

THE SEDIMENTOLOGY, GEOCHEMISTRY AND DIAGENESIS
OF WEST RAND GROUP SEDIMENTS IN THE HEIDELBERG
AREA, TRANSVAAL

by

P.M. Camden-Smith

Thesis submitted in fulfillment of the requirements
for the degree of Master of Science at the University
of Cape Town.

April, .

The University of Cape Town has been given
permission to reproduce this thesis in whole
or in part. Copyright is held by the author.

ABSTRACT

This study deals with the West Rand Group (formerly the Lower Division of the Witwatersrand System) sediments within an area of approximately 500 km² east of Heidelberg. The aim of the study was to interpret from the stratigraphy, lithology, petrology and sedimentary structures, the type of processes which were involved in the deposition of the arenaceous units of the West Rand Group, the current dispersal pattern and the probable, equivalent modern day depositional environment. The extent of diagenesis and metamorphism was investigated by using two white mica techniques. The chemistry of the shales was related to its mineralogy and a detailed study of the geochemical profile below the West Rand/Central Rand unconformity was undertaken.

The West Rand Group east of Heidelberg is made up of a thick (3400 m) succession of alternating arenaceous and argillaceous units. It has traditionally been subdivided into three Subgroups - the Hospital Hill, Government and Jeppestown. Each Subgroup is divided into three formations on the basis of laterally persistent markers.

Facies analysis has indicated that deposition occurred in the following environments in the different Formations : (1) the first shale horizon of the Orange Grove Quartzite Formation marks a change from "high" energy-wave dominated to lower energy - tide dominated conditions. The basal conglomerates and overlying trough crossbedded facies are interpreted as either platform beach or inlet deposits while ebb tidal deltas and local storm deposits characterise the rest of the arenaceous succession (2) the shales and thin sublitharenites of the Parktown Shale Formation were formed by suspension deposition of mud alternating with periodic sand influxes while the banded iron formations and magnetite rich zones probably represent distal shelf muds. (3) the 'sago'-textured units of the Brixton Formation were deposited by storm ebb surge currents in conjunction with tidal currents (4) at the base of the Promise Quartzite Formation offshore (subtidal shelf) marine conditions prevailed. Nearshore sequences and finally a braided stream setting of the Platte type is interpreted for the rest of the succession (5) the poor outcrop of 'tillite' in the Coronation Shale Formation made it impossible to delineate the facies associated with the till (6) the immature subgreywackes of the Witpoortjie Formation below the Government Reef represent subtidal shelf and inshore tidal flat deposits. The Government Reef marker represents an ancient beach deposit with onshore migrating sandbars and ripples moving in response to shoaling waves. The Blue Grit marker is interpreted as either a fossil submarine rockfall or a canyon and fan valley deposit (7) the shales of the Jeppestown Subgroup represent proximal shelf deposits

while the sandstones formed as a response to tidal, shelf and possibly fluvial processes.

The Weber crystallinity index indicates that the mineral assemblage (white mica, chlorite and quartz) are low grade. The West Rand Group's $H_b(\text{rel})$ value of 150 corresponds to an approximate temperature of 290°C . The study area's baric constraints are similar to the conditions for the Hercynian metamorphism in the eastern Alps.

The relative amounts of clay mineral present in a sample was calculated from its bulk chemistry. Chlorite, illite and muscovite (in that order) are the major clay phases present. The trace element abundance indicates that the source rocks for the West Rand Group in the study area are similar in petrology to the source rocks of the Fig Tree sediments. The trace elements - Sr, Ni, Rb, Ca, Zn, Cr - can be used to discriminate the shales of the West Rand, Central Rand and Fig Tree Groups. The Jeppestown shale immediately below the Main Conglomerate has a geochemical profile that has traits of a palaeosol which has subsequently been modified by diagenesis and the percolation of ground waters.

Two models are proposed for the deposition of the Hospital Hill Subgroup and the Government Subgroup by integrating the writer's detailed facies analysis approach with the work done by previous workers in other outcrop areas.

ACKNOWLEDGEMENTS

This M.Sc. research project was financed by the Economic Geology Research Unit, a bursary and loan from Southern Oil Exploration Corporation (SOEKOR) and a grant from Anglo American Corporation, all of whom are gratefully thanked. Professor A.J. Erlank of the Geochemistry Department, University of Cape Town, is thanked for permission to use the department's equipment and for reducing and in many instances waivering the instrument costs.

The writer is indebted to Professor D.A. Pretorius of the Economic Geology Research Unit, University of the Witwatersrand and Professor A.O. Fuller of the Geology Department, University of Cape Town for proposing the project. Guidance and encouragement was given by Professor A.O. Fuller ho is thanked for his useful comments against the final draft of the thesis. Special thanks are due to Dr. A. Button for many discussions on West Rand Group geology, and for his constructive criticisms in the field. The author's field method and interpretation benefitted considerably from discussions during field excursions with Professors A.O. Fuller and D.A. Pretorius, Drs. K.A. Eriksson, W.E. Minter, R.I. Hutchinson, H. de la R. Winter, Mr. P.M. Strydom, Mr. N. Tyler and my wife, Frances.

Mr. G. Payne, underground mine manager of Nigel Witwatersrand Pty. Ltd., is thanked for permission to sample and map the mines' longest crosscut. Union Corporation Ltd., Marievale, is also acknowledged for providing several core samples.

The following persons deserve special mention for their contributions at various stages of the research programme and in the preparation of this manuscript : Richard Zebblon, my field assistant; the farmers of the Heidelberg district for their hospitality; Dr. J.P. Willis, Mr. H.H.G. Fortuin and Mrs. M. Brautesteth for supervision of XRF analyses; Dr. A.R. Duncan, Miss. J. Crank and Mr. D. Murray for computing assistance; Mr. K.W. Kasch and Dr. C.W. Stowe for critical assessment of the chapters on metamorphism and structure respectively; Mr. R. Olivier for preparation of thin sections; Dr. J. McPherson, Mr. K. Behr and Mr. C. Basson for photographic reproduction and Miss. P. Eloff and my wife Frances, for meticulous drafting of many of the diagrams.

This thesis was typed in draft form by Mrs. W. Gordon and the final copy wa competently typed by Mrs. M. Grandia and Mrs. A.E. van Schalkwyk. A special word of appreciation is expressed to Mrs. G. Krummeck who kindly typed the review.

Finally, I thank my parents and friends, but particularly my wife Frances, for her support, advice and encouragement throughout my post-graduate career.

C O N T E N T S

	<u>Page</u>
<u>ABSTRACT</u>	i
<u>ACKNOWLEDGEMENTS</u>	iii
<u>CONTENTS</u>	iv
<u>FIGURES</u>	vi
<u>PLATES</u>	vii
<u>TABLES</u>	viii
<u>CHAPTER 1 INTRODUCTION</u>	1
1.1. <u>General</u>	1
1.2. <u>Study area</u>	2
1.3. <u>Purpose of study</u>	4
1.4. <u>Method of investigation</u>	5
1.4.1. Field procedure	6
1.4.2. Computer reduction	6
1.5. <u>Previous work</u>	7
<u>CHAPTER 2 STRUCTURE</u>	9
2.1. <u>Introduction</u>	9
2.2. <u>Subarea one</u>	10
2.3. <u>Subarea two</u>	11
2.4. <u>Subarea three</u>	14
2.5. <u>Discussion</u>	14
<u>CHAPTER 3 STRATIGRAPHY</u>	16
3.1. <u>Definition</u>	16
3.2. <u>Petrology of sandstones</u>	18
3.2.1. Textures	18
3.2.2. Composition	23
3.3. <u>Hospital Hill Subgroup</u>	25
3.3.1. Orange Grove Quartzite Formation	25
3.3.2. Parktown Shale Formation	33
3.3.3. Brixton Formation	37
3.4. <u>Government Subgroup</u>	44
3.4.1. Promise Quartzite Formation	44
3.4.2. Coronation Shale Formation	46
3.4.3. Witpoortjie Formation	48
3.5. <u>Jeppestown Subgroup</u>	52

	<u>Page</u>
<u>CHAPTER 4 DIAGENESIS AND METAMORPHISM</u>	55
4.1. <u>Introduction</u>	55
4.2. <u>Sample choice and preparation</u>	56
4.3. <u>Geothermometry</u>	56
4.4. <u>Geobarometry</u>	59
4.5. <u>Conclusion</u>	61
 <u>CHAPER 5 GEOCHEMISTRY</u>	 62
5.1. <u>Geochemistry of the West Rand Group - a review</u>	62
5.2. <u>Analytical procedure</u>	64
5.3. <u>Mineralogy from bulk chemistry</u>	65
5.4. <u>Distribution of trace elements</u>	73
5.4.1. Jeppestown Palaeosol	75
5.4.2. Correlation Coeffecients	76
 <u>CHAPTER 6 CONCLUSION</u>	 80
6.1. <u>Hospital Hill Subgroup Model</u>	81
6.2. <u>Government Subgroup Model</u>	82
6.3. <u>Jeppestown Subgroup Model</u>	84
 <u>REFERENCES</u>	
<u>APPENDICES</u>	
Appendix 1 Review of the West Rand Group	97
Appendix 2 Computer Programme for tilt correction	165
Appendix 3 Geochemical listings of Kaapvaal Craton Archaean sediments	175
Appendix 4 Calculation of bo cell dimension	221
Appendix 5 Estimates of precision and detection limit for each major oxide (Table 1) and estimates of the uncertainties due to counting statistics (Table 2)	223
Appendix 6 Several trace element and major element plots.	226

LIST OF FIGURES

<u>Figure</u>	<u>Page or following Page</u>
1.1. Four major outcrop areas of the West Rand Group	2
1.2. Map showing the distribution of the Witwatersrand Supergroup below cover of Karoo, Transvaal and Ventersdorp sequences.	3
1.3. Comparison of Mellor's (1917) stratigraphic column to that of SACS (1978).	4
1.4. Topography of study area.	4
1.5. Geology of study area showing traverse locations.	7
2.1. Division of study area into three subareas.	10
2.2. Lineation and fold axial readings recorded for subarea 2.	10
2.3. Classification of folds.	12
2.4. Parameters measured on a horizontal apparent profile section of a plunging fold.	13
2.5. Classification of folds in subarea 2.	14
3.1. The West Rand Group in the Heidelberg-Greylingstad-Delmas area.	18
3.2. Comparative stratigraphy of the West Rand Group in the East Rand.	18
3.3. Composite stratigraphic column of the West Rand Group in the study area.	18
3.4. Relative proportions of pebbles in the Government Reef and Black Grit.	25
3.5. Stratigraphic section for the Orange Grove Quartzite Formation.	28
3.6. Sedimentary structures observed and mapped at the base of the first shale horizon of the Orange Grove Quartzite Formation.	29
3.7. Paleocurrent direction analysis of the Orange Grove Quartzite Formation.	30
3.8. The stratigraphic column of the Parktown Shale Formation.	34
3.9. Composite stratigraphic section of the Brixton Formation.	38
3.10. Paleocurrent pattern of the Brixton Formation.	41
3.11. Sequence of sedimentary structures, textures and lithology in the Promise Quartzite Formation.	46
3.12. Paleocurrent dispersal pattern for the Promise Quartzite Formation.	46
3.13. Composite stratigraphic section of the Witpoortjie Formation.	49
3.14. Generalized stratigraphic sequence of the Jeppestown Subgroup.	
4.1. The cumulative frequency curves illustrating the distribution of b_0 in low grade zone metamorphic belts of various baric types.	61
5.1. Discriminate function analysis of West Rand, Central Rand and Fig Tree Group shales.	64
5.2. Distribution of major elements below West Rand/Central Rand unconformity.	76
5.3. Distribution of trace elements below West Rand/Central Rand unconformity.	76
6.1. Depositional model for the Hospital Hill Subgroup.	82
6.2. Depositional model for the Government Subgroup.	83

LIST OF PLATES

<u>Plates</u>		<u>Following page</u>
3.0.	Sedimentary structures in the West Rand Group.	19
3.1.	Textures in several thin sections.	20
3.2.	Orange Grove Quartzite Formation's sedimentary structures.	28
3.3.	Tidal flat structures in the Orange Grove Quartzite Formation.	28
3.4.	Parktown Shale Formation sedimentary structures.	36
3.5.	Government Subgroup's sedimentary structures.	45
3.6.	Coronation Shale Formations tillite horizon.	48
3.7.	Jeppeshtown Subgroup's sedimentary structures.	53.

CHAPTER 1

INTRODUCTION

1.1 GENERAL

The Witwatersrand Supergroup consists of about 7400 m of sediments lying in a roughly ovoid basin 350 km long and 200 km wide within the Kaapvaal craton (Pretorius 1974). Stratigraphically, the Witwatersrand Supergroup has been separated into two groups: a shale dominated West Rand Group (previously known as the Lower Division) and a quartzite and conglomerate dominated Central Rand Group (previously known as the Upper Division).

An interpolated age of the Witwatersrand Supergroup is defined by a maximum of 2720 ± 55 Ma (Rb-Sr) for the underlying granite (Allsopp 1964) and a minimum of 2620 ± 55 Ma (U-Pb) for lavas of the overlying Ventersdorp Supergroup (van Niekerk and Burgher 1978). On present evidence the Witwatersrand basin is therefore Archaean, i.e. >2500 Ma old. However, Pretorius (1974) noted that "the transition from Archaean to Proterozoic style of crustal evolution took place on the Kaapvaal craton at between 3000 and 3240 Ma ago. On other shield areas of the world, the age of transition has been dated at about 2500 Ma". This comment emphasises the Proterozoic aspect of the Witwatersrand Supergroup despite its formal position in the Archaean.

The scattered areas of West Rand Group outcrop are shown on Fig. 1.1. Borchers's map (Fig. 1.2, 1961, 1964) shows the distribution of the Witwatersrand Supergroup below the cover of Karoo, Transvaal and Ventersdorp sequences.

All these weakly metamorphosed sedimentary/volcanic successions rest with marked unconformity on a highly metamorphosed basement complex comprising the Older Granite and the Swaziland Sequence which together constitute an early Archaean granite-greenstone terrain.

Mellor (1911) constructed "an approximately representative section

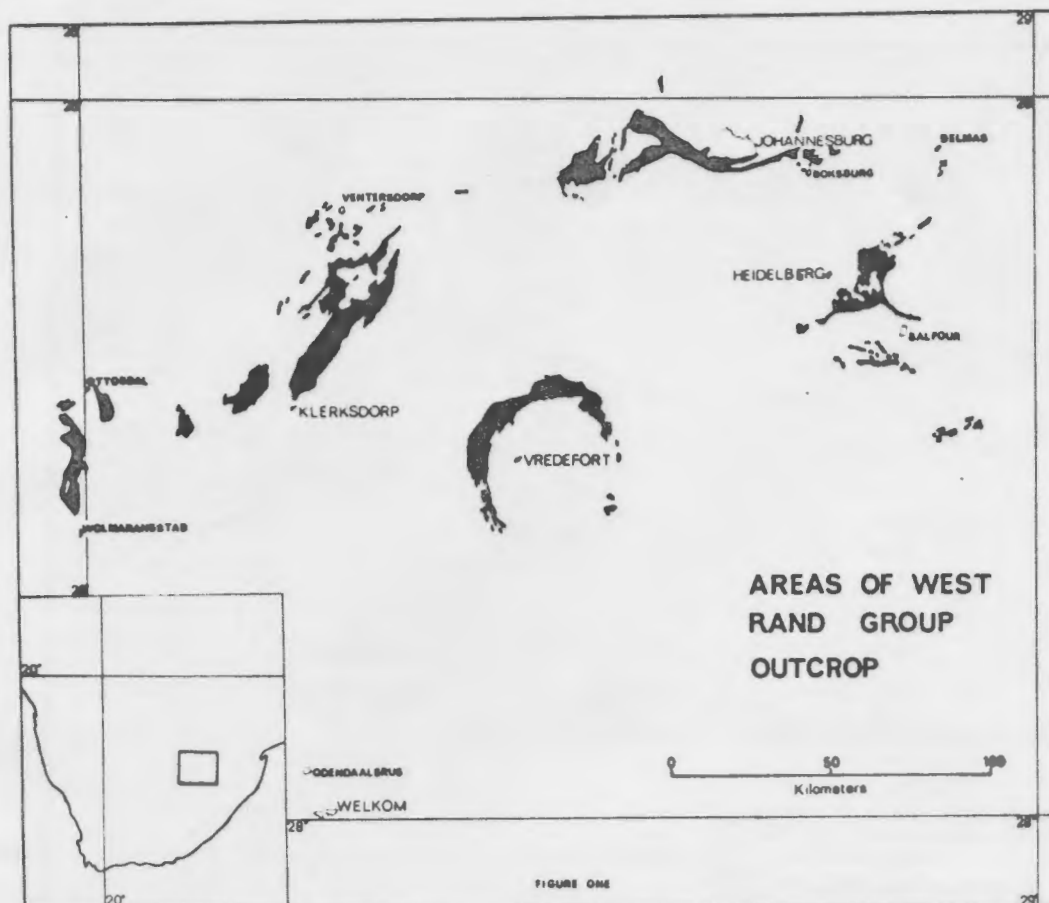


FIGURE 1.1 The four major outcrop areas of the West Rand Group.

of the lower Witwatersrand applicable to both the Central and at least the adjacent portions of the Western Rand". By 1939, the persistence of most of the West Rand Group lithologies described by Mellor had been confirmed by Rogers (1921) for the Heidelberg area and by Nel (1927, 1933, 1939) for the Vredefort, Klerksdorp and Ventersdorp districts. Mellor's (1917) stratigraphic column remained the basis for the subdivision of the West Rand Group for over forty years and it was only in 1960 that Collender questioned it. Winter (1978), the chairman of the Witwatersrand Working Group of SACS (South African Committee for Stratigraphy) proposed a lithostratigraphic subdivision of the Witwatersrand Supergroup. Fig. 1.3 compares Mellor's (1917) stratigraphic column to that of the South African Committee for Stratigraphy. In this thesis the terminology used by SACS will be followed.

1.2 STUDY AREA

The area described in this thesis is situated in south-eastern Transvaal.

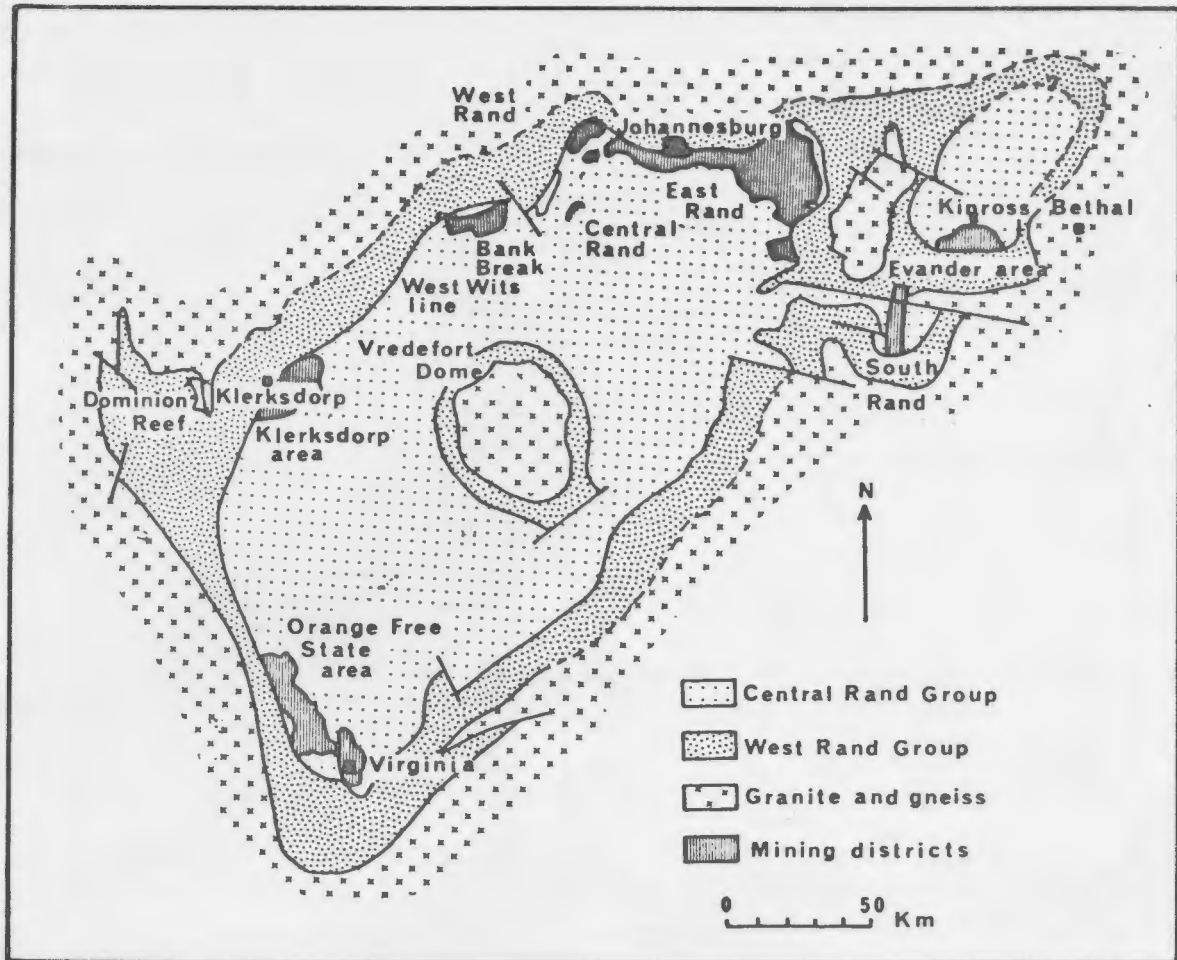


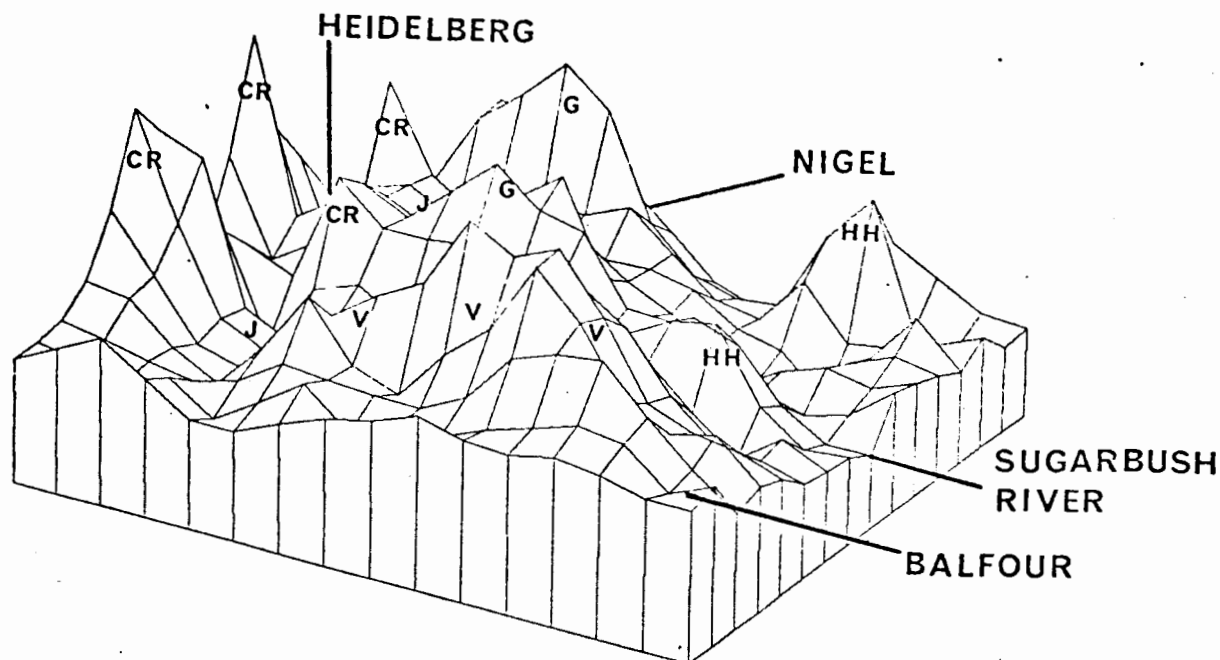
FIGURE 1.2 Map showing the distribution of the Witwatersrand Supergroup below the cover of Karoo, Transvaal and Ventersdorp sequences as revealed by diamond drilling (after Borchers 1964).

It is bounded by the Sugarbush fault in the south, the Blesbokspruit River in the north and the meridians $28^{\circ} 20'$ and $28^{\circ} 35'$. This is an area of approximately 500 km^2 of which nearly 180 km^2 is exposed rock. The three major towns in the area - Heidelberg, Nigel and Balfour - are linked by a network of provincial and district roads.

The Sugarbush River, a tributary of the Vaal River, follows a course that is independent of the lithological and structural setting, cutting across the Swaziland, Witwatersrand, Ventersdorp, Transvaal and Karoo sequences. Fig. 1.4 constructed with the use of the Sacant Graphics Package (U.C.T. version), gives a perspective picture of the topography of the study area. The data used in its construction were a set of points (X, Y, Z) defined over a rectangular grid arbitrarily placed over the four (2628CB, 2628AD,

after MELLOR (1917)				after SACS (1978)			
MEMBERS & BEDS (markers)		SERIES	Thickness (m)	FORMATIONS	MEMBERS & BEDS (markers)		
LOWER WITWATERSRAND SYSTEM		JEPPESTOWN SERIES	T	ROODEPOORT		JEPPESTOWN SUBGROUP	
			S				
				250	CROWN LAVA		
				300	FLORIDA QUARTZITE		
	Government reef	GOVERNMENT REEF SERIES	N ₃	WITPOORTJIE		GOVERNMENT SUBGROUP	
			N ₂		Government reef		
			M ₂				
			N ₁				
			M ₁				
	Coronation reef		K ₂		Coronation reef		
			L	CORONATION SHALE			
			X ₁	PROMISE QUARTZITE	Hamberg Quartzite Member		
					1000		
	Promise reefs		J		Promise reef		
Hospital Hill Quartzites	HOSPITAL HILL SERIES	H ₃	BRIXTON		HOSPITAL HILL SUBGROUP		
		H ₂					
		G ₁					
		H ₁					
		F		Observatory Shale Member Contorted Bed			
Speckled Bed		E	PARKTOWN SHALE	Speckled Bed			
		D		Red Shales			
Ripple-marked Quartzites		C		Ripple marked Quartzite			
		B		Water Tower Shale Member			
Orange Grove Quartzites		A ₂	ORANGE GROVE QUARTZITE				
		A ₁		200			

FIGURE 1.3 Mellor's (1917) stratigraphic column compared to that of the South African Committee for Stratigraphy (1978)



UCT VERSION OF (JULY 1976) SACLANTCEN THREE-D PACKAGE OCT 1978

FIGURE 1.4 The sandstone ridges of the Hospital Hill Subgroup (HH), Government Subgroup (G) and Central Rand Group contrasting against the flat lying shale dominated Jeppestown Subgroup (J). The Ventersdorp lavas (V) form E-W trending ridges opposed to the north-south trending parallel ridges of the Witwatersrand Supergroup.

2628BC, 2628DA) 1:50 000 topographic maps drawn by the Trigonometrical Survey Office. Although the vertical exaggeration is great, the "fish net" appearance of the topography shows at a glance the relative elevations of the area. The shale dominated Jeppestown Subgroup and the younger flat-lying Karoo strata have an average elevation of some 1600 metres above sea-level while the sandstones of the Witwatersrand Supergroup form several arcuate north-south trending parallel ridges, reaching heights of up to 1800 m in the north of the area and gradually decreasing in height towards the south. To the west of Heidelberg and around Balfour, the Ventersdorp lavas form prominent hills rising 200 m above the surrounding area. The largest pan in the area - Rietpan - is at present a drainage centre (Jansen *et al.*, 1972).

1.3 PURPOSE OF STUDY

A review on the stratigraphy, lithology, petrology and geochemistry of the West Rand Group was compiled by the writer in 1978 (Appendix 1). It became apparent that although the literature on the Witwatersrand Supergroup is voluminous very little work other than that of a pioneering nature (Mellor, 1911, 1917; Rogers, 1921; Nel, 1927, 1933, 1939) has been done on the West Rand Group. The auriferous and uraniferous reefs of the Central Rand Group have, on the other hand, received much attention in recent years (e.g. Pretorius, 1966, 1974; Armstrong, 1968; Minter, 1978). A consequence of this is that some geologists (e.g. Vos, 1975) have suggested that the depositional models proposed for the Central Rand Group (alluvial plain and lacustrine) are also applicable to the West Rand Group. One of the purposes of this study is an investigation based upon more quantitative and stringent sedimentological variables to test the above hypothesis and to refine the wide ranging models (littoral, estuarine, marine, alluvial plain, glacial, etc.) which have been proposed for the West Rand Group.

Furthermore, in the opinion of many geologists working in Archaean terrains (e.g. Glikson, 1971; Pettijohn *et al*; 1972; Turner and Walker, 1973; Naqvi, 1978) the geochemistry of sediments is useful in understanding the early history of crustal evolution. Because of the lack of severe deformation, metamorphism and protracted erosion, the geochemistry of the Witwatersrand shales should prove useful in this regard.

It was thus the aim of the author to interpret from the stratigraphy, lithology, petrography and sedimentary structures, the type of processes which were involved in the deposition of the arenaceous units of the West Rand Group, the current dispersal pattern of the Group and finally the probable, if any, modern day equivalent depositional environment. The geochemistry of the shales, tillite, greywackes and sandstones is used to determine whether the provenance of the various shale horizons was approximately the same throughout the deposition of the Witwatersrand strata, to see whether it is feasible to make conclusions of early crustal evolution from a sedimentological viewpoint and to compare the geochemistry of South African Archaean sediments.

1.4 METHOD OF INVESTIGATION

The method of investigation entailed the observation, measurement and

recording of geological variables in the field; subsequent laboratory investigation (XRD, XRF and thin-sections) and the computer reduction of the data collected.

1.4.1 Field procedure

Using aerial photographs (scale 1:50 000) and a geological map of the country around Heidelberg (mapped by Rogers between 1918-1921), eighteen traverses were selected along unfaulted routes, (Fig. 1.5). The system used for section and sample location numbering comprise four digits; two for the traverse and two for the sample location e.g. sample 03/15 would be sample 15 from traverse number 3. Thickness determinations were made using the Jacob's staff method (Robinson, 1959). The orientation of beds, sedimentary structures and joints was determined using "Toby's Clinoboard" and a Brunton compass. Forty shale samples within the Jeppestown Subgroup were sampled along a crosscut in the Witwatersrand-Nigel Mine.

Of the 247 samples collected, all were halved (duplicates of which were kept in the Economic Geology Research Units Storeroom); 27 samples (1 paleosol, 1 sandstone, 1 greywacke, 2 tillites and 22 shales) selected for major and trace element analysis (X-ray fluorescence); 60 thin sections cut and more than 60 X-ray diffraction traces run.

1.4.2 Computer reduction

The number of crossbed measurements taken at any one outcrop varied from less than ten (unimodal) to over thirty (polymodal or bimodal). Where possible the trough axes of the pi crossbeds were recorded. The processing of the crossbed data was initially done by hand but this proved to be cumbersome. A Fortran programme was thus written using the rotation formulae of van Eden (1969) and the calculations for grouped data as stated in Potter and Pettijohn (1977). The full programme together with a few examples appears in Appendix 2. A minor disadvantage of the programme is that it was formulated assuming a symmetrical unimodal density function. However, meaningful analysis of bimodal data requires estimation of parameters that relate to each mode individually. Rose diagrams of a set of readings

showing /7

OUTCROP PATTERN OF WEST RAND GROUP MARKER BEDS

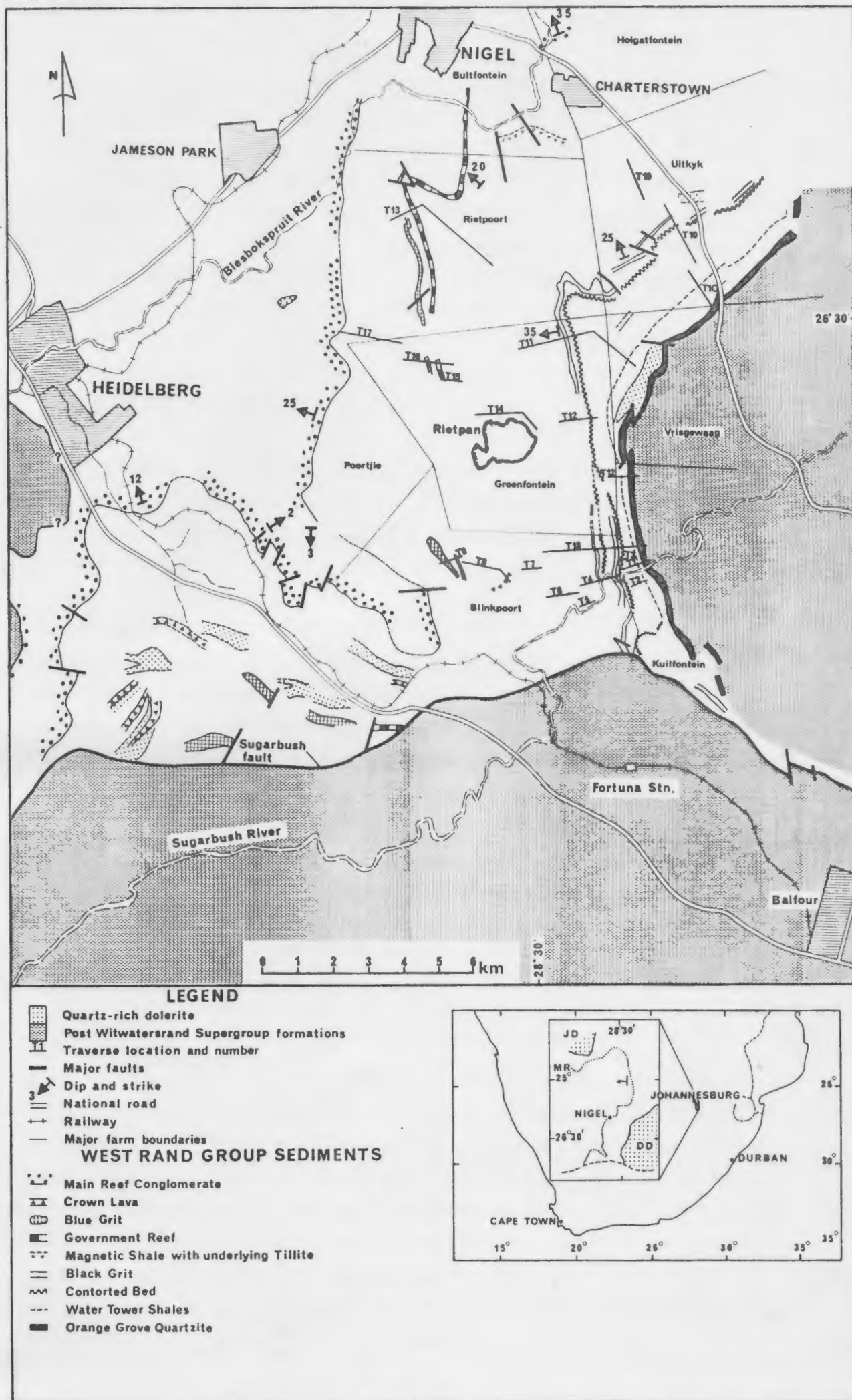


FIGURE 1.5 The geology of the study area with the locations of eighteen traverses (T)

showing bimodality were thus drawn, the two major modes separated and the programme rerun with the vectoral mean, vectoral magnitude, consistency ratio and arithmetic mean dip for each mode noted (see example in Appendix). An attempt was made to adapt the programme to synthesise data with a mixture of two or more circular normal distributions by a method of maximum likelihood as described by Jones and James (1969). However, the method of maximum likelihood only proves satisfactory if at least 500 crossbed readings at each locality are recorded and more than 1000 readings are needed for mixtures of more than two modes (Cohen 1966). None of these conditions were fulfilled in this study.

The programme, Datalist/NGP written by Dr. A.R. Duncan of the Geochemistry Department, University of Cape Town, was used to store the data needed to compare the geochemistry of the West Rand Group to that of the Central Rand Group, Fig Tree and Pongola Groups.

The Datalist/NGP programme provides listings of major element, trace element and Sr isotope data for bulk rock analyses. A substantial number of inter-element ratios are calculated. Although the programme has an igneous and metamorphic bias - for example it calculates the CIPW norms - it does have provision for an embedded listing of sample directories (i.e. sample name and number, database number, rock type code, locality information and reference code) and reference lists (Appendix 3). Furthermore, the programme can be used for data input to many other programmes such as genplot, triplot, histplot and various programmes in the BMDP and statjob packages. All the geochemistry data collected by the writer is available in the University of Cape Town's Earth Sciences Database.

1.5 PREVIOUS WORK

The only original published works of the geology of the West Rand Group in the study area, other than that of the author, are those of Luttmann-Johnson (1904), Corstorphine (1904) and Rogers (1921, 1922). Luttmann-Johnson mapped the Orange Grove Quartzite Formation together with other Witwatersrand Formations in the Fortuna Valley. He noted that the "Witwatersrand Beds were tilted and folded before the Ventersdorp volcanic outflows occurred". Corstorphine (1904) noted the relationship of the Old Granite to the Orange

Grove Quartzite Formation. Comparing the relationship to the Table Mountain Sandstone on Cape Granite he suggested that the sediments (Orange Grove Quartzite) were deposited on the slopes of an old granitic shore.

Roger's (1921) paper and map, which Mellor (1921) describes as involving "an enormous amount of detailed work both in the field and out of it" was used by the writer as a base map. The detailed stratigraphy of the West Rand Group compiled by Mellor (1917) in the Central Rand was confirmed by Rogers in the country surrounding Heidelberg. He also established the changes in thickness of the various formations and the presence of a tilite and volcanic horizon (Crown Lava). Rogers was the first to recognise and map the large Sugarbush fault. The detailed and accurate mapping of the individual marker beds revealed to Rogers the extensive and intricate nature of the faulting. The writer found no large errors in Rogers' mapping and agrees with his interpretation of the structure. A map redrawn from aerial photographs (scale 1:18 000) with all the subsequent roads, railways, farms, mines and towns is in the folder attached to the back of this thesis.

The geology of this area and the surrounding countryside has been reviewed by de Jager (1964), Pretorius (1964), Jansen et al., (1972) and more recently by Camden-Smith (Appendix 1).

STRUCTURE

2.1 INTRODUCTION

Much has been written on the structure of the study area and the adjacent South Rand Goldfield (area between the Sugarbush fault and Vaal River). Rogers (1922), Nel and Jansen (1957), Pretorius (1964) and Jansen et al, (1972) all agree that these areas have been subjected to folding and complex faulting both during and after deposition of the Witwatersrand, Ventersdorp and Transvaal Supergroups. Differences of opinion have arisen on the relative importance of pre-Ventersdorp and post-Transvaal movement.

Pretorius (1964a) is of the opinion that folding "started in Witwatersrand times and continued, probably in pulses, through Ventersdorp and Transvaal times, and might have lasted in a very much enfeebled form, right up to Karoo times". He states "it is not feasible to date the movements in any of the faults as being exclusively of any particular period in geological time" due to their continued reactivation up to and including Karoo times. The writer's aim with regard to the structural history of the study area was not to unravel the relationship between the different fracture and fold patterns (as was Roering's (1968) objective in the Krugersdorp-Florida Hills area), but rather to determine mean fold attitudes by means of stereographic plots in order to make the necessary corrections for meaningful paleocurrent vector analysis.

The study area is divided into three subareas (Fig. 2.1) on the basis of their respective fold and fracture patterns. Subareas 1 and 3 are areas with no folding (except for the disharmonically folded laminae in the Contorted Bed) but having an intricate fracture pattern. Owing to the complex folding and fracturing in subarea 2 no crossbed data were collected within this region.

Contours of poles to bedding planes were constructed by the use of the Kalsbeek counting net and show the respective dip azimuth modes of subareas 1 and 3 as two maxima (Fig. 2.2). Clearly, the combined bedding

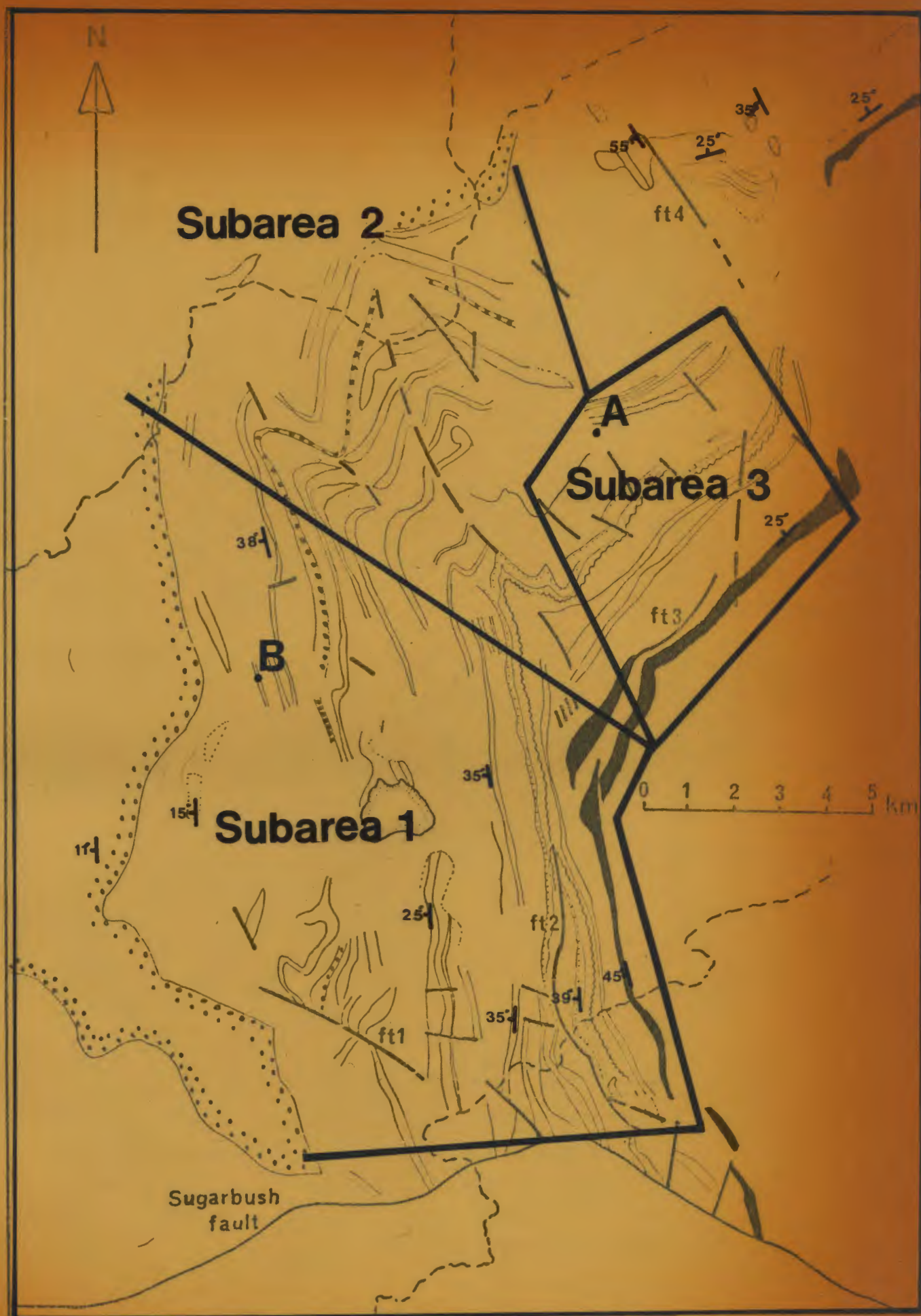


FIGURE 2.1 Map showing general structure and location of three subareas

plane data from subareas 1 and 3 simply define the macro-arcuate geometry as shown from the outcrop pattern. Also on Fig. 2.2 the lineation and fold axial readings are recorded for subarea 2. The scattered nature of the lineations made it difficult to ascertain whether they were tectonic or primary sedimentary structures. No significant preferred orientation directions were recorded in the study area, but this may be due to the poor exposure of shale.

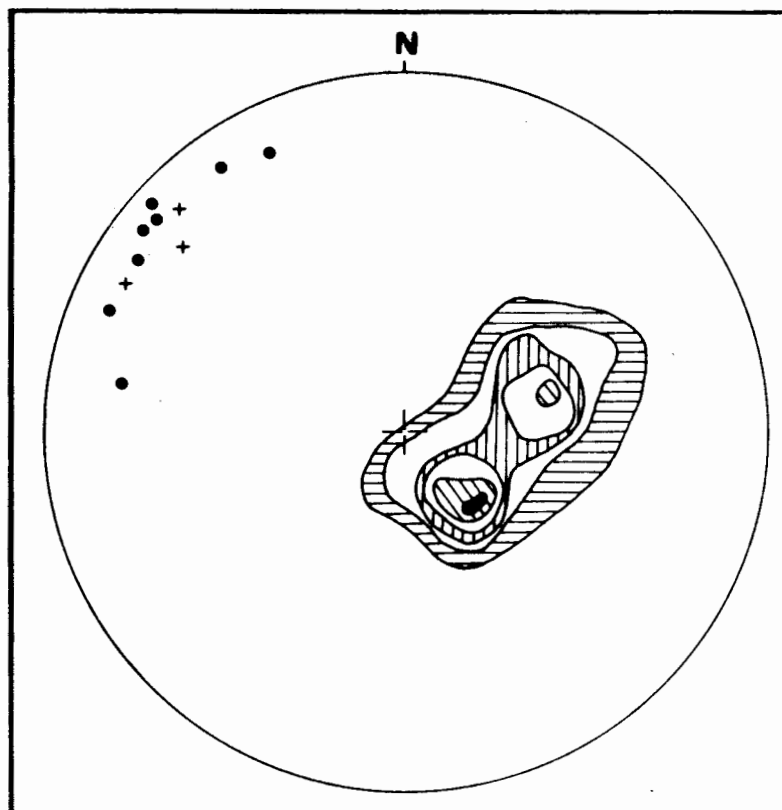


FIGURE 2.2 Equal area projection diagram of 187 poles to bedding planes from subareas 1 and 3 (Contours 0-5-10-15-20-25%). Crosses are fold axes readings and dots are lineation readings recorded in subarea 2.

2.2 SUBAREA 1

An east-west cross section through this subarea indicates that there is an orderly progression from a maximum dip of 45° for the Orange Grove Quartzite Formation, 40° - 35° for the Brixton Formation, 35° - 20° for the Government Subgroup and 20° - 15° for the Jeppestown Subgroup to a minimum dip of 5° for the overlying Central Rand Group. This feature is, according to Brock and Pretorius (1964a,b), a basin edge structure formed by

successive subsidences of the depositional basin.

Three major faults and numerous minor faults occur in subarea 1. A long slightly curved traverse fault (ft. 1) caused considerable drag on the Government Subgroup beds. This was the only site in subarea 1 where faulting markedly affected the strike of the beds. Towards the east, the largest strike fault (ft. 2) in the study area (5,5 km long with a minimum throw of 400 m) duplicates the Black Grit and Contorted Bed marker horizons of the Hospital Hill Subgroup. Similar thrust faults (ft. 3) inclined westwards, duplicate the Orange Grove Quartzite Formation and extend into subarea 3. Associated with the ft. 3 fault planes are quartz dolerite and diabase sills. The petrological differences between these rocks and Karoo dolerites were summarised by Rogers (1922). A minimum age of a similar dolerite south of the Sugarbush fault has been given as 1120 Ma (K-Ar) by McDougall (1963).

2.3 SUBAREA 2

The classification of folds in subarea 2 was based on Ramsay (1967). This is a geometrically based classification that allows individual folded layers to be compared unambiguously (Fig. 2.3). The classification involves measurement of orthogonal thickness (t_α) and the thickness parallel to axial surface (T_α) measured on the bounding surface of folded layers with equal amounts of inclination (α). The ratio of t_α/t_0 and T_α/T_0 where t_0 equals T_0 at the fold hinge are tabulated. A graph of these ratios versus α plotted on Ramsay's classification diagrams measures the changing shape and class of the fold.

One of the problems encountered was deciding whether an apparent fold profile (i.e. a horizontal cross section of a plunging fold as seen on aerial photographs) could be used in Ramsay's classification. As the axial planes of the folds in the study area are vertical there exists a simple trigonometrical function relating the angle of plunge (β) to the thicknesses T , T_1 and angles α , α_1 , where T and α are the parameters measured on a true fold profile and T_1 and α_1 the parameters measured on a horizontal apparent profile section of a plunging fold (Fig. 2.4). Since both T_1 and $\tan \alpha$ are proportional to $\sin \beta$ the angle of plunge can be ignored and apparent fold profiles used in Ramsay's classification. The orthogonal thickness varies from a minimum value in the fold limb to a maximum value in the hinge, there-

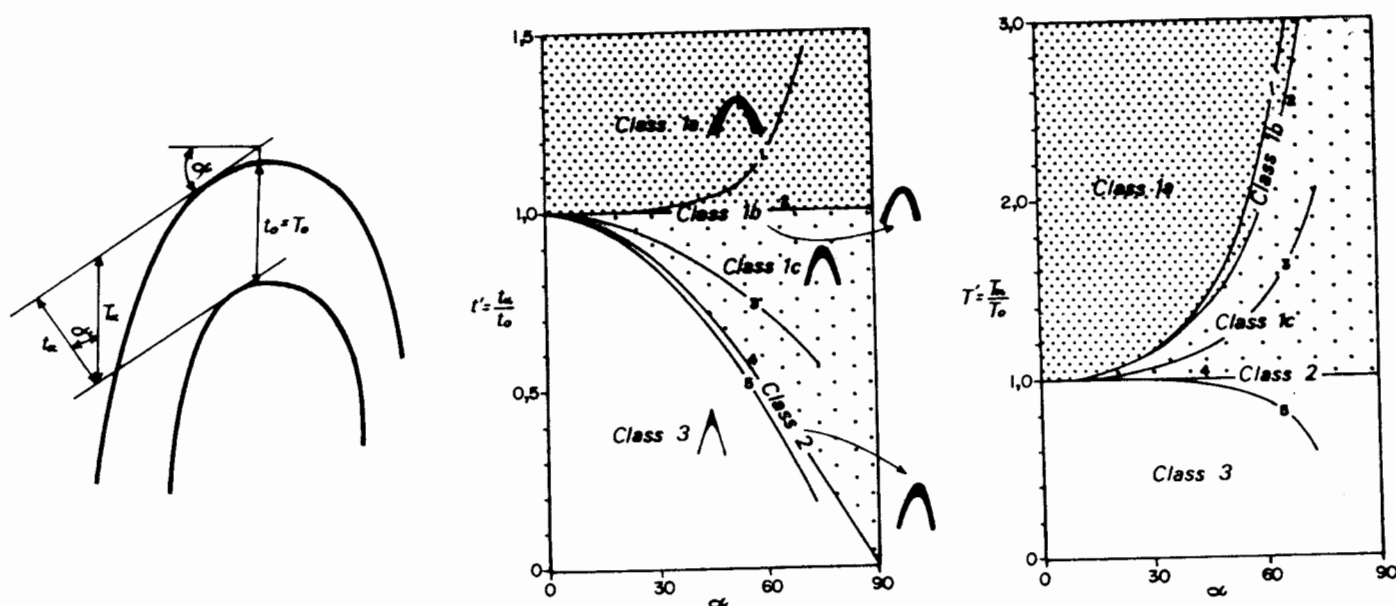


FIGURE 2.3 The classification of folded layers (Ramsay, 1967)

fore the simple aforementioned relationship no longer holds for t/α .

On T versus α plots (Fig. 2.5) it was found that the arenaceous units of two selected Hospital Hill Subgroup folds tended to give class 1C and 3 folds closely clustered about the class 2 dividing line. The northern limbs of the Government Subgroup folds plotted in the Classes 1C and 3 fields while the limbs on the southern side of the fold axis did not conform to Ramsay's classification having several points of inflexion and maxima and minima. Table 2.1 summarises the classification of the folds in subarea 2.

Dip isogons drawn on the folds in subarea 2 shows a complex converging - diverging pattern (Fig. 2.5). It was found that generally the isogons diverged from the outer to the inner arc of folds defined by argillaceous horizons, while the isogons in the arenaceous units revealed a wide array of complex patterns - either converging or diverging in some folds, both converging and diverging in others or neither converging or diverging. The three arenaceous units of the Government Subgroup, selected for T versus α plots had dip isogons that generally diverged from the outer to the inner arc of the folds.

Hobbs et al (1976) note that in a multilayered sequence in which individual

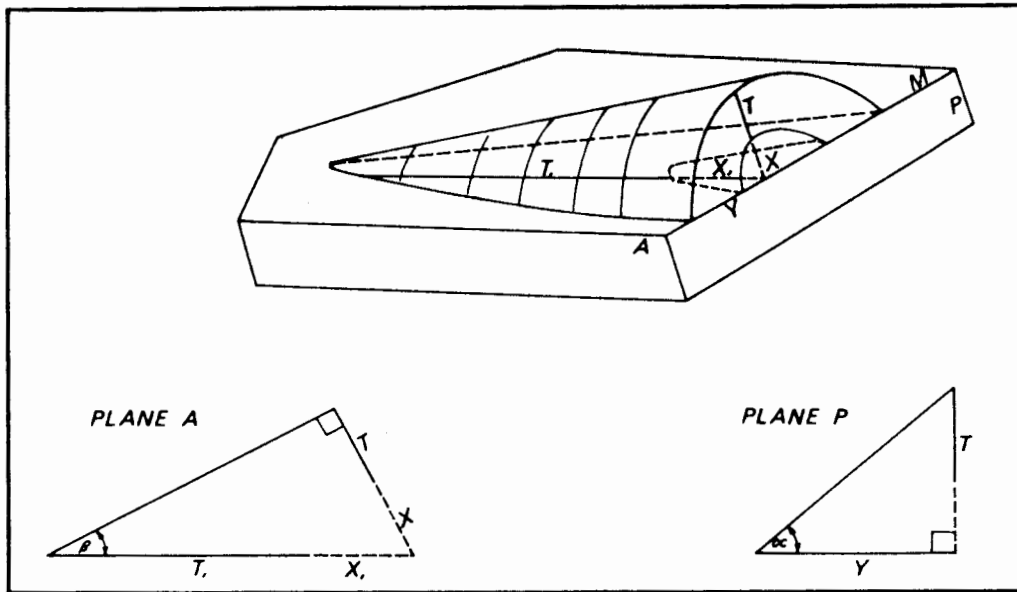


FIGURE 2.4 Use of horizontal projection (M) in place of fold profile projection (P) in Ramsay's classification.

On plane A.
$$\sin \beta = \frac{T + x}{T_1 + x_1}$$

$$T + x = \sin \beta (T^1 + x^1) \dots\dots\dots 1$$

$$\text{i.e. } T = T^1 \sin \beta \dots\dots\dots 2$$

On plane A.
$$\tan \alpha^1 = \frac{T^1 + x^1}{Y} \dots\dots\dots 3$$

On Plane P.
$$\tan \alpha = \frac{T + x}{Y} \dots\dots\dots 4$$

combining (1) and (4)

$$\tan \alpha = \frac{\sin \beta (T^1 + x^1)}{Y}$$

substituting (4)

$$\tan \alpha = \sin \beta \tan \alpha^1 \dots\dots\dots 5$$

From equation (2) and (5) it will be seen that both T^1 and $\tan \alpha^1$ are proportional to T and $\tan \alpha$ by a common factor ($\sin \beta$) and may therefore be substituted for T and $\tan \alpha$ in Ramsay's plots provided that plane A is vertical i.e. perpendicular to M.

Table 2.1

Variation of fold classes within individual layers in subarea 2

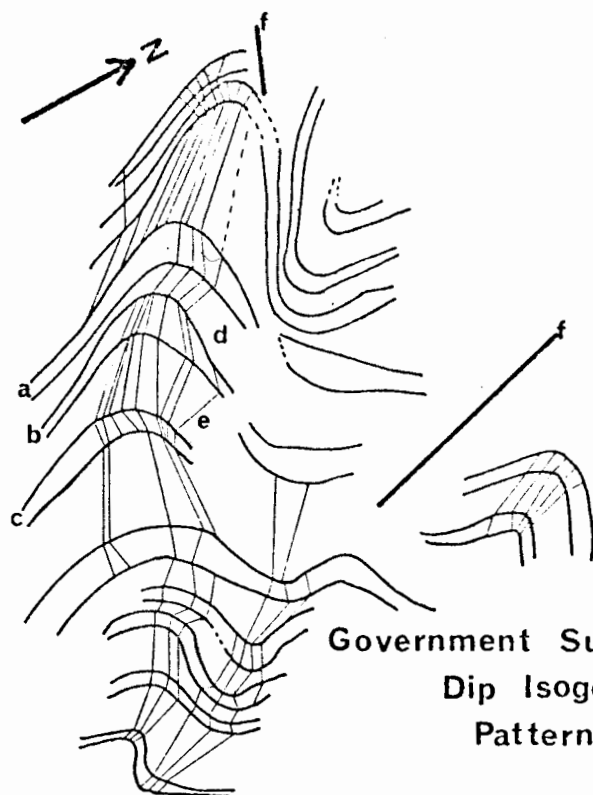
	0 - 10	10 - 20	20 - 30	30 - 40	40 - 50	50 - 60	60 - 70	70 - 80	80 - 90	CLASS MODE
a		2/2	3/2	3/2	3/1C	3/?				3/2
d		?/2	?/2	2/2	1C/1C	1C/1C	1C/1C	1C/1C	1C/?	1C/2
b	1A/?	1A/3	1B/3	1C/3	2/3	3/?	1C/?	1C/?		1C/3
e	3/?	3/1C	3/1C	3/1C	3/1C	3/?				3/1C
c	1A/3	1A/3	1A/3	1A/3	?/3					1A/3
f	?/2	1A/2	1A/3	2/3	1C/3	1C/2				?/3
g				1C/2	2/3	2/3	2/3	?/3		2/3

1C/₂ = southern limb
 = northern limb

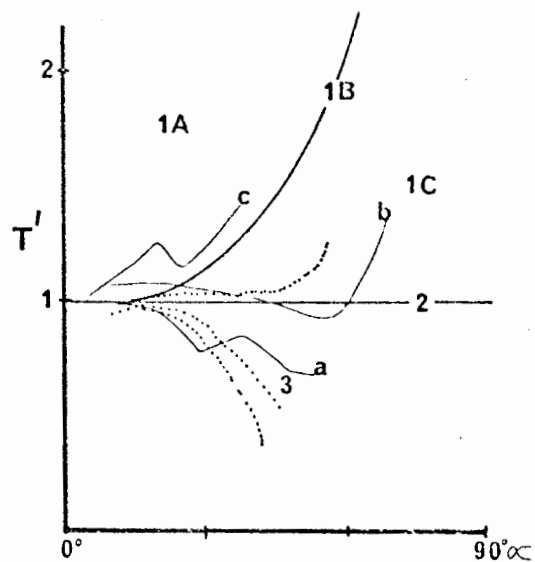
layers possess different thicknesses and competencies, only one or two layers begin to fold initially and it is these layers that control the subsequent deformation. If this applied in the study area, then class 2 folds in the argillaceous horizons should be bounded by class 3 and class 1C folds in the competent horizons whilst class 3 folds in argillaceous layers should be found between competent layers which are of the same class, i.e. class 3. This relationship has been noted in metamorphic terrains where quartzofeldspathic layers have behaved more competently than biotite schists (Toogood, 1976). Table 2.1 shows that in the study area not only do different layers have different classes of folds but that a single folded layer may belong to a number of classes. This large variability of classes cannot be accounted for by the sensitivity of Ramsay's fold classification as even the dip isogons show a complex pattern. Furthermore, owing to this variability, the three different processes operating during deformation, namely the pre-fold layer - parallel shortening, buckling and post-fold homogeneous flattening cannot be estimated.

The faulting in subarea 2 is marked by large traverse faults radiating from the area of maximum curvature in the Hospital Hill Subgroup horizons. Several markers have been displaced by these faults and as the fault is approached there is a systematic rotation of bedding planes. Several injective shale dykes penetrate the quartzite horizons of the Government Subgroup. They are well developed south-west of the farmhouse Rietpoort and are also present on the northern limbs of quartzite horizon 'a' (Fig. 2.5). The thickness of these dykes varies from 20 to 100 cm. Roering (1967) interprets similar 'dyke-like' structures in the Krugersdorp area as a macro-boudinage type of phenomenon formed by tensile stresses.

Roering (1968) noted that bedding plane data can be useful in defining the presence of fundamental faults in a basin-type structural environment. Furthermore, he stipulates, as did Brock and Pretorius (1964a,b), that a very intimate relationship exists between faulting and folding in the Witwatersrand Basin. Roering showed that in the Krugersdorp area not only do folds form adjacent to faults, but the strikes of the fold axes are generally parallel to these faults. This relationship exists in subarea 2 where the fold axes (Fig. 2.1) are near parallel to the trend of the faults. Ramsay's fold classification of the best developed folds in the area showed that there exists a complex fold pattern within a single folded layer. The formation of these folds is interpreted as not being due to progressive



Government Subgroup
Dip Isogon
Pattern



Hospital Hill Subgroup

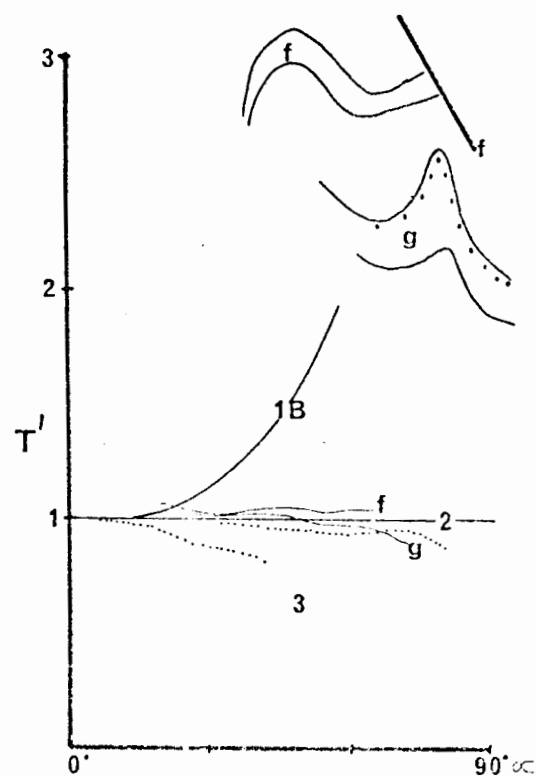
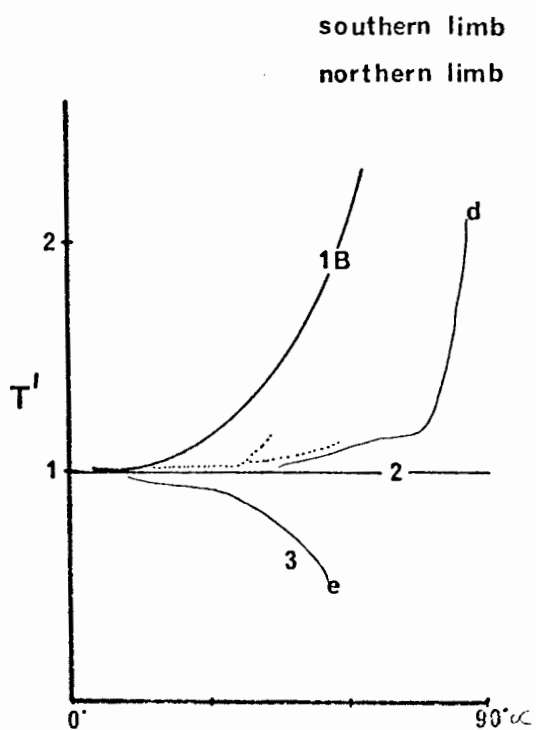


FIGURE 2.5 The classification of folded layers within subarea 2

Table 2.2

West Rand Group Palaeocurrent direction analysis-Heidelberg area

T10-QTZ after black grit

Locality Number	Azimuth Bedding	Dip Bedding	Azimuth cross-bedding	Dip cross-bedding	Corrected Azimuth	Corrected Dip
1	334.000	15.000	285.000	29.000	256.466	22.006
2	344.000	15.000	273.000	22.000	234.972	22.003
3	334.000	15.000	290.000	30.000	263.545	21.626
4	334.000	15.000	265.000	21.000	224.639	20.769
5	334.000	15.000	272.000	27.000	240.472	23.678
6	334.000	20.000	285.000	30.000	245.832	22.181
7	344.000	15.000	302.000	23.000	263.180	15.357
8	334.000	15.000	295.000	26.000	263.274	16.992
9	334.000	15.000	280.000	26.000	246.629	20.794

Vector Mean Azimuth = 249.

Vectoral Magnitude = 8.77

Consistency Ratio = 97.40

Sample Deviation = 14.

Arithmetic Mean Corrected Dip = 20.

Corrected by unfolding fold axis (306/14) - location (A) Figure 1.6

T10-QTZ after black grit

Locality Number	Azimuth Bedding	Dip Bedding	Azimuth cross-bedding	Dip cross-bedding	Corrected Azimuth	Corrected Dip
1	.000	.000	252.000	26.000	251.980	26.000
2	.000	.000	235.000	24.000	234.980	24.000
3	.000	.000	263.000	26.000	262.980	26.000
4	.000	.000	228.000	25.000	227.980	25.000
5	.000	.000	240.000	26.000	239.980	26.000
6	.000	.000	257.000	27.000	256.980	27.000
7	.000	.000	262.000	18.000	261.980	18.000
8	.000	.000	260.000	21.000	259.980	21.000
9	.000	.000	246.000	25.000	245.980	25.000

Vector Mean Azimuth = 249.

Vectoral Magnitude = 8.81

Consistency Ratio = 97.84

Sample Deviation = 13.

Arithmetic Mean Corrected Dip = 24

Table 2.2 (contd)

West Rand Group Palaeocurrent Direction Analyses-Heidelberg area

TR17 Jeppestown -1STQTZ

Locality Number	Azimuth Bedding	Dip Bedding	Azimuth cross-bedding	Dip cross-bedding	Corrected Azimuth	Corrected Dip
1	260.000	29.000	232.000	40.000	192.505	19.064
2	260.000	29.000	235.000	41.000	199.077	18.495
3	260.000	29.000	234.000	32.000	171.340	13.435
4	260.000	29.000	235.000	42.000	201.035	19.269
5	260.000	29.000	229.000	35.000	176.352	17.291
6	260.000	29.000	248.000	43.000	228.228	15.619
7	260.000	29.000	225.000	30.000	157.871	17.057
8	260.000	29.000	235.000	40.000	196.958	17.743
9	260.000	29.000	240.000	44.000	213.086	18.982
10	260.000	29.000	218.000	44.000	182.470	28.426
11	260.000	29.000	212.000	42.000	173.606	29.883
12	260.000	29.000	226.000	32.000	164.814	17.309
13	260.000	29.000	218.000	35.000	166.375	22.616
14	260.000	29.000	218.000	43.000	181.004	27.702
15	260.000	29.000	231.000	46.000	201.478	24.135

Vector Mean Azimuth = 187.
Vectorial Magnitude = 14.19
Consistency Ratio = 94.61
Arithmetic Mean Corrected Dip = 20

Corrected by unfolding fold axis(306/14)-location (B) Figure I.6

TR 17. Jeppestown -1STQTZ

Locality Number	Azimuth Bedding	Dip Bedding	Azimuth cross-bedding	Dip cross-bedding	Corrected Azimuth	Corrected Dip
1	.000	.000	202.000	20.000	201.980	20.000
2	.000	.000	206.000	15.000	205.980	15.000
3	.000	.000	184.000	10.000	183.980	10.000
4	.000	.000	116.000	18.000	215.980	18.000
5	.000	.000	185.000	15.000	184.980	15.000
6	.000	.000	242.000	15.000	241.980	15.000
7	.000	.000	161.000	14.000	160.980	14.000
8	.000	.000	213.000	15.000	212.980	15.000
9	.000	.000	226.000	18.000	225.980	18.000
10	.000	.000	190.000	25.000	189.980	25.000
11	.000	.000	178.000	25.000	177.980	25.000
12	.000	.000	170.000	15.000	169.980	15.000
13	.000	.000	173.000	19.000	172.980	19.000
14	.000	.000	184.000	25.000	183.980	25.000
15	.000	.000	206.000	20.000	205.980	20.000

Vector Mean Azimuth = 195.
Vectorial Magnitude = 13.94
Consistency Ratio = 92.96
Arithmetic Mean Corrected Dip = 17.

data. The similarity between the corrected and uncorrected versions of the vector mean azimuth, vectoral magnitude and consistency ratio in both the corrected and uncorrected versions is interpreted as indicating that the westerly-north-westerly crossbed azimuth dips in subareas 1 and 3 were not affected by the folding in subarea 2.

Further evidence supporting this conclusion comes from the 917 crossbeds measured in subareas 1 and 3. The arithmetic mean corrected dip of these crossbeds showed no systematic variation and was 10° below the generally accepted maximum original angle of repose (35°) of foresets in subaqueous sands. This contrasts with the findings of Pettijohn (1957) and Ramsay (1961) who found that in the limbs of folded rocks foreset beds are generally inclined at much higher (40°) or lower (15°) angles to the bedding surface. The only localities where the arithmetic mean dip exceeded or was near to the critical angle of 35° were those in the Government Subgroup sediments adjacent to the shear fault - ft. 1. In this case out of the total number of 55 readings the corrected dip was 33° with one locality having an average foreset dip of 38° .

The change in attitude between subareas 1 and 3 is therefore due to vertical tectonics related to faulting and not the result of a macro-fold. As a consequence no stereographic fold corrections need to be performed on palaeocurrent directions in subareas 1 and 3.

STRATIGRAPHY

3.1 DEFINITION

It has been long accepted that the Central Rand area (centred around Johannesburg and extending from Boksburg in the east to about twenty kilometres west of Krugersdorp in the west) is the type area of the West Rand Group. Here Mellor's (1911, 1917) stratigraphic classification was based on lithology only, with the boundaries between series and stages taken at the top or bottom of marker horizons. No consideration was given to unconformities, disconformities, depositional cycles and other tectonic and sedimentological features. Furthermore, as Mellor's breakdown was used for correlation by Rogers (1922) in the Heidelberg area and by Nel (1927) in the Vredefort area it was assumed that there exists no large facies variation between the different areas.

An attempt made to reclassify the West Rand Group stratigraphic column in the Klerksdorp area by Collender (1960) was not readily accepted. Pretorius (1965), noting that the West Rand Group sediments at Vredefort and in the Balfour - Greylingstad areas might have been deposited on the opposite edge of the Witwatersrand basin to those laid down in the Welkom, Klerksdorp, West Wits, Central Rand, East Rand, Delmas and Heidelberg areas, questions the concept of a type area. Should a type area be regarded as one containing rocks belonging to a proximal facies (e.g. Klerksdorp), or one with distal facies rocks (e.g. South Rand)? Is an area on the inflow side of the depository (North-west edge) more "typical" than an area on the opposite side? Pretorius (1965) further stipulates that "before any consideration can be given to possible revision on the stratigraphic classification of this Division a study will have to be undertaken of facies changes". As no substantial work of this kind has been done, the lithostratigraphic column (Fig. 1.3) presented by Winter (1978) and adopted by the writer serves only as an illustration of the revised stratigraphic nomenclature since Mellor's (1911, 1917) papers. The lithostratigraphic column is a useful framework and may be regarded as one which will be consistently revised as more sedimentological information (especially facies

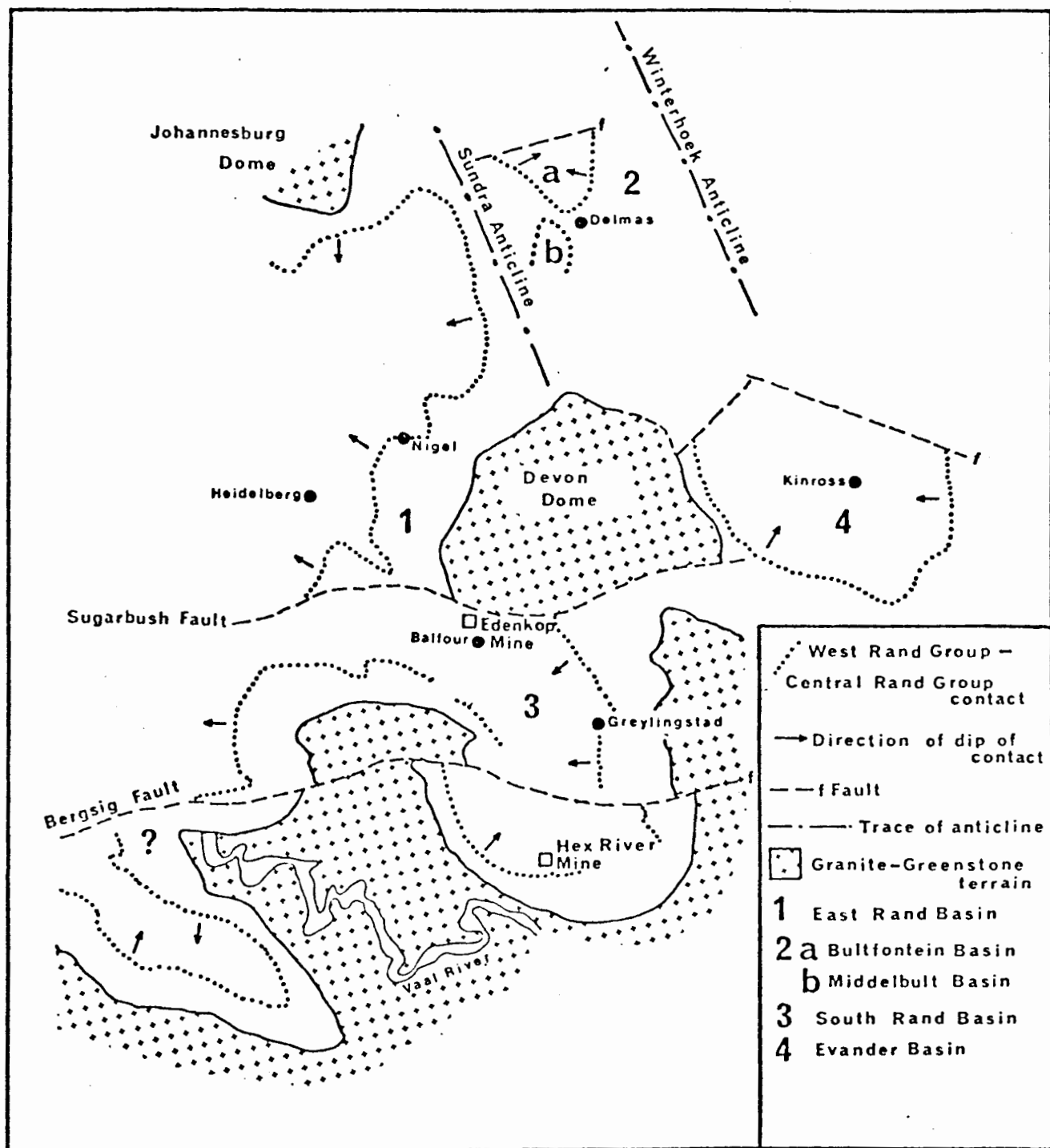


FIGURE 3.1 Simplified map showing the basin geometry of the Heidelberg-Delmas-Balfour area. The Sugarbush fault, Sundry anticline and Devon Dome divides the area into four parts:-
 1) East Rand Basin 2) Delmas area 3) South Rand

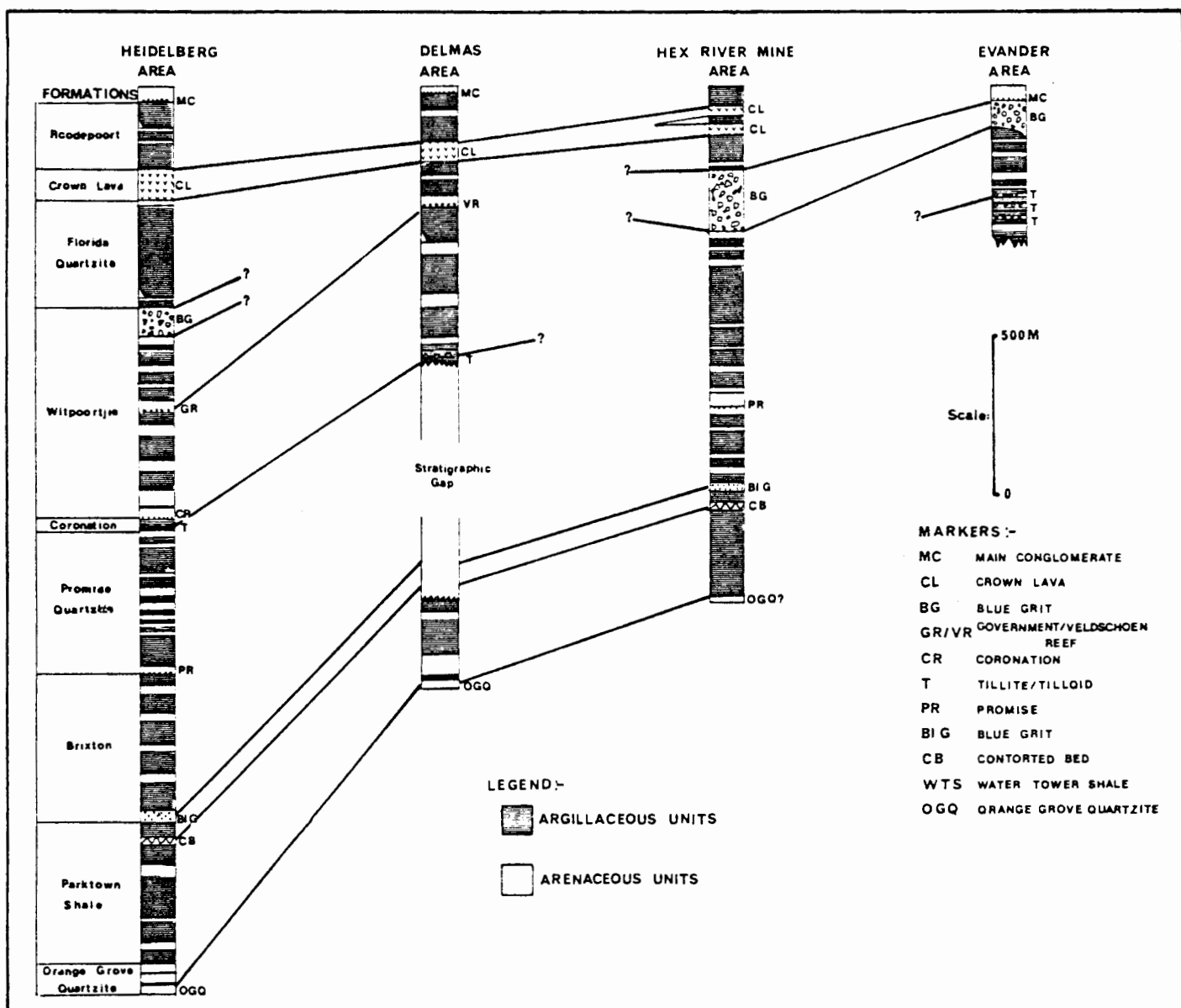


FIGURE 3.2 Comparative West Rand Group stratigraphy of the Heidelberg-Delmas-Balfour area (modified after Jansen *et al*, 1972; Button, 1970)

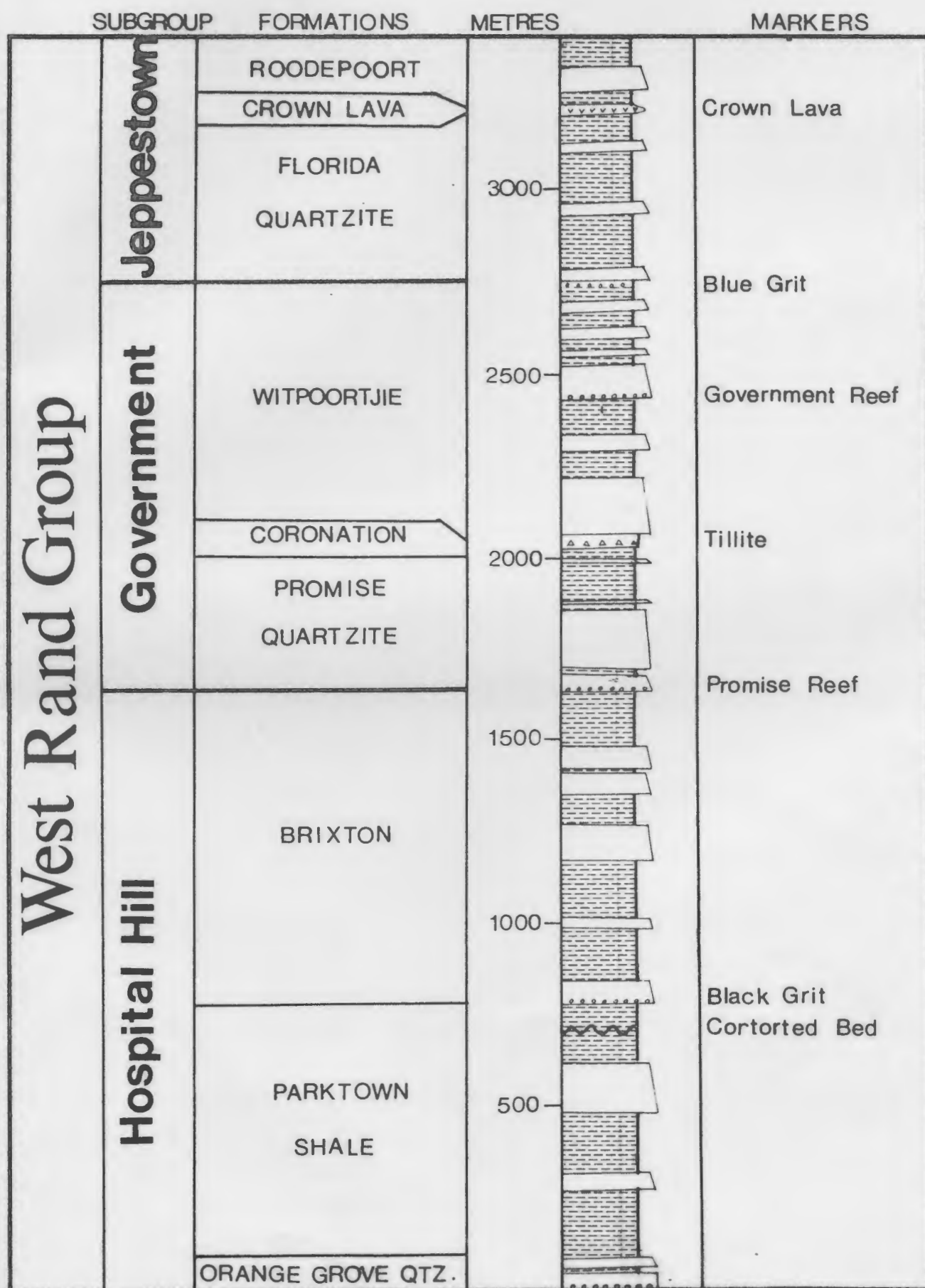


FIGURE 3.3

The composite stratigraphic column of the West Rand Group in the Heidelberg-Nigel-Balfour area

ses (and hence environments) at the time of deposition (Walther's Law, 1893) the main emphasis in describing the stratigraphy of the West Rand Group will be in the vertical distribution of sedimentary structures and paleocurrents present in the different lithologies.

Several examples of the different types of sedimentary structures observed in the study area are given in Plate 3.0. In the field subdivision of the arenaceous units was performed by meticulously measuring each sedimentary structure (thickness of individual plane beds, tabular crossbeds, trough crossbeds etc.) in the better exposed areas. In the laboratory these detailed profiles were then subdivided into constituent facies on the basis of the most frequently occurring sedimentary structures. In this way composite generalised stratigraphic sections were constructed for each formation. As many of the facies defined in the field have ambiguous environmental interpretations when treated individually, the writers final conclusions on the formation's environment of deposition is based upon the lithology, paleocurrent dispersal pattern and finally the communal association of the different facies.

3.2 PETROLOGY OF SANDSTONES

In the Klerksdorp area texturally and mineralogically supermature ortho-quartzite in the Hospital Hill Subgroup at the base of the West Rand Group contrast with immature subgreywackes and feldspathic quartzites in the overlying stratigraphic units (Fuller, 1958). According to Fuller (1958), "gross features of Witwatersrand rocks are maintained over considerable distances, so that discussion of the petrology of relatively few specimens might lead to a better understanding of the system as a whole". Although this is also the case in the Central Rand (Eriksson et al, in press), in the study area texturally diverse sandstones intertongue or overlies one another within individual members and it was clear that a more comprehensive representative sampling scheme was needed.

Over 240 samples were collected, halved and macroscopically described in the laboratory. From these approximately 40 thin sections from throughout the West Rand Group were examined in detail and 33 representative thin sections selected for grain size and modal analysis.

3.2.1 Textures

P L A T E 3.0

- a. Small trough crossbed (Orange Grove Quartzite, Uitkyk).
- b. Large tabular crossbed (Promise Foramtion, Blinkpoort).
- c. Multiple sets of trough crossbeds overlying sets of tabular crossbeds (Promise Formation, Blinkpoort).
- d. Multiple sets of tabular crossbeds (Brixton Formation, Blinkpoort).
- e. Convolutd large tabular crossbeds (Promise Formation, Groenfontein).
- f. Medium scale low angle cross-stratification overlying medium scale tabular crossbeds (Witpoortjie Formation, Groenfontein).
- g. Medium scale tabular crossbeds underlying large tabular crossbeds (base of Promise Formation, Blinkpoort).

Meaningful textural (fabric, grain size, grain shape) analysis of thin sections is a tedious and laborious operation especially when compared to the methods (settling tube, sieves) used in the analysis in present day environments (e.g. Flemming, 1977). According to Selley (1973) "statistical textural studies of ancient sediments have largely proved an unsatisfactory method of environmental diagnosis". The reason for this is the problem of granulometric analysis of sedimentary rocks and because the correlation of grain size and sorting to energy level may depend only on the nature of source material added. However, as individual sandstones derived from the same source within the West Rand Group consist of texturally dissimilar sands a comparison can be made between well sorted mature sediments and poorly sorted immature sediments in terms of high and low energy environments respectively.

Table 3.1 summarises the textures of the thin sectioned sandstones in the West Rand Group.

The sorting and maturity of the sandstones has been expressed in terms of Folk's (1968a) classification. Estimates of roundness were made on the clastic quartz grains with the use of the Amstrat grain shape comparator, which is similar to the one devised by Powers (1953). The grain size of the well sorted sandstones was determined with the use of an Amstrat grain size comparator. The mean grain size diameter of the poorly sorted sandstones was determined by measuring over 20 grain diameters chosen to be approximately representative of the mean. If the sandstones were unimodally distributed with a consistent shape the mean diameter was corrected to sieve equivalents (by the method of Adams, 1977).

About sixty five per cent of the thin sections examined have an homogeneous fabric; three samples (8/9, 6/4 and 15/5) show grading on a microscopic scale, while some specimens (e.g. 4/20, 8/9, 13/071) are layered with well sorted coarser grained sands being separated by subrounded to subangular sands and silts.

None of the samples had strongly developed preferred grain orientation. The layered specimens (e.g. 8/9, Plate 3.1A) have a slightly discernible orientation with the long axis of the grains being paral-

P L A T E 3.1

- A. Layered sample (8/9) with a slightly discernible orientation with long axis of grains parallel to banding.
- B. Thin section of a 'sago' textured rock sample (01/09). Note the very good rounding of the larger grains.
- C. Moderate sorted bimodal grain sized(2.2 ϕ and 0.5 ϕ) sandstones of the Orange Grove Quartzites Formation.
- D. Well sorted unimodal fine grained sandstone (3.12 ϕ with sericite and haematite layers (Promise Formation).
- E. Angular floating shale clasts surrounded by well rounded, bimodally sized quartz grains (Brixton Formation).
- F. Moderately to poorly sorted medium grained sandstones (Witpoortjie Formation).
- G. Co-existence of well rounded cherts and subangular quartz grain-(unit corresponds to Speckled Bed on Central Rand).
- H. Texture of polymodal, silty claystone of the Promise Reef.

Table 3.1

<u>Textures of the West Rand Group</u>				
SAMPLE	COLOUR	GRAIN SIZE (MEAN)	SORTING	MATURITY
<u>Hospital Hill Subgroup</u>				
01/04	10YR 8/2	1.75 ϕ	ms	Mature
01/05	10R 5/4	1.83 ϕ	ms	Submature
02/05	N7	0.84 ϕ	ws	Mature
BB/Gr	5YR 6/1	0.51 ϕ	vps	Submature
03/06	5YR 7/2	1.2 ϕ	vws	Supermature
04/02	10R 6/2	-2 ϕ and 0.5 ϕ	ms	Textural inversion
04/20	5YR 7/2	1.8 ϕ	ps	Submature
04/21	10R 6/2	2.55 ϕ and -0.5 ϕ	ms	Textural inversion
04/23A	5YR 6/4	2.8 ϕ and -0.23 ϕ	ms	Textural inversion
04/23B	10R 6/2	3.34 ϕ and -0.25 ϕ	ms	Textural inversion
04/23C	10R 6/2	3.55 ϕ and 0.0 ϕ	ms	Textural inversion
06/04	10R 6/2	1.17 ϕ	vws	Mature
10/03	10R 7/4	1.3 ϕ	ps	Submature
11/07	5YR 6/1	2 ϕ and 0.25 ϕ	ms	Supermature
12/04	N6	2.2 ϕ and 0.5 ϕ	ms	Textural inversion
18/16	5YR 7/2	1.3 ϕ	vps	Submature
18/22	10R 6/2	3.5 ϕ and -0.25 ϕ	ms	Mature
18/27	5YR 7/2	3.4 ϕ and 1.09 ϕ	ms	Mature
<u>Government Subgroup</u>				
07/03	10R 6/2	1.4 ϕ	ms	Mature
08/08	5YR 8/1	1.34 ϕ	ws	Mature
08/09	5GY 8/1	1.1 ϕ and 2.85 ϕ	lam	Textural inversion
13/03B	5YR 7/2	2.1 ϕ	ps	Submature
13/05	5YR 8/1	2.3 ϕ	recrystallised	
13/071	5P 4/2	3.12 ϕ	lam	Immature
13/08	10YR 8/2	0.0 ϕ and 1.75 ϕ	lam	Supermature
14/04	10YR 5/4	2.54 ϕ	ps	Immature
15/03	N9	1.06 ϕ	ms	Mature
15/05	5R 6/2	1.4 ϕ	ws	Mature
<u>Jeppestown Subgroup</u>				
26N		1.97 ϕ and 0.51 ϕ	ms	Mature

lel to the banding. The complete lack of strong preferred grain orientation is due to the high sphericity of the detrital grains. Many of the samples in the Hospital Hill Subgroup are characterised by supermature rounding (Plate 3.1B) (e.g. 2/5, 3/4, 4/21, 4/23, 12/4) while the grains in the Government Subgroup are generally more subrounded to subangular (e.g. 13/11, 14/4, 13/071) although supermature rounding (e.g. 13/08, 07/07) is still occasionally present.

Kuenen (1960) summarises a series of papers describing the experimental abrasion of sand grains by various processes. His data prove that wind action is a more effective rounding agent than running water. This is supported by the fact that dune sands are often well rounded (Greensmith, 1978). According to Klein (1977) supermature rounding is rather unique and owes its origin to long distances of grain transport on a tidal sand body. This rounding may be emphasised if coastal aeolian dunes are deposited in a tidal environment.

Middleton and Davis (1979), question Klein (1977), and note that intertidal sands within the Bay of Fundy are minerologically immature and have a mean roundness in the subangular category. They conclude, as did Keunen (1960), that tidal movement of sand appears to be more effective in producing new surface textures and in rounding grains than most fluvial transport, but less effective than high-energy wave action on beaches or wind action.

The "sago" textured bimodal grain sized samples of the Hospital Hill Subgroup (4/21, 4/23, 11/07, 12/04, 18/27) and Government Subgroup (13/08) *had coarser particles which were often more distinctly rounded* than the finer angular textured particles of the matrix. The difference in texture in a compacted bimodal sediment is thought to have originated in two ways:

- a) the larger fragments, propelled by rolling and saltation processes, suffer more collisions and consequently greater abrasion than the smaller particles which are partially suspended by water currents (Gilbert, 1914),
- b) as a result of post depositional changes due to pressure solution (Renton et al, 1969; Potter, 1977).

The presence of some subrounded smaller quartz grains (e.g. 01/09 Plate 3.1B) suggests to the writer that the difference in texture between the coarse and fine ingredients of the "sago" textured units in the study area, is likely to be exaggerated by pressure solution. Furthermore, although the "sago" textured sandstones are bimodal in their sand size distribution, the larger well rounded grains are always volumetrically dominant (up to 95 per cent of the whole rock). This contrasts with fluviially derived bimodal sediments where the fine grained constituents are greater in quantity than the coarser, rolled fragments (Udden, 1914; Potter, 1977). The origin of the bimodal "sago" texture (Plate 3.1B) may be due to the in situ breakdown of large rounded rock fragments.

The bimodal grain size of the Orange Grove Quartzite Formation (Plate 3.1C) is similar in texture to the specimen described by Fuller (1958). These sandstones are only moderately sorted overall and are composed of two distinct sand sized modes (2.2 ϕ and 0.5 ϕ) which are themselves well sorted and rounded. This form of textural inversion could have been caused by wind deflation (Folk, 1968b), beach fractionation (Fuller, 1962; McCave, 1978) or due to different source areas contributing different modal classes (Blatt, 1967) with both modes being redeposited together (Klein, 1977). Yet another form of grain size bimodality is illustrated in Plate 3.1A. Here a distinct lamina composed of moderately sorted and rounded large particles (1.1 ϕ) rests on a claystone drape and is overlain by particles that are subangular and up to seven times smaller. This thin section is the internal structure of a mud draped foreset and the unusual texture which has facets of both high energy (well sorted large particles) and low energy (the smaller angular particles) conditions is interpreted as being formed in an environment where alternating bedload transport and suspension settling processes prevail.

Other textures common to the sandstone of the West Rand Group includes:-

- a) Well sorted unimodal fine grained sand (3.12 ϕ), which have subangular to subrounded grains of medium sphericity. Sericite and secondary haematite are sometimes arranged in

definite layers (Plate 3.1D).

- b) Moderately to poorly sorted medium grained (1.83 ϕ) sandstones whose quartz grains usually show authigenic enlargement and intergrowth. Long contacts and triple junctions indicate some recrystallisation and interpenetration but it is evident that the grains were originally spherical and subrounded as can be seen on margins which have not been modified. (Plate 3.1F).

Textures that are rare in the West Rand Group but nevertheless interesting include:-

- a) Angular floating shale clasts that are surrounded by well rounded and spherical bimodally sized quartz grains (Plate 3.1E). According to Conybeare and Crook (1968) such a texture originates from the scouring action of sediment-laden water tearing up penecontemporaneous cohesive sediment and incorporating fragments of it in a subsequent deposit. This process of deposition is common in alluvial, near-shore marine and turbidity current deposits. Sedimentary structures and other criteria (which will be described in the next section) suggest a near-shore marine environment in this instance.
- b) A sample comprising a mosaic of subangular quartz grains (0.84 ϕ) formed by authigenic enlargement of clastic quartz particles and smaller spherical and super-rounded lithic fragments (mostly chert) which are often coated with haematite (Plate 3.1G). In all the other samples containing chert and quartz, including the two conglomerates (Fig. 3.4) chert is always larger and more angular than the adjacent quartz grains.

The groundmass of all three diamictitic markers in the West Rand Group (Promise Reef, Tillite and Blue Grit) have similar textures to that shown on Plate 3.1H. The polymodal, silty claystones (using the classification of Picard, 1971) consist of subangular to rounded, fine to coarse sized quartz grains set in a matrix of very fine sand size, silt size quartz grains and clays (most chlorite). Such rock types can originate from many processes (Frakes, 1978). These

include earthflows, mudflows, solifluction, subaqueous slumping and sliding and fluviatile activity.

In summary, the variable textures in the arenaceous horizons of the West Rand Group suggests that considerable winnowing and re-deposition of the sediments has taken place. This is manifested in the roundness and high sphericity of the well sorted grains in the "sago" textured arenites (Plate 3.1B), the bimodal grain size (Plate 3.1C) and the co-existence of well rounded cherts and sub-angular quartz grains (Plate 3.1G). Hydraulic processes operating on the bimodally distributed grains may generate laminated sand sized textures (Plate 3.1A). It has been suggested that most of these textures are diagnostic of marginal marine environments.

3.2.2 Composition

Table 3.2 summarises the compositional analyses for the sandstones of the West Rand Group. The classification used is that of Folk (1968a).

All the sandstones and conglomeratic rock slabs were stained for K-feldspar by the methods of Hutchinson (1974) and Nold and Erickson (1967). Reference control samples with known K-Feldspar were stained before each batch of 10 thin sections to check for possible dilution of saturated sodium cobaltinitrate and the strength of hydrofluoric acid. Minor K-feldspar yellow stains for all the thin sections and several rock slabs of the West Rand Group were observed.

Modal analysis of conglomeratic rock slabs was done by placing a sheet of transparent graph paper over the polished surface and the points of intersection of the lines on the graph paper counted visually for whichever feature they overlay, quartz, banded chert, unbanded chert, shale fragment, groundmass, etc. The modal analysis of several thin sections was performed using a polarising microscope with a Leitz manual point-counter stage unit attached to its stage. A visual assessment of the relative proportions of mineral grains was done on the well sorted orthoquartzites.

Two of the three conglomerates in the study area, the Government

Table 3.2

<u>Sandstone composition of the West Rand Group</u>				
SAMPLE	TOTAL QUARTZ %	ROCK FRAGMENTS %	MATRIX %	CLASSIFICATION (FOLK 1968a)
	<u>Hospital Hill Subgroup</u>			
01/05	95	3	2	Quartzarenite
BB/GR	93	5	2	Sublitharenite
03/06	95	2	1	Quartzarenite
04/02	45	54	1	Litharenite
04/11	70	26	4	Litharenite
04/20	87	8	4	Sublitharenite
04/21	89	5	6	Sublitharenite
04/23A	72	27	1	Litharenite
04/23B	72	20	7	Litharenite
04/23C	73	5	13	Sublitharenite
06/04	96	0	4	Quartzarenite
10/03	99	0	1	Quartzarenite
11/07	96	4	0	Quartzarenite
12/04	75	15	10	Litharenite
18/16	90	5	1	Sublitharenite
18/22	75	20	3	Sublitharenite
18/27	85	15	1	Sublitharenite
	<u>Government Subgroup</u>			
07/03	82	15	3	Sublitharenite
08/08	93	6	1	Sublitharenite
08/09	80	6	14	Sublitharenite
13/03B	95	5	1	Quartzarenite
13/05	91	2	7	Sublitharenite
13/071	56	14	30	Litharenite
13/08	92	5	3	Sublitharenite
15/03	90	6	4	Sublitharenite
15/05	83	15	2	Sublitharenite
15/01	95	4	1	Quartzarenite
	<u>Jeppestown Subgroup</u>			
26N	69	6	25	Litharenite

Reef and Black Grit are matrix supported, polymodal polymictic conglomerates consisting of pebbles of chert (black, white and unbanded), rock fragments and quartz. The relative proportions of these pebbles is shown on Fig. 3.4. The basal oligomictic conglomerate of the Orange Quartzite formation is clast and matrix supported and comprised of well rounded to rounded pebbles of quartz.

Folk (1968a) classified quartz into six types based on "strained shadows" (extinction). Following this method, the most common type in the study area are the single quartz grains which have a slightly undulose extinction followed by the highly "strained" type. In some samples (e.g. BBGr, 4/11, 6/4) the unstrained type is predominant. Composite grains make up about 15% of the quartz population in some samples (e.g. 2/5, 4/4, 4/23, 8/9, 9/10) while in others (e.g. 3/6, 4/2, 4/11) a few polycrystalline grains with sutured boundaries have overgrowths in optical continuity with detrital grains. No attempt was made to statistically quantify the relative proportion of each quartz type because in mature sandstones it has been shown that the ratio of non-undulation quartz to total quartz is not a reliable provenance indicator. Blatt (1967) showed that strained quartz grains are less stable than unstrained ones; hence an excess of unstrained quartz may be indicative of several episodes of recycling rather than provenance. Nevertheless it is interesting to note that the paleosol of the granite underlying the West Rand Group consists of 60 per cent quartz with strongly undulating extinction with the remaining 40 per cent made up of sericite (highly altered orthoclase and minor plagioclase).

Chert is the most common rock fragment. In the Black Grit conglomerate it consists of 75 per cent of the total pebble population while in the Government Reef it comprises 32 per cent. The presence of these angular cherts as well as the well rounded sand-sized cherts in the arenites is always diagnostic of an older sedimentary source (Folk, 1968a). Other sedimentary rock fragments include sandstone arenites (e.g. 3/6, 4/2, 8/8, 13/3, 13/8), litharenites (e.g. 12/4, 15/5, 18/22) and phyllarenites (e.g. 12/4, 13/3, 18/27).

The matrix of the sandstones consist primarily of sericite. Minor quartz and chlorite were also identified as matrix material (e.g.

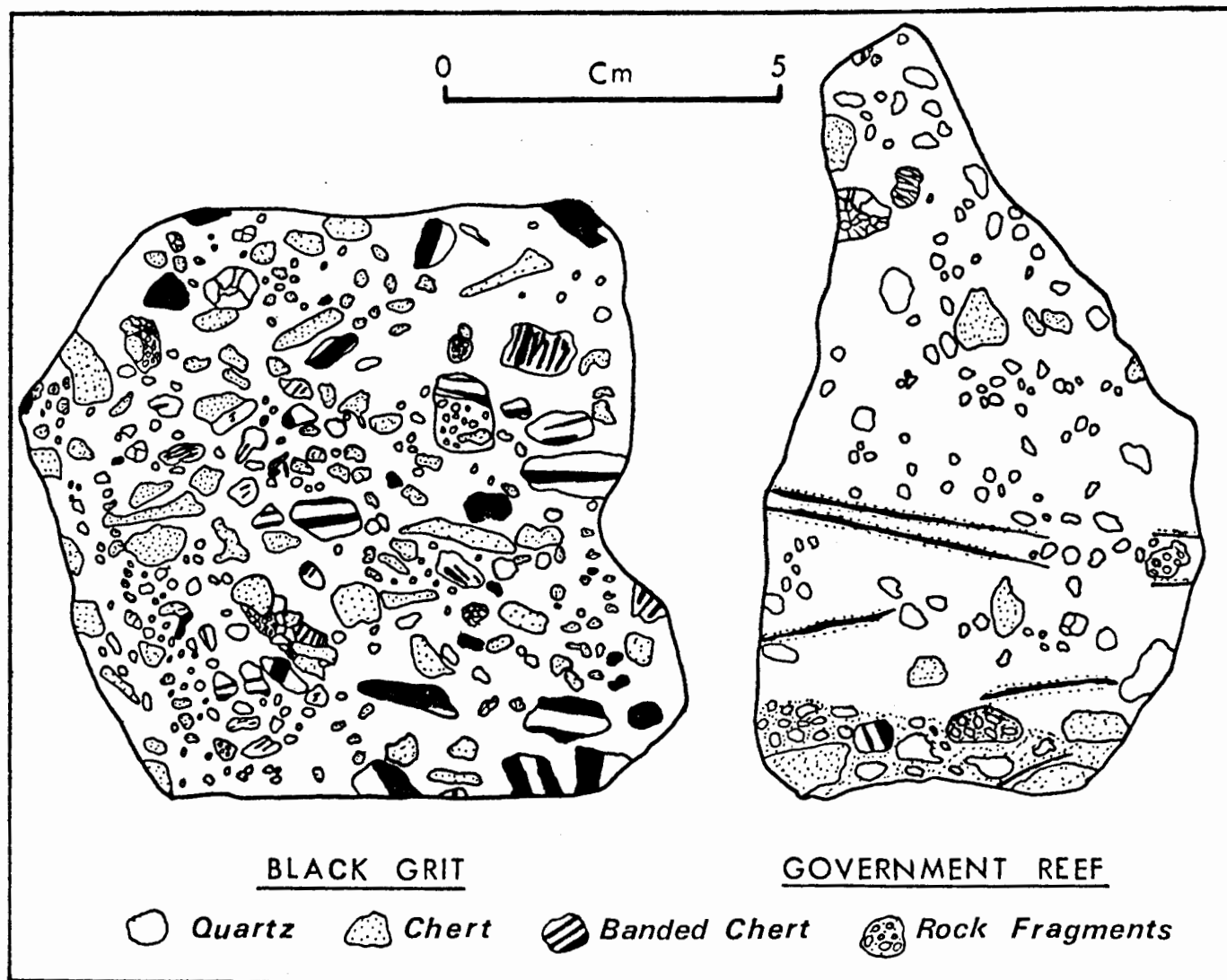


FIGURE 3.4 The relative proportions of clasts within the Balck Grit and Government Reef conglomerates. Black Grit's matrix totals 53.1% with white chert (20.3%), banded chert (11.5%), quartz (7.7%), rock fragments (4.4%) and black chert (3%) constituting the pebble fraction. The Government Reef consists of matrix (67.8%), quartz (18.2%), white chert (9.6%), rock fragments (3.4%) and black chert (1%).

13/11, 7/11). Haematite and occasionally limonite are the major replacement minerals. Ilmenite and magnetite, which are sometimes altered to haematite, are often rounded (e.g. 4/23, 7/3). Rounded grains of zircon with diameters of about 0,1 mm form less than 1 per cent of the total rock composition in five thin sections (4/1, 8/8, 8/9, 15/3, 15/5).

In summary, the extremely high quartz content, absence of feldspar, the presence of sedimentary rock fragments and ultra-stable heavy minerals and the texture of the sandstone suggests that repeated sedimentary redeposition of sediments derived from an older sedimentary environment has taken place. The presence of "strained" quartz and polycrystalline quartz suggests that, at least a portion of the original primary source was a plutonic igneous or metamorphic province.

3.3 HOSPITAL HILL SUBGROUP

This Subgroup has a measured thickness of 1620 m. Although there are more arenaceous units in this Subgroup in the Heidelberg - Balfour - Delmas area than on the Central Rand, the proportion of quartzite to shale is almost the same (38 per cent of the total thickness on the Central Rand and 36 per cent near Heidelberg). The Orange Grove Quartzite, Parktown Shale and Brixton Formations are well defined by the lateral continuity of the Orange Grove, Black Grit and Promise Reef markers.

3.3.1 Orange Grove Quartzite Formation

Definition

The Orange Grove Quartzite Formation is well developed between the farms Uitkyk and Rietfontein and poorly developed south of the Sugarbush River. It rests with marked unconformity on a granite paleosol (farm Uitkyk) or an aluminous schist (farm Kuilfontein).

Out of a total of five measured sections the two profiles most representative of the formation are those on the Sugarbush River (T1) and alongside the Nigel-Balfour Road (T10). These two profiles will be described in detail and because of the lateral homogeneity in thickness and lithology of the formation they may be considered

as type sections of the Orange Grove Formation in the Heidelberg-Nigel-Balfour triangle.

Lithology

The average thickness of the formation is 80 m (range 70-115 m). It is split into three sandstone units by two shale bands. The basal arenite unit (45 m) is overlain by a persistent shale horizon (7 m) which is marked by a strip of grass covered ground between the white arenites. The second shale band is only locally developed about 65 m above the base of the formation.

The first sandstone unit has a sharp base with discontinuous mature conglomerates (up to 0,5 m thick) containing well rounded and well sorted quartz pebbles (up to 2 cm in diameter) developed as lags in well defined trough crossbeds. The matrix of the conglomerate consists wholly of well sorted quartz sands. On the farm Kuilfontein, three conglomeratic horizons (0,4 and 8 cm above the base) occur at the bottom of fining upward cycles. About 5 m above the last impersistent conglomeratic layer, medium to fine moderately sorted white sands which weather to a very pale orange colour (10 YR 8/2) make up the next 30 m of the formation. Some coarse grained lags follow and the top of the unit is marked by very fine sand and silts comprising the base of the first shale unit.

The main shale horizon of the Orange Grove Quartzite Formation is often banded with lighter and darker grey bands and weathers to a greyish-pink colour (5 YR 7/2). It is highly cleaved and in places complex arrays of quartz veins are present. The shale displays no diagnostic primary sedimentary structures, although intercalated between the shales are rare well-sorted lensoid sand bodies up to 20 cm thick which have finely laminated "hummocky" bedding. These sand bodies are fine-grained (3.5 - 3.0Ø) and are pale red purple (5 RP 6/2) weathering to a greyish orange (10 YR 7/4).

Overlying the shale horizon is a loosely packed, 0,5-2 m sandstone unit which is coarse grained and often graded (e.g. in the Nigel-Balfour Road quarry, there are four fining upward cycle 8,43, 10 and 9 cm thick). This facies is succeeded by poorly sorted immature coarse grained (mean 1.0 - 0.5Ø) haematite stained arenites

ORANGE GROVE QUARTZITE FORMATION

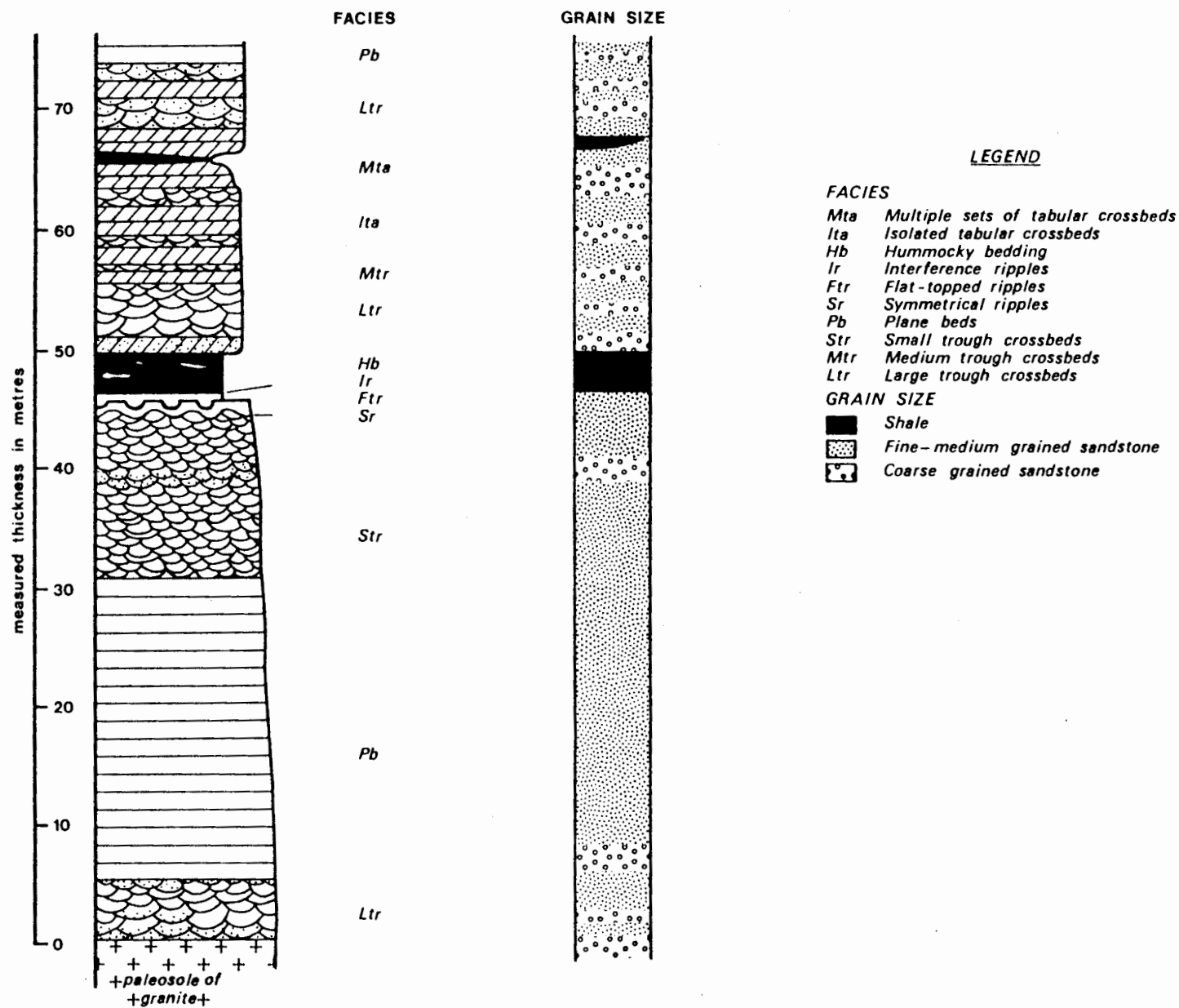


FIGURE 3.5 Stratigraphic section for the Orange Grove Quartzite Formation

P L A T E 3.2

- a. Plane-bedded succession near the base of the Orange Grove Quartzite Formation.
- b. Interference ripples developed on top of some of the plane-beds shown on Plate 3.2a.
- c. Wind obstacle marks developed on plane-beds. The compass is pointing towards the north. In this case wind blowing in a south-easterly direction produced the 'tails' behind the obstacles.

PLATE 3.2



(coloured pale red 10R 6/2).

The remaining 10 to 15 m of the Formation is similar in texture and lithology to the first 5 m. South of the Sugarbush River two discontinuous oligomictic conglomerates, a metre apart occur in ill defined troughs 58 m above the base. The conglomerates are poorly to moderately packed and in places are mineralised. Medium grained (mean 1.3Ø) moderately well sorted quartzarenites overlies the conglomerates. The upper contact of the formation is sharp.

Sedimentary facies

The Orange Grove Quartzite Formation has been divided into 10 facies on the basis of its sedimentary structures. Facies were only defined formally after the sections were measured on the basis of the most frequently occurring sedimentary structure. Unlike the other Formations, the variability associated with each proposed facies is very small. Of the ten facies identified only the small, medium and large trough crossbedded facies are inter-gradational. Fig. 3.5 shows the vertical stacking of the different facies.

The thick trough crossbedded basal conglomeratic horizons are overlain by thinner trough crossbedded units. These are succeeded by 30 m of internally plane bedded and solitary low angled crossbedded arenites (Plate 3.2A). Asymmetrical ripple marks, runnel marks, primary current lineation, interference ripples (Plate 3.2B) and wind obstacle marks (Plate 3.2C) are present between the plane beds. The ripple marks are common features 10 to 15 m above the base of the formation while the runnel marks are generally best preserved 25 to 30 m above the conglomerate. The top 15 m of the first sandstone unit comprise trough crossbedded units (Pi-type, Allen, 1963) with some local coarse grained lags developed in the middle of this facies. At one locality (a quarry on the Nigel-Balfour Road) the contact between the first shale and sandstone unit has been excavated and reveals an excellent outcrop of flat-topped wave ripples (Plate 3.3A) with intervening ladder back ripples (Plate 3.3B), two types of interference ripples (Plate 3.3C and Plate 3.3D), mudcracks, possible late stage runoff erosion marks cutting into the lee side of flat topped ripples and washout structures.

P L A T E 3.3

- A. Excavated contact between first shale and sandstone horizon revealing outcrop of laterally persistent flat-topped wave ripples.
- B. Ladder back ripples developed between major wave ripples.
- C. and D - Two types of interference ripples. C are commonly termed 'tadpole' structures while D represents the typical type of interference pattern produced in sands and muds of tidal flats (Reineck and Singh, 1975).

PLATE 3.3

A



B

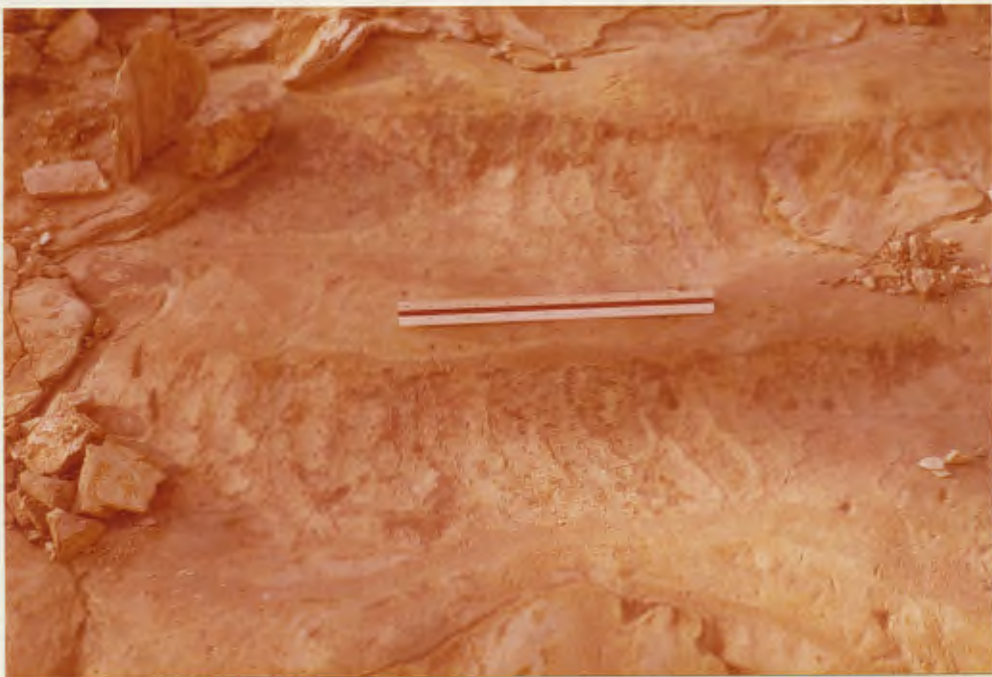


PLATE 3.3(contd.)

C



D



Using a one metre square grid a portion of this interface was mapped in detail and cross sections of the ripples measured. One of the four stations selected for detailed work shows the sinuous trend of the ripples (Fig. 3.6). Some of the crests terminate and are replaced by others and there are rare instances where well developed bifurcation of the crests occur. It was observed that symmetrical ripples with primary and secondary crests are overlain by flat-topped ripples and these in turn are overlain by interference ripples. The larger ripples have a length of between 30 and 60 cm and a mean of 48 cm while the intervening ladder-back ripples have a length of between 2 and 6 cm.

Reineck and Wunderlich (1968) and Tanner (1967) noted that the ripple index, RI (ratio of ripple length to ripple height), and the ripple symmetry index, RSI (ratio of length of horizontal projection of stoss side to length of horizontal projection of lee side), are the most important indices for distinguishing between current and wave produced ripples. The measured RI of larger ripples had a range of 5.19 to 10 and a mean of 7.7. This value falls in the region of overlap (i.e. between 4 and 15) of the two types of ripples. However, the mean RSI (1.64) measured is well inside the category of wave produced ripples. The RSI for the smaller-scaled ladder-back ripples is greater than 3 classifying them as current produced ripples. The average grain size of the symmetrical and flat-topped ripples is 0.75 ϕ while the intervening ladder-back ripples and overlying interference ripples are finer grained (less than 3.5 ϕ).

Overlying the main shale horizon is the loosely packed graded sandstone facies which is followed by large trough crossbedded units. An upward decrease in trough crossbedded thickness is apparent. Isolated tabular crossbeds with an average thickness of about 20 cm often truncate the troughed crossbedded facies. Multiple sets of smaller scaled tabular crossbeds are rare and are best observed on the farm Vrisgewaag (T11). The inconsistent second shale horizon is closely associated with this facies and often overlies it. Large coarse grained trough crossbedded units followed by massive structureless units are the facies developed at the top of the Formation on the farm Kuilfontein (T1).

Paleocurrent Dispersal Pattern

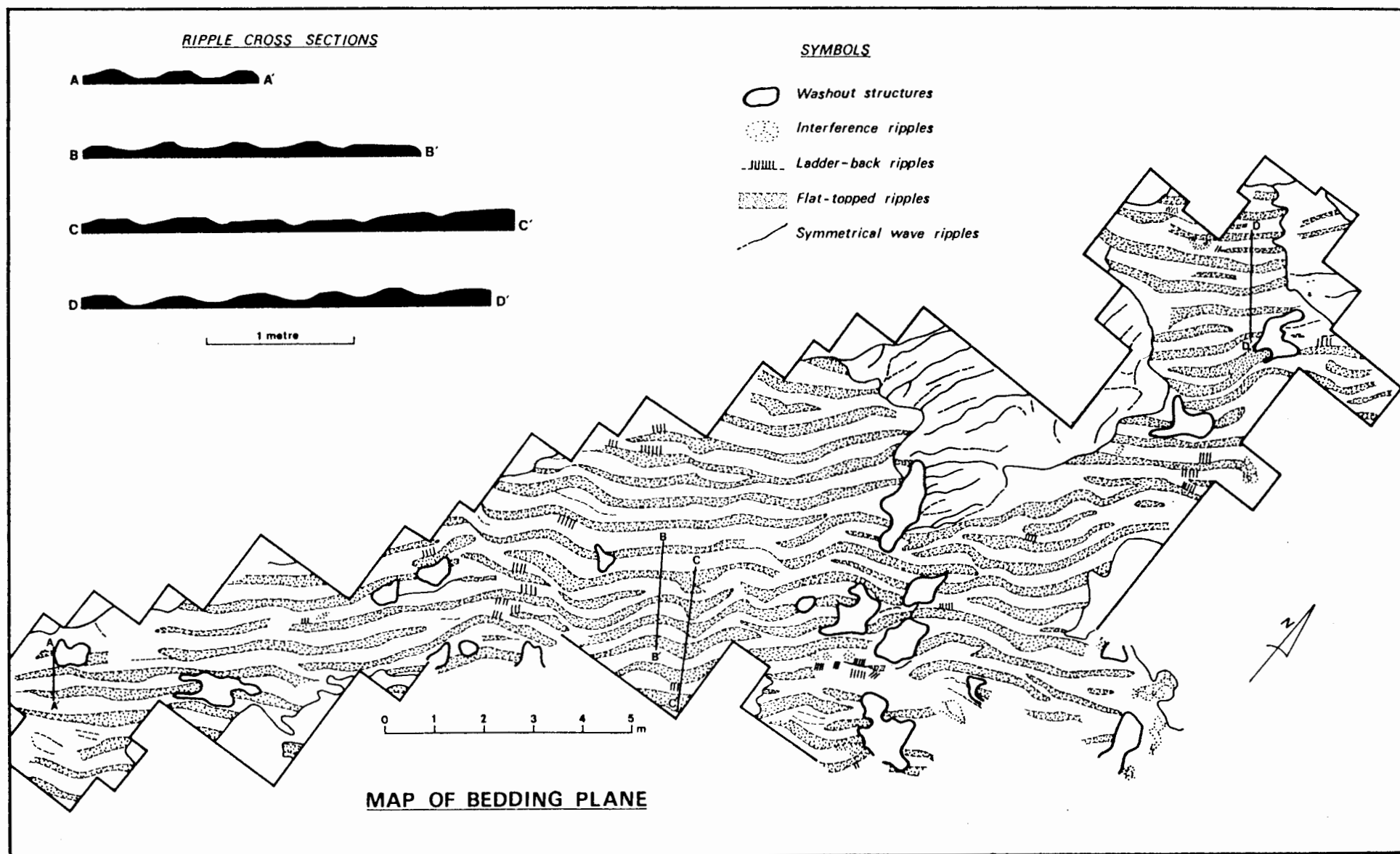


FIGURE 3.6 Sedimentary structures observed and mapped at the base of the first shale horizon of the Orange Grove Quartzite Formation

The Orange Grove Quartzite Formation shows a complex composite poly-modal paleocurrent pattern (Fig. 3.7). It would be an oversimplification to interpret the composite rose diagram of the Formation as being due to the relative interplay of waves, tidal and fluvial influences. Rather each sandstone unit with its respective facies should be considered individually. In this way the relative influence of each can be evaluated up the stratigraphic column. Ideally, paleocurrent measurement should be made using a grid design. However, the large dip and the fact that 40 per cent of the strike length is repeated by strike faulting makes this exercise futile. Therefore, the lateral change in paleocurrent direction of each facies which might have indicated either the geometry of a coastline or the presence of topographic paleohighs cannot be shown. The variations in crossbedding azimuths which reflect changes in the direction of current flow at different stratigraphic levels within the Formation are shown on Fig. 3.7.

The direction of the trough axis of the basal conglomerates is NW. This is the only unimodal current rose in the whole of the Orange Grove Quartzite Formation. The ripple marks on some of the overlying plane beds are quadrimodal while the primary current lineations show a good NW-SE direction. The wind direction obtained from the wind obstacle marks is consistently S-SE.

The trough crossbedded facies below the first shale horizon is trimodal north of the Sugarbush River but a strong N-NE mode develops south of it. The wave ripples near the Nigel-Balfour Road quarry have a sinuous north westerly trend. The orientation of the washout structures is N-NW. Overlying the shale horizon, the trough crossbedded arenite and both isolated and multiple sets of tabular crossbeds have a strong NE mode south of the quarry while the section measured at the quarry has a SW mode. No crossbed data are available from the overlying poorly developed structureless arenites near the Sugarbush River.

Excluding the impersistent trough crossbedded conglomerates, the consistency ratio always increases from a mean value of 38 for the arenites below the prominent shale to a value of 60 for the overlying feldspathic arenites. Likewise the vectoral magnitude increases from

Figure 1 consists of a stratigraphic column on the left and a 3x3 grid of circular diagrams on the right. The stratigraphic column shows measured thickness in metres (0 to 70) and various sedimentary patterns including ripple marks and pebbles. The grid on the right shows circular diagrams for three locations: Sugarbush River (T1), T10, T11, T12, T18, and Quarry. The diagrams illustrate the development of primary current lineations (l=8), ripple mark directions (r=23), and wind directions (w=7).

Legend:

- $l=8$ primary current lineation
- $r=23$ ripple mark direction
- $w=7$ wind direction

Locations: Sugarbush River (T1), T10, T11, T12, T18, Quarry

FIGURE 3.7 Paleocurrent direction analysis of the Orange Grove Quartzite Formation

4 to 8.

Environment of Deposition

Apart from the vertical stacking of facies shown in Fig. 3.5, which the writer will use in reconstructing the depositional environmental of the Orange Grove Quartzite Formation, two further points need to be considered. These are the lateral persistence of the facies, especially the facies developed below the first shale horizon, and the recognition of similar sequences in other major outcrop areas (e.g. Central Rand, Erickson et al; in press).

The thin sheets of oligomictic conglomerate at the base of the formation have been recorded in most of the other outcrop areas (Appendix 1) and probably occur over an area of more than 30 000 km². The development of basal conglomerates over such extensive areas are common in the Cambrian and, according to Bourgeois (1978), they are strictly of marginal origin marking periods of widespread transgressions of an advancing sea and are comparable to the well sorted gravels of many modern beaches. Kumar and Sanders (1974) suggested that many "blanket sands" in basal parts of transgressive sequences would be recognised as inlet filling sands and this is what Eriksson et al; (in press) proposed for the sequence developed below the first shale horizon of the Orange Grove Quartzite Formation in the Central Rand.

Parts of the sequence of sedimentary structures and lithologies described by Eriksson et al; are developed in the study area but certain facies are better developed than others (e.g. the plane bedded facies in the Central Rand reach thicknesses of up to 5 m while in the study area the average thickness is 25 m). Furthermore, in the Heidelberg area sedimentary structures indicative of intertidal sand bodies formed by the "late stage emergency runoff" (Klein, 1977) of water have been recognised (i.e. flat topped ripples, ladder back ripples, mud cracks).

According to Eriksson et al; the whole of the sequence developed below the first shale horizon is analogous to Holocene tidal inlet deposits. The conglomerates at the base they interpret as a tidal inlet channel floor lag gravel with the overlying upward decrease in

size /31

size of trough crossbeds being indicative of tidal inlet channels. The plane bedded facies resting on the channel deposits are interpreted as upper flow regime swash-generated deposits while a tentative paleoenvironmental interpretation for the overlying trough crossbedded facies is dune migration on a tidal delta fronting the inlet. The vertical superimposition of these facies resulted from the longshore migration of tidal inlets.

One of the problems in applying Eriksson's et al; tidal inlet model to the study area is the presence of such thick sequences of upper flow regime plane beds. The sedimentary structures (runnel marks, primary current lineations and wind obstacle marks) recognised in this facies are common features on the fore and backshore of beaches. Although the beach and associated dune facies constitute the most "visible" subenvironments of a barrier island today (the other subenvironments being back-barrier, tidal inlet and barrier "toe"), they would have very little chance of preservation, especially during a transgression (Kumar, 1978). The reason for this is that as the sea level rises (or land subsides) erosion takes place during submergence and the only facies having a high probability of escaping erosion are the inlets because they are generally deeper than the lagoonal facies on the landward side of the barrier and the shelf immediately seaward of the barrier (Kumar, 1978; Barwis and Makurath, 1978). Clearly a refinement of Eriksson's et al; (in press) model needs to be proposed which takes the following into account (a) the presence of a 25 m plane bedded beach facies, and, (b) the recognition of sedimentary structures diagnostic of intertidal flat sediments (Fig. 3.6).

The writer is of the opinion that the sequence from the conglomerate facies at the base to the top of the first shale horizon has subenvironments which are present in modern strand plain and tidal flat environments. However, as there is a complete gradation from high destructive deltas through strand plains to barrier islands it is impossible to distinguish between these three models on the basis of vertical sequence (Fisher and Brown, 1972).

The basal conglomerates and overlying trough crossbedded facies are interpreted as either platform beach (Clifton et al; 1971) or inlet

deposits (Kumar and Sanders, 1974). In the study area no features associated with the seaward end of the platforms or inlets are preserved and it is suggested that the sands that accumulated here were redistributed to form beach ridges on the adjoining side of the migrating inlets. The thick sequence of swash sands in the study area compared with the thinner facies developed in the Central Rand was probably caused as a response to variation in basin subsidence rate. Such a sequence would be retained if sediment supply and rate of subsidence (or sea level rise) were rapid. A present day example of such thick occurrences of beach facies is the sequence of beach ridges on the coast of Nagarit, Mexico, studied by Curray et al; (1969).

The trimodal paleocurrent pattern of the overlying trough crossbedded facies is similar to the hypothetical crossbedding pattern on ebb tidal deltas (Hayes, 1976). Other factors suggesting a tidal origin for this sequence include the association of wave and current ripples, interference ripples, ladderback ripples and flat topped ripples. The features on Fig. 3.6 originate when normal wave ripples are modified by a falling water level so that the sediment from ripple crests is transferred into ripple troughs. The flattening of the crests takes place during subaerial emergence and is caused by "capillary waves" which are produced by strong winds on the water surface (Reineck and Singh, 1975). During emergence some water is retained in the troughs and the ripple crests show marked erosional planes on the side while some ripple crests are sometimes broken through, producing washout structures. All these features and processes forming them have been observed on the tidal flats surrounding the North Sea (Reineck and Singh, 1975).

The overlying shale unit is interpreted as having been deposited on a shelf. The coastal deposits must have undergone rapid submergence if this is correct. The complete lack of sedimentary structures and the fact that the texture of the lensoid sandbodies in the shale are not related to that of the underlying tidal and beach facies overrides the argument that the shale unit is a back barrier lagoonal deposit. The "hummocky" laminated nature of the sand bodies could have originated by periodic flushing of sands through the coastal areas during storms.

The overlying graded sandstone facies are similar to modern shoreface storm generated sequences (Kumar and Sanders, 1976). The grading was probably caused by the sands being held in suspension during the height of the storm and as the storm wanes (and so do the hydrodynamic conditions caused by the storms) suspension settling takes place. The absence of segregated layers of heavy minerals, ripple cross laminae and high angle, large scale cross strata all suggest relatively fast deposition and distinguishes these deposits from foreshore deposits.

The fining upward textures, upward decrease in thickness of the trough and tabular crossbeds, and bimodal current roses for the following 15 m are characteristics of progradational intertidal flat sequences observed by Evans (1965) in the Wash, and van Straten (1964) in the Wadden Sea. The structureless well sorted sands recorded at the top of the sequence on Blinkpoort probably represent a local high energy environment (beach?).

In summary, the first shale horizon in the vertical succession of the Orange Grove Quartzite Formation marks a change from high energy-wave dominated to lower energy-tide dominated conditions. Below the first shale horizon the mature sediments have probably systematically undergone a wave dominated transgressive autochthonous regime which caused the retreating of the shoreline and formed the persistent swash and platform beach or inlet deposits. The recognition of storm deposits is also taken to be indicative of a robust hydraulic regime. This is also manifested in the paleocurrent pattern which is laterally inconsistent. From the wave ripple trend and orientation of primary current lineations the shoreline trend was probably NE-SW. However, the current rose patterns do not conform with this indicating the complex interaction of wave, wind and tidal current bedforms on a strand plain of negligible slope. The lower energy conditions are manifested in the presence of offshore shale deposits followed by sands which are immature and deposited by tidal currents.

3.3.2 Parktown Shale Formation

Definition

Strike faulting north of the Sugarbush River has resulted in the duplication and thickening of members making up the Parktown Shale

PARK TOWN SHALE FORMATION

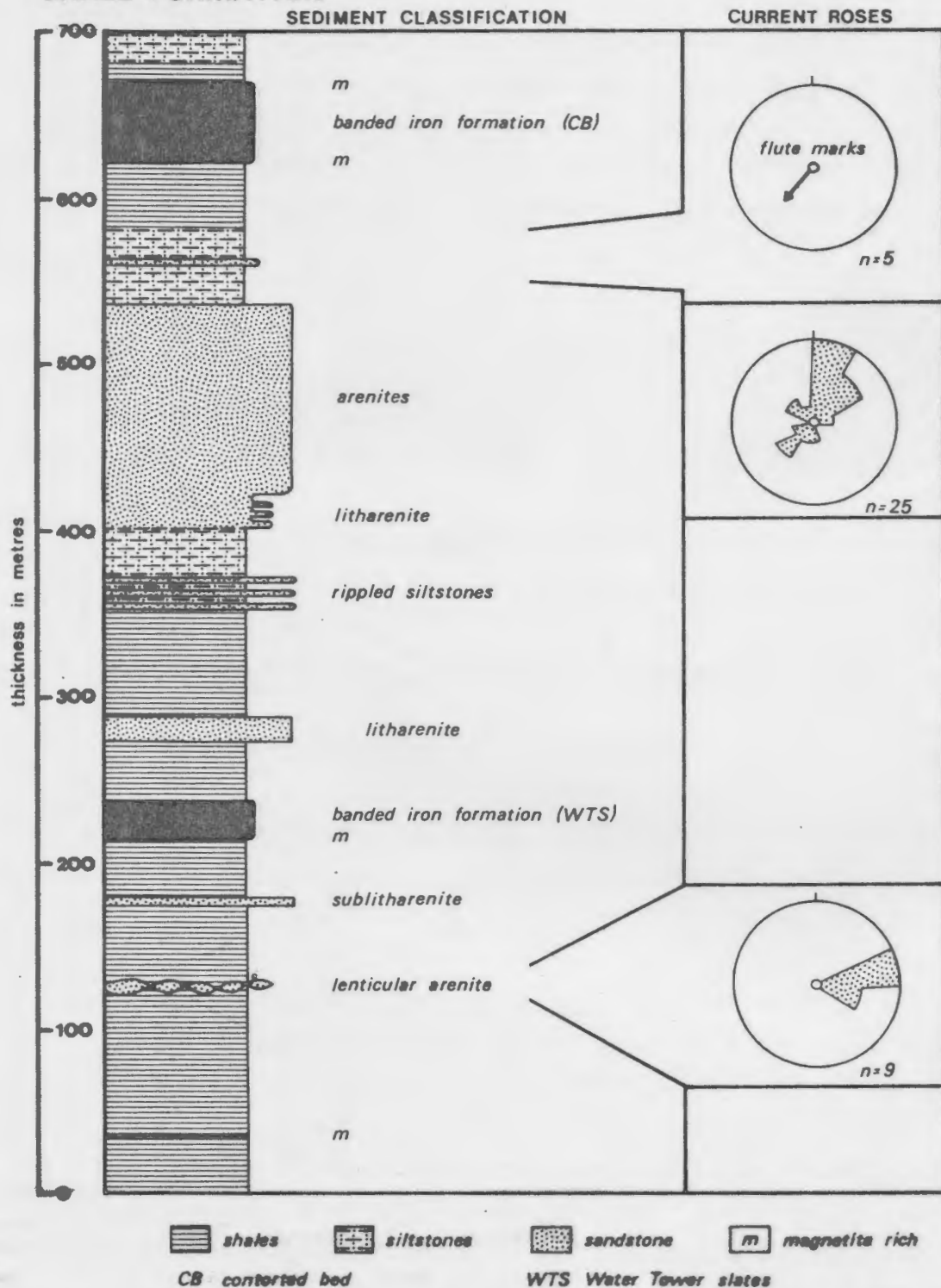


FIGURE 3.8 The stratigraphic column of the Parktown Shale Formation

Formation. The type section of the formation is thus the area next to, and south of, the Sugarbush River on the farms Blinkpoort and Kuilfontein.

Lithology and Sedimentary Structures

The Formation comprises two banded ironstones correlated with Mellor's (1911) Contorted Bed, and Water Tower Slates (Rogers, 1922), a 140 m arenaceous horizon and several thinner sandstone units separated by mudstones and horizontally laminated and ripple marked siltstones (Fig. 3.8). The mudstones weather either to a pale red (5R/ 6/2) or a dark reddish brown (10R 3/4).

The first two lenticular sandstone units below the first banded ironstone are coarse grained sublitharenites. The sand grains are poorly sorted and angular with a mean grain size of 0.75 ϕ (range 4 to 1.0 ϕ). The lithic fragments consist of smaller well rounded micaceous litharenites and cherts. The rock is cemented by very fine grained quartz. Small green grains found as inclusions in the larger quartz grains have a high relief, high dispersion and are isotropic. This spotted rock (Plate 3.1G) below the Water Tower Slate Unit is similar to the speckled bed, identified by Mellor (1911) in the Central Rand and West Rand areas. However, the speckled bed in these areas is only a short distance below the Contorted Bed and the two Units cannot be correlated. Nevertheless, it is significant that both in the Johannesburg area and in the study area an immature sandstone with an interesting texture is associated with the chemically precipitated magnetic horizons.

The Water Tower Slates are poorly developed banded ironstones comprising a microrhythmic alternation of magnetite (mean thickness of 20 cm), white chert and iron-rich mudstones (mean thickness of 2,5 cm). The third sandstone unit 40 m above the banded ironstone, is classified as a poorly sorted immature sublitharenite and is succeeded by a 120 m thick argillaceous horizon. The lower half of this horizon consists of alternating horizontally laminated siltstones and shales while the top half comprises mudstones with intercalated rippled siltstones and sandstones with clay drapes. Near the base of the thickest sandstone unit load casts of fine sand in silty

black shales are common (Plate 3.4A)

The main sandstone unit of the Parktown Shale Formation has a gradational base and a sharp top. The unit consist of bimodal white arenites. This texture is well known in the quartzites of the Brixton Formation in the Johannesburg area. The arenites are sparsely cross-bedded.

Intercalated between the overlying argillaceous horizon is a 2 m sandstone unit which has a fluted base (Plate 3.4B). The shales and siltstones above this unit are greyish yellow green (5 G7 7/2) and weather to a moderate brown (5 7R 4/4). The proportion of siltstones to shale decreases upwards. The shales grade into black magnetite - rich layers.

The base of the Contorted Bed is marked by a 26 m magnetite rich zone which in places is infiltrated by pegmatitic quartz veins. This zone is followed by interlaminated mesobands of chert (light grey), jasper (red) and shale (black). Over a thickness of 18 m this unit is contorted into Class 1C type folds which are steeply inclined (Plate 3.4C). Boudins or possible ball and pillows are rare. Overlying the contorted region are shales and siltstones with weakly magnetic lenses constituting the only chemical precipitate.

Paleocurrent Dispersal Pattern

It was only possible to obtain reliable current directions at two stations alongside the Sugarbush River. The thickest "sago textured" sandstone unit has a bipolar current rose with its major modes orientated N-NE and SW. The current rose for the first lenticular sandstone units is unimodal with its vector mean azimuths showing bed-load transport influenced by an easterly flowing current. The down current direction of the flute marked uppermost sandstone unit of the Parktown Shale formation is south-west.

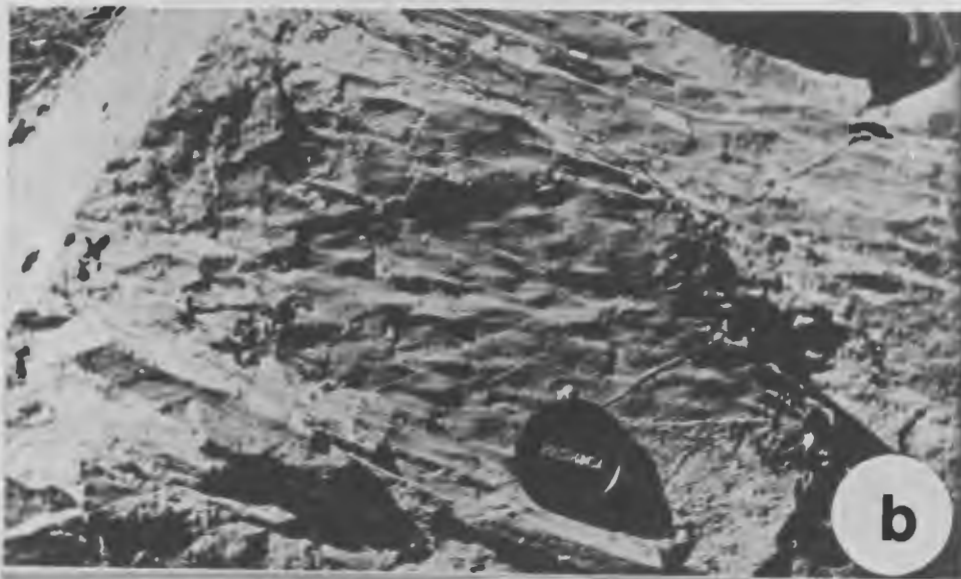
Environment of Deposition

Although relatively little is known about the sedimentology of iron formations with most previous workers concentrating on the mineralogy

P L A T E 3.4

- a. Isolated lenticular load casts probably produced by load deformation of underlying hydroplastic mud(shale); due to yielding under unequal load.
- b. Small ill-defined flute casts preserved at base of sandstone. Current probably from top left to bottom right.
- c. Folding of the Contorted Bed.

PLATE 3.4



of these rocks (e.g. James, 1966), Dimroth (1979) has proposed a model of physical sedimentation relating the sedimentary structures and textures of iron formations to hydrodynamic processes during deposition. Based on Dimroth's (1979) model and classification the two banded ironstones of the Parktown Shale Formation are of the laminated micrite type, cherty iron formations in the "detrital chemical sediment class". According to Dimroth (1979) such iron formations are very similar to limestones deposited on the shallow marine shelf of the Persian Gulf.

Parallel laminations and stratification are visible as the only depositional features in the Contorted Bed indicating a depositional environment below wave base. Such laminations are based from shelf muds of the Persian Gulf because of bioturbation. The finely-alternating ferruginous and siliceous layers in the two banded iron formations may form as a response to cyclically fluctuating Eh and Ph conditions (Walter, 1972) but Dimroth (1979) is of the opinion that iron formations were precipitated as CaCO_3 (probably aragonite) which have subsequently been replaced by silica and iron compounds during early diagenesis. The latter hypothesis is plausible as samples with as much as 25 per cent carbonate have been identified within the Parktown Shale Formation in the Central Rand area (Rogers, 1933). Whatever the origin of the iron formations, they probably represent intervals of non-detrital deposition and are interpreted as the most distal facies within the Hospital Hill Subgroup.

The discontinuous immature sublitharenites below the first banded iron formation are probably nearshore shelf storm deposits with the first lenticular arenite being deposited by longshore currents flowing at right angles to the paleoslope. This is assuming that the flute marks on the base of the uppermost sandstone unit indicate scouring action down a south westerly slope. The main sandstone unit of the Parktown Shale Formation with its gradational base, sharp top, mature sands, sparse crossbedding and bimodal current rose is interpreted as being formed by the migration of flood (? and wave) dominated bed-forms along a NW-SE trending coastline.

In summary, the shales and thin sublitharenites of the Parktown Shale

Formation were formed by suspension deposition of mud alternating with periodic sand influxes (? distal storm layers) while the banded iron formations and magnetite - rich zones probably represent distal shelf muds. The presence of a thick sandstone unit within the formation in the study area, which is absent in other outcrop areas (Appendix 1), indicates that the alternating transgressive-regressive sequences in the study area include proximal sand facies which are influenced by tides. The differences in thickness and character of the Parktown Shale Formation within the study area and other outcrop areas (Appendix 1) is probably a result of fluctuations in the rate and extent of transgressions and regressions in the shoreline environment, controlled by the rate of deposition and rate of sea-level change (Curry, 1964).

3.3.3 Brixton Formation

Definition

This formation is best exposed on the farms Blinkpoort in the south and Uitkyk in the north of the study area. Sands and clays of the Karoo Supergroup partly cover the Brixton Formation between the two farms. A composite type section constructed from traverses 4, 5, 6, 10, 11 and 12 is shown on Fig. 3.9.

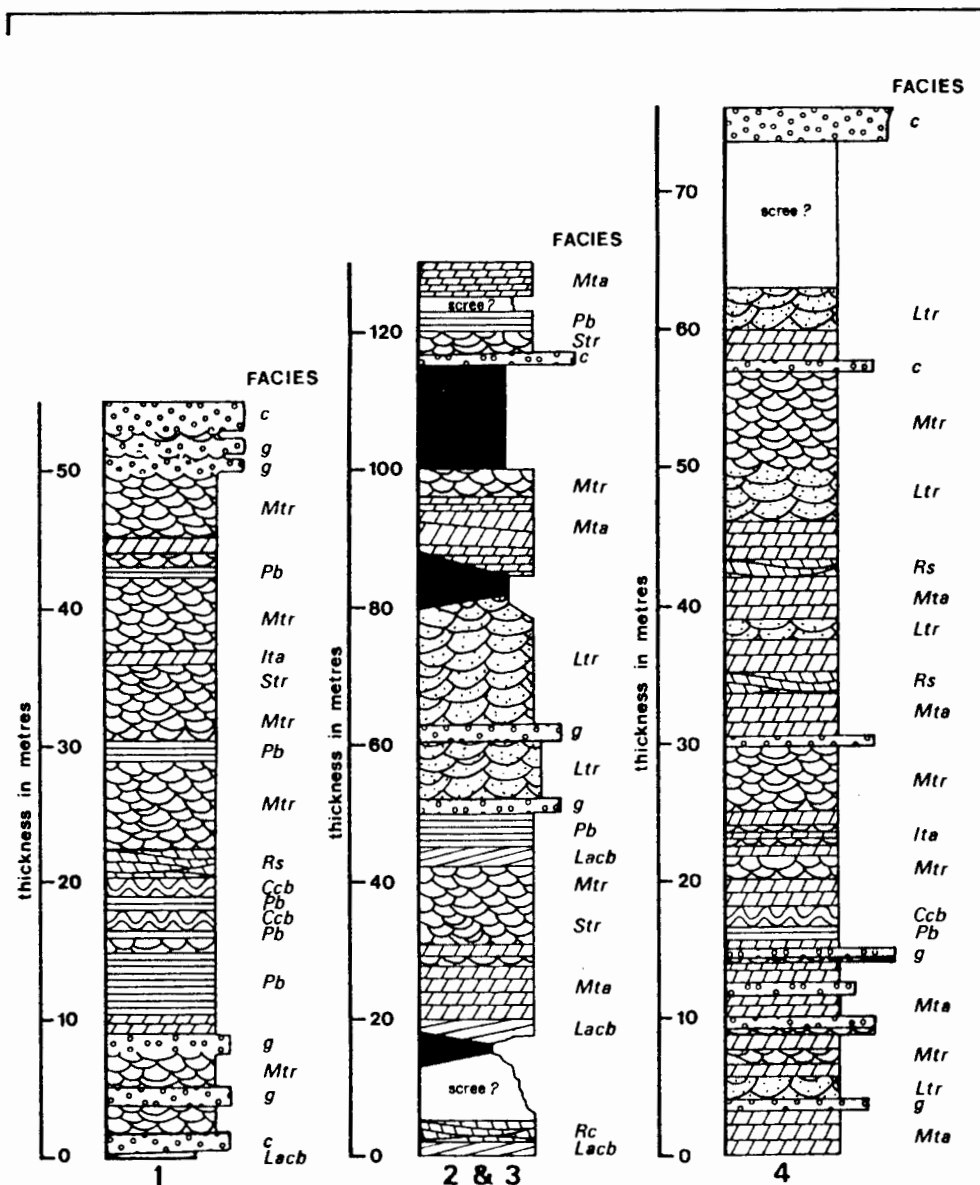
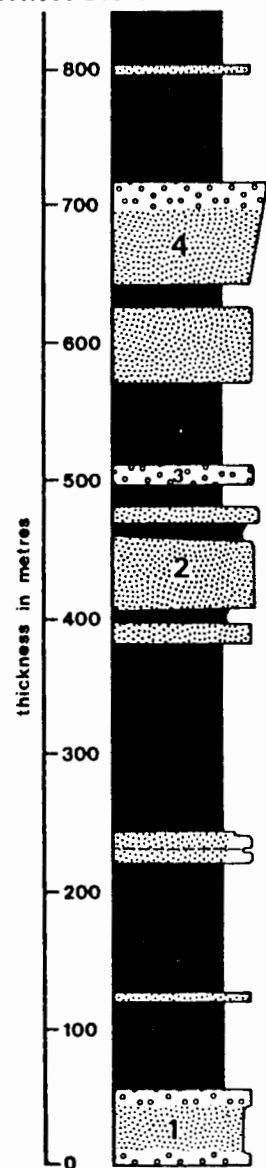
Lithology

The Brixton Formation measures about 850 m in thickness. It consists of five thick and several thinner laterally discontinuous sandstone units separated by shales and siltstones.

The first arenaceous horizon (55 m) serves as a useful marker in both the east and south Rand. It is a medium grained sandstone characterised throughout the study area by the presence of black conglomerate lenses at the base and at the top. The unit was appropriately named the Black Grit by Sawyer (1907). The impersistent conglomeratic layers are thin - the thickest measured was 35 cm - locally mineralised, and comprise angular fragments of black, white and banded chert. On the farm Uitkyk the base of the unit is classified as an immature, coarse grained (mean diameter 0,45 ϕ) poorly sorted sublitharenite with skeletal euhedral haematite being the only

BRIXTON FORMATION

MEMBERS OF THE BRIXTON FORMATION



FACIES

FACIES

- c Conglomerates
- g Coarse grained lags
- Str Small trough crossbeds
- Mtr Medium trough crossbeds
- Ltr Large trough crossbeds (generally coarse grained subarkose)
- Ita Isolated tabular crossbeds
- Mta Multiple sets of tabular crossbeds (often mud-draped)
- Rs Reactivation surfaces
- Pb Plane beds (current lineation on some surfaces)
- Ccb Convoluted bedding
- Lacb Medium-scale low angle cross-stratification (generally separated by claystone drapes)

GRAIN SIZE

- Shale
- Fine-medium grained sandstone
- Coarse grained sandstone

FIGURE 3.9 Composite stratigraphic section of the Brixton Formation

replacement mineral, but near the Sugarbush River it is a mature, moderately sorted, coarse grained (mean diameter 0.0Ø) arenite with sericite as a matrix. On the farm Rietpoort the Black Grit's base comprises well sorted bimodal grain sized sublitharenites. Green fuchsitic staining, aggregated stylolytic surfaces and characteristic "sago textured" quartz arenites are common features between the basal and upper conglomerates.

The third arenaceous unit of the Brixton Formation consists of coarse grained (mean diameter 1.0Ø) immature litharenites which become finer grained and more mature 4 m above the undulating gradational base. Several fining upward cycles characterise this unit. Lithologically the next sandstone unit (labelled 2 and 3 on Fig. 3.9), is very diverse. Three thin shales are separated by litharenites and quartzarenites near the Sugarbush River (T4) while in the north of the area the thin shales thicken at the expense of the sandstones. On T11 this unit is not recognised at all. The topmost arenaceous unit has a sharp erosive base with shale clasts and jasperitic chert clasts loosely packed in a mature, coarse grained litharenite (Plate 3.1E). Pyritic pitting and green fuchsitic staining is common 2 m above the base.

The last major arenaceous unit of the Brixton Formation consists of a coarsening upward sequence of intertonguing coarse grained, immature sublitharenites and mature fine grained arenites. Coarse "sago" textured units or pebbly washes with very little matrix were recognised 4, 9, 12, 15, 30 and 57 m above the base of the unit. Very coarse sandstones and discontinuous poorly packed mineralised conglomerates composed mainly of well rounded quartz clasts and angular cherts make up the last 13 m of the unit.

Sedimentary Facies

The Brixton Formation's arenaceous units have been divided into several sedimentary facies (Fig. 3.9). Although the approach is similar to the method used in dividing the Orange Grove Quartzite Formation into its respective facies on the basis of the most frequently occurring sedimentary structure it was necessary also to include some textural facies (conglomerates and coarse grained lags). The reason for this is that more often than not the coarse grained lags and conglomerates

are not well exposed and no diagnostic sedimentary structures within them could be recognised. As all evidence relative to the environment must be utilised to build a consistent, convincing and realistic picture of the conditions that existed at the time of sedimentation it was decided to include the structureless coarse grained facies.

The Black Grit (labelled 1 on Fig. 3.9) consists predominantly of small and medium trough crossbeds (mean trough thickness is 15 cm, range 5-50 cm) which are often convoluted and overturned, rare plane bedding, rippling and vague parting-current lineation were also observed. These features are randomly stacked throughout the 55 m thick unit with no one facies being laterally persistent (e.g. plane bedded facies were in some places cut into and replaced by overlying troughs).

A sandstone unit about 150 m above the upper conglomerate of the Black Grit consists of trough and tabular crossbedded units with thin muddy drapes defining the tabular and trough foresets. Ripples with wavelengths of 15 cm are abundant and the upper contact is sandwaved with wavelengths of up to 10 m.

The sedimentary facies present in the four sandstone units 165 m above the sandwaved contact are shown on Fig. 3.9. As in the Black Grit the most frequently occurring sedimentary facies are the trough crossbedded units. However, multiple sets of tabular crossbeds which are often mud-draped and range from small to large scaled sets are more common. Furthermore, the vertical stacking of different facies is not as random as that for the Black Grit. Coarse grained lags are always followed by a trough crossbedded facies which in turn are often overlain by low-angle or plane-stratified units.

The last major arenaceous horizon (labelled 4 on Fig. 3) has multiple sets of tabular crossbeds (4 m thick) at the base of the unit which are cut into by very coarse grained trough crossbedded sublitharenites. The next 45 m is characterised by diverse randomly stacked sedimentary structures which include convoluted bedding, reactivation surfaces and trough and tabular crossbedded units. Coarse-grained medium and trough crossbedded sets become more dominant in the upper part of the succession.

Paleocurrent Dispersal Pattern

The vertical and lateral distribution of the paleocurrent pattern of the Brixton Formation is shown on Fig. 3.10.

The Black Grit marker shows well developed bipolar pi-crossbeds with two major modes orientated south west ($210-220^{\circ}$) and north east ($25-35^{\circ}$) alongside the Sugarbush River. On the farm Uitkyk (T10) a similar bi-polar current rose is evident while between these two localities (T18 and T12) the bedform orientation is more complex. However, there is always a dominant primary mode orientated N-NE. The significance of this will be discussed later. The only other well developed bipolar-bimodal current rose within the Brixton Formation is present in the third arenaceous horizon of the Brixton Formation measured on the Sugarbush River is S-SE. Except for the sandstone labelled 3 on Fig. 3.9, all the other units are unimodal with the vector mean azimuth indicating bedload transport towards the S-SW. The exception is interesting in that the small trough crossbedded units above the rip-up shale clast conglomerate have a westerly paleocurrent direction while the overlying multiple sets of tabular crossbeds have a E-NE direction.

Environment of Deposition

The thick arenaceous units of the Brixton Formation all have sedimentary structures which indicate that tidal processes were operative during their deposition.

The most common feature in all the sandstone units are either medium scale trough or tabular crossbeds. The mud draped foresets of the planar crossbeds are common features in tidal sand deposits (e.g. Reineck, 1963; Raaf and Boersma, 1971). The suggestion that the mud drapes formed by fall-out of fine grained suspended sediment during the slack water period of the tidal cycle (e.g. Klein, 1970) has been questioned by McCave (1970). Because of the long settling time of the suspended mud, McCave (1970) is of the opinion that mud drapes in tidal sand deposits are not the result of diurnal and semi-diurnal tidal fluctuations. Instead they are more likely to be due to a combination of abnormally high suspended sediment concentrations, low

SANDSTONE PALEOCURRENT PATTERN OF THE BRIXTON FORMATION

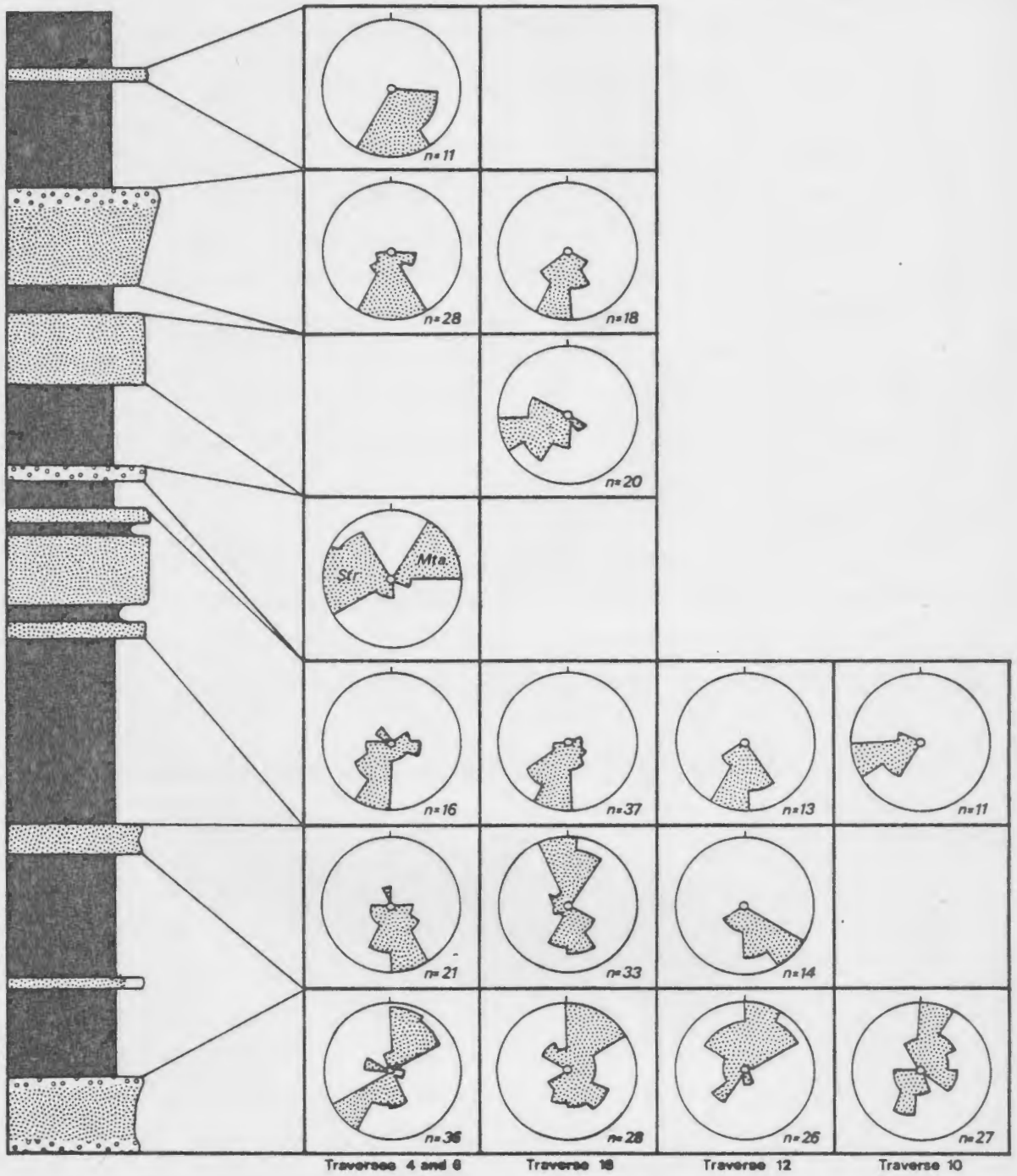


FIGURE 3.10 Paleocurrent pattern of the Brixton Formation

current velocities and low wave intensity over a long period. Johnson (1978) suggests that these conditions prevail following a storm when suspended concentrations are high. The trough cross-beds are interpreted as products of migrating three-dimensional dunes (probably linguoid) and the infilling of erosional scours.

The lateral extent of the Black Grit's coarse grained and conglomeratic facies probably indicates erosion under a laterally extensive sheet of water of relatively uniform depth. The Black Grit (together with many other sandstone units of the West Rand Group) has a sharp basal contact with no deep channels and scours but is characterised by coarse grained sheet sandstones. This factor, plus the bimodal - bipolar paleocurrent pattern and the recognition of thin sets of plane beds and reactivation surfaces in an apparent random vertical sequence, suggests to the writer that the Black Grit was deposited in an environment comprising a shallow tidal sea bordered by exposed beaches. The paleocurrent patterns for the Black Grit north of the Sugarbush River indicate the superior strength of the flood current (N-NE). Erikson *et al.* (in press) noted that ebb currents (S-SW) were stronger, especially during deposition of the lowermost Brixton Quartzites in the Central Rand, and this fact again indicates the uniqueness of the cherty conglomerate marker on the East Rand.

The unidirectional paleocurrent patterns for the remaining six units of the Brixton Formation are not diagnostic of fluvial environments as these patterns are common in tide and wave influenced environments (Johnson, 1978). Thus, although parts of the sequence resemble sections of braided stream environments of the Platte type (Miall, 1977), reactivation surfaces and thick sequences of plane beds in this unit are more indicative of a marine setting. The stacking of facies in these units (labelled 2, 3 and 4 on Fig. 3.9) is often punctuated by fining upward cycles with coarse grained lags overlain by a trough crossbedded and a plane bedded facies. These sequences were probably formed by channels cut by storm ebb currents which are infilled as the storm subsides to deposit a waning flow sequence with the final ripples being reworked by waves (plane beds). Such processes Banks (1973) visualised in the deposition of the lithologically diverse late Precambrian deposits from northern Norway.

The complex alternation of silts and muds in the latter area were deposited in sublittoral environments which never established a shoreline. The absence of these fine grained facies in the study area is probably because the above process was operative on an established shoreline with a high sediment rate. The unimodal regional paleocurrent patterns for these units which shows a S-SW transport direction are consistent with modern analogues where storm ebb surge currents are the most likely seaward flowing currents (Hayes, 1976; Gadow and Reineck, 1969). However, though this "catastrophic sedimentation regime" is preserved in parts of the sequence the presence of reactivation surfaces and mud draped tabular crossbeds indicates that the sequence also shows more normal noncatastrophic (tidal) processes. In these facies the unimodal paleocurrent pattern may be explained by the main ebb currents following mutually exclusive paths to those of the flood currents (Johnson, 1978). Thus the sediments of the arenaceous units of the Brixton Formation were probably deposited under the same conditions as the Jura Quartzite (Scotland) where, although storm deposits are invoked as the major process for preserving sediment, it is only effective because it acts in conjunction with tidal currents (Anderton, 1976). The convolute bedding facies which is best developed 15 m above the base of the last major sandstone unit of the Brixton Formation (labelled 4 on Fig. 3.9) is attributed by Coleman (1969) and Wunderlich (1970) to emergence-draining of pore water from rapidly sedimented material, although the deformation may also be a product of differential loading.

The shaleclasts at the base of the unit labelled 3 on Fig. 3.9 together with the unusual paleocurrent pattern which is interpreted as running parallel with the shoreline are difficult to explain in terms of tidal and storm processes acting normal to a shoreline. Such a current pattern and shaleclast texture may occur within a back-barrier tidal channel environment where shaleclast filled washouts are produced by tidal scour. Similar barrier-protected sequences with trough crossbeds and planar crossbeds overlying a base characterised by a few clasts and overlain by a plane bedded sand facies have been described by Carter (1978) in the Upper Tertiary Cohansey Sand of New Jersey.

In summary, the consistency of the major current modes in most of the

Brixton Formation sandstone units, the bimodality of some of its units and the roundness and maturity of the "sago textured" grains all suggest that the units were deposited along a coastline that was subjected to tidal and wave surge forces. The orientation of the shoreline was probably NW-SE. The majority of bedforms indicate bedload transport towards the SW and it has been suggested that the ebb dominance of these structures was enhanced by storms washing out sediments in the nearshore regions and then winnowing material from a flat floor. However, the recognition of possible barrier island subenvironments indicates that longshore processes were still operative but, unlike the conditions which were present during the deposition of the lower Orange Grove Quartzite Formation, were subordinate to wave beat and tidal forces. Although Eriksson *et al* ; (in press) suggest that the tidal range was greater than 4 m during the deposition of the Brixton Formation in the Central Rand area it is likely that tidal fluctuations were modified by factors of basin geometry and mesotidal (2-4 m) wave dominated conditions probably prevailed in the study area.



Eastward panoramic view of West Rand Group sediments cut by Sargarbush River with flat lying Karoo strata in the background

3.4 GOVERNMENT SUBGROUP

The thickness of the Government Subgroup is approximately 1 300 m in the study area, compared with 750 m near the Hex River Mine (South Rand) and 1 860 to 2 000 m on the Central Rand. The Subgroup is divided into three formations: The Coronation with its tillite and magnetic marker horizons, the Promise Quartzite and the Witpoortjie Formations. The Promise Reef and Blue Grit are both diamictic markers delineating the base and the top of the Subgroup respectively.

Plate 3.5 shows several sedimentary structures which are present within the Government Subgroup. Although many of these structures are also present within the Hospital Hill Subgroup, the communal association of the structures is quite different. In general, herringbone crossbeds (Plate 3.5a) and tabular crossbeds overlying either low angle cross stratified laminae (Plate 3.5d) or mud draped symmetrical ripples (Plate 3.5c) are more abundant in the Government Subgroup. Thick coarse grained tabular crossbeds (Plate 3.5b) and "water escape" structures (Plate 3.5e) are also common. Symmetrical wave ripples (Plate 3.5g) and runnel marks on plane beds (Plate 3.5f) indicate, as in the Hospital Hill Subgroup, that wave processes were still operative. The following profiles indicate subtle differences in the relative influence of wave and tidal processes when compared with the sections of the Hospital Hill Subgroup.

3.4.1 Promise Quartzite Formation

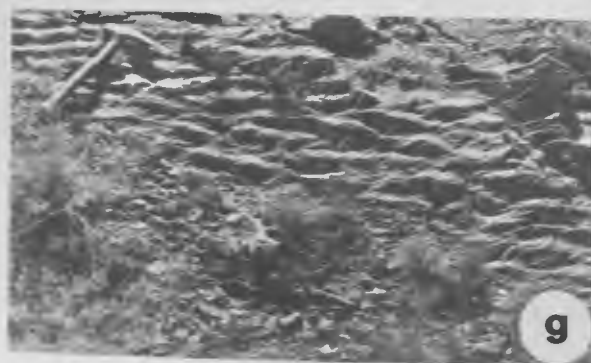
Definition

The base of this formation is seldom seen because it is generally covered by thick soil or remnants of Karoo Supergroup beds. However, on Blinkpoort and the neighbouring part of Groenfontein the base consists of coarse grits exposed in ten prospecting pits. The diamictite is as much as 3 m thick in one pit and has quartz pebbles 5 cm long scattered sparsely through it, but it thins and disappears along the 4 km of occasional outcrops traced on the two farms. On Rietpoort, Bultfontein and Uitkyk, this marker is seldom seen and the Promise Quartzite Formation succession cannot be correctly ascertained on these farms. Fig. 3.11 is a composite type section constructed from traverses 7, 14 and 18.

PLATE 3.5

- a. Herringbone crossbedding at the base of the thickest sandstone in the Promise Formation (Groenfontein).
- b. Large coarse grained tabular (fluvial) crossbeds near top of thickest sandstone in Promise Formation (Groenfontein).
- c. Oblique view of medium scaled tabular crossbeds overlying -near symmetrical small mud draped wave ripples (Promise Formation).
- d. Large tabular crossbeds overlying low angle cross-stratified laminae (Witpoortjie Formation).
- e. Water escape structures (T14 - Groenfontein).
- f. Runnel marks on plane beds, Promise Formation (Blinkpoort).
- g. Irregular symmetrical wave ripples (T14 Groenfontein).

PLATE 3.5



Lithology

The Promise Quartzite Formation measures some 240 m in the study area. Thin shales near the base and at the top of the formation bound the thickest arenaceous unit of the West Rand Group. Subsequent to Roger's (1922) mapping, farming activity has covered the top two arenaceous horizons of the Promise Quartzite Formation.

The base of the formation is composed of scattered pebbles of granite, feldspar and quartz set in a muddy matrix. This horizon was correlated with the Promise Reef of the Central Rand by Rogers (1922). It is overlain by crossbedded mature sublitharenites which are medium grained (mean diameter of about 1.4Ø) and which sometimes have graded foresets. Several fining upward cycles are present 50 m above the diamictite. The variation in grain size up the stratigraphic column is generally correlative with the sedimentary structures observed. The coarser sands are more often than not present in the trough crossbedded facies while the fine to medium grained sands are generally confined to the tabular crossbedded facies.

Sedimentary facies

Ten facies have been identified within the Promise Quartzite Formation (Fig. 3.11). Facies which are well developed within the formation include convoluted large tabular crossbeds and thick sequences of herringbone crossbedding. The formation is characterised by its predominance of multiple sets of tabular crossbeds over the trough crossbedded facies. The tabular sets vary in thickness from 0,02 to 1,2 m.

Although larger tabular crossbeds are generally more common at the top of the thickest arenaceous unit, the vertical stacking of the other facies alternate in an apparently random manner.

Paleocurrent Dispersal Pattern

The paleocurrent dispersal pattern of the Promise Quartzite Formation is given on Fig. 3.12.

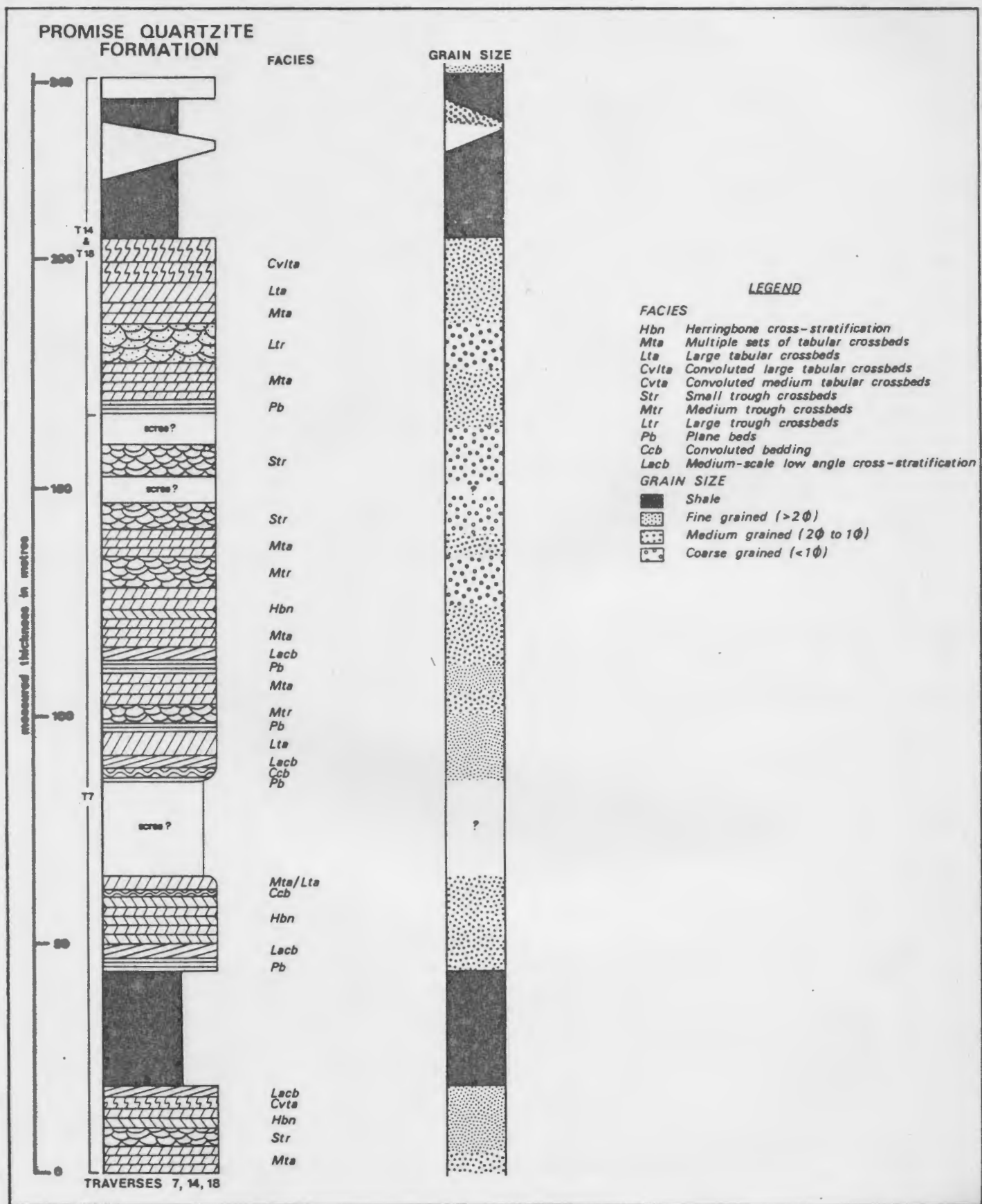


FIGURE 3.11

Sequence of sedimentary structures, textures and lithology in the Promise Quartzite Formation

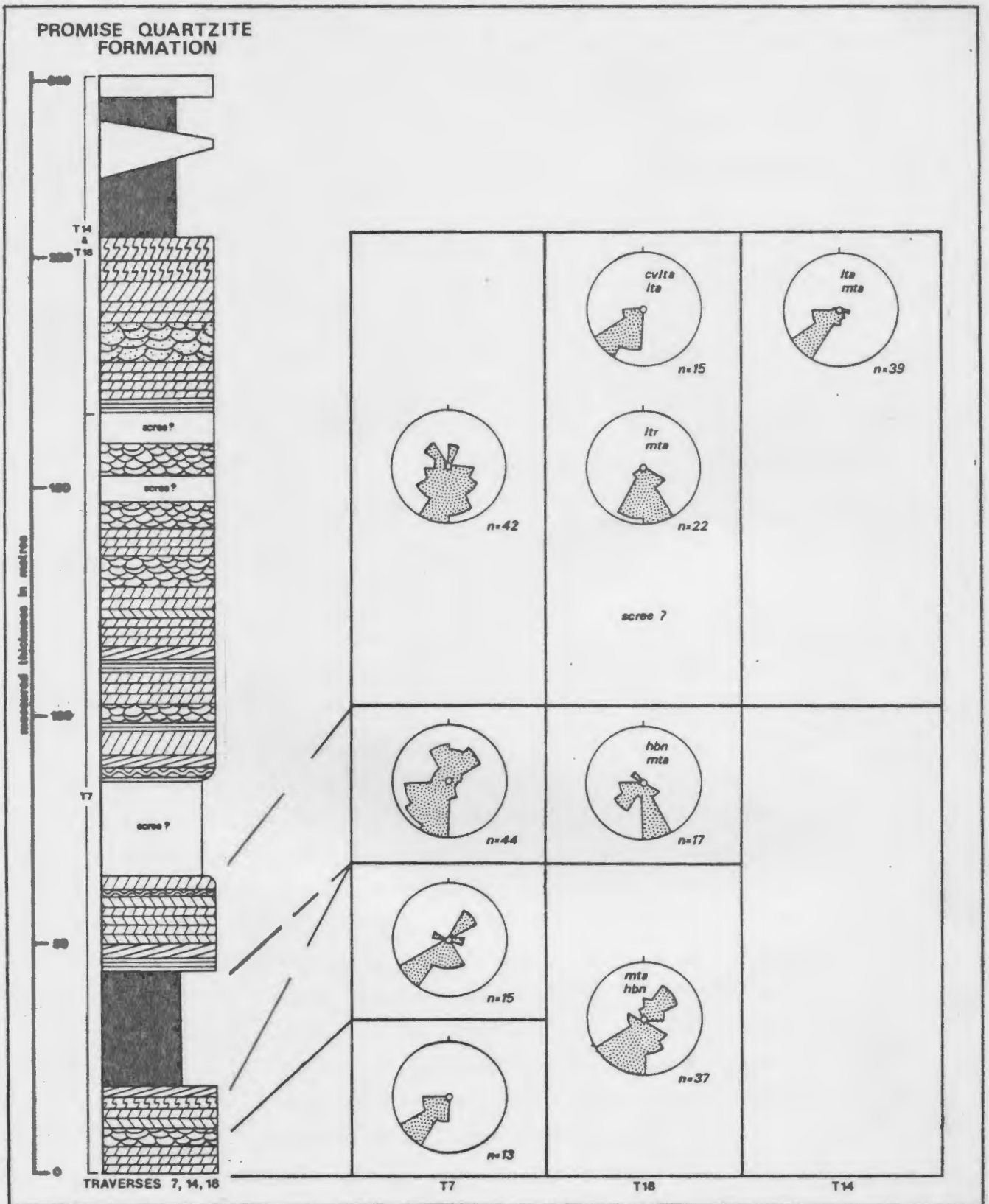


FIGURE 3.12 Paleocurrent dispersal pattern for the Promise Quartzite Formation

Multiple sets of tabular crossbeds and herringbone crossbedded facies give bipolar-bimodal current roses while the larger convoluted and trough crossbedded facies are strictly unimodal. At all stations the dominant vector mean azimuth is towards the south. The thickest arenaceous horizon current roses change from being strongly bipolar at the base to unimodal further up the succession.

Environment of Deposition

The tabular and trough crossbeds overlying the diamictite marker at the base of the Promise Quartzite Formation were probably deposited in an offshore (subtidal shelf) environment. About 7 m above the base of the formation herringbone and low angle cross-stratification indicate shallower tidal processes. The absence of typical inshore fining upward tidal flat sequences suggest that the bedforms resulted from the migration of storm surge (trough crossbeds) and ebb orientated (tabular crossbeds) sand waves in a subtidal environment. This is substantiated by the dominance of a major mode (S-SW) in the bipolar current roses for these facies.

The base of the thickest sandstone unit of the West Rand Group is characterised by thick sequences of herringbone crossbeds which are interpreted as being indicative of an intertidal or subtidal environment. The coarser sands and unimodal directions for the remaining 100 m of this unit could either be interpreted as marine or fluvial deposits. The writer is of the opinion that the sequence is similar to a braided stream deposit of the Platte type (Camden-Smith, 1979a, b). The convoluted large tabular crossbeds were probably formed by strong sediment laden currents that drag the upper parts of the foresets into folds (McKee *et al*, 1962). This type of feature has been commonly observed in fluvial deposits (Reineck and Singh, 1975). The presence of planar bedding within the unit indicates that sand was transported under upper flow regime conditions. Such deposits are common in braided streams that are subjected to catastrophic floods (McKee *et al*, 1967).

3.4.2 Coronation Shale Formation

The Coronation Shale Formation comprises a 6 m thick tillite horizon

and a banded shale unit containing much magnetite. The two units are best observed on the farm Blinkpoort in the south and Bultfontein in the north. The magnetite rich unit can be traced between these two farms through Rietpoort and Groenfontein.

Lithologically, the tillite is nonstratified and poorly sorted (Plate 3.6a). The boulders and pebbles within the tillite are composed dominantly of sandstones although slate and lava pebbles have been noted (Rogers, 1922). The matrix of the tillite is much the same as that of the two diamictitic markers and so too is its geochemistry. However, one of the most distinctive features of the till is the presence of several striated and faceted clasts which are rare and difficult to extract in the hard lithified rock (Plate 3.6b and Plate 3.6c). As no striated pavements were observed in the study area the faceted clasts are the only evidence that the pebbles originated from glacial abrasions.

Environmental Significance

The tillite marker extends over an area of many thousands of square kilometres. It has been recognised in the West Rand area, the Klerksdorp area, in the Orange Free State Goldfields, in the Delmas area and in the Evander area. The Coronation Shale Formation is best developed in the Evander area where interbedded magnetic shales and quartzites with two tillite bands total some 169 m (Jansen et al, 1972). In the Klerksdorp area the "tillite" lacks striated pebbles, has a restricted areal extent and is in some cases lenticular (Watchorn - pers. comm.). The glacial origin of some diamictites has been refuted for these very reasons (e.g. Dott, 1961; Schermerhorn, 1974). Nevertheless, the areal extent of this marker contrasts with the limited coverage of the other diamictites (the Blue Grit on the East Rand, the tilloid associated with the Promise Reef on the West Rand and the Promise Reef in the study area). This fact suggests to the writer that a synchronous glaciation occurred in West Rand Group times and may have contributed not only to marine tills but also to unstable sediment piles, leading to subaqueous slumps, slides and flows. However, the evidence is inconclusive, in that the poor outcrop of the tillite makes it difficult to delineate the facies associated with the till.

P L A T E 3.6

- a. Outcrop of tillite on farm Rietpoort.
- b. Pebbles extracted from tillite matrix. Note the faceted surface
of pebble 6 cm to the left of scale.
- c. Striations on two of the pebble surfaces.

PLATE 3.6



The oldest evidence for widespread glaciation is in the Middle Precambrian (2150-2500 m.y., Pettijohn, 1975) of the Canadian Shield. The best known tillite from this time is the Gowganda Formation, which extends over an area of many thousands of square kilometres (Young, 1973). New age data for the Ventersdorp Supergroup restricts the age of the Witwatersrand Supergroup to between 2620 and 2800 m.y. making the tillite within the Coronation Shale Formation the oldest recorded deposit.

3.4.3 Witpoortjie Formation

Definition

The Witpoortjie Formation is best developed on Bultfontein and is less well preserved on Rietpoort and Blinkpoort. In the western part of Blinkpoort the units above this marker are difficult to decipher because of complex faulting.

The choice of any one specific type section is difficult because of the cover of post Witwatersrand strata together with the complicated structure. Fig. 3.13 is thus a composite type section prepared from traverse numbers 3,9,14,15,16 and 13.

Lithology

The Witpoortjie Formation is about 680 m thick in the study area. Directly above the shales containing the Coronation Shale Formation 6 sandstones alternate with shale units. The top of the formation is marked by a marker, the Blue Grit diamictite, the other marker being the Government Reef at the base of the fourth sandstone unit. Without these two markers it would be difficult to distinguish between the different sandstone units.

As in the Delmas area (Button, 1970) the shales below the Government Reef are all dark grey to black in colour and often grade into siltstones which in turn grade into sandstones. This feature contrasts with the sharp contact between the two lithologies in the Hospital Hill Subgroup. The sandstones below the Government Reef weather to a pale red (10R 6/2) or greyish orange pink (10R 8/2). The laminated siltstones also weather to a greyish orange pink

WITPOORTJIE FORMATION

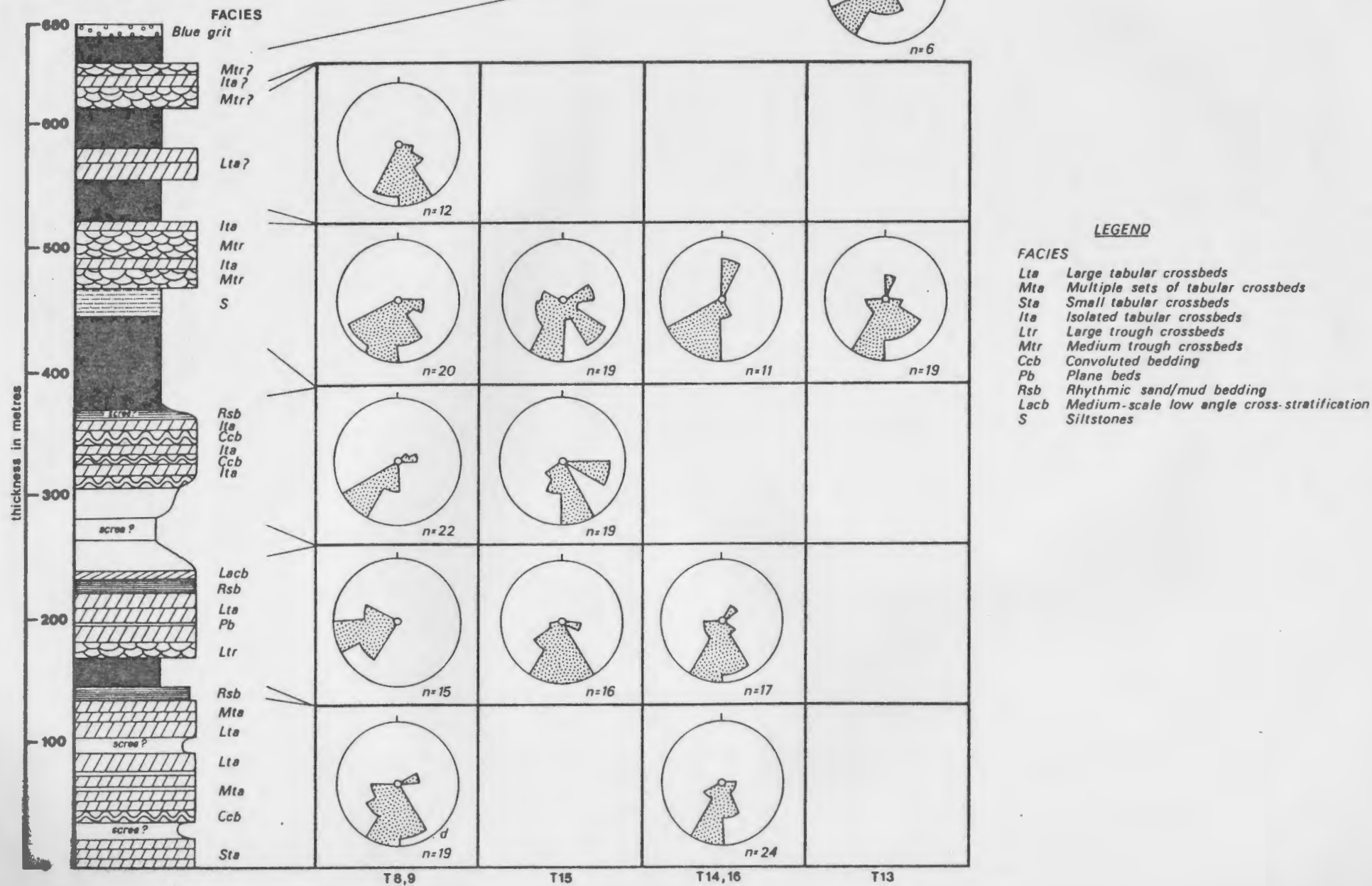


FIGURE 3.13 Composite stratigraphic section of the Witpoortjie Formation

while the arenaceous units above and including the Government Reef are generally pale to light brown (5YR 6/4). The poorly sorted submature and immature units below the Government Reef were classified as subgreywackes by Fuller (1958). As a large proportion of sandstones of the Witpoortjie Formation are "dirty" and consist of mega-rythmically interbedded sand-shale sequences as opposed to many of the moderately to well sorted cleaner sands of the Hospital Hill Subgroup they can be termed greywackes in the field (Blatt et al, 1972). However, following Folk (1968a) and Blatt et al, (1972) the word greywacke has no place as a term for use in laboratory, where the writer classified the sandstone of the Witpoortjie Formation precisely on the basis of all essential sand size constituents with the percentage of clay matrix being ignored (Table 3.2).

The Government Reef is a small pebble conglomerate (Fig. 3.4) which reaches thicknesses of up to 0,6 m. On the farm Holgatfontein in an old prospectors pit, two conglomerates are developed at the base of the sandstone. The basal conglomerate is 35 m thick with the second one being less developed with an average thickness of 15 cm. The quartz pebbles (which constitute about 65 per cent of the total pebble population) are well rounded and sorted. The sandstones above the conglomerate (e.g. 13/08) are mature, bimodally sized (0.0 and 1.75 ϕ) sublitharenites.

South of Heidelberg and near the Sugarbush fault, the Blue Grit, which Rogers (1922) describes as a rock of "remarkable character", has an heterogeneous matrix composed of quartz, chlorite, epidote, zoisite, actinolite, tremolite, white mica and chloritoid. The chloritoid and amphiboles are rare minerals and were not identified by the writer but were recorded in one thin section by Rogers (1922). Angular fragments of chert, fresh feldspar, phyllite, granite, syenite and porphyritic lava measure between 1.5 to 75 mm and are randomly scattered throughout the unit. On the Evander Goldfield, Jansen et al, (1972) have observed that this unit has occasional boulders up to 30 cm in size and is up to 590 m thick. In the study area the Blue Grit's type area of development is in the south where its thickness is approximately 230 m. It is, however, recognisable as far north as Rietpoort where it measures 15 m. This large

variation in thickness of the Blue Grit is an exception to the general trend of laterally consistent thicknesses in the units below the marker.

Sedimentary Facies

The vertical stacking of the 10 facies identified within the Brixton Formation is shown on Fig. 3.13.

The units below the Government Reef differ from the ones above (and including) the marker by the relative absence of medium trough cross-beds and the presence of rhythmic sand/mud bedding, convoluted bedding and medium-scale low angle cross-stratification. On all the traverses no thick cosets of herringbone crossbedding were observed as was the case in the units below the Witpoortjie Formation. One facies that is common at the top of the basal arenaceous units of the formation is the facies termed "rhythmic sand/mud bedding". This field term proposed by Reineck and Singh (1975) includes lenticular and flaser bedding, coarsely interlayered sand/mud bedding and thinly interlayered sand/mud bedding. In the study area the facies is characterised by thinly layered wavy mud layers which alternate with sandy layers.

Paleocurrent Dispersal Pattern

The paleocurrent dispersal pattern within the arenaceous units of the Witpoortjie Formation is given in Fig. 3.13.

As in the Promise Quartzite Formation most of the current roses have a vector mean azimuth which indicates bedload transport towards the S-SW. The bipolar current patterns obtained from the Government Reef on the farms Groenfontein (T16) and Rietpoort (T13) contrast with the divergent unimodal patterns of the marker beds at localities (T15 and T9) south of these farms. Although the arenaceous horizons below the Government Reef have well developed primary modes, minor secondary modes are also present with the two modes separated by 120° or, in two cases, 60° .

Environment of Deposition

The immature subgreywackes of the Witpoortjie Formation below the

Government Reef probably represent subtidal shelf and inshore tidal flat deposits. The units often fine upward ending with finely laminated sand/mud bedding which is typical of inshore tidal flat sequences. As in other ancient deposits, the differentiation between subtidal and intertidal deposits is problematical (Raaf and Boersma, 1971). The absence of thick sequences of herringbone crossbeds and the unimodal and weakly bimodal current roses suggest that a subtidal environment was more prominent. Rapid deposition or a proximal source area accounts for the textural immaturity of the sediments. The convolute bedding and water escape structures in the unit below the Government Reef occur in modern shallow marine environments (Lowe, 1975) and have been described in their ancient counterparts (Anderson, 1976; Johnson, 1977).

The Government Reef marker, which consists almost wholly of medium trough crossbeds and has a laterally complex paleocurrent pattern, probably represents ancient beach deposits. Onshore migrating sand bars and ripples moving possibly in response to shoaling waves were probably the chief processes operative.

The sparse paleocurrent data and outcrop of the two upper arenaceous units of the Witpoortjie Formation makes it impossible to draw conclusions as to their origin.

The poorly sorted Blue Grit with its wide range of particle size and pebble composition may have originated from subaqueous mass-transport processes. The full spectrum of submarine mass-transport processes has recently been reviewed by Carter (1975). The Blue Grit's restricted extent and lenticular nature suggests that it may well represent either a fossil submarine rockfall or a canyon and fan valley deposit. The large boulder sized pebbles, admixtures of pebbles of widely divergent compositions and the absence of distinct boundaries within the Blue Grit support the suggestion that it was transported over a relatively short distance and across a steep or moderate slope. However, according to Carter (1975), there is already evidence to show that the generation of inertia flow (as opposed to turbidity flow) may not require slopes of more than a few degrees. Whatever its origin, the Blue Grit's petrology and outcrop pattern classifies it as a gravitite (Carter, 1975).

In summary, the proposed depositional environments for the Government Subgroup are similar to those of the Hospital Hill Subgroup in that many of the arenaceous units are interpreted as tide influenced shoreline deposits. However, the relative absence of both complex paleocurrent patterns and thick sequences of supermature bimodal sized sediments and the presence of immature subgreywackes distinguishes the units of the Government Subgroup from the Hospital Hill Subgroup. Eriksson *et al.* (in press) explains this difference as a result of tidal reworking of sediments in the Hospital Hill Subgroup. However, the writer believes that high-energy wave action on beaches and/or wind action accounts for the mature sands of the Hospital Hill Subgroup whilst the immature subgreywackes of the Government Subgroup were generally deposited in a less robust yet tide - influenced environment. This fact can be substantiated in that Middleton and Davis (1979) have shown that the intertidal sands in the Bay of Fundy are mineralogically immature yet the mean tidal range here exceeds 6 m. The only supermature rounded grains within the Bay of Fundy are the small pocket beach deposits.

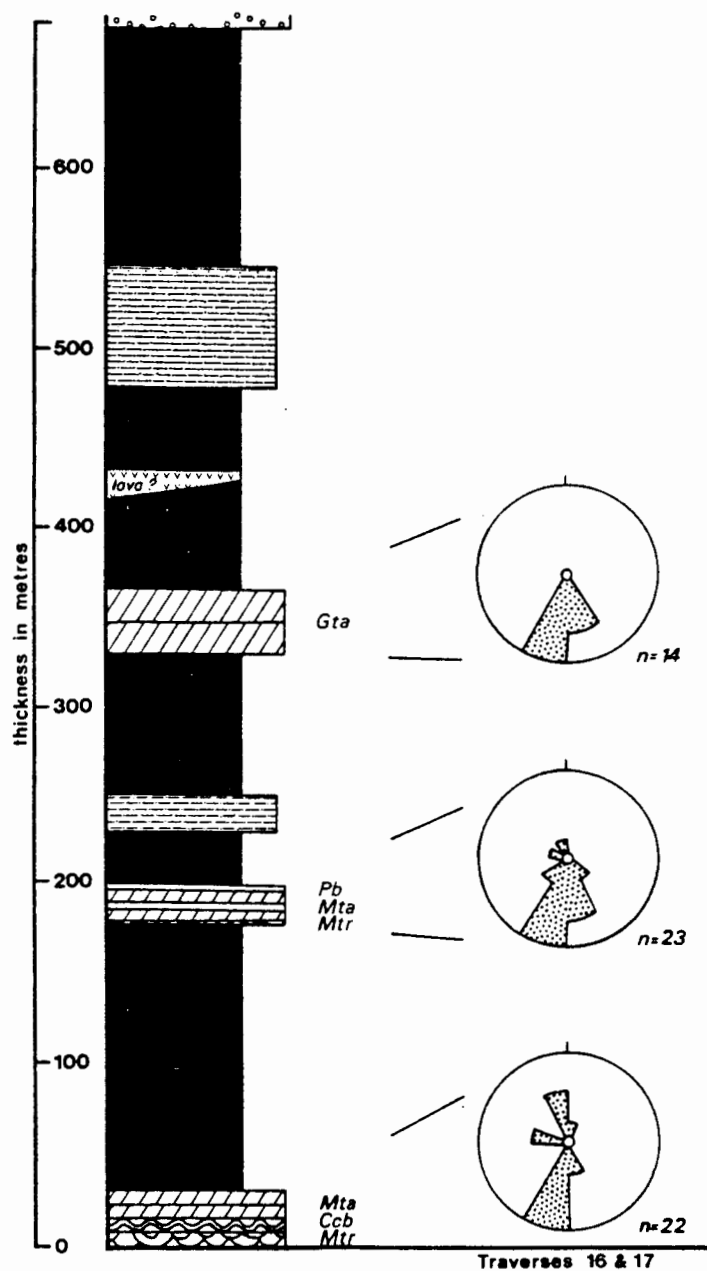
3.5 JEPPESTOWN SUBGROUP

Definition

The numerous intrusions of norites and quartz dolerites in the south of the study area together with the extensive cover of Karoo Supergroup sediments towards the north made the stratigraphic surface analysis of the Jeppetown Subgroup a difficult task. Plate 3.7a shows the poor exposure of the Jeppetown Subgroup. This complication was enhanced by the writer not recognising the Crown Lava in the field although it has been drilled in the area. The Crown Lava (or Jeppetown Amygdaloid) is a marker which splits the Subgroup into three formations. The approximate position of the marker is taken from Rogers (1922) and shown in Fig. 3.14.

The type area of development for the bottom half of Jeppetown Subgroup is the succession seen above the Blue Grit on the farm Groenfontein (T16 and T17). The upper half of the Formation was described by the writer by sub-surface stratigraphic analysis along a cross cut in the Witwatersrand-Nigel Mine.

JEPPESTOWN SUBGROUP



LEGEND

FACIES

- Mtr Medium trough crossbeds
- Gta Gigantic tabular crossbeds
- Mta Multiple sets of tabular crossbeds (often with mud drapes)
- Pb Plane bedding
- Ccb Convoluted bedding

LITHOLOGY

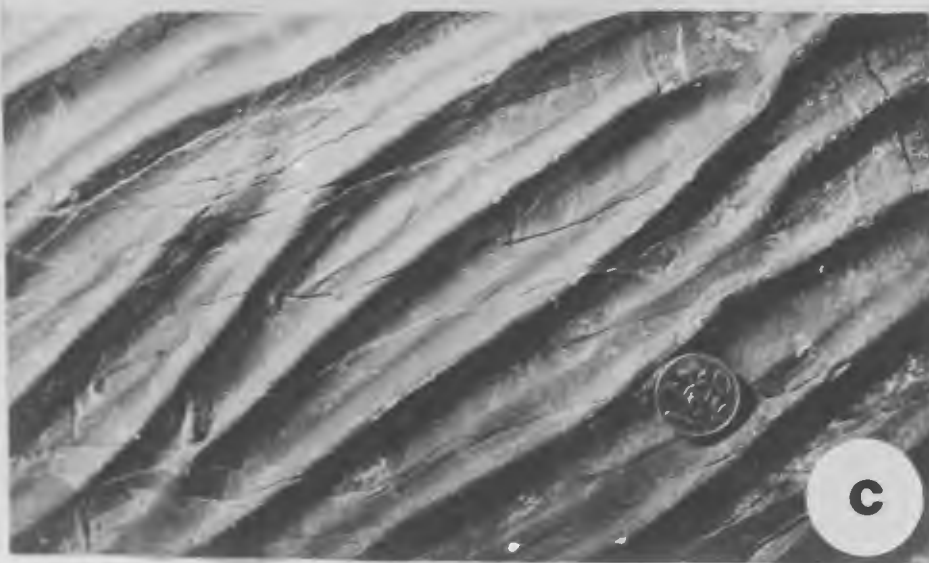
- Shales
- Siltstones (often graded)
- Sandstones

FIGURE 3.14 Generalized stratigraphic sequence of the Jeppestown Subgroup

P L A T E 3.7

- a. Poor outcrop of the Jeppestown Subgroup (Poortjie).
- b. Large tabular crossbeds developed within the third sandstone member of the Jeppestown Subgroup.
- c. Symmetrical, branching ripple marks with pointed crests and flat troughs photographed within the Witwatersrand-Nigel mine.

PLATE 3.7



Lithology

The Jeppestown Subgroup consists of three thick sandstone units, two siltstones units and an amygdaloidal lava all of which are separated by shale. The shale at the base of the Subgroup is distinctive in that intercalated thin bands of ferruginous rock are often present. The siltstones above the Crown Lava are often graded. Symmetrical, branching ripple marks with pointed crests and flat troughs (Plate 3.7c) which are cut by later calcite and quartz veinlets of later tectonic origin occur towards the top of the second siltstone unit. Ripple length varies generally from 8 cm to 30 cm. The geochemistry and mineralogy of the overlying shales will be described later in the chapter on geochemistry.

Sandstone units are much the same as those in the Government Subgroup, i.e. they are poorly sorted, submature and weather to a moderate orange pink (10R 7/4). One exception to this generalisation is the third and last thick arenaceous unit of the Jeppestown Subgroup. This sandstone is a submature, moderately sorted litharenite with a bimodal sand size distribution, (two sizes being 0.51 ϕ and 1.97 ϕ). The geochemistry (Appendix 4) of this sandstone is similar to the lithic arenites (sub-greywackes) as tabled in Pettijohn et al, 1973. The sediments above this horizon are chiefly shales and siltstones with thin discontinuous sandstones occurring within them.

Sedimentary Facies

The five facies indentified within the Jeppestown Subgroup are shown on Fig. 3.14.

The two lowermost sandstone units are dominated by multiple sets of tabular crossbeds which often have mud draped-foresets. Convolute and planar bedding are also common. The bases of the two units are characterised by medium sets of trough crossbeds. The third sandstone unit consists wholly of very large tabular crossbeds (Plate 3.7b). The overall geometry of the sets could not be ascertained because of the poor outcrop. The individual sets are up to 2.2 m thick. The length of the foresets exceeded 3 m and had an arithmetic mean corrected dip of 21 $^{\circ}$.

Paleocurrent Dispersal Pattern

Fig. 3.14 shows the paleocurrent dispersal pattern of the three sandstone

DIAGENESIS AND METAMORPHISM

4.1 INTRODUCTION

X-ray diffraction and petrographic descriptions of selected West Rand Group shale samples have been undertaken to establish the mineral assemblage present. Table 4.1 summarises the results. Most of the samples consist of quartz and chlorite and illite (or muscovite). Winkler (1974) notes that this assemblage persists unchanged from the diagenetic stage through the very low grade and low grade metamorphic stages to the beginning of medium grade metamorphism, disregarding the changes of crystallinity and structural order in the micas. As no diagnostic low grade metamorphic minerals such as laumontite, lawsonite, glaucophane, paragonite nor pyrophyllite were identified, the writer relied heavily on the white micas as petrogenetic indicators. The lattice spacing in white micas (muscovite, illite and sericite) is sensitive to compositional variations which in turn reflect the pressure or temperature conditions.

Muscovite belongs to only two main solid solution series. These include the muscovite - paragonite series where Na replaces K and the muscovite - celadonite (phengite) series where substitution of Fe/Mg for Al occurs. The effects of these end-member substitutions have been experimentally and theoretically researched (e.g. Velde, 1965). At low grade metamorphism an increase in temperature results in an increase of the Na content which causes a decrease in the basal spacing $d(002)$ of the mica. Likewise, an increase in the celadonite content with increasing pressure results in an increase in the $d(060)$ spacing (Cipriani *et al*; 1971). This relationship means that indirect chemical analysis is possible by means of XRD and depends on the change of $d(002)$ and $d(060)$ spacing with changes in composition. A review by Guidotti and Sassai (1976) summarises the theory on how the compositional variation of white mica is used as a geothermometer and geobarometer.

Table 4.1

Sample type and sample mineralogy as determined by X-ray diffraction										
SEDIMENT TYPE	SAMPLE	SUBGROUP			MINERALOGY					
		JEPPE- TOWN	GOVERN- MENT	HOSPITAL HILL	QUARTZ	CHLORITE	WHITE MICA	FELD- SPAR	MAGNE- TITE	CALCITE
Shale	PSC-1N	x			x	x	x			
Shale	PCS-2N	x			x	x	x			
Shale	PCS-4N	x			x	x	x			
Shale	PCS-8N	x			x	x	x			
Shale	PCS-11N	x			x	x	Trace			
Shale	PCS-13N	x			x	x	x	x		x
Shale	PCS-16N	x			x	x	x			
Shale	PCS-18N	x								
Shale	PCS-35N	x			x	x	x			
Sahle	PCS-32N	x			x	x	x			
Quartzite	PCS-26N	x			x	x	x			
Shale	PCS-31N	x			x	x	x			
Graded Siltstone	PCS-25N	x			x	x	x			
Tillite	TA		x		x	x	x			
Tillite	TB		x		x	x	x			
Shale	PWR	x			x	x	x	x		x
Graded Siltstone	WPGS	x			x	x	x			
Granitic Paleosol	PGR	Underlying Supergroup			x		x	x		
Shale	01/09			x	x	x	x		x	
Shale	04/13			x	x	x	x			
Magnetic Shale	05/01			x	x	x	x		x	
Shale	09/10		x		x	x	x			
Ironstone	11/04			x	x				x	
Diamictite	13/11		x		x	x				
Shale	15/14		x		x	x	x			
Shale	16/01		x		x	x	x			
Shale	17/01				x	x	x			

Two XRD techniques were used. The "illite crystallinity" method of Weber (1972) serves as a geothermometer while the method of Sassi and Scolari (1974) proved useful as a barometric indicator. The latter method involves the calculation of the b_0 cell dimension from measurement of the $d(060)$ spacing.

4.2 SAMPLE CHOICE AND PREPARATION

The choice and collection of samples was limited to a large degree by the poor quality of exposure. Furthermore, very quartz rich rocks and rocks in which k-feldspar and chlorite occur as essential components were to be avoided. In all these cases the b_0 values turn out to be higher than expected (Sassi and Scolari, 1974).

The first shale horizon in the Orange Grove Quartzite Formation fulfilled the above conditions, however, many shales within the Jeppestown Subgroup contained substantial amounts of chlorite (see Table 5.4). Nevertheless, the methods were attempted as chlorite does not affect the geothermometry results and the baric b_0 values for these samples (which is small anyway) can be regarded as an absolute maximum.

As the grain size of the samples affects the height and width of the white mica peaks, the writer used lightly polished rock slices cut parallel to cleavage (for geothermometry) and perpendicular to cleavage (for geobarometry). This quick and easy method of preparation was recommended by Guidotti and Sassi (1976) and proved successful in the study of Malmesbury shales (Spector, 1977; Antrobus, 1977) and Damaran pyllites (Kasch, 1979).

The XRD traces were run on a Philips Diffractometer. The angles scanned for the "illite crystallinity method" were from 9° - 10° for the mica peak and 19° - 21° for the external quartz standard (100 peak). Angles scanned for measurement of mica (060) peaks were from 59° - 63° as this included the mica and the quartz (211) peaks. The settings and calculations involved for the determination of both the b_0 cell dimension from measurement of the $d(060)$ spacing and the "crystallinity" of illite appear in Appendix 4.

4.3 GEO THERMOMETRY

Weaver (1960) used a sharpness ratio, defined as the ratio of the height

of the (002) illite peak at 10 Å to the height at 10,5 Å, to define the relative degree of diagenesis and metamorphism in pelitic rocks. Kubler (1966, 1968) on the other hand, used peak width (HS) in millimetres at half height above background. Modifying this method, Weber (1972) calculated the peak width of the mica peak (002) at half peak height and related it to the width at half peak height of the quartz (100) peak in an external standard. He defined the relative value as:-

$$Hb(rel) = \frac{Hb(002) \text{ illite (mm)}}{Hb(100) \text{ quartz (mm)}} \times 100$$

The object of using Hb(rel) is to normalise the Hb values relative to a standard, thus minimising instrument errors and rendering comparable the data

Table 4.2

Illite crystallinity HB(rel) of some selected West Rand Group shales			
SAMPLE	MEAN Hb(rel)	RANGE	NO. OF XRD RUNS
01/07	153	145 - 156	3
16/1	177	169 - 191	3
WPGS	168	160 - 182	5
PWR	121	111 - 149	4
TA	148	143 - 153	2
PCS-36	153	151 - 155	2
PCS-31	170	157 - 178	3
PCS-16	118	110 - 131	4
PCS-2	147	147 - 147	2
PCS-1	150	146 - 154	2
MEAN Hb(rel) = 150,5 ± 18,3			

Table 4.3

Relative degree of diagenesis and metamorphism of shales in the <u>West Rand Group</u>			
	KUBLER INDEX (Hb)	WEBER INDEX (Hbrel)	TEMP °C
DIAGENESIS	7	210	200
ANCHIZONE (very low grade)		150 (West Rand Group)	290
	4	130	350
EPIZONE (low grade)			
	2,7	85	520
MEDIUM GRADE			

from different workers.

Table 4.2 summarises the Hb(rel) values for several samples examined. The average Hb(rel) of 150 falls in the region of very low grade metamorphism (Table 4.3). Except for two samples the Weber indices are consistently below 210 (Kubler index = 7) and above 130 (Kubler index = 4). These two values define the anchizone (Frey, 1970). The two anomalous specimens both have a Weber index that is below 130. This indicates that some of the white micas are "well crystallised".

The regional distribution of the illite crystallinity does not show variations of metamorphism which can be correlated to different burial depths. The

1968). Using this fact Sassi and Scolari (1974) found that the b_0 cell dimension values for 140 samples increased with increasing pressure, and that it is practically identical in the micas from very different regions belonging to the same baric type of metamorphism. A b_0 scale was thus prepared which allows the distinction of six different facies series within low grade metamorphic terrains.

Table 4.4 summarises the results obtained. Of the 17 samples selected only 12 proved useful. The reproducibility of the b_0 values is good. On average the mean of two or more b_0 values of the same sample deviates by 0,00019 Å on successive runs. The mean b_0 value is $9,0019 \text{ Å} \pm 0,0204(1\sigma)$. However, excluding the thin Orange Grove Quartzite shale horizon, whose bulk composition is different to the thick green Jeppestown shales, the mean b_0 value is $9,0017 \text{ Å} \pm 0,0060(1\sigma)$. Because chlorite content increases the b_0 spacing, the value $9,0017 \text{ Å}$ probably represents a maximum value.

Figure 4.1 shows the cumulative frequency curves illustrating the distribution of b_0 in low grade zone metamorphic belts of various baric types. The West Rand Group rocks lie on the low pressure side (low b_0 values) of the Sassi and Scolari (1974) cumulative frequency curves between the Bosot and Northern New Hampshire curves. The metamorphism of the latter region belongs to the "low pressure intermediate group" of Miyashiro (Green, 1963) while Bosot metamorphism is characterised by the absence of a chlorite-rich zone and the occurrence of andalusite and cordierite (Zwart, 1963). Because the bulk composition of the Bosot rocks differs to that in the study area a direct comparison cannot be made. The mean b_0 value (9,0017) of the Jeppestown Subgroup falls between facies series 2 ($b_0 = 8,995$) and 3 ($b_0 = 9,010$) on the Sassi and Scolari (1974) empirical scale. These two series represent low pressure metamorphism (e.g. Hercynian metamorphism in Eastern Alps) and low-intermediate pressure metamorphism (e.g. Northern New-Hampshire). Remembering that 9,0017 is probably too high, the West Rand Group metamorphism is probably closer to the former.

As "the pressure values assigned to the various facies series are imprecise, much debated and susceptible to even drastic variations", Sassi and Scolari (1976) have not, as yet, attempted to establish a b_0 - P curve. Nevertheless, the relative barometric values obtained for the West Rand Group shales indicate that they have not been subjected to intermediate pressures (i.e. greater than 3,5 K-bar).

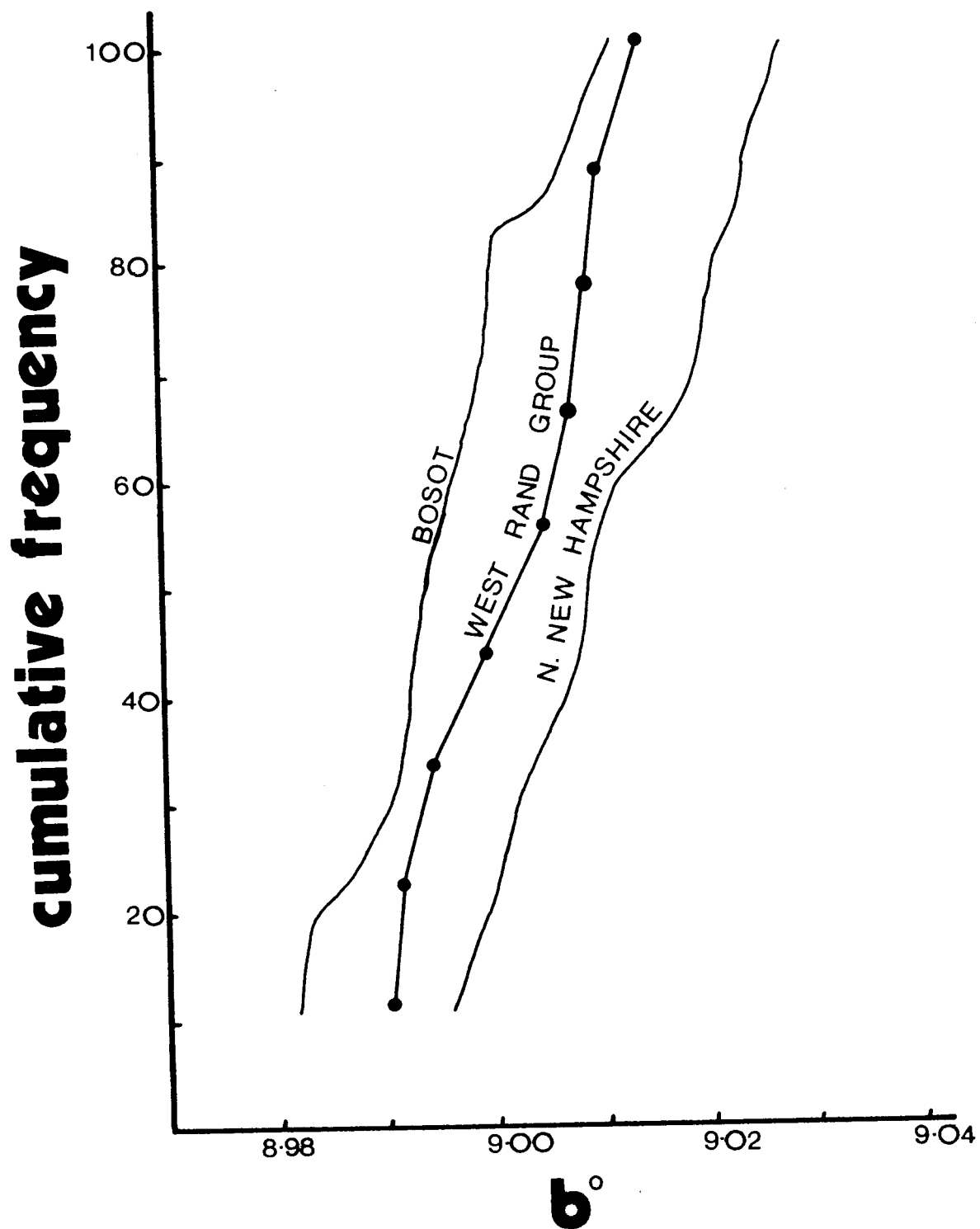


FIGURE 4.1 Cumulative frequency curves concerning the West Rand Group analytical data with comparative curves from Sassi and Scolari (1974)

4.5 CONCLUSION

The mineral assemblage in the shale of the West Rand Group is white mica and chlorite and quartz. The Weber crystallinity index indicate that these are low-grade rocks. The West Rand Group's $H_b(\text{rel})$ value of 150 corresponds to an approximate temperature of 290°C . The pressure regime can be distinguished on the basis of b_0 values. The study area's baric constraints are similar to the conditions as defined by Sassi and Scolari (1974) for the Hercynian metamorphism in the eastern Alps and by Di Pierro *et al.* (1973) for the pre-Alpine rocks in Calabria. Variations in P-T conditions in these areas have been studied by various workers (e.g. Hoffmann, 1970; Sassi, 1972) on the basis of paragenesis. There is considerable discordance in their interpretation. Therefore, until a P- b_0 curve is constructed, the geothermal gradient of the West Rand Group remains unknown.

GEOCHEMISTRY

5.1 GEOCHEMISTRY OF THE WEST RAND GROUP - A review

For obvious reasons, the coarse grained sedimentary rocks of the Witwatersrand Supergroup have been studied in great detail while a handful of workers (Fuller, 1958; Nel, 1968; Danchin, 1970; Hofmeyer, 1971; Fuller *et al*, 1979 and Sprague, 1979) have concentrated on the mineralogy and geochemistry of the shales.

Nel's (1968) study on the boron content of West Rand Group shale is of special importance as boron and other trace elements may be used to indicate their environment of deposition (Shimp *et al*; 1969). The basis of this concept is that certain trace elements such as boron, chlorine, lithium, sulphur and vanadium are concentrated more in sediments of marine origin than those of fresh water origin. The Jeppestown and Government shales yield average boron contents of 11ppm (range 5-21) and the average boron/potassium ratio is 8.3 p.p.m. (range 4.4-13). Although Nel (1968) concludes that the shales "are compared of the weathering products of igneous rocks deposited in a fresh water environment", he does emphasize the probability that little or no boron absorption occurred due to the small amounts of illite (which has a high absorptive capacity of boron, Harder, 1961).

Danchin (1970) and Hofmeyer (1971) have analysed 10 shale horizons within the Government and Jeppestown Subgroups. They found that the average MgO, total iron, P₂O₅, Na₂O, Ni, Cr and Co contents and the Ni/Co and V/Cr ratios are far closer to those of the Fig Tree Subgroup than the average South African shale. According to Danchin (1970) and Hofmeyer (1971) this correlation indicates that the source rocks for the Witwatersrand Supergroup must have been similar in petrology to the source rocks of the Fig Tree sediments although they probably contained a smaller ultrabasic component as the Ni concentrations and therefore the Ni/Co ratios are significantly lower.

Recently Sprague (1979) and the writer's geochemical results have been reviewed by Fuller et al; (1979). Using discriminant function analysis, Sprague (1979), characterised and distinguished Kaapvaal Craton shale. The data listings of the datasets (geochemical listings of shales within the West Rand, Mozaan and Fig Tree Groups) used in this exercise, were compiled by the writer, and are reproduced in Appendix 3. Fig. 5.1 summarises Sprague's (1979) results. The plots are a graphical display of how successfully pre-assigned groups are separated on the basis of geochemical criteria alone. In Fig. 5.1a the West Rand Group shales from the East Rand and from the Klerksdorp area plot in clearly separated clusters. Likewise, the Fig Tree and Central Rand shales form distinct clusters. The variables used in the construction of this display included both major and trace elements. When trace elements are omitted from the analysis the separation of the different groups is ill-defined (Fig. 5.1b). Only variables which discriminate most clearly between groups should therefore be used. Sprague (1979) does not delve into this problem although the discriminant function BMDP programme (P7M) used prints the F value for each variable. Before any variable is entered into the discriminant function, an F-statistic is computed from a one-way analysis of variance (ANOVA) on the variable for the groups used in the analysis. The highest F-statistic (F-to-enter) is the variable that discriminates the best between groups. These values for each variable (element) are given in Table 5.1. Sprague (1979) concludes "that with a much larger number of samples, it will be possible to positively identify an 'unknown' sample on the basis of the group it plots into on a canonical variable plot". From Table 4.1 much effort and time would be saved in reaching this goal if all the major elements and only the following trace elements - Sr, Ni, Rb, Ca, Zn, Cr, - were analysed.

In summary, the information that has been gained thus far on the chemistry of the West Rand Group includes:-

- i) The inability of boron - potassium ratios to distinguish marine from fresh-water shales within the West Rand Group
- ii) the validity of relating the chemistry of these rocks to the chemistry of potential source rocks (Granite - Greenstone terrains)
- iii) the ability to distinguish, on the basis of chemistry alone, the different argillaceous units on the Kaapvaal craton.

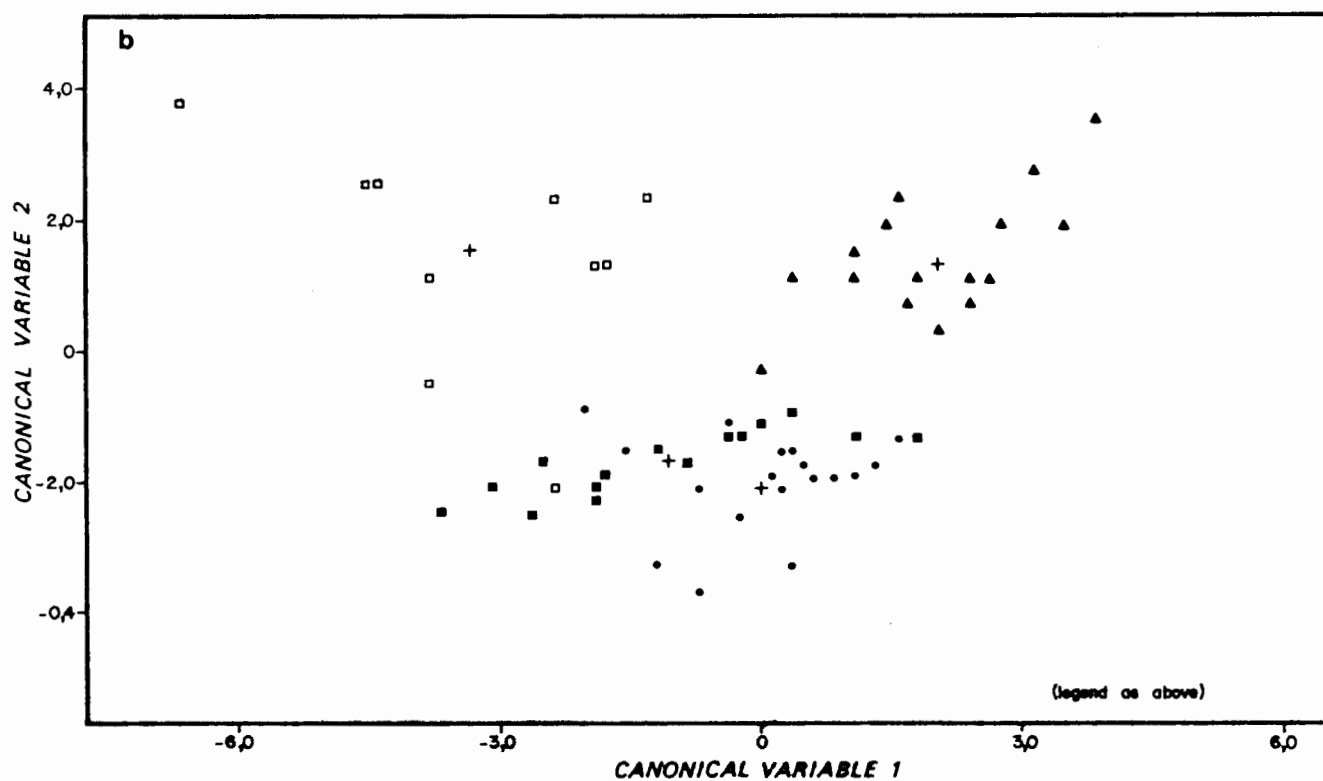
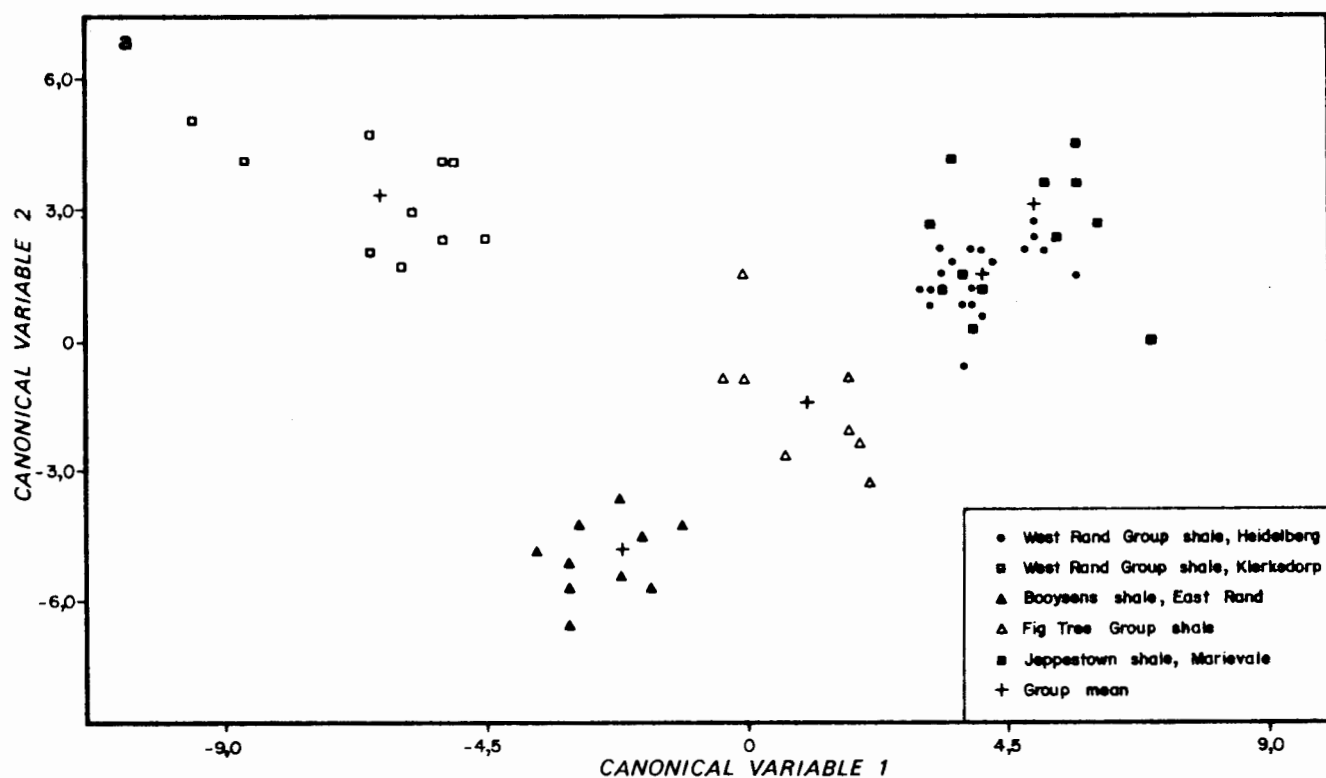


FIGURE 5.1 Discriminate function analysis of West Rand Group shales.

Very little is known about how the chemistry of a particular sample is related to its mineralogy, to what extent diagenesis has affected the original mineralogy of the sediment, and the geochemical profile of the shale immediately below the West Rand/Central Rand unconformity in the study area. These problems were investigated by the writer.

5.2 ANALYTICAL PROCEDURE

X-ray fluorescence spectrometry (XRF) has been increasingly utilised in the analysis of sedimentary materials (e.g. Danchin, 1970; Hofmeyer, 1971; Pearson, 1978). The general principles of the technique are described by Jenkins and de Vries (1967). All major elements (with the exception of Na)

Table 5.1

F-statistics for those elements which discriminates the best between Groups on the Kaapvaal Craton		
ELEMENT	F VALUE TO ENTER OR REMOVE	APPROXIMATE F-STATISTIC
Majors and trace elements (Figure 5.1a)		
Sr	56.59	56.59
Ni	29.16	40.82
SiO ₂	8.60	28.82
Rb	5.35	22.73
Al ₂ O ₃	9.17	21.34
Fe ₂ O ₃ *	8.57	20.65
K ₂ O	6.68	19.83
CaO	4.49	18.65
Major elements only (Figure 5.1b)		
Na ₂ O	43.42	43.42
Al ₂ O ₃	20.27	30.17
K ₂ O	19.18	32.54
Fe ₂ O ₃ *	5.63	28.22
* Fe ₂ O ₃ as Total Fe.		

were analysed by XRF, using the lithium tetraborate fusion of Norrish and Hutton (1969). Na was analysed by XRF on pressed powder briquettes, prepared using the method of Baird (1961). The operating conditions used are routine procedures adopted in the Department of Geochemistry, University of Cape Town, for the analysis of terrestrial, lunar and meteoric samples (Willis *et al*; 1971, 1977). Estimates of the precision and detection limit for each major oxide are given in Appendix 5 (Table 1). All trace elements were analysed by XRF using pressed powder briquettes. Success of this method for obtaining good quality trace element data is the similarity between the data produced by Willis *et al*; (1971) from lunar rocks and soils and that published by Carmichael *et al*; (1967) from standard rocks. Estimates of the uncertainties due to counting statistics are given in Appendix 5 (Table 2).

The concentration of twelve major elements (SiO_2 , TiO_2 , Al_2O_3 , Fe_2O_3 (Total Fe), MnO , MgO , CaO , Na_2O , K_2O , P_2O_5 , S, H_2O) and sixteen trace elements (Sr, Rb, Y, Zr, Nb, Zn, Co, Cu, Ni, V, Cr, Ga, Sc, U, Ba, Sc) have been determined in twenty-six West Rand Group samples. The geochemical data are reproduced in Table 5.2. The classification of the rocks together with their mineralogical composition, is summarised in Table 4.1.

5.3 MINERALOGY FROM BULK CHEMISTRY

Introduction

The identification of most minerals by x-ray diffraction is now routine (e.g. Table 4.1) but quantitative studies of clay minerals have only had a limited success. Schoen *et al*; (1972) reported variations in accuracy of up to 10 per cent in the most accurate techniques (that of Gibbs, 1967) used in clay mineral quantification studies. Gibbs (1967) set up and studied mixtures of standard clays, as did Schultz (1964). However, Gibbs obtained his standards by painstaking separation from his unknowns. The advantages of Gibbs's method are the close relationship between standard and unknown as well as the elimination of absorption problems by use of an internal standard. The minerals within the compact fine grained West Rand Group samples must be separated before quantification - a long and tedious process with complete separation (by crushing and pipetting) of the different fractions, an impossible aim. Pierce and Siegel (1969) show that almost any quantitative method (Johns *et al*; 1954; Schultz, 1964; Gibbs, 1967 and Brindley, 1961), applied consistently and carefully, will

Table 5.2

Geochemistry of West Rand Group shales - Heidelberg area (March 1979)														
MAJORS	PCS-1	PCS-2	PCS-4	PCS-8	PCS-11	PCS-13	PCS-16	PCS-18	PCS-25	PCS-31	PCS-32	PCS-36	PCS-26	TA
SiO ₂	58.60	60.68	53.79	53.81	57.11	48.36	55.62	51.78	73.04	56.13	57.30	57.57	89.48	70.49
TiO ₂	1.09	1.02	.65	.54	.50	.35	.65	.59	.34	.66	.64	.65	.11	.42
Al ₂ O ₃	23.84	22.41	13.84	12.74	11.07	8.67	14.39	13.47	9.66	15.05	14.47	14.90	5.32	10.81
Fe ₂ O ₃	3.76	5.55	20.40	20.98	19.43	9.52	16.14	21.26	6.67	13.63	14.37	12.62	1.36	10.65
MnO	0.02	0.04	0.17	0.17	0.17	.15	.09	.09	.05	.07	.07	.09	.02	.04
MgO	1.58	2.28	5.79	5.65	5.22	14.11	6.40	6.54	4.32	6.82	5.71	5.74	.97	2.42
CaO	0.03	0.02	0.15	0.28	0.35	6.94	.17	.25	.40	.11	.47	.67	.14	.04
Na ₂ O	0.19	0.16	0.01	0.01	0.01	.01	.02	.01	1.37	.03	.07	.03	.05	.00
K ₂ O	6.78	5.91	0.45	0.43	0.22	.01	1.64	.59	.64	2.02	1.95	2.81	1.55	2.01
P ₂ O ₅	0.00	0.02	0.09	0.07	0.09	.01	.09	.11	.01	.06	.09	.10	.00	.04
LOI	3.83	3.70	3.43	4.58	4.24	10.74	4.65	4.99	2.59	4.77	4.62	4.47	1.09	2.78
H ₂ O	0.17	0.12	0.13	0.14	0.13	.16	.17	.10	.15	.17	.09	.11	.11	.17
S	0.14	0.06	0.10	0.05	0.06	.03	.03	.04	.07	.05	.05	.02	.04	.15
TOTAL	100.03	101.97	99.00	99.45	98.60	99.06	100.06	99.82	99.32	99.58	99.92	98.50	100.28	100.02
TRACES														
Ba	748.5	659.8	92.5	118.0	64.4	0.0	346.0	120.8	141.3	438.5	428.8	775.1	377.3	343.5
Sc	40.2	42.4	21.6	18.5	18.2	29.5	23.2	21.3	9.0	23.2	24.0	25.0	4.0	13.2
Sr	16.4	13.2	3.7	7.1	6.9	221.2	25.0	6.6	87.8	8.0	15.8	8.7	7.7	8.6
Rb	221.4	190.2	16.9	20.3	9.8	0.0	71.7	26.2	23.5	77.5	77.8	107.8	49.4	85.9
Y	16.7	16.6	21.1	21.7	23.5	9.3	21.3	19.1		21.5	12.8	22.0	5.3	19.3
Zr	189.5	169.6	154.0	131.6	126.1	32.9	136.2	127.1	100.8	131.8	125.4	142.4	48.4	136.5
Nb	12.0	10.4	8.7	7.4	7.9	0.0	7.0	7.6	4.2	8.2	7.0	6.9	0.0	5.8
Zn	20.3	27.9	97.8	105.6	102.2	62.0	78.7	89.1	61.4	85.7	75.5	84.5	12.3	49.6
Cu	13.0	10.9	13.3	15.6	47.0	34.5	18.5	57.6	22.2	32.3	56.1	44.6	4.6	38.4
Co	72.6	48.3	40.4	34.2	30.8	73.6	37.4	38.8	0.8	39.2	41.2	41.6	6.1	20.2
Ni	280.5	331.6	333.5	286.3	241.6	427.9	307.9	288.6	150.8	306.0	277.6	317.2	30.5	140.3
V	276.1	227.4	141.6	126.8	123.1	140.2	147.8	143.9	62.8	150.0	148.3	155.3	23.1	88.2
Cr	1412.0	1370.0	780.5	642.4	598.6	1971.0	670.5	682.6	462.3	674.2	673.6	718.9	78.6	348.1
Ga	27.6	25.9	17.4	16.9	14.7	8.5	18.6	17.0	10.2	18.3	18.0	19.3	5.5	13.1
U	12.7	1.6	0.0	1.1	0.0	0.0	00	0.0	0.0	0.0	0.0	0.2	0.0	0.4

provide good precision. As progressive changes in the relative amounts of clay minerals are required for most applied studies, good precision and not good accuracy is the only requisite. In this study, the writer used a technique developed by Pearson (1978) which uses both XRD and XRF methods yielding more accurate and equally precise results than the aforementioned workers.

Method

Pearson (1978) devised a scheme to calculate mineral abundance from bulk chemical analyses of fine grained sedimentary rocks. The assumptions about element location are essentially the same as those made in the schemes of Imbrie and Poldervaart (1959) and Nicholls (1962) in that free SiO_2 , Ti, S, P and CO_2 are assigned to quartz, rutile, pyrite, apatite and carbonates respectively. The remainder is assigned to clay silicates on the assumption that these are dominated by non-expanding clays (muscovite and illite), chlorite and/or kaolinite. The method of clay mineral calculation is detailed and only the briefest summary is given here. For further information, the reader is referred to the papers by Nicholls (1962), Mietsch (1962) and Pearson (1978).

The chemical composition of any rock type can be related to its known mineral constituents' compositions by a set of simultaneous equations of the type:

$$a_i x + b_i y + c_i z + 100k_i \dots\dots\dots (1)$$

where a_i , b_i , c_i and k_i , are the percentages of element i in mineral phases X, Y, Z and the bulk rock respectively and x , y and z are the percentages of phases X, Y and Z present in the rock. Assuming that the average clay composition of the West Rand Group shales can be partitioned between three phases, muscovite, illite and chlorite, and that their compositions can be adequately approximated by analyses from the literature of clay minerals from rocks of a similar type, equations of type (1) can then be applied. Table 5.3 shows some analyses from Deer et al; (1974) which have been chosen according to the above criteria. The composition of one of the chlorites used was that of brunswigite which was identified by Fuller (1958) in a sample 20 m below the Main Conglomerate on the East Rand. Readjusting components in the muscovite and chlorite in Table 5.3 was helped by the predominance of only one clay phase noted in certain XRD traces. For example,

samples /67

samples PCS-4 and 13/11 consist essentially of two phases - chlorite and quartz - while PCS-1 contained quartz and muscovite with very little chlorite. By recalculating the bulk chemical compositions, a crude approximation was obtained for the chemistry of chlorite and muscovite. Ideally, if available, microprobe analysis of the three individual clay phases run on a number of West Rand Group samples would yield far superior average chlorite, muscovite and illite compositions.

Of the major constituent oxides which could be used to set up equations

Table 5.3

Reference analyses of clay minerals (weight percent)							
	MU			CH		KA	IL
	1	2	1	2	3		
SiO ₂	45.87	48.42	25.07	26.40	27.11	45.77	56.92
Al ₂ O ₃	38.69	27.16	19.78	18.23	17.42	39.07	18.50
K ₂ O	10.08	11.23	00.50	00.27	00.00	00.31	05.10
MgO	00.10	00.10	11.67	10.35	09.75	00.08	02.07
FeO	00.00	7.38	21.66	31.57	33.89	00.04	00.26
Fe ₂ O ₃	00.00		07.54			00.30	04.99
CaO	00.00	00.01	01.04	00.82	00.21	00.26	01.59
Na ₂ O	00.64	00.25	00.18	00.01	00.00	00.17	00.43
H ₂ O ⁺	04.67	04.31	10.82	10.01	11.07	13.68	05.98
FM ⁺	00.10	07.39	40.87	42.92	43.64	00.42	07.32

MU 1	Clear flawless muscovite, New Mexico. Analysis 1, Deer et al (1974) pg. 196.
MU 2	Analysis 2, Deer et al (1978), pg. 198.
CH 1	From Pearson (1978).
CH 2	Analysis 8, Deer et al (1978), pg. 235, with adjusted K ₂ O, MgO, FeO, Fe ₂ O ₃ .
CH 3	Brunswigite, New Zealand. Analysis 6, Deer et al (1974), pg. 235.
KA	From Pearson (1978).
IL	Illite, Fithian, Illinois. Analysis 3, Deer et al (1974), pg. 251.
FM ⁺ = MgO + FeO + Fe ₂ O ₃	

of the type (1), SiO_2 , Al_2O_3 , and K_2O are the most reliable but errors are only slightly increased if total $\text{Fe}_2\text{O}_3 + \text{MgO}$ is substituted for SiO_2 (Pearson, 1978). It is known that K_2O resides almost wholly in mica, MgO and FeO reside mainly in chlorite while Fe_2O_3 may reside in mica or chlorite or both. Thus, taking MU, IL and CH as the compositions of muscovite, illite and chlorite respectively, and applying equation (1) to SiO_2 , for PCS-1, PCS-2, PCS-4 etc., gives a linear equation. By applying the same procedure to Al_2O_3 , MgO and K_2O a set of simultaneous equations is set up and may be solved either graphically (Meitsch, 1962) or with the help of a computer whereby solutions for up to eight phases can be obtained by matrix inversion (Pearson, 1978).

With very minor modification the writer used the programme written by Pearson (1978). The data input file includes analyses on Table 5.3 and the writer's bulk major chemical analyses of West Rand Group sediments (Table 5.2). As the programme has a facility whereby oxides not used in solving the equations can be recalculated and compared with their input values, any large deviation indicates that one or more of the clay mineral compositions chosen (Table 5.3) is a poor approximation to the real phase. A different permutation is then attempted to minimise the deviation.

In summary, using Pearson's (1978) method acceptable clay mineral analyses can be produced from XRF analyses supplemented by a knowledge of the amount of quartz in each sample. The determination of the number of clay mineral phases and the amount of quartz in each sample are the only operations performed by XRD.

Results

a) Mineralogical Analysis

Table 5.4 summarises the mineralogical analyses of seventeen shales, two tillites and one diamictite. The average quartz content of the shales is 28.57 per cent while the mean clay content is 67.70 per cent indicating that over ninety-five per cent of the sample is made up of these two components.

Using recent mineralogical information, and average chemical composition data, Yaalon (1961) calculated the mineralogical composition of a variety of shales. Contrary to earlier workers, he found

Table 5.4

Mineralogical analysis of bulk sample (weight percent)								
SAMPLE	QUARTZ	PYRITE	APATITE	RUTILE	CALCITE	Mn 0	TOTAL CLAY	MISC*
PCS-1	27.40	0.26	00.00	1.29	0.05	0.02	72.26	-1.28
PCS-2	26.6	0.11	00.05	1.02	0.02	0.04	69.26	2.9
PCS-4	24.4	0.19	00.21	0.65	0.13	0.17	72.20	2.05
PCS-8	26.3	0.09	0.17	0.54	0.50	0.17	66.99	5.24
PCS-11	28.0	0.11	0.21	0.50	0.63	0.17	68.88	1.5
PCS-16	16.9	0.06	0.21	0.65	0.30	0.09	76.71	5.08
PCS-18	15.8	0.07	0.26	0.59	0.44	0.09	71.75	10.9
PCS-31	28.7	0.09	0.14	0.66	0.19	0.07	72.89	-2.74
PCS-32	28.3	0.09	0.21	0.64	0.83	0.07	74.13	-4.27
PCS-36	27.4	0.04	0.24	0.65	1.19	0.09	68.84	1.55
PWR	35.9	0.30	0.14	0.64	4.80	0.11	56.15	1.96
WPGS	23.2	0.04	0.21	0.64	2.32	0.11	75.73	-2.25
01/09	33.72	0.02	1.16	0.57	0.05	0.03	69.29	-4.84
04/03	38.8	0.02	0.17	0.53	0.02	0.22	56.2	4.04
09/10	46.0	0.02	0.21	0.81	0.03	0.05	52.83	0.05
16/01	24.5	0.02	0.05	0.44	0.05	0.03	62.15	12.55
17/01	33.8	0.02	0.02	0.65	0.02	0.04	64.79	0.66
TA	59.4	0.28	0.04	0.42	0.13	0.04	36.4	4.3
TB	37.9	0.30	0.02	0.42	0.11	0.04	?	?
13/11	75.9	0.02	0.02	0.24	0.01	0.11	?	?

* Miscellaneous minerals which include feldspar, magnesite, siderite and other unidentified minerals. Note that the XRD method for the estimation of quartz (Johns et al, 1954) has an accuracy of less than 10%. This error is included within Misc.

a major decrease in feldspar and an approximate doubling of the clay content. Shaw and Weaver (1965) determined the mineral composition of 400 shale samples from 60 formations in North America. They noted that the average clay content of 61% was similar to that calculated by Yaalon, although the quartz content (31%) was significantly higher. Furthermore, they have demonstrated on a regional basis, the significant relationship between bulk mineralogical content and environment of deposition. These authors have prepared a series of mineral variation diagrams for environments ranging from fluviatile to deep-sea. In the former the quartz content is 52% and clays 29% while the deep-sea quartz content is 16%. The clay/quartz ratio of the West Rand Group (2.37) falls closest to the environment termed "deltaic" on Shaw and Weaver's plot. The clay/quartz ratios here is 2.24 while the ratios in the lagoonal and slope environments are 0.85 and 4.00 respectively. Clearly, Shaw and Weaver's (1965) plots are generalisations and large variations in the quartz/clay ratios within a single delta may occur. However, because of the lack of exposure in the Jeppestown Subgroup and the absence of significant sedimentary structures, knowledge of its depositional environment is extremely scant and this broad (if somewhat arbitrary) classification is justifiable.

Rutile occurs mainly in beach sediments, dune sands, and shelf placers (Pettijohn et al, 1972). Its high concentration in two of the shale specimens (PCS-1, PCS-2) sampled immediately below the Main Conglomerate horizon is therefore difficult to explain in terms of depositional environment. The enrichment of rutile in these two samples may be explained by its resistance to weathering. In acid rich soil profiles von Engelhart (1940) found 2.4% TiO_2 in soil horizon A, 1% TiO_2 in soil horizon B and 0.4% TiO_2 in unweathered material. Here the accumulation of TiO_2 in the soil is explained by the migration of Ti. The geochemical profile below the Main Conglomerate is probably a paleosol and will be elaborated upon later. The average rutile content in the 15 shales below this profile is 0.61%. This value is slightly lower than the TiO_2 contents found elsewhere (e.g. Russian platform (0.86%) and Caucasian geosyncline (0.7%), Ronov and Yaroshevskiy, 1968).

The low calcite content in the two samples immediately below the

Main Conglomerate was expected because of its decomposition due to chemical weathering. The erratic distribution of CaCO_3 below the paleosol profile may be due to Ca mobilisation during low grade metamorphism (Usdowski, 1968). It was noted that secondary calcite was prolific along many fault and joint planes. Though extreme care was taken in not sampling such specimens, the erratic distribution of the minerals may also suggest that the sorting of fresh from altered material by naked eye inspection was not satisfactory.

The average Na_2O content of the shale is 0.06 (wt %). Van Houten (1965) has shown that shales with a high Na content contain more Na feldspar. The complete lack of feldspar (Table 4.1) in most of the West Rand Group shales probably accounts for the low Na content. The only sample with an appreciable amount of Na was PWR. However, even in this case its Na_2O (0.37%) content is way below the mean content (0.8 ± 0.03 wt %) of 1,152 shales as quoted by Heier and Billings (1978).

Excluding sample 01/09 which has an anomalous amount of apatite (P_2O_5) and the two samples immediately below the Main Conglomerate, the average P_2O_5 content for the West Rand Group shales is 0.153%. Koritnig (1978) has summarised numerous data on the phosphorus content of sedimentary rocks and noted the following average data for clastic rocks:-

Deep sea clay	0.28% P_2O_5
Shelf clays and shales	0.15%
Greywackes	0.13%
Quartzite	0.06%

The conclusion reached by the writer in the chapter on stratigraphy was that most of the shales in the West Rand Group were deposited in a shelf environment. The data is thus in accordance with Koritnig's (1978) findings.

The erratic distribution of pyrite indicates that it is probably secondary. Sprague (1979) noted the close relationship that pyrite has with quartz veins when he observed that pyrite occurs as angular grains, idiomorphic crystals and irregular aggregates with numerous

quartz inclusions. The pyrite must therefore have been precipitated from solution.

b) Clay Mineral Abundances

Table 5.5 shows the distribution of kaolinite, muscovite, illite and chlorite within twenty samples. Seven shale samples were routinely examined by X-ray analysis for the identification of kaolinite, montmorillonite and different types of chlorite as described by Carrol (1970). Heat treatment and glycolation indicated that neither kaolinite nor montmorillonite group minerals were present. When samples PCS-4, PCS-8, PCS-11 and PCS-2 were heated at 650°C the 14 Å spacing was intensified. This indicates that the chlorites are Mg-chlorites. Although kaolinite was not identified the mineral was experimentally included as a fourth phase in Pearson's programme. Surprisingly, when this was done, four samples (PCS-32, PWR, 09/10, 17/01) had smaller deviations of recalculated oxides than when only three phases (chlorite, muscovite and illite) were used.

All the shales are coloured various shades of green (5GY 7/2) due to the presence of illite and chlorite. The green colour may also be due to the presence of ferrous (reduced) iron in the clay minerals (Weaver, 1978). The great abundance of chlorite and illite is probably due to regressive diagenesis (catamorphism) and anchimeta-morphism. The lack of kaolinite and montmorillonite indicates that the following diagenetic sequence probably occurred:-

- i) Formation of chlorite from kaolinite (Frey, 1970)
- ii) Montmorillonite (smectite) is transformed to mixed layer montmorillonite and then illite (Dietz, 1941).

However, although angular to sub-angular idiomorphic laths of chlorite which grew during diagenesis were recognised in thin section, rounded detrital chlorite grains were also present - albeit rare. This is interesting in that it indicates rapid deposition from a diagenetically advanced to low grade metamorphosed source. Compaction and recrystallisation of clay minerals during burial are irreversible. Chlorites are extremely sensitive to chemical weathering and undergo dissolution, transformation and neoformation

in soils. The source area must, therefore, have been a continental region where physical, as opposed to chemical, weathering processes were dominant. The original primary genesis of the chlorites and

Table 5.5

<u>Clay mineral abundances as weight percent clay fraction</u>					
SAMPLE	KAOLINITE	MUSCOVITE	ILLITE	CHLORITE	TOTAL MICA
PCS-1		80.92	2.13	6.95	93.05
PCS-2		57.62	25.02	17.36	82.64
PCS-4			18.88	81.02	18.88
PCS-8			22.71	77.89	22.71
PCS-11			24.53	75.47	24.53
PCS-16			46.34	53.66	46.34
PCS-18			29.92	70.08	29.92
PCS-31		6.94	34.91	58.15	41.85
PCS-32	0.13	1.54	43.19	55.14	44.73
PCS-36		17.82	32.74	49.44	40.56
PWR	3.81	16.44	32.58	47.17	49.01
WPGS		1.71	34.70	63.59	36.41
01/09		1.89	50.78	47.33	52.67
04/13		26.82	51.70	21.48	78.52
09/10	0.86	26.34	16.32	56.48	42.66
16/01			62.66	37.34	62.66
17/01	3.31	28.10	37.79	30.79	65.90
TA		51.84		48.16	51.84
TB			62.83	37.17	62.83
13/11				100.00	

illites which were not formed diagenetically was probably due to the uplift of igneous and metamorphic rocks with the consequent formation of illite in feldspar and chlorite in mafic minerals (Lelong and Millot, 1966).

There is very little variation in the abundances of the clay suite through the vertical section (chlorite > illite) except for the two shale samples (PCS-1, PCS-2) immediately below the Main Conglo-

merate, the tillites (TA, TB), the diamictite (13/11) and the two shales (04/13, 06/01) sampled in the Hospital Hill Subgroup. Weaver (1978b) notes that continental flood-plain and lacustrine shale deposits have clay suite compositions that show wide variations while geosynclinal marine shales and thin, epicontinental shales have a uniform clay suite. Although different depositional environments have different clay mineral suites and subtle environmental differences can be detected by changes in the clay suite (e.g. Weaver, 1967; Keller, 1970) the writer's sample size is far too small for such inferences. Furthermore, as the clay suite at the site of sampling is not only a function of source material and climatic conditions but also of advanced diagenesis and possible neoformation such a study would have probably been fruitless.

Conclusion

In summary, as the major element chemical composition of shales is closely related to their mineralogy, the relative amounts of clays present in a sample can be calculated from its bulk chemistry. A computer programme and technique, developed by Pearson (1978), proved useful in quantifying mineral analyses from the bulk chemistry of West Rand Group sediments.

The results indicate that - in most cases - chlorite, illite and muscovite (in that order) are the major clay phases present. Small amounts of kaolinite were also identified in four specimens. The samples immediately below the Main Conglomerate show interesting variations in their calcite, rutile and clay mineral abundances. These mineralogical variations are, by definition, closely related to the distribution of the major elements. Fig. 5.2 shows the distribution of major elements in four specimens (PCS-1, PCS-2, PCS-4 and PCS-8) sampled at different depths below the base of the Main Conglomerate. Comparing Fig. 5.2 and Table 5.5 the increase in chlorite with depth is concomitant with an increase in MgO and Fe_2O_3 . Likewise, a sympathetic relationship exists between the total mica, K_2O and Al_2O_3 contents.

5.4 DISTRIBUTION OF TRACE ELEMENTS

As over 95 per cent of the West Rand Group shales are made up of quartz and clay minerals, most of the elements present in trace amounts are located

in the clay fraction. The clay mineral suite of any particular shale reflects the combined effects of the source material, of the diagenetic history and possibly the depositional history. The trace elements could therefore conceptually become incorporated in clay mineral structures at any of these three different stages.

The exceptionally high content of Cr in the Fig Tree shale suggested to Danchin (1970), that the source rocks were either ultramafic or, less likely, mafic in composition. Some trace elements (Cr, Co, Ni) retain their relative abundances during physical weathering, transportation and deposition and are indicative of the nature of the source area. Shaw (1954) studied the geochemistry of sixty three rocks of the pelitic Devonian Littleton Formation of New Hampshire. The samples represent all grades of diagenesis and metamorphism from shales to sillimanite schists to gneisses. He showed that the concentration of most trace elements remained constant during regional metamorphism, exceptions being Ni and Cu, which showed a slight decrease, and Li and Pb a well defined increase. Hence, diagenesis does not markedly affect trace element distribution. Those trace elements which are often more concentrated in shales than in igneous rocks because of sorption by the clay colloidal particles in the environment of deposition are the most promising environmental discriminants and indicators (Wedepohl, 1971). However, in the review on the West Rand Group (Appendix 1), it was concluded that, though these elements (B, CL, Li, S, V, Cr) are generally more abundant in marine shales than in continental clays in both modern and ancient environments, their applicability in Archaean shales is limited (Nel, 1968).

Previous work, thus suggests, that during diagenesis and early metamorphism when K or Mg are reconstituted by absorption between the layers of illite and chlorite, the trace element distribution is not affected and thus strongly reflects the character of their provenance. Table 5.6 contains the means, variances, standard deviations and coefficient of variations for ten major and fifteen trace elements of seventeen representative shale samples. The elemental averages of 316 South African shales (from Hofmeyer, 1971 and Danchin, 1970) are included for comparison.

Clearly, Ni, Cr and Co contents are far higher than the average South African shale. The writer's data thus agrees with Danchin's (1970) and Hofmeyer's (1971) work in the Klerksdorp area, and the source rocks for the West Rand Group in the study area must have been similar in petrology to the source

Table 5.6

The average elemental abundances of seventeen
selected West Rand Group shales

ELEMENT	MEAN	VARIANCE	STANDARD DEVIATION	COEFF. OF VARIATION	AVERAGE S.A. SHALE (316 SAMPLES)
Si	56.93	19.57	4.42	0.078	66.21
Ti	0.59	0.01	0.10	0.175	0.90
Al ₂ O ₃	13.38	2.42	1.56	0.116	18.97
Fe ₂ O ₃	15.89	36.79	6.07	0.382	6.18
MnO	0.11	0.00	0.07	0.656	
MgO	5.00	2.39	1.55	0.309	1.86
CaO	0.57	1.67	1.29	2.270	0.78
Na ₂ O	0.05	0.01	0.09	1.674	
K ₂ O	1.71	0.83	0.91	0.523	
P ₂ O ₅	0.09	0.01	0.11	1.141	
Ba	388.0	66171.4	257.2	0.663	
Sr	17.0	362.5	19.0	0.110	
Rb	79.5	2126.4	46.1	0.580	
Y	20.4	15.1	3.9	0.191	
Zr	147.2	2487.3	49.9	0.339	215.0
Nb	7.6	3.1	1.8	0.242	15.7
Zn	86.0	562.8	23.7	0.276	83.9
Cu	44.3	548.7	23.4	0.258	
Co	35.5	58.5	7.7	0.216	15.9
Ni	280.7	13204.7	114.9	0.409	34.3
V	129.3	566.2	23.8	0.184	103.0
Cr	703.8	107650.8	328.1	0.456	99.2
Ga	17.0	2.7	1.7	0.098	20.4
Sc	20.4	17.22	4.1	0.203	14.3
U	0.3	0.4	0.6	2.058	
Th	0.0	0.0	0.0	0.000	

rocks of the Fig Tree sediments. Indeed, the lower Ni, Co and Cr values of the West Rand Group compared to the Fig Tree Group, together with the petrology of the sandstones, suggest that sediments characteristic of the Fig Tree Group itself, constituted the provenance for the West Rand Group.

5.4.1 Jeppestown Paleosol

No characteristic paleosol colour changes occur within the upper Jeppestown shale. All the shales sampled within the Witwatersrand-Nigel mine were green (5GY 7/2). Nevertheless, the absence of flame structures at the base of the Main Conglomerate horizon and the unconformable relationship between the West Rand Group and Central Rand Group indicate a hiatus between the two Groups. Whether the Upper Jeppestown shale was wholly exposed to subaerial weathering is not known but Button (pers. comm.) noted that the Central Rand Group at Houtpoort, 15 km south west of the Witwatersrand-Nigel Mine, consisted of a braided stream facies at the base overlain by a tidal-marine facies. Subaerial exposure is thus likely and several specimens (PCS-1, PCS-2, PCS-4, PCS-8) were sampled to ascertain whether geochemical criteria, as opposed to colour changes, could define the Jeppestown paleosol.

The distributions of trace elements and major elements in four samples below the Main Reef Conglomerate are shown on Fig 5.3 and 5.2 respectively. It is readily seen that SiO_2 , TiO_2 , Al_2O_3 and K_2O decrease with depth below the Conglomerate while total Fe and MgO increase. The only trace element that increases with depth is that of Zn. These increases and decreases in weight percentages can be regarded relative because of the open system. To test these relative increases and decreases, the ratios of all the major and trace elements to Ti were calculated because of the limited mobility of Ti under weathering conditions. When this ratio is plotted with depth the same trends are evident and thus the elemental variations on Fig. 5.2 and 5.3 are real.

The decrease in K_2O and increase in Fe_2O_3 and MgO is due to the clay minerals present. Muscovite and chlorite show an inverse relationship with muscovite (K_2O) decreasing and chlorite (total Fe and MgO) increasing with depth (Table 5.5). Ti is locally accumulated in

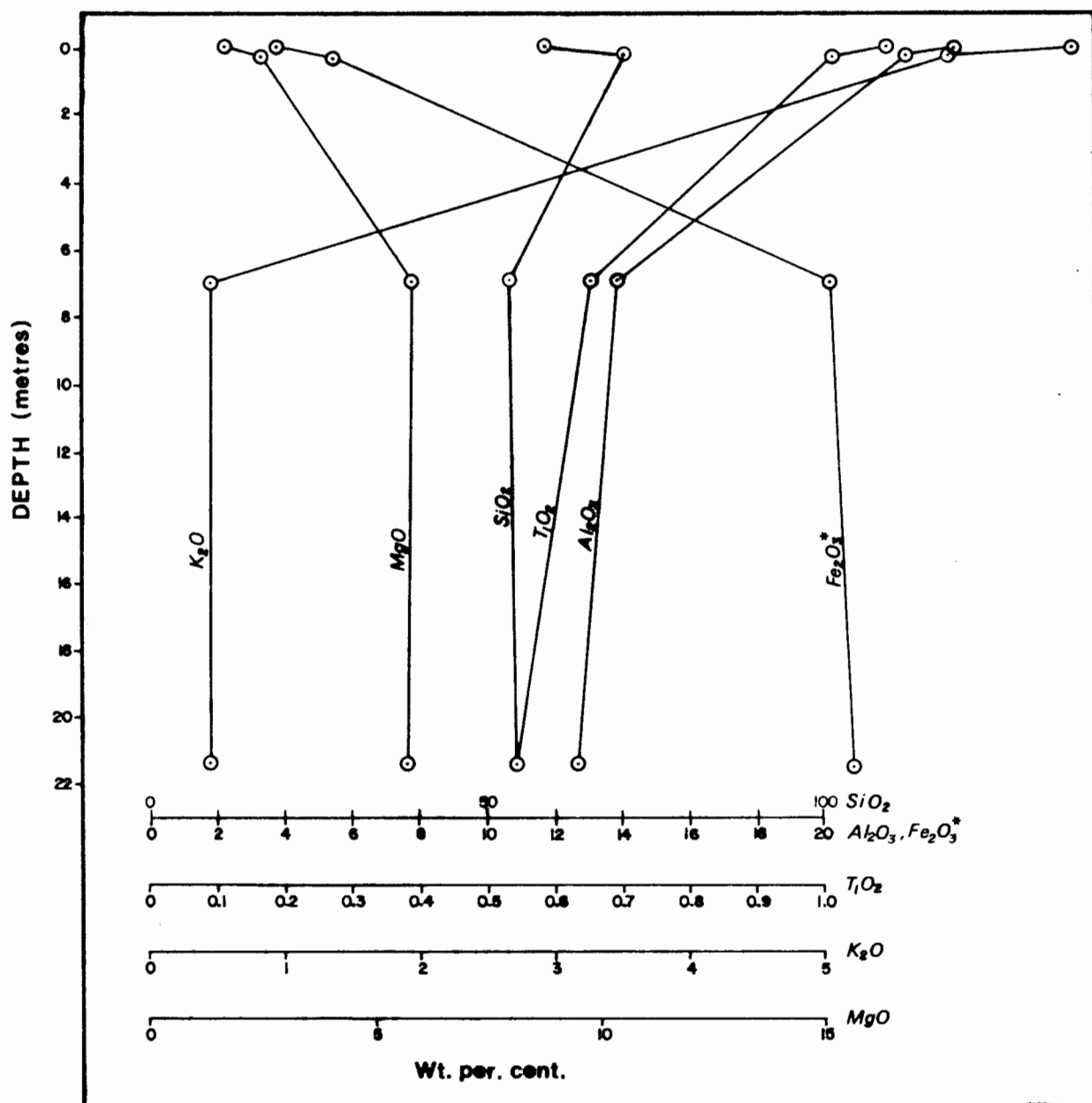


FIGURE 5.2 Distribution of major elements below West Rand/Central Rand unconformity

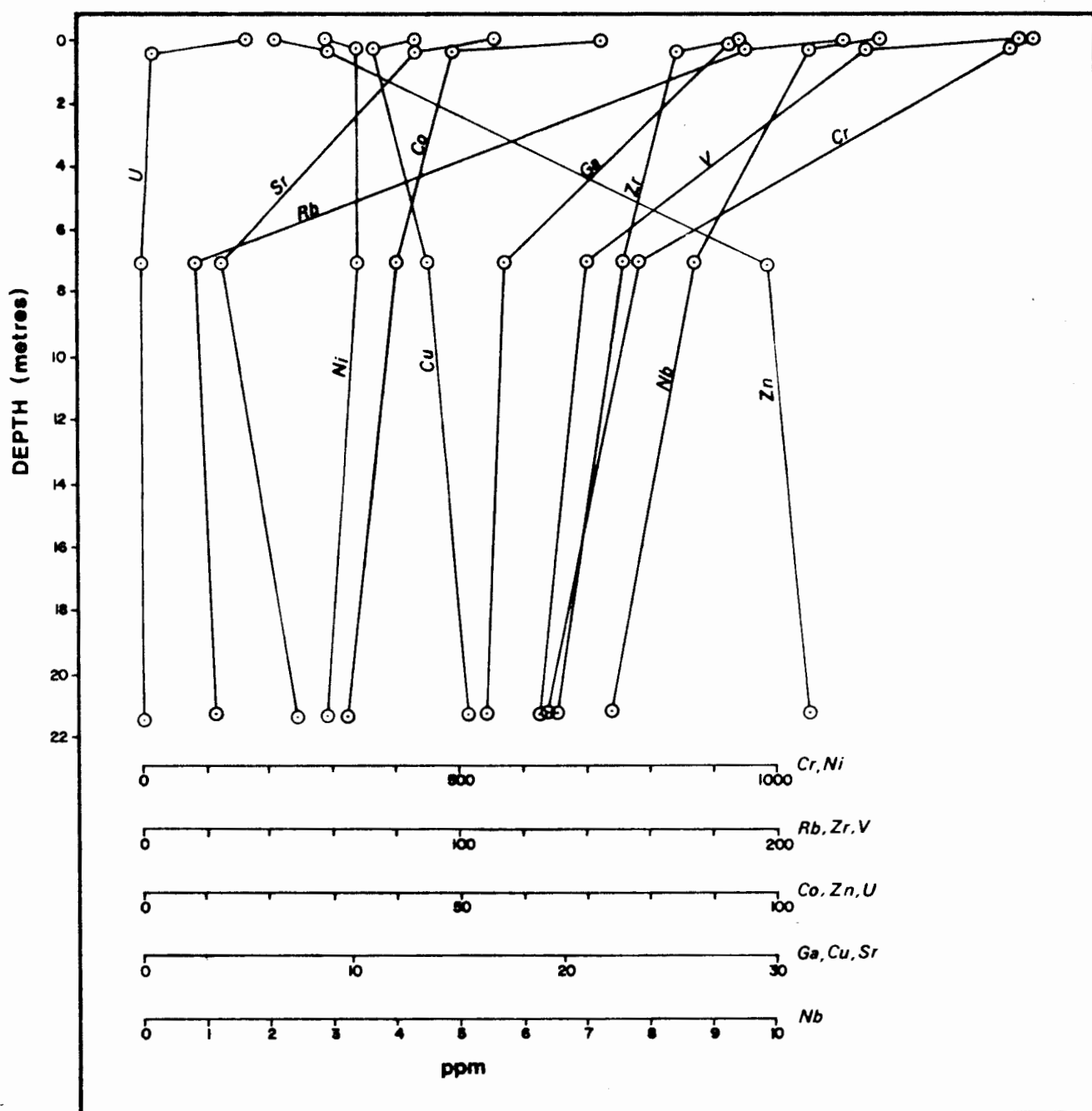


FIGURE 5.3 Distribution of trace elements below West Rand/Central Rand unconformity

weathering processes and so is Al. The SiO_2 content is governed by the amount of quartz in the sample.

Cr present in chromite, magnetite and ilmenite is concentrated in residual weathering products. According to Shiraki (1978) "no element exists besides Cr which is as effectively fixed in its weathering products without appreciable losses to the surface run off". Zn often has a higher concentration in soils than in unweathered rocks. White (1957), however, noted that 45% Zn was leached out of soils while 35% was incorporated in mineral structures. The decrease in Zn content with weathering in the study area is thus explained by leaching. The increase in Zr is not surprising as it accumulates in soils (Köster, 1961). According to Erlank *et al.* (1978), Zr is also released during the weathering of minerals other than zircon. The remaining trace elements which show a marked increase in concentration with weathering - Ba, Rb, Co, Ni, U and Ga are probably related to the clay mineral present (Ba, Rb, Ga), mobilization during weathering (Ni, Co) or migration from the overlying uraniferous Main Conglomerate (U).

In conclusion, the Jeppestown shale immediately below the Main Conglomerate has a geochemical profile that has characteristics of a paleosol which has subsequently been modified by diagenesis and percolation of ground waters. Thus the expected increase in total iron and decrease in K_2O with an increasing degree of alteration is marred by the absorption of K_2O during diagenesis. In addition, the varied clay mineral abundances and trace element distribution indicate that the geochemical profile has been further modified by the percolation of ground waters and/or hydrothermal solution along the upper shale/Main Conglomerate interface.

5.4.2 Correlation Coefficients

Correlations (BMDP 8D) between the major element and trace element data are given in Table 5.7. Because of the small number of samples used the correlation coefficients must be treated with caution. There was no exclusion of any sample which had trace element values that deviated from the mean. This would have reduced the sample size further and arbitrary selection might have produced artificial

Table 5.7

Correlation coefficients of twenty West Rand Group shales

	S102	3	1102	4	AL203	5	FE203	6	MNO	8	MGU	9	CAO	10	NA2O	11	K2O	12	P2O5	13	BA	17
S102	3	1.0000																				
1102	4	.4607	1.0000																			
AL203	5	.3870	.9233	1.0000																		
FE203	6	-.5752	-.6405	-.5638	1.0000																	
MNO	8	-.4347	-.4501	-.4458	.4842	1.0000																
MGU	9	-.4956	-.3586	-.4717	-.0807	.2020	1.0000															
CAO	10	-.3976	-.2691	-.3766	-.2937	.1639	.7440	1.0000														
NA2O	11	.2797	.4850	.4219	-.6217	-.2639	-.1568	.3720	1.0000													
K2O	12	.5064	.8025	.8969	-.6190	-.3998	-.5765	-.2849	.5055	1.0000												
P2O5	13	.2770	-.0767	-.1489	.0045	-.1188	-.0996	-.1641	-.2038	.1564	1.0000											
BA	17	.6209	.5368	.5872	-.4983	-.1616	-.4697	-.3066	.3664	-.7846	-.1841	1.0000										
SR	18	-.5742	-.2980	-.3592	-.3036	.1182	.7735	.9278	.1659	-.2483	-.1925	-.2993										
RB	19	.5424	.5748	.7033	-.4436	-.2414	-.6995	-.3588	.3834	.9226	-.0454	.8299										
Y	20	.5977	.1623	.1440	-.1305	.0023	-.1639	-.3041	.1202	.0155	.0722	.2632										
ZR	21	.7616	.6083	.5052	-.5112	-.3676	-.3860	-.4030	.2807	.4553	.4048	.5075										
NH	22	.6070	.6403	.7267	-.2936	-.2176	-.6571	-.6686	.1946	.6394	.2020	.5694										
ZN	23	.1523	-.2307	-.3813	.0295	-.0013	.3267	.0421	-.1010	-.5478	.3714	-.2622										
CU	24	.2561	-.1823	-.2271	-.1757	-.2968	.1249	.1284	.1300	-.1828	.4247	.0283										
CU	25	-.2959	.3608	.3613	-.5467	-.1610	.4423	.6266	.4376	.3066	-.2038	-.0328										
NI	26	.2502	.2689	.2265	-.6379	-.4400	.4663	.2917	.2100	.0555	-.0607	.0522										
V	27	.1197	.8827	.8765	-.6076	-.3474	-.0823	-.0353	.4277	.7319	-.2334	.3863										
CR	28	.0737	.4381	.2268	-.6601	-.1755	.4522	.5337	.3282	.2353	-.1418	.0695										
GA	29	.3147	.8504	.9617	-.3606	-.3605	-.5976	-.5255	.3262	.8450	-.1396	.5639										
SC	30	.0092	.7748	.7748	-.6466	-.4237	.0370	.1508	.4308	.6591	-.4073	.2655										
U	31	.2155	.6706	.6841	-.4452	-.3381	-.3668	-.1503	.3392	.6875	-.0190	.3176										
TH	32	.0000	.0000	.0000	.0000	.0000	.0000	.0000	.0000	.0000	.0000	.0000										

	SR	18	RB	19	Y	20	ZR	21	NH	22	ZN	23	CU	24	CU	25	NI	26	V	27	CR	28
SR	18	1.0000																				
RB	19	-.5152	1.0000																			
Y	20	-.4574	.0212	1.0000																		
ZR	21	-.4303	.3894	.6001	1.0000																	
NH	22	-.6951	.6080	.5428	.7635	1.0000																
ZN	23	-.0700	.5976	.6389	.4187	.0184	1.0000															
CU	24	.0358	-.1697	.3399	.4402	.0772	.6567	1.0000														
CU	25	.6344	-.0708	-.3556	-.1403	-.1371	-.3213	-.1475	1.0000													
NI	26	.5248	-.1913	.3734	.3973	.1273	.4729	.3777	.3869	1.0000												
V	27	-.0075	.4457	-.0249	.3308	.4535	-.3547	-.2444	.6881	.3392	1.0000											
CR	28	.6360	.0180	-.2875	.1571	-.1979	-.0893	-.0529	.6673	.4567	.5445	1.0000										
GA	29	-.5427	.6946	-.2031	.4481	.7544	-.3892	-.2737	.1999	.0510	.7780	-.0026	1.0000									
SC	30	.2112	.5545	-.2015	.1085	.1713	-.4425	-.2921	.7215	.4009	.9370	.6395	.3638	1.0000								
U	31	-.0857	.5608	-.1447	.3216	.4411	-.4365	-.2441	.5254	-.0046	.7287	.3176	.0000	.0000	1.0000							
TH	32	.0000	.0000	.0000	.0000	.0000	.0000	.0000	.0000	.0000	.0000	.0000	.0000	.0000	.0000	.0000	1.0000					

	GA	29	SC	30	U	31	TH	32
GA	29	1.0000						
SC	30	.6459	1.0000					
U	31	.6217	.5402	1.0000				
TH	32	.0000	.0000	.0000	1.0000			

correlations. Instead, several trace elements and major elements were plotted against each other (BMDP 6D) to ascertain the true relationship. Several of these plots are reproduced in Appendix 6. Good correlation is revealed by a tendency toward a linear distribution; poor correlation is shown by a scattered distribution. Good linear distributions were obtained when Al_2O_3 were plotted against TiO_2 , K_2O , Nb, Zr, V, Cr, Ga and Sc, Ba vs. K_2O and Cr vs. TiO_2 . Scattered distributions are shown for Fe_2O_3 vs. Co, and Fe_2O_3 vs. Sc. The large number of negative correlations in Table 5.7 is not surprising as Chayes (1960) has shown that where the sum of variables cannot exceed a certain constant, as is the case when percentage data is being handled, then positive correlations tend to be suppressed and negative correlations enhanced.

The most obvious feature in Table 5.7 is the lack of significant correlation between total Fe and the other elements. This indicates that total Fe did not play a major role in the incorporation of trace elements. On the other hand, Al_2O_3 , shows positive correlation with all but three (Zn, Ca, Sr) of the trace elements. The best inter-correlated groups of elements (coefficients of greater than seven) include Al_2O_3 - TiO_2 - K_2O - Rb - Nb - V - Ga - Sc, K_2O - Ba - Rb, CaO - Sr, Zr - Nb and V - U.

The very high correlations between Al_2O_3 and K_2O (which reside in the clay minerals) and Rb - Nb - V - Ga - Sc - Ba suggest that the trace elements are largely detrital (or inherited, Nicholls, 1963) entering the depositional environment in close association with the mineralogical clay phases. The strong positive correlation between CaO and Sr can probably be accounted for by co-precipitation during deposition or diagenesis.

The good correlations between Ti and other elements indicates that it is not only restricted to the mineral rutile. This was the assumption Pearson (1978) made when computing the clay mineral abundances from whole rock chemistry. Porrenga (1967) noted the unexpectedly high concentrations of Ti in separated clay mineral fractions and suggested that it was a detrital element, closely associated with the clay fraction. Weaver and Pollard (1973) found that an illite and chlorite from Scotland contained as much as 2.13%

and 1.03% TiO_2 respectively. Clearly, the illites and chlorites within the West Rand Group shales contain a substantial amount of TiO_2 (see TiO_2 vs. Al_2O_3 plot in Appendix 6).

The low correlation coefficients of Cu and Zn suggest that these elements do not occupy structural sites in the clay minerals. Hofmeyer (1971) showed good intercorrelations of the group Cu, Zn, Cr, V, Ni and Co in West Rand Group shales in the Klerksdorp area. He suggested that these elements were absorbed by chlorite and goethite with neither mineral playing a controlling role. The absence of this relationship in the study area is attributed to the absence of goethite. The moderate correlations between Cu, Zn and P_2O_5 suggests that these elements were absorbed by apatite. Krauskopf (1956) and Heydemann (1959) showed in a set of experiments that apatite and iron oxide are good absorbants of copper and zinc.

Significant Zr correlations include those with SiO_2 , TiO_2 , Al_2O_3 , K_2O , P_2O_5 , Ba, Nb, Ga and U. The large number of correlations and their moderate strengths suggest that Zr is not only present in the discrete mineral phase zircon but in other phases. The Zr - U correlation is explained by the presence of small amounts of zircon which is a favourable host for U. Nicholls and Loring (1962) suggest that some Zr proxies for Al (as does Ga) in clay minerals formed during source rock weathering. The relationship existing between Zr, Si, Ba and Ti, suggest that a significant proportion of Zr is located in ilmenite, rutile and/or fersite. The Ti, Zr and Nb correlations emphasise the fact that a proportion of these elements is located in heavy mineral fractions.

On theoretical grounds nickel and cobalt should have reasonable correlations as they have similar ionic potentials. Likewise plots of Co against Fe for shales should produce a good linear correlation (e.g. Carr and Turekian, 1961). Table 5.7 indicates that neither of these correlations exist in the study area. According to Burns and Burns (1978), nickel and/or cobalt occur in numerous minerals with pyrite and related structure types. The erratic distribution of secondary pyrite may explain the lack of Co - Ni - Fe correlation.

In summary, the correlation matrix reveals a number of highly significant correlations. Most trace elements are clearly largely controlled by the clay minerals although several exceptions may be explained by the distribution of heavy minerals and other accessory minerals.

CONCLUSION

The present study has led to a better understanding of the structure, sedimentology, diagenesis and geochemistry of the West Rand Group in the Heidelberg-Nigel-Balfour triangle. Study of the vertical succession of rock types and sedimentary structures has demonstrated that wave-dominated mineralogically mature arenites occur at the base of the Group contrasting with tide-dominated and fluvial litharenites and "subgreywackes" in the Government Subgroup. Although the geochemistry of the shales indicate that they are diagenetically advanced they still possess a trace element distribution indicative of the West Rand Group's original source area.

Correlating the major and trace elements it was shown that most of the minor elements were absorbed or occupied structural sites either in the clay fraction or in the heavy minerals.

The complicated strike-slip faulting, variation in dip and lack of borehole control did not permit construction of regional isopach maps of the intervals between the different "marker horizons" in the West Rand Group. Ideally these isopachs would represent the external form of the sand-shale bodies enabling formulation of paleoenvironmental models. As isopachs could not be drawn an attempt has been made to construct models detailing the depositional history and subenvironments of the sandstones of the West Rand Group. The depositional models integrate the writer's detailed facies analysis of the study area and observations of stratigraphic variations (lithology, thickness, sand/shale ratio) recorded in the basin as a whole (Appendix 1).

Seven major trends have emerged as a result of this detailed study:-

- 1) persistence of the dominant paleocurrent direction (SW) from the Hospital Hill Subgroup arenites up to the Jeppestown sandstones and into the Central Rand Group (Button, 1979),
- 2) a general increase in sandstone immaturity up the stratigraphic column,
- 3) the sand/shale ratio of the Government Subgroup is higher than that

of the Hospital Hill and Jeppestown Subgroup,

- 4) a consistent decrease in dip occurs from the Orange Grove Quartzite Formation to the Central Rand Group (even where there is no post-lithification faulting),
- 5) presence of tidal, longshore and wave currents implying that the Witwatersrand Basin was connected to an open ocean during Hospital Hill times,
- 6) presence of tidal and possible braided stream sediments in the Government Subgroup,
- 7) the presence of sand shoals in the Jeppestown Subgroup.

The depositional models established for the study area and basin as a whole are constrained by two assumptions:-

- 1) Structuring of the basin (major faulting and related folding) occurred after deposition of the Hospital Hill Subgroup while faulting and sedimentation were contemporaneous with the depositional history of the Government Subgroup
- 2) The regional markers are assumed to represent either a) widespread marine transgressive facies (e.g. Orange Grove Quartzites, Brixton Quartzites) or b) contemporaneous blankets of widespread chemical sediments (e.g. Contorted Bed). The more local diamictite markers probably represent submarine fan complexes on an ancient slope (e.g. Blue Grit).

Sediments bounded by regional stratigraphic markers constitute a "systems tract" defined by Brown and Fischer (1977) as contemporaneous depositional systems e.g. intergradational fluvial, shelf and slope systems. This would account for the differences in sand/shale ratios between markers in the four major outcrop areas.

In the following section the writer summarises the depositional models for the different Subgroups under the subtitles of a) regional markers, b) stratigraphic variables, c) depositional system tract and finally d) principal depositional modes. Schematic representation of the major depositional tracts in each Subgroup are presented in Fig. 6.1 and 6.2.

6.1 HOSPITAL HILL SUBGROUP MODEL (Fig. 6.1)

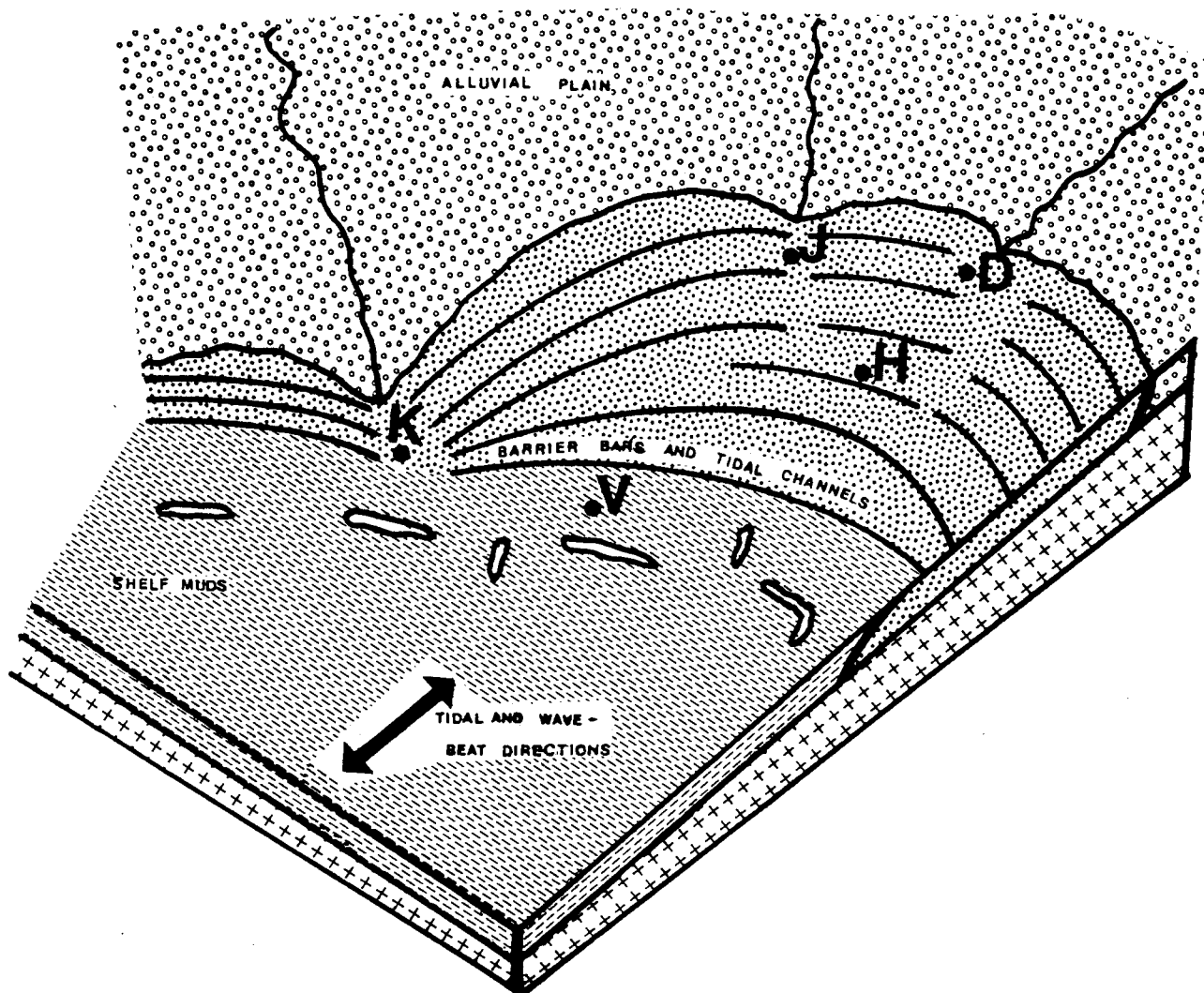


FIGURE 6.1 General depositional model of alluvial plain, coastal barrier bars and/or beaches, tidal channels and shelf mud systems in Hospital Hill Subgroup model. This style of deposition reflects development of laterally persistent mature arenites and shelf muds. Eustatic sea level rise (or subsidence) would account for the thick alternating sequences of arenites and shales. The towns of Johannesburg (J), Delams (D), Heidelberg (H), Klerksdorp (K) and Vredefort (V) are included for reference purposes.

Regional markers - The Orange Grove Quartzites, Water Tower Slates, Contorted Bed and Brixton arenites form regional markers. Orange Grove Quartzites occur as ripple marked, plane-bedded arenites in the Central Rand and East Rand and as thick coarse grained arkosic units in the Delmas area. In the Klerksdorp area these quartzites are poorly developed with lavas and mudstones (Dominion Group) resting on basement. The Water Tower Slates and Contorted Bed occur in all four major outcrop areas. The fuchsitic stained "sago" textured Brixton arenites form excellent markers in the Central and East Rand areas while in the Mazista area, Western Transvaal they are poorly developed.

Stratigraphic variables - Thicknesses of the Hospital Hill Subgroup decrease eastwards. The sand/shale ratios in Klerksdorp (0.80) area are higher than the ratios calculated in the Vredefort (0.70), Central Rand, West Rand and Heidelberg areas (0.55).

Depositional systems tract - Large volumes of clastics, shales and chemical sediments formed a depocentre characterised by widespread shallow marine coastal tracts and a distal shelf.

Depositional system mode - An elevated source area along an ancient margin north of Delmas and Mazista supplied broad stable platforms with clastic sediments. Tidal, wave-induced and longshore currents redistributed and winnowed these sediments in the major outcrop areas.

In coastal systems, sand belts usually develop where waves first impinge upon the seafloor and extend landward to the limit of tidal action. It is proposed that many of the Brixton sandstones represent ancient transgressive sand belts (tens of kilometres wide and hundreds of kilometres long). A low energy zone prevailing in the open sea below wave base developed the argillaceous horizons. Facies analysis in the study areas indicate that the waves and tides propagated in a NE-SW direction. Transgressions and regressions acting on this simple model explain the laterally persistent argillaceous - arenaceous sequence of the Hospital Hill Subgroup.

6.2 GOVERNMENT SUBGROUP MODEL

Regional markers - The Government Reef, Coronation Shale and Coronation

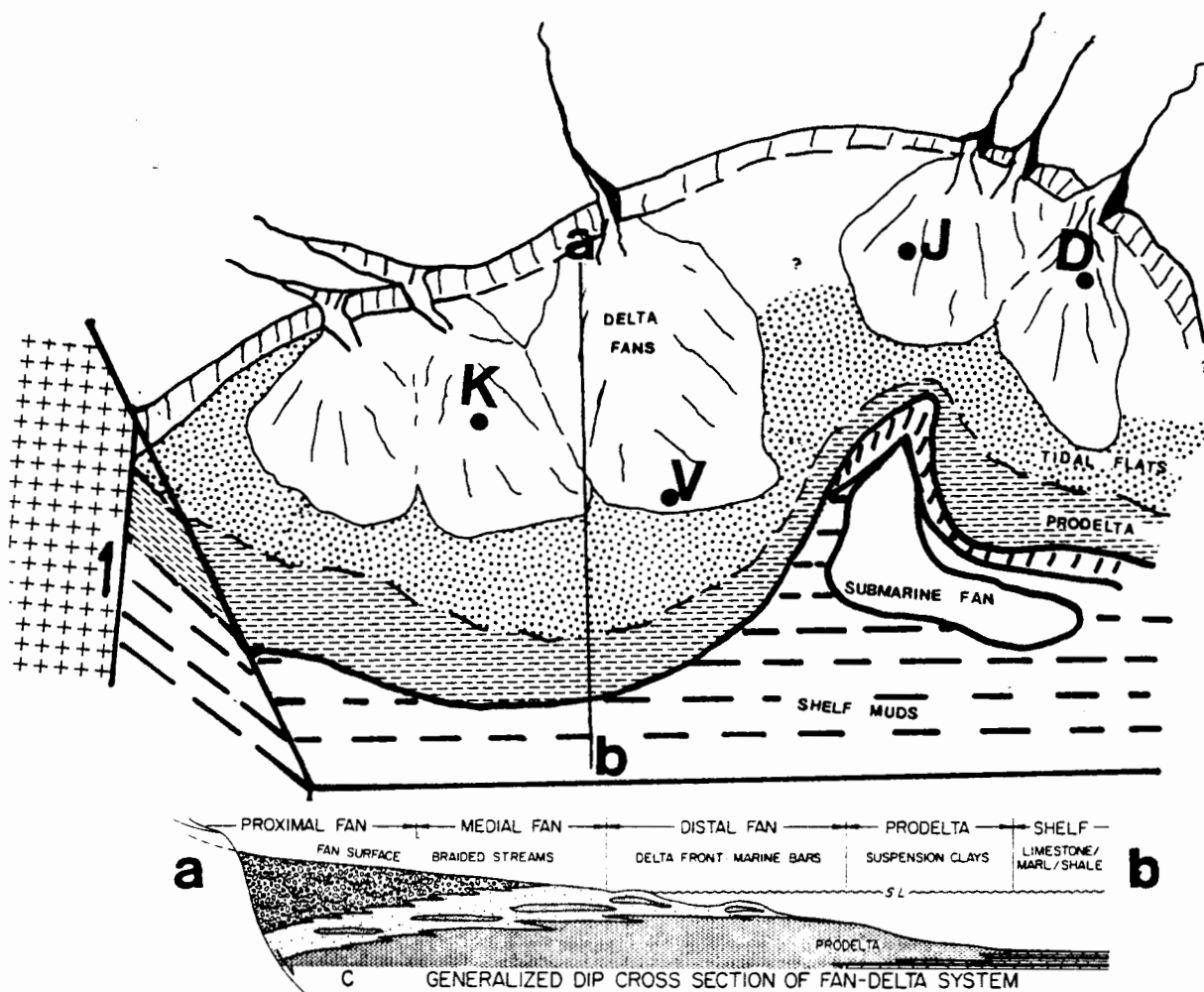


FIGURE 6.2 General depositional model of fan-delta, shelf and slope systems in Government Subgroup showing schematic representation of possible terrigenous input areas. Tidal direction was still NE-SW. The towns of Johannesburg (J), Delmas (D), Heidelberg (H), Klerksdorp (K) and Vredefort (V) are included for reference purposes. A general cross section (a-b) showing principal types of facies assemblages within the fan-delta system is included (after Brown and Fischer, 1977).

tillite form three regional markers. The Government Reef is a persistent, mature to submature arenite or litharenite in the Orange Free State, Central and East Rand areas. The markers are absent in the Vredefort area and in the Klerksdorp area it consists of thick loosely packed conglomerates (locally known as Big Pebble, Buffelsdoorn or White Reef). The Veldschoen Reef in the Delmas area occupies a similar stratigraphic position to the Government Reef in the East Rand. The tillite and diamictite markers (e.g. Blue Grit) are best developed towards the east of the East Rand and in the South Rand.

Stratigraphic variables - Thicknesses decrease in a southerly and easterly direction. Likewise, the sand/shale ratio decreases eastwards from a value of 2.6 in the Klerksdorp area to 1.48 in the Heidelberg area. The Government Reef overlies laminated shale.

Depositional systems tract - Alluvial fan(?), fan delta, localised shallow coastal deposition and slope systems typify the Government Subgroup sequence.

Principal depositional mode - Faulting along the northern margin of the semi-stable platform supplied alluvial fan and fan delta systems with very coarse grained sediments. In the study area and Delmas areas fans prograded southwestwards over extensive tidal-flat environments. The fans were only locally reworked by wave processes and tidal currents which propagated in a SW-NE direction. Terrigenous clastic sediment supply slowly diminished by the end of Promise Formation time. A major transgression then occurred depositing the Coronation shale in the Central, East, Free State Goldfields, Delmas and Evander areas. Renewed uplift along the margins supplied coarse grained sands (Government Reef) which were redistributed by tidal and wave processes in the East, Central and Orange Free State areas. Local slope sedimentation was probably concentrated in front of delta fans where prodelta and delta front deposits were reworked and transported into deeper water by gravity processes (e.g. Blue Grit). At present there is some controversy as to whether the genetic term tillite should be applied to certain beds within the Coronation Formation. If this marker is a true tillite, the depositional model proposed would have to be modified to include glacial outwash fans in place of fan deltas as the supplier of terrigenous material.

6.3 JEPPESTOWN SUBGROUP MODEL

Regional markers - The Crown Lavas were described by SACS (1978) as "dark green, often slightly brown, fine grained to cherty lavas, occasionally finely porphyritic, often amygdaloidal with associated minor quartzite, tuffaceous or agglomerate sediments" and occur in all four major outcrop areas. The lavas are thickest in the Orange Free State Goldfield area where they total some 106 m.

Stratigraphic variables - The sand/shale ratio is highest in the Klerksdorp area (1.27) and lowest in the Heidelberg area (0.54). However, no consistent trend is evident in the other areas - Vredefort (0.65), South Rand (0.68) and Central Rand (0.77). The thickness of the Subgroup decreases south-eastwards. In the Evander area the Jeppetown succession is absent with the Main Conglomerate overlying the Blue Grit marker. Erosional truncation of the Subgroup is also evident in the Delmas and East Rand areas where large scour channels, slump deposits and poorly sorted pebbly and sandy mudstones are present at the base of the Central Rand Group (Antrobus and Whiteside, 1964).

Depositional tract and principal mode - Isopach maps (Brock and Pretorius, 1964) indicate that the shape of the West Rand Group basin became shallower and smaller during Jeppetown Subgroup times. The Subgroup encompasses two major types of basin fill - shelf deposition in the East Rand area and fluvial deposition in the Klerksdorp and Vredefort areas.

REFERENCES

- Adams, J., 1977. Sieve size statistics from grain measurement. *J. Geol.*, 85: 209-227
- Allsopp, J.L., 1964. Rubidium - strontium ages from the Western Transvaal. *Nature*, 204(4956): 361-363
- Anderson, R., 1976. Tidal shelf sedimentation: an example from the Scottish Dalradian. *Sedimentology*, 23: 429-458
- Armstrong, G.C., 1968. Sedimentological control of gold mineralization in the Kimberley reefs of the East Rand Goldfield. *Inform. Circ. econ. Geol. Res. Unit, Univ. Witwatersrand, Johannesburg*, 47: 24pp.
- Antrobus, E.S.A. and Whiteside, H.C.M., 1964. The geology of certain mines in the East Rand. In: Haughton, S.H. (Editor), *The Geology of Some Ore Deposits in Southern Africa*, *Geol. Soc. S.Afr., Johannesburg*, 1: 125-160
- Antrobus, B., 1977. Metamorphic and structural aspects of the geology around the Vanrhynsdorp district and their relationships with the postulated Nama/Malmesbury fault; an application of potassic, white micas as petrogenetic indicators. Unpub. *Geol. Honours Proj.*, Univ. Cape Town, Cape Town, 32pp.
- Baird, A.K., 1961. A pressed specimen die for the Norelco vacuum - path X-ray spectrograph. *Norelco. Rep.*, 8: 108
- Balazs, R.J. and Klein, G. de V., 1972. Roundness-mineralogical relations of some intertidal sands. *J. sedim. Petrol.*, 42: 425-433
- Banks, N.L., 1973. Tide - dominated offshore sedimentation, Lower Cambrian, North Norway. *Sedimentology*, 20: 213-228
- Barwis, J.H. and Makurath, J.H., 1978. Recognition of ancient tidal inlet sequences: An example from the Upper Silurian Keyser Limestone in Virginia. *Sedimentology*, 25: 61-82
- Blatt, H., 1967. Original characteristics of clastic quartz grains. *J. sedim. Petrol.*, 37(2): 401-424
- Blatt, H., Middleton, G. and Murray, R., 1972. *Origin of sedimentary rocks*. Prentice Hall Inc., New Jersey. 634pp.
- Borchers, R., 1961. Exploration of the Witwatersrand System and its Extensions. *Proc. geol. Soc. S.Afr.*, 64: 67
- Borchers, R., 1964. Exploration of the Witwatersrand System and its Extensions. In: S.H. Haughton (Editor), *The Geology of Some Ore Deposits in Southern Africa*. *Geol. Soc. of S.Afr., Johannesburg*, 1: 1-23

- Bourgeois, J., 1978. Conglomerates. In: R.W. Fairbridge and J. Bourgeois (Editors), *The Encyclopedia of Sedimentology*. Dowden, Hutchinson and Ross Inc., Stroudsburg, 901pp.
- Brindley, G.W., 1961. Quantitative analysis of clay mixtures. In: G. Brown (Editor), *The X-ray identification and crystal structures of clay minerals*, Mineralogical Society, London.
- Brock, B.B. and Pretorius, D.A., 1964a. An introduction to the stratigraphy and structure of the Rand Goldfield. In: S.H. Haughton (Editor), *The Geology of Some ore deposits in Southern Africa*. Geol. Soc. of S.Afr., Johannesburg, 1: 25-61.
- Brock, B.B. and Pretorius, D.A. 1964b. Rand basin sedimentation and tectonics. In: S.H. Haughton (Editor), *The Geology of Some ore deposits in Southern Africa*. Geol. Soc. of S. Afr., Johannesburg, 1: 449-499.
- Brown, L.F. and Fischer, W.L., 1977. Seismic stratigraphic interpretation of depositional systems: Examples from Brazillian rift and pull-apart basins. In: C.E. Payton (Editor), *Seismic stratigraphy - applications to hydrocarbon exploration*, AAPG Memoir 26, Oklahoma, 213-249.
- Burns, R.G. and Burns, V.M. 1978. Nickel. In: K.H. Wedepohl (Editor) *Handbook of Geochemistry*, Vol. 11/3, Springer-Verlag, Berlin-Heideberg-New York.
- Button, A., 1970. The stratigraphy of the Witwatersrand System in the Delmas area, Transvaal. Inform. Circ. econ. Geol. Res. Unit, Univ. Witwatersrand, Johannesburg, 58: 20pp.
- Button, A., 1979. Upper Witwatersrand strata in the Heidelberg area. 20th Ann. Rep., Econ. geol. Res. Unit, Univ. Witwatersrand, Johannesburg.
- Camden-Smith, P.M., 1979a. Stratigraphy and current dispersal patterns of the West Rand Group in the Heidelberg-Nigel-Balfour triangle. Abstracts, Geokongress 1979, 1: 73-78.
- Camden-Smith, P.M., 1979b. The Lower Witwatersrand project. 20th Ann. Rep., Econ. geol. Res. Unit, Univ. Witwatersrand, Johannesburg.
- Carmichael, I.S.E., Hampel, J. and Jack, R.N., 1968. Analytical data on the U.S.G.S. standard rocks. Chem. Geol. 3: 59-64.
- Carr, M.H. and Turekian, K.K., 1961. The geochemistry of cobalt. *Geochim. Cosmochim. Acta.*, 23: 9pp.
- Carrol, D., 1970. Clay minerals: A guide to their X-ray identification. Geol. Soc. Am. Spec. Pub., 26: 80pp.
- Carter, R.M., 1975. A discussion and classification of subaqueous mass-transport with particular application to grain-flow, slurry-flow, and fluxoturbidites. *Earth-Sc. Rev.*, 11: 145-177.
- Carter, C.H., 1978. A regressive barrier and barrier-protected deposit: Depositional environment and geographic setting of the late Tertiary Cohansey sand: J. sedim. Petrol., 48: 933-950.

- Chayes, F., 1960. On correlation of variables of constant sum, *J. Geophys. Res.*, 65: 4185-4193.
- Cipriani, C., Sassi, F.P. and Viterbo-Bassani, C., 1968. La composizione delle miche chiare in rapporto con le costanti reticolarie col grado metamorfico. *Rend. Soc. Ital. Miner. Petrol.*, 24: 153-187.
- Cipriani, C., Sassi, F.P. and Scolari, A., 1971. Metamorphic white micas: Definition of paragonetic fields. *Schweiz. Miner. Petrogr. Mitt.*, 51: 259-302.
- Clifton, H.E., Hunter, R.E. and Phillipps, R.L., 1971. Depositional structures and processes in the non-barred high-energy nearshore. *J. sedim. Petrol.*, 41: 651-670.
- Cohen, A.C., 1966. Discussion of paper "Estimation of parameters for a mixture of normal distributions" by Hasselblad, V., *Technometrics*, 8: 445-446.
- Collender, D.F., 1960. The Witwatersrand System in the Klerksdorp area as revealed by diamond drilling. *Trans. geol. Soc. S. Afr.*, 63: 189-226.
- Coleman, J.M., 1969. Brahmaputra river: channel processes and sedimentation. *Sedim. Geol.*, 3: 129-239.
- Conybeare, C.E.B. and Crook, K.A.W., 1968. Manual of sedimentary structures. B.M.R. Bull. 102, Canberra, 327pp.
- Corstorphine, G.S., 1904. The geological relation of the Old Granite to the Witwatersrand Series. *Trans. geol. Soc. S. Afr.*, 7(1): 9-12.
- Curray, J.R., 1964. Transgressions and regressions. In: R.L. Miller (Editor), *Papers in marine geology (Shephard Commemorative volume)*. MacMillan, New York, 179-203.
- Curray, J.R., Emmel, F.J. and Crampton, P.J.S., 1969. Holocene history of a strand plain, lagoonal coast, Nayarit, Mexico. In: A.A. Castanares and F.B. Phleger (Editors), *Coastal lagoons, a symposium Mexico: Universidad Nacional Autónoma*.
- Danchin, R.V., 1970. Aspects of the geochemistry of some selected South African fine grained sediments. Unpub. Ph.D. thesis, Univ. Cape Town, Cape Town, 215pp.
- Deer, W.A., Howie, R.A. and Zussman, J., 1974. An introduction to the rock forming minerals. Longmans, London, 528pp.
- De Jager, F.S.J., 1964. The Witwatersrand System in the Springs-Nigel-Heidelberg sector of the East Rand Basin. In: S.H. Haughton (Editor), *The Geology of Some Ore Deposits in Southern Africa*. *Geol. Soc. of S. Afr.*, Johannesburg, 1: 161-190.
- Di Pierro, M., Lorenzoni, S. and Zanaettin-Lorenzonni, E., 1973. Phengites and muscovites in alpine and pre-alpine phyllites of Calabria (Southern Italy). *Neues Jb. Miner. Abh.*, 119: 57-64.
- Dietz, R.S., 1941. Clay minerals in recent marine sediments. Ph.D. thesis, Univ. of Illinois, Illinois, U.S.A.

- Dimroth, E., 1979. Diagenetic facies of iron formations. In: R.G. Walker (Editor), *Facies Models*, Geoscience Canada, Reprint Series 1, 211 : pp. 183-189.
- Dott, R.H., Jr., 1961. Squantum "tillite", Massachusetts - evidence of glaciation or subaqueous movements? *Bull. geol. Soc. Am.*, 72: 1289-1306.
- Engelhardt, W., von., 1940. Zerfall und aufbau von Mineralen in Norddeutschen Bleicherdewaldböden. *Chem. der Erde*, 13(1).
- Eriksson, K.A., Turner, B.R. and Vos, R.G., (in press). Evidence of tidal processes from the lower part of the Witwatersrand Supergroup, South Africa.
- Erlank, A.J., Smith, H.S., Marchant, J.W., Cardoso, M.P. and Ahrens, L.H., 1978. Zirconium. In: K.H. Wedepohl (Editor), *Handbook in Geochemistry*, Vol. 11/5, Springer-Verlag, Berlin-Heidelberg-New York.
- Evans, G., 1965. Intertidal flat sediments and their environments of deposition in the Wash. Quart. Jl. *geol. Soc. Lond.*, 121: 209-245.
- Fischer, W.L. and Brown, L.F., 1972. Clastic depositional Systems - a genetic approach to facies analysis. *Bur. econ. Geol., Univ. Texas*, Austin, Texas, 97-128.
- Flemming, B.W., 1977. Depositional processes in Saldanha Bay and Langebaan Lagoon. *N.R.I.O., Prof. Res. Series No. 2*, 215pp.
- Folk, R.L., 1968a. Petrology of sedimentary rocks. *Hemphill's, Univ. of Texas*, 170pp.
- Folk, R.L., 1968b. Bimodal supermature sandstone: product of the desert floor. *XXXIII Int. geol. Congress.*, 8: 9-32.
- Frakes, L.A., 1978. Diamictite. In: R.W. Fairbridge and J. Bourgeois (Editor), *The Encyclopedia of Sedimentology*. Dowden, Hutchinson and Ross Inc., 901pp.
- Frey, M., 1970. The step from diagenesis to metamorphism. *Sedimentology*, 15: 261-279.
- Fuller, A.O., 1958. A contribution to the petrology of the Witwatersrand System. *Trans. geol. Soc. S. Afr.*, 61: 10-50.
- Fuller, A.O., 1962. Systematic fractionation of sand in the shallow marine and beach environment off the South African coast. *J. sedim. Petrol.*, 32(3): 602-606.
- Fuller, A.O., Sprague, A., Waters, D., Willis, J.P. and Camden-Smith, P.M., 1979. Chemistry and mineralogy of Archaean shales from the Witwatersrand Supergroup. *Abstracts, Geokongress 79*, 1: 158pp.
- Gadow, S., Reineck, H.E., 1969. Ablandiger Sandtransport bei Sturmfluten. *Senckenbergiana Marit*, 1: 63-78.
- Gibbs, R.J., 1967. Quantitative X-ray diffraction analysis using clay mineral standards extracted from the samples to be analysed. *Clay Miner.*, 7: 79-90

- Gilbert, G.K., 1914. The transportation of debris by running water: Prof. Pap. U.S. geol. Surv., Vol. 86.
- Glikson, A.Y., 1971. Archaean geosynclinal sedimentation near Kalgoorlie, Western Australia. Sp. Publ. geol. Soc. Austr., 3: 343-360.
- Green, J.C., 1963. High-level metamorphism of pelitic rocks in Northern New-Hampshire. Am. Miner., 48: 991-1023.
- Greensmith, J.T., 1978. Petrology of the sedimentary rocks. 6th Edition. George Allen and Unwin Ltd., 241pp.
- Guidotti, C.V. and Sassi, F.P., 1976. Muscovite as a petrogenetic indicator mineral in pelitic schists. Neues. Jb. Miner. Abh., 127: 97-142.
- Hayes, M.O., 1976. Tidal inlets. In: M.O. Hayes and T.W. Kana (Editors), Terrigenous clastic depositional environments. Technical report No. 11-CRD, Columbia, South Carolina.
- Harder, H., 1961. Beitrag zur geochemie des Bros III. Bor in metamorphen gesteinen und im geochem-ischen Kreislauf. Nachr. Akad. Wiss. Göttingen. Math-Phys. Kl No. 1: 1.
- Heier, K.S. and Billings, G.K., 1978. Sodium. In: K.H. Wedepohl (Editor), Handbook of Geochemistry, Vol. 11/1, Springer Verlag, Berlin-Heidelberg-New York.
- Heydemann, A., 1959. Absorption aus sehr verdünnten Kupferlösungen an reinen Tonmineralen. Geochem. cosmochim Acta., 15: 305.
- Hobbs, B.E., Means, W.D. and Williams, P.F., 1976. An outline of structural geology. John Wiley, New York, 571pp.
- Hoffmann, C., 1970.. Die glaukophangesteine, ihre stofflichen equivalente und um wandlungsprodukte in Nordcalabre (Süditalien). Contr. Miner. Petrol., 27: 283-320.
- Hofmeyr, P.K., 1971. The abundances and distribution of some trace elements in some selected South African shales. Unpub. Ph.D. thesis, Univ. Cape Town, Cape Town, 218pp.
- Hutchinson, C.S., 1974. Laboratory handbook of petrographic techniques. J. Wiley and Sons, New York, 527pp.
- Imbrie, J. and Poldervaart, A., 1959. Mineral compositions calculated from chemical analyses of sedimentary rocks. J. sedim. Petrol., 29: 588-595.
- James, H.L., 1966. Chemistry of the iron-rich sedimentary rocks. Prof. Pap. U.S. geol. Surv., 440W: 61pp.
- Jansen, H, Schalk, K.E., Leube, A., Snyman, A.A., Steyn, A.P.A., de Jager, F.S.J. and Beer, H.M., 1972. Geology of the country around Standerton. Explanation of sheets 2628D and 2629C. Geol. Surv. S. Afr., Pretoria, 27pp.
- Jenkins, R. and de Vries, J.L., 1967. Practical X-ray spectrometry. Philips Technical Library.

- Johns, W.D., Grim, R.E. and Bradley, W.F., 1954. Quantitative estimation of clay minerals by diffraction methods. *J. sedim. Petrol.*, 24: 242-251.
- Johnson, H.D., 1977. Water escape structures in shallow marine sandstones. *Sedimentology*, 24: 389-411.
- Johnson, H.D., 1978. Shallow siliciclastic seas. In: Reading, H.G. (Editor), *Sedimentary environments and facies*. Blackwell Scientific Publications, London, 557pp.
- Jones, T.A. and James, W.R., 1969. Analysis of bimodal orientation data. *Math. Geology*, 1(2): 129-135.
- Kasch, K.W., 1979. Tectonothermal evolution of the Southern Damara Belt and its geodynamic implications. *Abstracts, Geokongress 79*, 1: 227-231.
- Keller, W.D., 1970. Environmental aspects of clay minerals. *J. sedim. Petrol.*, 40(3): 788-854.
- Klein, G. de V., 1970. Depositional and dispersal dynamics of intertidal sand bars. *J. sedim. Petrol.*, 40: 1095-1127.
- Klein, G. de V., 1977. *Clastic tidal facies*, CEPCO, Illinois, 149pp.
- Koritnig, S., 1978. Phosphorus. In: R.H. Wedepohl (Editor), *Handbook of Geochemistry*, Vol. 11/2, Springer-Verlag, Berlin-Heidelberg-New York.
- Köster, H.M., 1961. Vergleich einiger Methoden zur Untersuchung von Geochemischen Vorgängen bei der Verwitterung. *Beitr. Mineral. Petrogr.*, 8: 69pp.
- Krauskopf, K.B., 1956. Factors controlling the concentrations of thirteen rare metals in sea water. *Geochem. cosmochim. Acta.*, 9: 1.
- Kubler, B., 1966. Cristallinité de l'illite et le zones tout à fait supérieures du méta morphisme. In: *Colloque sur les Etages Tectoniques*, 105-122.
- Kubler, B., 1968. Evaluation quantitative du métamorphisme par la cristallinité de l'illite. Etat des progrès réalisés ces dernières années. *Bull. Centre Rech. Pau - S.N.P.A.*, 2: 385-397.
- Kuenen, Ph., 1960. Experimental abrasion: 4. Eolian action. *J. Geol.*, 68: 427-449.
- Kumar, N., 1978. Tidal inlet and tidal delta facies. In: R.W. Fairbridge and J. Bourgeois (Editors), *The Encyclopedia of Sedimentology*, Dowden, Hutchinson and Ross Inc., 901pp.
- Kumar, N. and Sanders, J.E., 1974. Inlet sequence: a vertical succession of sedimentary structures and textures created by the lateral migration of tidal inlets. *Sedimentology*, 21: 491-532.
- Kumar, N. and Sanders, J.E., 1976. Characteristics of shoreface deposits: modern and ancient. *J. sedim. Petrol.*, 46: 145-162.
- Lelong, F. and Millot, G., 1966. Sur l'origine des minéraux micacés des altération latéritiques. Diagenèse régressive. Minéraux en transit, *Bull. Serv. Carte Géol. Alsace - Lorraine, Strasbourg*, 19: 271-287.

- Lowe, D.R., 1975. Water escape structures in coarse-grained sediments. *Sedimentology*, 22: 157-204.
- Luttman-Johnson, H., 1904. Notes on the geology of the Fortuna Valley, Heidelberg, Transvaal. *Trans. geol. Soc. S. Afr.*, 7(3): 136-139.
- McCave, I.N., 1970. Deposition of fine grained suspended sediment from tidal currents. *J. Geophys. Res.* 75., 4151-4159.
- McCave, I.N., 1978. Grain size trends and transport along beaches: Example from eastern England. *Mar. Geol.*, 28: 43-51.
- McDougall, T., 1963. Potassium-Argon measurements on dolerites from Antarctica and South Africa. *J. Geophys. Res.*, 68pp.
- McKee, E.D., Reynolds, M.A. and Baker, C.H., 1962. Laboratory studies on deformation in unconsolidated sediments. *Prof. Pap. U.S. geol. Surv.* 450-D, 151-155pp.
- McKee, E.D., Crosby, E.J. and Berryhill, H.L., 1967. Flood deposits, Bijou Creek, Colorado, June 1965. *J. sedim. Petrol.*, 39: 829-851.
- Mellor, E.T., 1911. The normal section of the Lower Witwatersrand System. *Trans. geol. Soc. of S. Afr.*, 14: 93-131.
- Mellor, E.T., 1917. The geology of the Witwatersrand: Explanation of Sheet 52 (Johannesburg). *Geol. Surv. S. Afr.*, Pretoria, 3: 46pp.
- Mellor, E.T., 1921. Discussion of paper "The geology of the neighbourhood of Heidelberg". *Proc. geol. Soc. S. Afr.*, 24: 39-42.
- Miall, A.D., 1977. A review of the braided-river depositional environment. *Earth-Sc. Rev.*, 13: 1-62.
- Middleton, G.V. and Davis, P.M., 1979. Surface textures and rounding of quartz sand grains on intertidal sandbars, Bay of Fundy, Nova Scotia. *Can. J. Earth-Sc.*, 16(11): 2071-2085.
- Mietsch, A.T., 1962. Computing mineral compositions of sedimentary rocks from chemical analyses. *J. sedim. Petrol.*, 32: 217-225.
- Minter, W.E.L., 1978. A sedimentological synthesis of Placer Gold, Uranium and Pyrite concentrations in Proterozoic Witwatersrand sediments. In: A.D. Mial (Editor), *Fluvial Sedimentology*, Can. Soc. Petroleum Geol., 859: pp 801-829.
- Naqvi, S.M., 1978. Geochemistry of Archaean meta sediments, evidence for prominent anorthosite-norite-troctolite in the Archaean basaltic primordial crust. In *Archaean Geochemistry*, Edited by Windley, B.F. and Naqvi, S.M. Elsevier, Scientific Publishing Company, Amsterdam, 406pp.
- Nel, L.T., 1927. The geology of the Country around Vredefort. *Spec. Publ. geol. Surv. S. Afr.*, Pretoria, No. 6.
- Nel, L.T., 1933. The Witwatersrand System outside the Rand. *Proc. geol. Soc. S. Afr.*, 36: 23-48.

- Nel, L.T., Truter, F.C., Willemse, J. and Mellor, E.T., 1939. The geology of the country around Potchefstroom and Klerksdorp. Explanation of Sheet No. 61 (Potchefstroom), Geol. Surv. S. Afr., Pretoria, 156pp.
- Nel, L.T. and Jansen, H., 1957. The geology of the country around Vereeniging: Explanation of sheet No. 62. Geol. Surv. S. Afr., Pretoria.
- Nel, W.A., 1968. The estimation and distribution of boron in fine grained South African Sediments. Unpub. M.Sc. thesis, Univ. Cape Town, Cape Town, 69pp.
- Nicholls, G.D., 1962. A scheme for recalculating the chemical analyses of argillaceous rocks for comparative purposes. *Am. Miner.*, 47: 34-46.
- Nicholls, G.D., 1963. Environmental studies in sedimentary geochemistry. *Science Progress*, 201: 372-398.
- Nicholls, G.D. and Loring, D.H., 1962. The geochemistry of some British Carboniferous sediments. *Geochim. cosmochim. Acta.*, 26: 181-196.
- Nold, J.L. and Erickson, K.P., 1967. Changes in K-feldspar staining methods and adaptations for field use. *Am. Miner.*, 53: 278-282.
- Norrish, K. and Hutton, J.T., 1969. An accurate X-ray spectrographic method for the analysis of a wide range of geological samples. *Geochim. cosmochim. Acta.*, 33: 431-453.
- Pearson, M.J., 1978. Quantitative clay mineralogical analyses from the bulk chemistry of sedimentary rocks. *Clays and clay Minerals*, 26: 423-433.
- Pettijohn, F.J., 1957. Paleocurrents of Lake Superior Precambrian quartzites, *Bull. geol. Soc. Am.*, 68: 469-480.
- Pettijohn, F.J., 1975. *Sedimentary rocks*. Harper and Row, New York, 628pp.
- Pettijohn, F.J., Potter, P.E. and Siever, R., 1972/3. *Sand and sandstone*. Springer-Verlag, Berlin: 618pp.
- Picard, M.D., 1971. Classification of fine-grained sedimentary rocks. *J. sedim. Petrol.*, 41(1): 179-195.
- Pierce, J.W. and Siegel, F.R., 1969. Quantification in clay mineral studies of sediments and sedimentary rocks. *J. sedim. Petrol.*, 39: 187-193.
- Porrenga, D.H., 1967. Clay mineralogy and geochemistry of recent marine sediments in tropical areas. *Publ. van het Fysisch-Geografisch Lab., Univ. van Amsterdam*, 9: 1-145.
- Potter, J.F., 1977. The texture of compacted bimodal sediments. *J. sedim. Petrol.*, 47(4): 1539-1541.
- Powers, M.C., 1953. A new roundness scale for sedimentary particles. *J. sedim. Petrol.*, 23: 117-119.
- Pretorius, D.A., 1964a. The geology of the South Rand Goldfield. In: S.H. Haughton (Editor), *The Geology of Some Ore Deposits in Southern Africa*, Geol. Soc. of S. Afr., Johannesburg, 1: 219-282.

- Pretorius, D.A., 1965. Lower division of the Witwatersrand system. Unpub. report to Ad. Hoc. committee on stratigraphic nomenclature of the Witwatersrand Triad, Johannesburg, 4pp.
- Pretorius, D.A., 1966. Conceptual geological models in the exploration for gold mineralisation in the Witwatersrand Basin. Inform. Circ. econ. Geol. Res. Unit, Univ. Witwatersrand, Johannesburg, 33: 39pp.
- Pretorius, D.A., 1974. The nature of the Witwatersrand gold - uranium deposits. Inform. Circ. econ. Geol. Res. Unit, Univ. Witwatersrand, Johannesburg, 86: 50pp.
- Potter, P.E. and Pettijohn, F.J., 1977. Paleocurrents and Basin Analysis. 2nd Edition, Springer-Verlag, Berlin-Heidelberg-New York, 425pp.
- Raaf, J.F.M. de. and Boersma, J.R., 1971. Tidal deposits and their sedimentary structures. Geologie Mijnb., 50: 479-504.
- Ramsay, J.G., 1961. The effects of folding on the orientation of sedimentation structures. J. Geol., 69: 84-100.
- Ramsay, J.G., 1967. Folding and fracturing of rocks. McGraw-Hill, New York, 568pp.
- Reiche, P., 1938. An analysis of crosslamination of the Coconino sandstone. J. Geol., 44: 905-932.
- Reineck, H.E., 1963. Sedimentgefüge im Bereich der südlichen Nordsee. Abh. senckenbergische naturforsch. Ges., 505:138pp.
- Reineck, H.E. and Singh, I.B., 1975. Depositional sedimentary environments - with reference to terrigenous clastics. Springer-Verlag, Berlin, 439pp.
- Reineck, H.E. and Wunderlich, F., 1968. Zur unterscheidung von asymmetrischen oszillations rippeln und strömungs rippeln. Senckenbergiana Lethaea, 49: 321-345.
- Renton, J.J., Heald, M.T. and Cecil, C.B., 1969. Experimental investigations of pressure solution of quartz. J. sedim. Petrol., 39: 1107-1117.
- Robinson, G.D., 1959. Measuring dipping beds. Geotimes, 4(1): 24-25, 27.
- Roering, C., 1968. The tectonics of the West Rand syncline: a field study of brittle failure in the Witwatersrand Basin. Inform. Circ. econ. Geol. Res. Unit, Univ. Witwatersrand, Johannesburg, 48: 28pp.
- Rogers, A.W., 1921. The geology in the neighbourhood of Heidelberg. Trans. geol. Soc. S. Afr., 24: 17-52.
- Rogers, A.W., 1922. The geology of the country around Heidelberg. Explanation of sheets 52B (Heidelberg), Spec. Publ. geol. Surv. S. Afr., Pretoria, No. 4.
- Rogers, A.W., 1933. Calcareous sediments in the Witwatersrand system. Trans. geol. Soc. S. Afr., 36: 65-68.
- Ronov, A.B. and Yaroshevskiy, A.A., 1968. Chemical structure of the earth's crust. Geochemistry Inter., 5: 1041.

- Sassi, F.P. and Scolari, A., 1974. The b_0 values of the potassic white micas as a barometric indicator in low grade metamorphism of pelitic schists. *Contr. Miner. Petrol.*, 45: 143-152.
- Sassi, F.P., 1972. The petrologic and geologic significance of the value of potassic white micas in low-grade metamorphic rocks. An application to the Eastern Alps. *Tschemm's Miner. Petrol. Mitt.*, 18: 105-113.
- Sawyer, A.R., 1907. New Rand Goldfield, Orange River Colony. *Trans. Inst. Min. Eng. Newcastle (England)*, Vol. 33.
- Schermerhorn, L.J.E., 1974. Late Precambrian mixtites: Glacial and/or nonglacial? *Am. J. Sc.*, 274: 673-824.
- Schoen, H.R., Foord, E. and Wagner, D., 1972. Quantitative analysis of clays- problems, achievements, and outlook. *Int. Clay Conf.*, Madrid.
- Schultz, L.G., 1964. Quantitative interpretation of mineralogical composition from X-ray and chemical data for the Pierre Shale. *Prof. Pap. U.S. geol. Surv.*, 391-C: 31pp.
- Selley, R.C., 1973. Ancient sedimentary environments. Chapman and Hall, London, 237pp.
- Shaw, D.M., 1954. Geochemistry of pelitic rocks. Part 1 and Part 11. *Bull. geol. Soc. Am.*, 65: 1152-1182.
- Shaw, D.B. and Weaver, C.E., 1965. The mineralogical composition of shales. *J. sedim. Petrol.*, 35: 213-222.
- Shimp, N.F., Witters, J., Potter, P.E. and Schleidher, J.A., 1969. Distinguishing marine and fresh water muds. *J. Geol.*, 77: 566-530.
- Shiraki, K., 1978. Chromium. In: R.H. Wedepohl (Editor), *Handbook of Geochemistry*, Vol. 11/3, Springer-Verlag, Berlin-Heidelberg-New York.
- Spector, D.L., 1977. Aspects of Malmesbury metamorphism in the Brandwacht area near Worcester, application of white mica geothermometry and geobarometry. Unpub. Geol. Honours Proj., Univ. Cape Town, Cape Town, 39pp.
- Sprague, A.R.G., 1979. A contribution to the chemistry and petrology of the Witwatersrand Supergroup. Unpubl. Geol. Honours Proj., Univ. Cape Town, Cape Town, 37pp.
- Tanner, W.F., 1967. Ripple mark indices and their uses. *Sedimentology*, 9: 89-104.
- Toogood, D.J., 1976. The structural and metamorphic evolution of a gneiss terrain in the Nanaqua belt near Onseepkans, South West Africa. *Precambrian Res. Unit, Univ. Cape Town, Bull.* 19.
- Turner, C.C. and Walker, R.G., 1973. Sedimentology, stratigraphy and crustal evolution of Archaean greenstone belts near Sioux Lookout, Ontario. *Can. J. Earth Sc.*, 10: 817-845.
- Udden, J.A., 1914. Mechanical composition of clastic sediments. *Bull. geo. Soc. Am.*, 25: 655-744.

- Usdowski, H.E., 1967. Die genese von dolomit in sedimenten. Springer-Verlag, Berlin- Heidelberg-New York.
- Walther, J., 1893-94. Einleitung in die Geologie als historishce Wissenschaft; Beobachtung uber die Bildung der Gesteine und ihrer organischen Einschlusse. Jena, G. Fischer, Bd. 1.
- Walter, M.R., 1972. A hot spring analog for the depositional environment of Precambrian iron formations of the Lake Superior region. *Econ. Geol.*, 67: 965-972.
- Weaver, C.E., 1960. Possible uses of clay minerals in the search for oil. *Proc. 8th National Conf. on Clays and clay Minerals*, 8: 214-227.
- Weaver, C.E., 1967. Significance of clay minerals in sediments. In: B. Nagy and U. Colombo (Editors), *Fundamental aspects of petroleum geochemistry*.
- Weaver, C.E., 1978. Clay minerals. In: R.W. Fairbridge and J. Bourgeois (Editors), *The Encyclopedia of Sedimentology*, Bowden, Hutchinson and Ross Inc., 901pp.
- Weaver, C.E. and Pollard, L.D., 1973. The chemistry of clay minerals. *Developments in Sedimentology*, 15.
- Weber, K., 1972. Notes on determination of illite crystallinity. *Neues. Jb. Miner. Mh.*, 6: 268-275.
- Wedepohl, K.H., 1971. Environmental influences on the chemical composition of shales and clays. In: L.H. Ahrens *et al* (Editors), *Physics and Chemistry of the Earth*, 8: 305-333, Pergamon Press, Oxford.
- White, M.L., 1957. The occurence of zinc in soil. *Econ. Geol.*, 52: 645-653.
- Willis, J.P., Ahrens, L.H., Danchin, R.V., Erlank, A.J., Gurney, J.J., Hofmeyer, P.K., McCarthy, T.S. and Orren, M.J., 1971. Some inter-element relationships between Lunar rocks and fines and stony meteorites. *Proc. 2nd Lunar Sci. Conf.*, Houston, Texas, 1971, 2: 1123-1138.
- Willis, J.P., Fortuin, H.H.G. and Eagle, G.A., 1977. A preliminary report on the geochemistry of recent sediments in Saldanha Bay and Langebaan Lagoon. *Trans. Roy. Soc. S. Afr.*, 42: 497-509.
- Winkler, H.G.F., 1974. Petrogenesis of metamorphic rocks. Springer-Verlag, Berlin, 320pp.
- Winter, H. de la R., 1978. Subdivisions of the Witwatersrand triad: the Dominion Group, the Witwatersrand Supergroup and the Ventersdorp Group. Unpubl. provisional stratigraphic subdivisions, S. Afr. committee for stratigraphy, *Geol. Surv.*, Pretoria.
- Whiteside, H.C.M., Glasspool, K.R., Hiemstra, S.A., Pretorius, D.A. and Antrobus, E.S.A., 1976. Gold in the Witwatersrand Triad. In: C.B. Coetzee (Editor), *Mineral resources of the Republic of S. Afr.*, *Geol. Surv. S. Afr.*, Pretoria, 462pp.
- Wunderlich, F., 1970. Genesis and environment of the "Nellenkopf chenschichten" (Lower Emsian, Rheinian Devon) at Locus Typicus in comparison wiht modern coastal environment of the German Bay. *J. sedim. Petrol.*, 40: 102-130

- Yaalon, D.H., 1961. Mineral composition of the average shale. Clay Miner. Bull., 27: 31-36.
- Young, G.M., 1973. Tillites and aluminous quartzites as possible time markers for middle Precambrian (Aphebian) rocks of North America, Geol. As. Canada Spec. Publ., 12: 92-127.
- Zwart, H.J., 1963. Metamorphic history of Central Pyrenees. Part II, Valle de Aran, Sheet 4. Leidse Geol. Mededel., 28: 321-376.

APPENDIX ONE

A REVIEW OF THE WEST RAND GROUP

BY

P.M. Camden - Smith

(Accepted for publication in the Economic Geology Research
Unit Information Circular, University of the Witwatersrand)

January, 1979.

C O N T E N T S

	<u>Page</u>
1. INTRODUCTION	1
1.1 Location of West Rand Group	1
1.2 Historical Note	1
1.3 Purpose of Review	2
2. AGE OF THE WITWATERSRAND SUPERGROUP	3
2.1 Geochronology	3
2.2 Possible Correlatives	4
3. STRATIGRAPHY	6
3.1 The Central and West Rand area	6
3.2 The Heidelberg - Balfour - Delmas area	13
3.3 Vredefort area	22
3.4 Klerksdorp - Ventersdorp - Ottosdal area	27
3.5 Northernmost West Rand Group outlier	36
3.6 Orange Free State goldfield (Odendaalsrus area)	37
4. MARKERS	41
5. STRUCTURE	42
5.1. Folding	43
5.2. Faulting	44
6. PETROLOGY	45
6.1 Mineralogy of the shales	45
6.2 Sandstones in the West Rand Group	46
7. GEOCHEMISTRY	48
7.1 Shales	48
7.2 Sandstones	49
8. METAMORPHISM	50
9. BASIN ANALYSIS	51
9.1. Arrangement and type of fill	52
9.2. Tectonic setting	53
9.3. Depositional environment	54
REFERENCES	

L I S T O F F I G U R E S

- Figure 1 : The four areas of West Rand Group outcrop.
- Figure 2 : Distribution of the Witwatersrand Supergroup below cover of Karoo, Transvaal and Ventersdorp sequences.
- Figure 3 : Comparison of West Rand Group stratigraphy as defined by Mellor (1917) and S A C S (1978).
- Figure 4 : Stratigraphy of the West Rand Group in the West Rand and Central Rand areas (after Mellor 1911,1913).
- Figure 5 : Simplified map showing the basin geometry of the Heidelberg-Delmas-Balfour area.
- Figure 6 : Comparative West Rand Group stratigraphy of the Heidelberg-Delmas-Balfour area (after Jansen et al,1972; Button, 1970).
- Figure 7 : Cyclic sedimentation in some West Rand Group sediments (after Button, 1968).
- Figure 8 : Comparison of lithology and thickness of West Rand Group stratigraphy in the Klerksdorp, Central-West Rand, Vredefort and Odendaalsrus areas.
- Figure 9 : Map showing the location of the northernmost West Rand Group outlier.
- Figure 10 : Fripp and Gay's (1972) model for the simultaneous formation of folds in the Contorted Bed and cleavage in the argillaceous rocks.
- Figure 11 : Map showing the periphery of the West Rand Group/Central Rand Group basins and the major faults.
- Figure 12 : The extrapolated isopachs (metres) of the West Rand Group (after Pretorius, 1974).
- Figure 13 : Schematic illustration of Vos's (1975) proposed manner of evolution for the Witwatersrand basin.

L I S T O F T A B L E S

- Table 1 : Age measurements relevant to the dating of the Witwatersrand Supergroup.
- Table 2 : Comparison of the thickness of the Orange Grove Quartzite Formation in the Heidelberg and Delmas areas.
- Table 3 : Government Subgroup in the Heidelberg-Delmas-Balfour area.
- Table 4 : Breakdown of the Government Subgroup in the Klerksdorp area.
- Table 5 : Markers within the West Rand Group.
- Table 6 : Correlation of magnetic anomalies in the West Rand Group.
- Table 7 : Major element analyses in the West Rand Group.
- Table 8 : Average trace and alkali abundances (in ppm) in West Rand Group rocks.
- Table 9 : Nature of metamorphism exhibited by the sediments of the West Rand Group.
- Table 10: Composite stratigraphic thickness of West Rand Group and areally and structurally related Groups.

1. INTRODUCTION

1.1 Location of West Rand Group

The Witwatersrand Supergroup consists of about 7400 m of sediments lying in a roughly ovoid basin 350 km long and 200 km wide within the Kaapvaal craton (Pretorius 1974). Stratigraphically, the Witwatersrand Supergroup has been separated into two groups: a shale dominated West Rand Group (previously known as the Lower Division) and a quartzite and conglomerate dominated Central Rand Group (previously known as the Upper Division).

The scattered areas of West Rand Group outcrop are shown on Figure 1. Borchers' (1961; 1964) map (Figure 2) shows the distribution of the Witwatersrand Supergroup below the cover of Karoo, Transvaal and Ventersdorp

sequences. All these weakly metamorphosed sedimentary/volcanic successions rest with marked unconformity on a highly metamorphosed basement complex comprising the Older Granite and the Swaziland Sequence which together constitute an early Precambrian granite-greenstone terrain.

1.2 Historical Note

Fred Strubens discovered gold in the quartz veins of the West Rand Group at Wilgespruit in 1884. A year later, he drew the first geological section through the Witwatersrand, showing the position of the Confidence Reef and three other units containing auriferous quartz veins - the Surprise, Governor and Mirella Reefs. The discovery of the auriferous banket reefs by George Harrison and George Walker in March 1886, and the proclamation of the Witwatersrand as a goldfield in September 1886, contributed to geological enquiry being focused in this part of South Africa. Numerous papers (mostly German and French) were published on the geology of these strata before the turn of the century.

Draper (1896; 1897), Molengraaff (1904), Sawyer (1911), Hatch (1898; 1904; 1913) and Corstorphine (1904) were the first geologists to systematically describe Witwatersrand strata. However, it was only during the period from 1910 to 1930 that Mellor (1911; 1913; 1917) undertook a regional study of the Supergroup. Mellor (1911) explained the differences in thicknesses of strata mapped by former geologists as "a consequence of the original conditions of deposition and also as one which is subject to the appearance of the great bodies of sediment in some localities which have no representatives in adjacent areas".

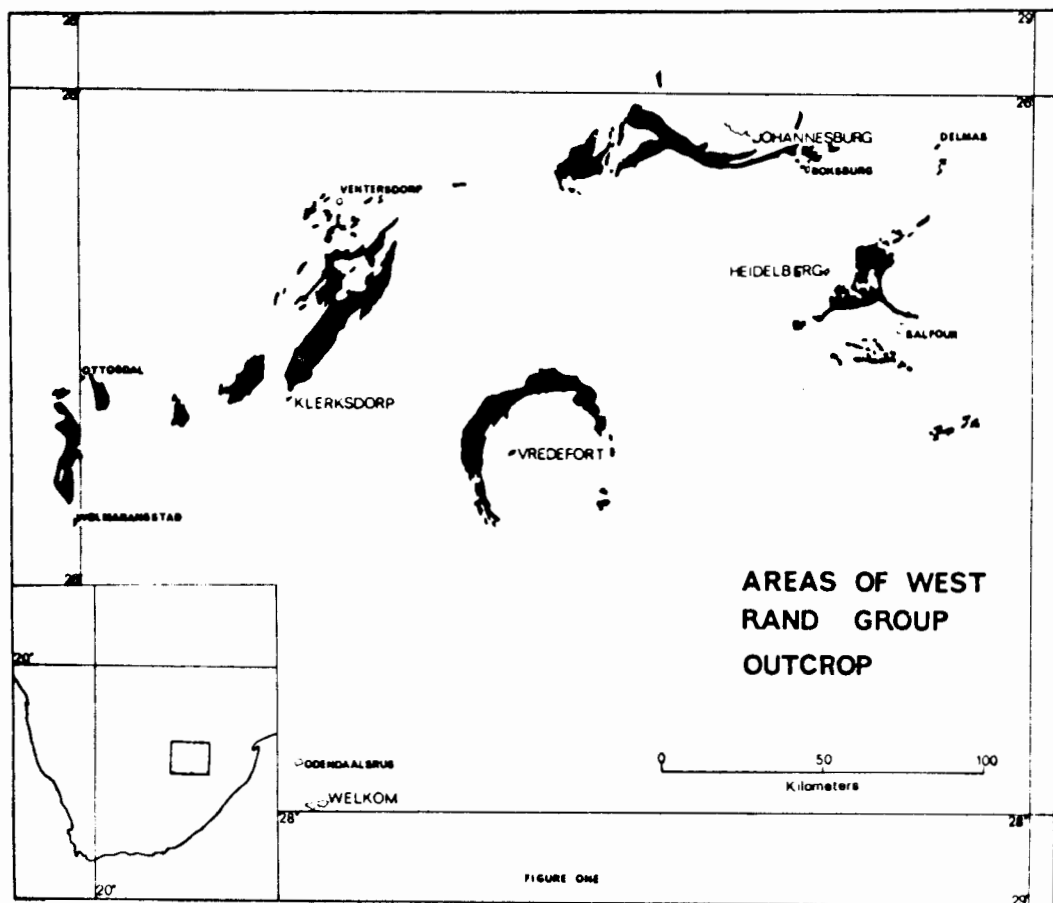


FIGURE 1 The four major outcrop areas of the West Rand Group.

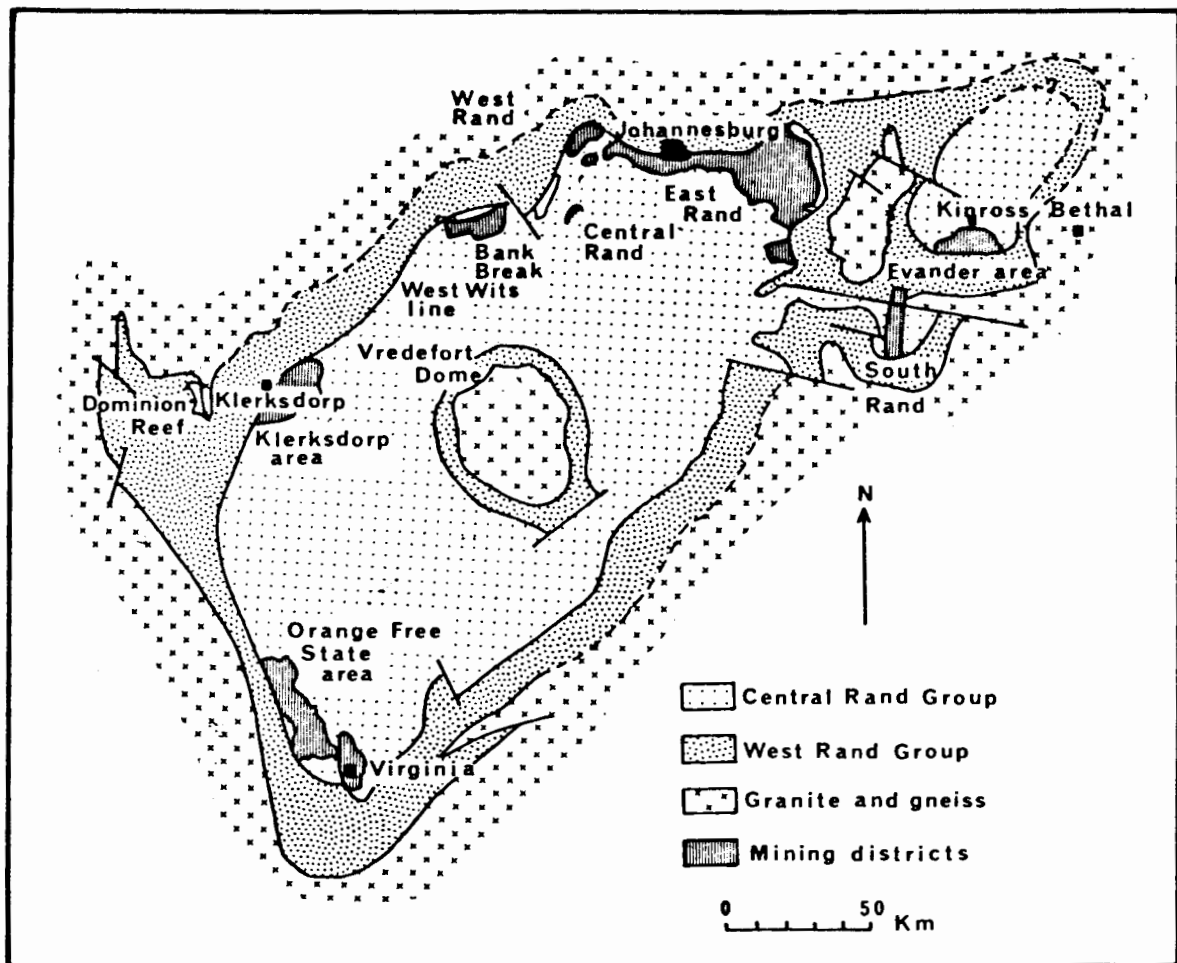


FIGURE 2 Map showing the distribution of the Witwatersrand Supergroup below the cover of Karoo, Transvaal and Ventersdorp sequences as revealed by diamond drilling (after Borchers 1964).

Realising the complexity of the problem and having a knowledge of the extensive faulting in the West Rand Group, Mellor (1911) constructed "an approximately representative section of the lower Witwatersrand applicable to both the Central and at least adjacent portions of the Western Rand". By 1917, the detailed stratigraphy of the West Rand Group had been deciphered by Mellor in the faulted country on the Central and West Rand, and since then the persistence of most of the lithologies has been confirmed by Rogers (1924) for the Heidelberg area and by Nel (1927; 1933; 1939) for the Vredefort, Klerksdorp and Ventersdorp districts. During the 1930's magnetic geophysical methods traced the magnetic shales of the West Rand Group beneath younger strata (Krahmann 1930; 1936, Reinecke and Krahmann 1935; Weiss 1936; 1950) and by 1940 deep diamond drilling began to provide direct evidence of the extension of the Witwatersrand Supergroup and a cover of younger strata.

Mellor's work (1911; 1917) remained the basis of subdivision of the West Rand Group for over forty years and it was only in 1960 that Collender questioned it. Verwoerd (1964) and Truswell (1967) reviewed the nomenclature used in the South African Stratigraphic column, and subsequently, a new classification of the Witwatersrand sediments was compiled by Wagener (1972). Winter (1978), the chairman of the Witwatersrand Working Group of SACS (South African Committee for Stratigraphy) proposed a lithostratigraphic subdivision of the Witwatersrand Supergroup. Figure 3 compares Mellor's (1917) stratigraphic column to that of the South African Committee for Stratigraphy. In this review the terminology used by SACS will be adhered to.

1.3 Purpose of Review

The literature on the Witwatersrand is voluminous and there is hardly an aspect of the deposits that has not been studied. Most papers, books and reviews, however, are concerned with the auriferous and uraniferous reefs of the Central Rand Group. The purpose of this review, together with the bibliography, is to summarise what is currently known about the West Rand Group.

The significance of understanding more about the West Rand Group is threefold. Firstly, sedimentological and geophysical marker horizons within these strata have long been used to correlate rock-units over large areas. It has, however, become clear that these marker horizons are not as

after MELLOR (1917)				after SACS (1978)			
MEMBERS & BEDS (markers)		SERIES	Thickness (m)	FORMATIONS	MEMBERS & BEDS (markers)		
LOWER WITWATERSRAND SYSTEM		JEPPESTOWN SERIES	T		ROODEPOORT		
				500			
			S				
				250			CROWN LAVA
			R				
			GOVERNMENT REEF SERIES	Q	300	FLORIDA QUARTZITE	
		P					
		O					
	Government reef	N ₃					
		N ₂					
			GOVERNMENT REEF SERIES	M ₂	500	WITPOORTJIE	Government reef
		N ₁					
		M ₁					
	Coronation reef	K ₂					
		L			CORONATION SHALE	Coronation reef	
			GOVERNMENT REEF SERIES	K ₁			Hamberg Quartzite Member
				1000	PROMISE QUARTZITE		
	J						
Promise reefs	I						
	H ₂						
		HOSPITAL HILL SERIES	H ₁	700	BRIXTON		
	G ₁						
	H ₁						
	F						
	E						
		HOSPITAL HILL SERIES	D	700	PARKTOWN SHALE	Observatory Shale Member Contorted Bed	
						Speckled Bed	
Speckled Bed	C					Red Shales	
	D					Ripple marked Quartzite	
Ripple-marked Quartzites	B					Water Tower Shale Member	
		HOSPITAL HILL SERIES	A				
				200	ORANGE GROVE QUARTZITE		
Orange Grove Quartzites	A						
					JEPPESTOWN SUBGROUP	WEST RAND GROUP	
					GOVERNMENT SUBGROUP		
					HOSPITAL HILL SUBGROUP		

Figure 3: Comparison of West Rand Group stratigraphy as defined by Mellor (1917)

persistent as previously thought. Secondly, the environment of deposition has been attributed to littoral (Becker 1896; Gregory 1908; Young 1917) deltaic or estuarine (Mellor 1916), marine (Graton 1930; Sharpe 1949), alluvial (Reinecke 1928; Bain 1955; 1960), and alluvial plain and lacustrine (Pretorius 1966; Vos 1975). An overall synthesis of previous work done by Whiteside et al (1976) concluded that the "lower division strata preserved around the periphery of the basin are almost exclusively composed of distal facies sediments, deposited for the most part beyond the fan base". A better knowledge of the geochemical and sedimentological characteristics of the West Rand Group would refine these wide-ranging models for the depositional environment of the Witwatersrand. Lastly, although conglomerates within the West Rand Group are lenticular and their gold content erratic, they have been mined in the Rietkuil Syncline and at the Buffelsdoorn Mine to the north west and the north of the Klerksdorp Goldfield. This review will thus provide a basis for further consideration of the nature and origin of the strata and the extent of mineralisation.

2. AGE OF THE WITWATERSRAND SUPERGROUP

2.1 Geochronology

Previously, an interpolated age of the Witwatersrand Supergroup was defined by a maximum of 2720^{+55} m.y. (Rb-Sr) for underlying granite (Allsopp 1964) and a minimum of 2300^{+100} m.y. (U-Pb) for lavas of the overlying Ventersdorp Supergroup (van Niekerk and Burger 1964). Rundle and Snelling (1977) assigned a younger age limit of the Witwatersrand Supergroup at 2290^{+85} m.y. (Ventersdorp lava) and suggested an older limit of 2740^{+19} m.y. (weighted mean age of the Schweizer Reneke granite and the Dominion Reef lava). These wide time limits for the deposition of the Witwatersrand Supergroup have resulted in several, more precise estimates being attempted. Pretorius (1974) suggested an age of between 2500 and 2750 m.y. whereas Reimer (1975) calculated, on the basis of approximated accumulation rates, that the Witwatersrand Supergroup was deposited over a period of 30-40 m.y. between 2470 m.y. and 2370 m.y.

New age-data for the Ventersdorp Supergroup restricts the age of the Witwatersrand Supergroup to between 2620 and 2800 m.y. The lower limit is set by van Niekerk and Burger's (1978) dating of a rhyolite within the Makwassie Formation of the Platberg Group in the Ventersdorp Supergroup (2620^{+55} m.y., U-Pb). However Allsopp (1978) (personal communication) considers the 2620 m.y. date to be too high and suggests that the zircons on which the age was determined are relic. Clearly, a direct age determination on either the Crown lava in the Jeppestown Subgroup or on the Bird

amygdaloid lava in the Central Rand Group would be invaluable in helping to decide between the widely divergent ages outlined above. Reviewing all the geochronological data published on the West Rand Group, a tentative estimated age of 2750 m.y. was put on the Contorted Bed, Hospital Hill Subgroup by SACS (1978). Table 1 is a tabulation of all radiometric dates pertinent to the Witwatersrand Supergroup.

On present evidence the Witwatersrand basin is therefore Archaen, i.e. >2500 m.y. old. However, Pretorius (1974) noted that "the transition from Archaen to Proterozoic style of crustal evolution took place on the Kaapvaal craton at between 3000 and 3250 m.y. ago. On other shield areas of the world, the age of transition has been dated at about 2500 m.y." This comment emphasises the Proterozoic aspect of the Witwatersrand Supergroup despite its formal position in the Archaen.

2.2 Possible Correlatives

The Dominion Group, Witwatersrand Supergroup and Ventersdorp Supergroup (generally known as the Witwatersrand Triad) are considered to be areally and structurally closely related (Brock and Pretorius 1964a). Cloud (1976) prefers to group the Pongola Group, Dominion Group, Zoetlief Group, and Witwatersrand Supergroup together, on the basis that the entire sequence, from the Pongola Group to the Witwatersrand Supergroup, is unique in the record of crustal evolution.

The Economic Geology Research Unit (E.G.R.U.) of the University of Witwatersrand evaluated the following possible correlatives of the Witwatersrand Supergroup:

(i) Nzuzi and Mozaan Subgroups:- On the 1955 maps of the Geology of South Africa compiled by the Geological Survey, the Mozaan Subgroup of the Pongola Group is correlated with the Witwatersrand Supergroup and the Nzuzi with the Dominion Group based on the work of Humphrey (1931) and Truter (1949). Allsopp et al (1962) date of a granite (3070 m.y.) intruded into the Mozaan near the Swaziland border and Davies et al (1969) age of 2900 m.y. for the Usushwana Complex in Swaziland, which is intrusive into the Nzuzi Subgroup, confirm Pretorius' (1964) conclusions that the Mozaan is older than the Witwatersrand Supergroup based on studies in the Mahlangatsha area of Swaziland.

(ii) Dominion Group:- Molengraaf (1905) considered the sediments in this group to be equivalent to the Orange Grove quartzite of the West Rand

TABLE 1: Age measurements relevant to the dating of the Witwatersrand Supergroup

UP/SUPERGROUP	MATERIAL DATED	METHOD	AGE IN M.Y.	REFERENCE
<u>MAXIMUM AGE OF WITWATERSRAND SUPERGROUP</u>				
EMENT PLEX	Granite	Rb-Sr	2700 ⁺ 55	Allsopp (1964)
	Granite	Rb-Sr	2900 ⁺ 150	Nicolaysen <u>et al</u> (1962)
	Granite (uraninite, monzanite)	U-Pb	3100 ⁺ 100	Nicolaysen <u>et al</u> (1962)
UNION IP	Spherulitic andesite (apatite, sulphide)	U-Pb	2800 ⁺ 60	van Niekerk and Burger (1969b)
	Quartz porphyry (sulphide)	U-Pb	2800	van Niekerk and Burger (1969a)
	Conglomerate (uraniferous minerals)	U-Pb	3050 ⁺ 50	Nicolaysen <u>et al</u> (1962) Rundle and Snelling (1977)
	Dacite	U-Pb	2820 ⁺ 110	van Niekerk (1968)
	Andesite	U-Pb	2830 ⁺ 110	van Niekerk (1968)

MINIMUM AGE OF WITWATERSRAND SUPERGROUP

TERS DORP ER GROUP	Rhyolite (zircons)	U-Pb	2620 ⁺ 50	van Niekerk and Burger (1978)
	lava (zircon)	U-Pb	2300 ⁺ 100	van Niekerk and Burger (1964)
	lava (zircon)	U-Pb	2290 ⁺ 85	Rundle and Snelling (1977)
	lava (zircon)	U-Pb	2285 ⁺ 50	Rundle and Snelling (1977)
	lava (zircon)	U-Pb	2245 ⁺ 90	van Niekerk (1968)
	lava	U-Pb	2238 ⁺ 110	van Niekerk and Burger (1964)

Group and the lavas he assigned to the Ventersdorp Supergroup. Nel (1934) included the overlying lavas in the Dominion Group, but still allocated it to the West Rand Group. Truter (1949) correlated the Dominion Group with the Uitkyk, Godwan and Koras Formations and suggested that they be regarded as separate groups. This view was supported by Von Backström (1952; 1962), Nel and Verster (1962) and Van Eeden et al (1963). Pretorius⁽¹⁹⁷⁴⁾ rejects the concept of the Dominion Group succession as a separate group and suggests that it should again be relegated to the West Rand Group of the Witwatersrand Supergroup, because it represents the initial phase of volcanic activity and sedimentation within the Witwatersrand basin.

(iii) The Zoetlief, Wolkberg and Uitkyk Formations and the rocks between Thabazimbi and the Botswana border (termed the Buffalo Springs Group by Tyler 1978) are all lithologically similar to the Dominion Group at the base of the Witwatersrand Supergroup (Pretorius 1966).

Recent lead isotope dating of acid lavas indicate that the Zoetlief volcanic sequence was extruded 2500 - 2700 m.y. ago (Van Niekerk and Burger 1968) which suggests on present geochronological evidence that the coarse feldspathic sediments of this formation could have been deposited while the Witwatersrand Basin was being filled.

The Wolkberg Formation, named by Truter (1949) and correlated with the Witwatersrand sediments, is now regarded as an integral part of the Transvaal Supergroup, grading into, and being conformably overlain by, the Black Reef Quartzite (Button 1973).

Van Rooyen (1947) mapped a small group of rocks lying north east of Potgietersrust which he named the Uitkyk Formation and tentatively correlated them with the Witwatersrand Supergroup. Pretorius (1964) noted the close structural and lithological resemblance between this Formation and that of the Moodies and Fig Tree sediments in the Swaziland Supergroup. Pretorius concludes, as did Hall (1911), that the Uitkyk Formation is a synclinal remnant outlier of the Swaziland Supergroup.

The rocks between Botswana and Thabazimbi have been correlated with the Dominion Reef Group (Truter, 1949; Schatte et al 1960), the Ventersdorp Supergroup (Kynaston 1911; Jansen 1974) and more recently with the Wolkberg Group of the Transvaal Supergroup (Tyler 1978).

(iv) The Godwan Formation in the Kaapsehoop area of the eastern Transvaal was mapped by Hall in 1905 and 1918 and was thought to be a Ventersdorp equivalent. Truter (1949) correlated the succession with the Nzuzi Subgroup of the Pongola Supergroup. Recently, Button (1978) correlated the Formation with the Central Rand Group based on stratigraphic and structural

trends in the Witwatersrand Basin. He rejects Truter's (1949) correlation on the basis that 'the nearest Pongola sediments are in the Amsterdam area, 110 km south of Kaapsehoop across the tectonic grain of the Kaapvaal craton'. Furthermore, the Ventersdorp correlation is not favoured because the nearest known Ventersdorp rocks at Evander are not of significant thickness and a West Rand Group correlation is unlikely because the Godwan contains no magnetic shales and orthoquartzites. Button (1978) concludes that the Godwan Formation is probably 'the easternmost exposure of the Upper Witwatersrand basin'.

(v) A borehole (441JP) drilled by the Geological Survey south of Mazista in the Western Transvaal penetrated shales and quartzite of the Hospital Hill Subgroup. The location of this borehole is outside the presently known boundary of the Witwatersrand basin, and proved that the West Rand Group extends considerably farther to the north-west than previously thought (Martini 1975). Furthermore, the only difference between the Hospital Hill subgroup drilled in this area to that mapped by Nel (1935) in the Klerksdorp-Ventersdorp area is the greater number of arenaceous units present in the former.

3. STRATIGRAPHY

The variations in thickness within the Jeppestown, Hospital Hill and Government subgroups, the presence of stratigraphic markers unique to certain areas and the recognition of cyclic sedimentation in local areas makes it convenient to consider the stratigraphy of the West Rand Group in four separate areas: the Central and West Rand, Heidelberg-Balfour-Delmas (including the South Rand Goldfield), Vredefort-Parys and the Klerksdorp-Ventersdorp areas. In addition to these areas, the West Rand Group sediments have been described in five synclinal outliers; the Bultfontein and Middelbult basins, which lie north and south-west of the village of Delmas (Button 1970); the Evander basin - 110 km southeast of Johannesburg (Jansen ^{et al} 1972); the most northerly outlier of the West Rand Group, situated fifteen kilometers north of Krugersdorp (Hendriks 1961); and the Orange Free State goldfield (Coetzee 1960). The first three named will be described under the heading Heidelberg-Balfour-Delmas Area while the fourth and fifth will be discussed separately.

3.1 The Central and West Rand area

The Central and West Rand area centered around Johannesburg and extends from Boksburg in the east to about twenty kilometers west of Krugersdorp in the west. The West Rand group is best exposed near Krugersdorp where

faulting has resulted in the duplication and thickening of the succession. Two of these faults, the Witpoortjie and Roodepoort, define a horst containing the West Rand Group, and it is this structure which forms the boundary between the West and Central Rand. The stratigraphic column in these two areas will be described together. [Figure 4 compares the composite sections of the West and Central Rand (after Mellor 1911; 1913) and it is apparent that the succession on the West Rand is thicker than those on the Central Rand.]

Mellor's (1911; 1913; 1917) stratigraphic columns for the Central and West Rand area have been refined by Pretorius (1964), Roering (1968), Wagener (1972) and Cousins (1965; 1973). The following subdivisions, stratigraphic terminology and stratigraphic marker horizons have been taken from the above-mentioned authors and also SACS (1978).

3.1.1 The Hospital Hill Subgroup

On the Central Rand the Hospital Hill Subgroup is divided into three formations: the Orange Grove Quartzites (200 m), Parktown Shale (700 m) and Brixton (700 m). The subgroup consists of 60 per cent shales which are frequently ferruginous and magnetic and 40 per cent fine grained quartzites. It occupies the stratigraphic column from the base of the Witwatersrand succession to the base of the quartzite containing the Promise Reef.

3.1.1.1 The Orange Grove Quartzites

The Orange Grove Quartzites rest unconformably on the Johannesburg granite dome and on the Muldersdrif Ultramafic Complex. It is a dominantly arenaceous formation made up of two major orthoquartzitic units (103 m and 52 m) separated from each other by shaly or locally schistose members (not more than 45 m thick). The thickness of the formation remains fairly constant, although laterally the outcrop is "very variable in appearance and character" (Mellor 1911). For instance, the first major orthoquartzitic unit may in some places consist of three quartzite members separated from each other by thin green to grey shales. The typical bluish black colour of the first shale band on the West Rand serves as a significant marker (Roering 1968).

Intermittent thin bands of conglomerate at the base are followed by thinly bedded, yellowish white to brown, fine to medium grained recrystallized quartzites. The Orange Grove Quartzites do not have a sharp upper contact, the arenaceous sediments being succeeded by a fine grained facies through a gradual transition zone (Roering 1968).

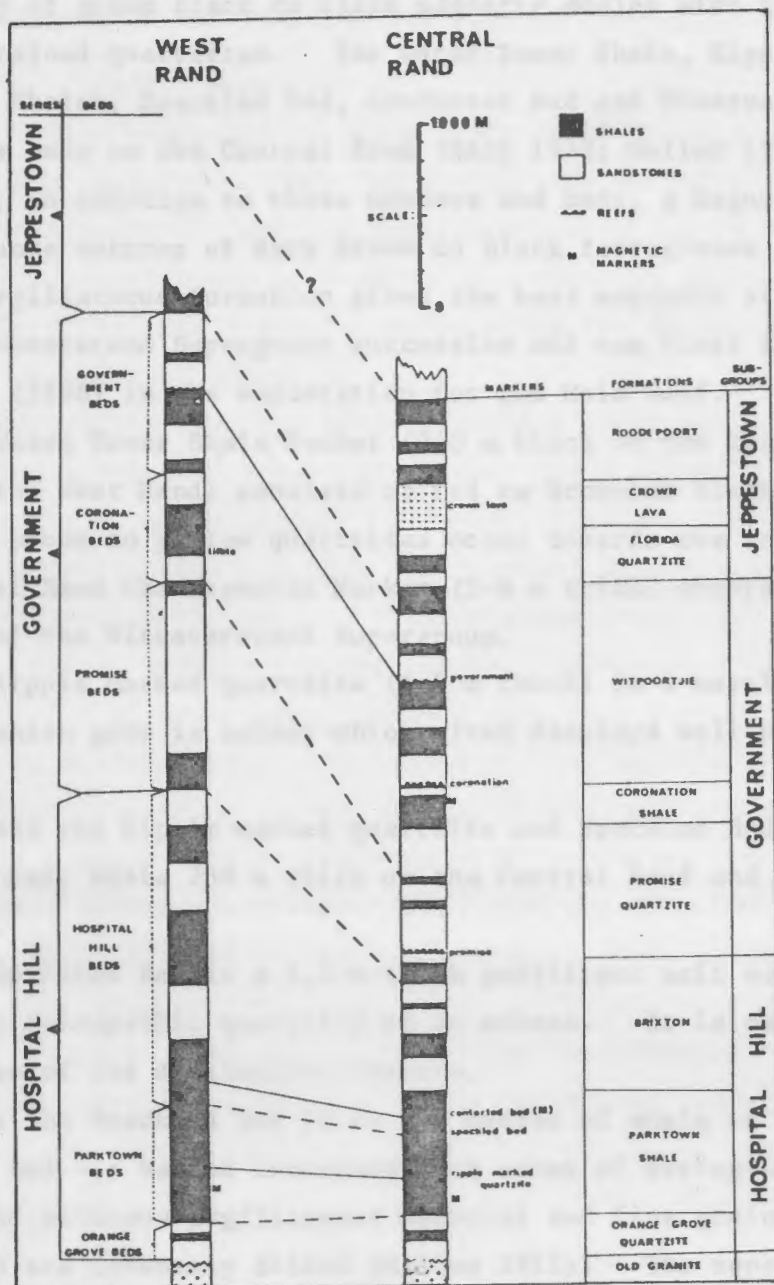


Figure 4: Stratigraphy of the West Rand Group in the West Rand and Central Rand areas (after Mellor 1911,1913).

3.1.1.2 Parktown Shale

The Parktown Shale formation has a thickness of approximately 700 m on the Central Rand and 1000 m on the West Rand. The formation consists dominantly of green black to black magnetic shales with interbedded medium to fine grained quartzites. The Water Tower Shale, Ripple Marked Quartzite, Red Shales, Speckled Bed, Contorted Bed and Observatory Shale Members are marker beds on the Central Rand (SACS 1978; Mellor 1911) while on the West Rand, in addition to these members and beds, a Magnetic Marker forms a conspicuous outcrop of dark brown to black ferruginous shale. This dominantly argillaceous formation gives the best magnetic signature of the whole Witwatersrand Supergroup succession and was first identified and used by Draper (1896) in the exploration for the Main Reef.

The Water Tower Shale Member (240 m thick on the Central Rand and 290 m thick on the West Rand) consists of red to brownish black ferruginous shales. Lenses of brown to yellow quartzites occur towards the top of the member. On the West Rand the Magnetic Marker (3-6 m thick) occurs about 370 m above the base of the Witwatersrand Supergroup.

The Ripple Marked quartzite (6-8 m thick) is a massively bedded quartzite, greenish grey in colour which often displays well preserved ripple marks.

Between the Ripple marked quartzite and Speckled Bed is an inconspicuous soft, red, shale 230 m thick on the Central Rand and 320 m thick on the West Rand.

The Speckled Bed is a 1,5 m thick persistent unit varying in composition from a feldspathic quartzite to an arkose. It is called the Speckled Bed because of its distinctive texture.

Above the Speckled Bed 70 to 120 metres of shale is followed by the Contorted Bed - a banded ironstone with zones of ferruginous chert, thinly interbedded siliceous argillaceous material and fine grained magnetic quartzite which are intensely folded (Mellor 1911). The zone of folding is confined to a 3-9 m thick horizon and according to Fripp and Guy (1972) there is a strong geometrical control (i.e. can be classified into a particular class of fold (after Ramsay 1967)) over the formation of the folds. However, Truswell (1977) sees no pattern in the disharmonic contortions and suggests the folding and contortions are slump features. The Contorted Bed is the most conspicuous marker on both the Central and West Rand.

The Observatory Shale Member overlying the Contorted Bed is 130 m thick on the Central Rand and more than 240 m thick on the West Rand. It is reddish, purplish or brownish black in colour and is markedly ferruginous just above the Contorted Bed. On the West Rand immediately underlying

the quartzites of the Brixton Formation is a 3-6 m discontinuous magnetic shale bed which has 2-12 cm pitted solution cavities (Roering 1968).

The Parktown Shale, as defined by SACS (1978) includes Mellor's (1911; 1913) Parktown Beds and about 20 per cent of his Hospital Hill Beds.

3.1.1.3 Brixton Formation

The Brixton Formation is 700 m thick on the Central Rand and about 1600 m on the West Rand. Roering (1968) regards the three major quartzite units of this formation and the overlying quartzites in the Government Subgroup as an "entire group of dominantly arenaceous sediments belonging to a new cycle of sedimentation following after the deposition of the dominant argillaceous sequence below".

On the Central Rand the three quartzite units are similar to the Orange Grove quartzites, except in places, for a greenish colour due to chrome bearing mica, fuchsite. The quartzites are fine to medium grained with the coarser grains set in a fine grained matrix, which give rise to a distinctive 'sago structure'. The first quartzite (190 m) is exceptionally fine grained and has few sago bands. The second (140 m) and third quartzites (100 m) are coarser grained with more frequent sago textures. According to Mellor (1917), the number of beds which make up the quartzites of the Brixton Formation (Hospital Hill Quartzites) decreases eastwards, there being three quartzite horizons at Witpoortjie, two at Maraisburg, and only one from Johannesburg eastwards. The intercalated shales are dark grey to black, often ferruginous and magnetic and occasionally banded and cherty as with the Contorted Bed.

SACS' Hospital Hill Subgroup includes the shale unit (110 m) above the last Brixton quartzite whereas Mellor's Government Reef Series begins at the base of this shale unit.

3.1.2 The Government Subgroup

SACS (1978) divides the Government Subgroup (approximately 1700 m) into three formations - Promise Quartzite (1000 m), Coronation Shale (200 m) and Witpoortjie (500 m) which do not correspond to the Government Stage, Coronation Stage and Promise Stage of previous workers (Pretorius 1964; Mellor 1911). Coarse quartzites with occasional conglomerates make up about 70 per cent of the succession. Mellor (1917) found the Government Reef quartzites to be less purely siliceous than those of the Hospital Hill Subgroup. The subgroup is taken from Mellor's Promise Reef Beds (J) to the top of the shale (O) overlying the 'Upper Government Quartzite' N2 (Figure 3).

3.1.2.1 Promise Quartzite

The Promise Quartzite Formation consists of three sandstone units with two shale units on the Central Rand and two sandstone units and a shale unit on the West Rand. The individual units show great variations in thickness and are ill-defined due to the rapid alternations of fine grained sericitic sandstones, shales and coarse grained dirty quartzite (or sub-greywackes).

The lower arenaceous unit is about 310 m thick on the Central Rand and 870 m on the West Rand. About 80 m above the base of this unit, a 0,3 m thick pebble conglomerate, the Promise Reef, containing pebbles varying from 2 to 5 cm in diameter occurs on the Central Rand. At about the same stratigraphic level as the Promise Reef on the Central Rand, Roering (1968) has recognised a tilloid on the West Rand which has "a reddish weathering quartzite matrix in which occur widely disseminated rounded pebbles of varying sizes".

Two 30 m shale bands separated by a 90 m sandstone unit overly this arenaceous unit on the Central Rand while on the West Rand there is only one 70 m thick shale band.

The quartzite (250 m thick on the Central Rand and 200 m on the West Rand) underlying the Coronation Shale is a coarse grained white to yellowish quartzite with numerous coarse grit bands. It is known as the Lower Coronation Quartzite (Mellor 1911) of Hamberg Quartzite Member (SACS 1978). Cross bedding is very common within this thin bedded unit.

3.1.2.2 Coronation Shale

The Coronation Shale (or West Rand Shale) is about 180 m thick on the Central Rand and 230 m on the West Rand. It is a "series of flaggy, shaly beds, passing up into highly ferruginous sandstone and shales" (Mellor 1917). According to Cousins (1973) they "closely resemble a varved shale". Near Roodepoort on the West Rand, tillites below the Coronation Shale are markers which are correlated with the tillites in Heidelberg, East Rand, West Wits Line and Klerksdorp areas (Pretorius 1964). According to Truswell (1970), the Coronation Shale is of special significance because it is the stratigraphically highest of the three magnetic horizons within the West Rand Group (the others being the magnetic horizons within the Water Tower Slates and the Contorted Bed of the Hospital Hill Subgroup). However, higher up the succession SACS (1978) noted that there are numerous conglomerate bands and associated grey to black often highly magnetic shales. Mellor (1911) used the term 'ferruginous' in many descriptions in place of the term 'magnetic'. Furthermore, according to Mellor, a "large proportion of the shales show this property to some degree".

3.1.2.3 The Witpoortjie Formation

The Witpoortjie Formation is about 1150 m thick on both the Central and West Rand. SACS' (1978) thickness of 500 m for this formation appears to be too low as even the thinnest portion of the West Rand Group in this area - that along the Witpoortjie fault - measures 620 m. The Witpoortjie formation consists of dark green magnetic shales, green silty shales and siltstones and argillaceous to gritty quartzites. Two of the four arenaceous units have persistent conglomerate bands while the four shale units in this formation have no distinctive markers.

The first quartzitic sandstone (180 m thick on both the Central and West Rand) consists of an alternation of hard coarse gritty quartzites with finer grained bands. A few centimetres above the base a persistent conglomerate band, the 'Coronation Reef' outcrops on the Central Rand. On the West Rand this 1 m thick conglomerate layer is not present although coarse, gritty to pebbly bands are present near the base. The quartzites fine upwards and are gradually replaced by a series of soft reddish brown shaly sandstones and shales (150 m thick).

The second quartzitic unit (90 m) is medium to coarse grained, thin bedded and is yellowish to brown in colour. The top metre is fine grained and often green in colour. This is followed by a 140 m thick sandy shale which tends to get more ferruginous at the base of the following quartzitic unit.

The third quartzitic unit begins with a well defined 'reef' on both the Central and West Rand. The Government Reef is a conglomerate with pebbles up to 6 cm in diameter. It is 1 m thick on the West Rand thinning eastwards to a single line of pebbles on the Central Rand. It is followed by a quartzitic unit (150 m) which is fine grained in places but generally rather coarse. 36 m above the Government Reef a well developed pebble bed - often better developed than the Government Reef itself - known as the Government Reef Leader occurs between Roodepoort and Florida (Mellor 1911). A 40 m shale overlies this distinctive quartzitic unit.

The uppermost quartzitic unit (150 m thick) in this formation is fine grained at the base and grades upwards into medium to rather coarse grained quartzites, with occasional bands of grit. The contact with the overlying shale is transitional with thick bedded, purplish red sandstones passing into ferruginous slaty shale. The shale (150 m thick) is fairly massive and is incorporated into the Jeppestown Series by Mellor (1917).

3.1.3. The Jeppestown Subgroup

The Jeppestown Subgroup consists of three formations - the Florida Quartzite (300 m), Crown Lava (250 m) and Roodepoort (500 m). ^(SACS 1978) Cousins (1965)

noted the persistence of the Crown lava (formerly the Jeppestown lava) into the Central Rand area and thus refined the succession compiled by Mellor (1911) as cited by Pretorius (1964). However, Cousins (1973) points out "that Mellor was handicapped severely in his field mapping by the lack of exposures in the wide, flat valley which follows the Jeppestown beds from Johannesburg to Roodepoort".

3.1.3.1 The Florida Quartzite Formation

This formation consists of two quartzitic units separated by a 90 m thick slaty shale. The lower quartzitic unit (70 m) has an erratically occurring thin pebble band at its base and fines upwards. The upper quartzite (140 m thick) is strongly cross bedded, rather coarse and massive in places. The interbedded shale is magnetic (Cousins 1973).

3.1.3.2 The Crown Lava

These lavas are described as "dark green, often slightly brown, fine grained to cherty lavas, occasionally finely porphyritic, often amygdaloidal with associated minor quartzitic, tuffaceous or agglomeratic sediments" (SACS 1978).

3.1.3.3 The Roodepoort Formation

This formation consists of three shale units separated from each other by two fine grained argillaceous quartzites. The lower shaly unit seldom outcrops and has a thickness of about 95 m. No distinctive features have been recorded for the overlying quartzite (72 m), shale (108 m) and quartzite (95 m) units.

More information is available for the uppermost shale unit probably because of its frequent occurrence in the footwall of the Main Conglomerate on the Central Rand. Cousins (1965) noted that "the upper shales of the Jeppestown subgroup grade gradually from fine to coarser-grained sediments. Above the massive shale, argillaceous quartzite with shale bands is found for some 15 metres. The shale bands first become subordinate and then absent, while the argillaceous quartzite grades slowly upwards into cleaner, less argillaceous and coarser grained quartzite. The change is progressive without any sudden variation. Furthermore, chloritoid and 'square pebbles' have been recorded between the uppermost shale and Main Conglomerate (Roberts and Kransdorff 1938; Pegg 1950 and Wiebels 1951). Wiebels (1955) believes that these and other similar rocks are of glacial origin. North of the Witpoortjie Fault Toens and Griffiths (1964) describe chert and quartz cobbles which are usually about 15 cm in diameter occurring midway between the shale and the Main Conglomerate. SACS (1978) has named all these arenaceous sediments between the Main Conglomerate (which is the Main Reef, Leader reef,

South reef, etc) and shale horizon the Maraisburg Quartzite and incorporated them into the Central Rand Group. Cousins (1965) suggested that the base of the Main Conglomerate, not the top of the upper shale of the Jeppestown Subgroup, should be taken as the contact between the West and Central Rand Group. In all the outcrop areas, bar the proximal arenaceous sediments of the Klerksdorp area where no argillaceous unit exists in the Roodepoort Formation the SACS (1978) stratigraphic nomenclature will be adopted.

3.2 The Heidelberg-Balfour-Delmas Area

East of Heidelberg the entire West Rand Group succession crops out almost continuously along the eastern rim of the Witwatersrand basin, whereas south of the Sugarbush Fault and near Delmas only scattered outcrops occur due to the covering of younger formations. The exact outline of the Witwatersrand basin is still unknown in this area because of the limited drilling that has taken place (Whiteside et al 1976). The Heidelberg-Balfour-Delmas area has in the past been divided into four separate areas - the Heidelberg area, South Rand area, Evander area and Delmas area (Figure 5).

In the Heidelberg area, West Rand Group strata crop out in an area bounded by the towns of Nigel, Heidelberg and Balfour. De Jager (1964) reviewed the geology of this area (the East Rand) which was first mapped by Rogers in 1918.

The South Rand area (which incorporates the South Rand Goldfields as delineated by Pretorius 1964) is situated between the Sugarbush Fault and the Vaal River. The area has been intensively drilled (Sawyer 1904) and a review of its geology has been presented by Pretorius (1964). The three subgroups of the West Rand Group are all represented but they thin from a total thickness of 2710 metres in the northernmost portion of the area to 1615 metres in the south eastern area where the field is terminated by granite and Swaziland Supergroup rocks.

The Witwatersrand Supergroup in the Delmas area has been mapped by Button (1970). The small amount of data (Fox 1939) available on the West Rand Group in the Evander basin has been collated by Jansen et al (1972).

The comparative stratigraphy of the West Rand Group in these four areas is given in Figure 6 and it is apparent that the succession decreases in thickness and becomes more argillaceous both in an easterly and a southerly direction. Furthermore, although some of the stratigraphic markers typical on the West and Central Rand are identified in the Heidelberg area, there are other markers (eg. Black grit and Blue grit) which are unique to this region.

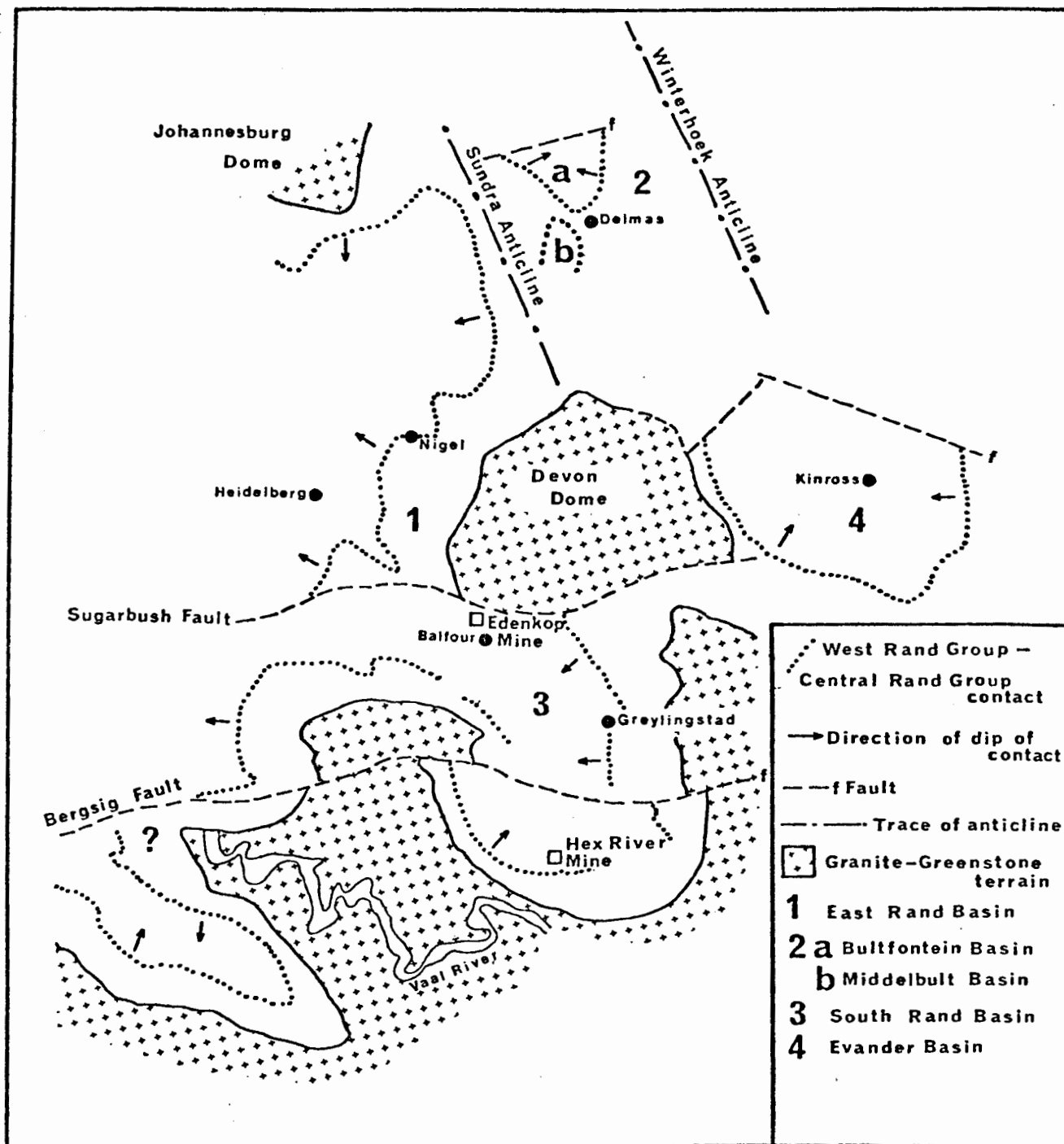


Figure 5: Simplified map showing the basin geometry of the Heidelberg - Delmas-Balfour area. The Sugarbush fault, Sundra anticline and Devon Dome divides the area into four parts:- 1. East Rand basin; 2. Delmas area; 3. South Rand basin and 4. Evander basin (after Pretorius 1964, Button 1970, Whiteside et al., 1976).

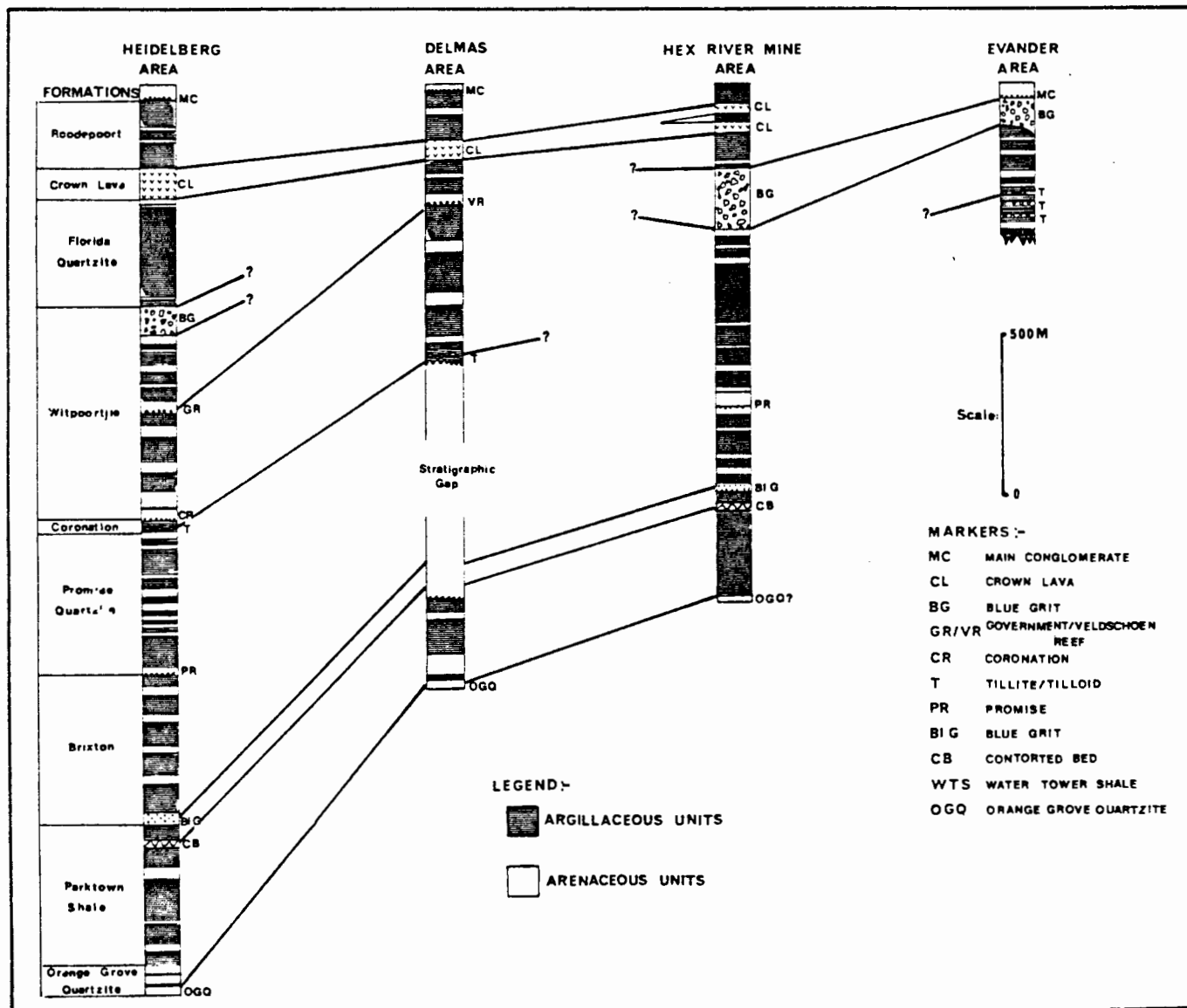


Figure 6: Comparative West Rand Group stratigraphy of the Heidelberg-Delmas-Balfour area (modified after Jansen et al, 1972; Button, 1970)

3.2.1 Hospital Hill Subgroup

This subgroup is 1000 m thick near Heidelberg and 600 m in the South Rand as compared to 1600 m on the Central Rand (Rogers 1922; Pretorius 1964). In the Delmas area there is a stratigraphic break of some 750 m within the Parktown Shale, Brixton and Promise Quartzite Formations. Although there are more quartzite units in this subgroup in the Heidelberg-Balfour-Delmas area than on the Central Rand, the proportion of quartzite to shale is almost the same (about 38 per cent of the total thickness on the Central Rand and 36 per cent near Heidelberg).

3.2.1.1 The Orange Grove Quartzite

This formation is poorly or not at all developed in the South Rand area whereas on the East Rand and near Delmas it measures 72-107 and 150 meters respectively (Rogers 1922; Button 1970). In these two areas the Orange Grove Quartzite formation is split into three quartzite units by two shale bands. In the Heidelberg area the basal quartzite rests unconformably on red weathering schistose shale, a magnetic quartzite which may be tentatively correlated with the Fig Tree Group of the Swaziland Supergroup (Jansen et al 1972) and in parts on a granitic palaeosoil. Near Delmas the Orange Grove Quartzite lies on Basement Granite.

At the base of the first plane-bedded, light gray to white, orthoquartzite unit in the Heidelberg area is an erratically distributed quartz and chert pebble conglomerate (up to 1 m thick), whereas near Delmas an arkose with lenses of grit and conglomerate is of variable thickness (up to 3 m). The following table compares the thickness of the Orange Grove quartzite and shale units in the Heidelberg and Delmas areas.

TABLE 2

<u>Heidelberg (after Rogers 1922)</u>		<u>Near Delmas (Button 1970)</u>	
Basal quartzite	29 m	Basal Quartzite	48 m
Shale	6 m	Shale	8,5 m
Quartzite	16 m	Quartzite	56 m
Shale	4,5 m	Shale	1 m
Quartzite	19 m	Quartzite	40 m
	<u>74,5 m</u>		<u>151,5 m</u>

Near Delmas the first shale unit is ripple marked and dark coloured. The overlying quartzite is siliceous, medium grained and varies in colour from light to dark gray. An inconspicuous shale band which lenses out in places is followed by the uppermost siliceous to argillaceous quartzite.

3.2.1.2 Parktown Shale

This formation measures about 400 m in the Heidelberg area, is at least 128 m in the Delmas area and is very poorly developed (8-30 m) in the South Rand area. In the Evander basin Fox (1939) correlated portions of borehole sections with the West Rand Group and a tentative thickness of 420 m for Parktown Shale was proposed. However, Jansen et al (1972) and Whiteside et al (1976) have reviewed the geology in this area and both correlate the 958 m of rocks drilled below the Main Reef horizon as belonging to the Government Subgroup. The lenticular graywacke (0-580 m) with cobbles and boulders described by Fox as probably belonging to the Ventersdorp Supergroup is now correlated with the Blue Grit unit of the South Rand-Heidelberg area (Figure 6).

On the Central Rand the sum of the two quartzite units within the Parktown Shale Formation is less than 10 meters whereas in the Heidelberg area there are five quartzite units totalling 97 m. The magnetic shales in the Water Tower Shale members have been identified in both the Heidelberg and Delmas areas. The five quartzitic units all display well preserved cross beds and ripple marks making it impossible to correlate any one unit with the Ripple-Marked Quartzite marker of the West and Central Rand. Furthermore, in the Heidelberg area feldspathic quartzites occur well below the usual position of the Speckled bed on the Central Rand (a short distance below the Contorted Bed). The Contorted Bed has been recognised in both the South Rand and East Rand areas. In the former area it is identified more by its alternating laminations of magnetic quartzite and chert than on its folded contorted nature.

3.2.1.3 Brixton Formation

The Brixton formation consists of three thick arenaceous units and three argillaceous units on the West and Central Rand while in the Heidelberg area it contains five arenaceous units and four argillaceous units measuring about 505 m in thickness. In the South Rand area six arenaceous units with intervening shale belong to this formation and measure about 300 m (Pretorius 1964).

The first quartzite in this formation (about 55 m thick in the Heidelberg area and between 30 and 8 m in the South Rand area) serves as a useful marker in both the East and South Rand. It is a medium to coarse grained quartzite which has conglomerate lenses containing angular chert pebbles (up to 2.5 cm) and is known as the Black Grit (Sawyer 1907; Rogers 1922; Nel 1933). In addition to the black chert fragments it may contain pebbles of less than 1.3 cm diameter of white and gray quartz, quartzite, calcareous quartzite, shale and limestone (Sawyer 1907). Rogers (1922) described a thin section

cut from the Black Grit and noted that a peculiarity in this rock is the presence of liquid inclusions and muscovite in the quartz grains.

Above the Black Grit quartzite unit the remaining "sago textured" white weathered quartzites in the Heidelberg area vary in thickness from 23-52 m and are separated by red weathered shales, some of which are slightly magnetic. Rogers (1922) distinguishes these shales from the shales within the Parktown Shale by the fact "that they do not become as strongly magnetic nor are they so well banded with slightly or non ferruginous layers". The topmost quartzite (23 m) of the Hospital Hill Subgroup is orthoquartzitic while the arenaceous units succeeding it are micaceous, gritty and red weathered.

On the South Rand two quartzite bands succeed the Black Grit and these, in turn, are overlain by 137 m of shale which become more ferruginous upwards (Pretorius 1964). Two quartzite units overly this shale in which is sporadically developed a conglomerate horizon 0.3 m thick with pebbles up to a maximum of 1.3 cm in diameter set in a fine grained matrix. The top of the Hospital Hill Subgroup is marked by a thick succession of hard, yellowish or reddish quartzites which are fine grained and contain lenses of feldspathic quartzite with sago structures.

3.2.2 Government Subgroup

Rogers (1922) correlated the Government Reef Beds near Heidelberg with those of the Central Rand and in addition mapped a tillite. Pretorius (1964) distinguished the three formations of the Government Subgroup in the poorly exposed South Rand areas where it consists of alternating white, yellow or red quartzite and ferruginous shale. The Government Subgroup is 1200 m thick near Heidelberg, 750 m near Hex River Mine and 1200 m in the Edenkop Mine on the South Rand compared to 1860 to 2000 m on the Central Rand. The best markers in the Government subgroup are tillites on the East Rand, Delmas and Evander basins; a magnetic shale, conglomerate units and a diamictite (the Blue Grit) in the East Rand, South Rand and Evander basins.

The three formations of the Government Subgroup - Promise Quartzite, Coronation Shale and Witpoortjie - delineated by SACS (1978) on the Central Rand are present in the East and South Rand by the recognition of the Promise Reef, Coronation Shale and the Coronation Reef (Rogers 1922; Pretorius 1964). Table 3 is a breakdown of the Government Subgroup into its three formations in the Delmas, Heidelberg, Evander and South Rand areas (Button 1970; Rogers 1922; Jansen *et al* 1972 and Pretorius 1964). The composite thickness of the faulted and poorly exposed Government Subgroup on the South Rand taken from Pretorius' (1964) detailed succession in both the Edenkop and Hex River

Mines, is approximately 1230 m. However, Jansen et al (1972) suggests that the succession near the Hex River Mine (750 m) is a closer approximation to a representative thickness.

3.2.2.1 Promise Quartzite Formation

The Promise Reef marker horizon is not widespread in the Heidelberg area although there are erratic, micaceous gritty conglomerates at the base of the first arenaceous unit (120 m) which have been pitted by early prospectors (Rogers 1922). In the southeastern corner of the area, near the Sugarbush River, scattered pebbles of feldspar up to 1.3 cm in diameter and a few pebbles of coarse "microcline quartz granite" set in a muddy matrix, are, according to Rogers (1922), possible equivalents of the Promise Reefs of the Central Rand. The overlying shale is magnetic in places and could be used as a local marker near Heidelberg. On the South Rand the Promise Quartzite Formation comprises Pretorius' (1964) Promise Stage and the Coronation D, Coronation C and first quartzite of the Coronation C 'substages'. In the Edenkop Mine an estimated 60 m of the basal portion of the Promise Stage, including the Promise Reef are not exposed (Pretorius 1964). However, near the Hex River Mine on the South Rand the lowest exposures of the Government Subgroup consist of four narrow bands of fine grained quartzite with intercalated shales and infrequent bands of black chert. The Promise Reef marker has not been identified (Leube 1956).

The alternating thick quartzites and thin shale units which make up the rest of the formation have no distinctive characteristics.

3.2.2.2 The Coronation Shale

Compared to the Central Rand, the Coronation Shale formation in the Heidelberg-Delmas area has better developed tillites or tilloids. It is only south of the Sugarbush Fault that tillites and magnetic shales have not yet been recognised (Pretorius 1964). However, in the Evander area the Coronation Shale Formation is about 170 m thick, in the Delmas area 31 m thick and in the East Rand 26 m thick.

In the Evander area the base of the formation is marked by a magnetic shale 15 m thick and is in turn overlain by an argillaceous quartzite 17 m thick, another magnetic shale (30 m) and the first tillite horizon (13 m) (Jansen et al 1972). A thin (5 m) thick quartzite separates the first and second tillite bands (32 m). The second tillite has a magnetic matrix and is overlain by a magnetic ironstone (13 m). The third tillite horizon is poorly developed and is situated between the ironstone and a dominantly

TABLE 3: Government Subgroup in Heidelberg-Balfour-Delmas area

CENTRAL RAND	EAST RAND	SOUTH RAND EDENKOP	DELMAS	EVANDER
WITPOORTJIE (± 800 m)	<div>584m</div> <div> <div>Blue Grit 37</div> <div>Quartzite and Grit 4</div> <div>Four shale with Three Quartzite units 129</div> <div>Quartzite with Government Reef 49</div> <div>Four Quartzite and Five Shale units 347</div> <div>Coronation Quartzite with Grit 18</div> </div>	<div>440m</div> <div> <div>Blue Grit (Hex River) 180</div> <div>Not exposed (faulted out) 95</div> <div>Government Reef 20</div> <div>Coronation Reef 144</div> </div>	<div>472m</div> <div> <div>Shale 71</div> <div>Veldschoen Reef 85</div> <div>Three shale and Three Quartzite units 316</div> </div>	<div>290m</div> <div> <div>Blue Grit - disconformity 120</div> <div>Five Quartzite and Five Shale units 210</div> </div>
CORONATION SHALE (m)	<div>26m</div> <div> <div>Magnetic Shale 18</div> <div>Tillite 8</div> </div>	<div>3</div> <div>Shale (non magnetic) 3</div>	<div>31m</div> <div> <div>Magnetic Shale 7</div> <div>Tilloid 24</div> </div>	<div>169m</div> <div> <div>GT 3</div> <div>GT 2 Tillites</div> <div>GT 1</div> </div>
PROMISE QUARTZITE (1000 m)	<div>487m</div> <div> <div>Quartzite 24</div> <div>Shale 24</div> <div>Quartzite 18</div> <div>Shale 137</div> <div>Quartzite 128</div> <div>Shale 18</div> <div>Quartzite 12</div> <div>Magnetic shale 6</div> <div>Quartzite with grit(Promise Reef) 120</div> </div>	<div>790m</div> <div> <div>Quartzite 100</div> <div>Shale 30</div> <div>Quartzite 18</div> <div>Shale 34</div> <div>Quartzite(Coronation b) 229</div> <div>Shale 134</div> <div>Quartzite 85</div> <div>Shale 3</div> <div>Quartzite 61</div> <div>Shale 34</div> <div>Promise Reef 60</div> </div>	<div>± 10</div> <div>Quartzite</div> <div>?</div>	?

argillaceous unit (40 m) which is culminated by a black shale marker horizon (3 m). Overlying the black shale is a dominantly arenaceous succession with interbedded shales (34 m).

In the Delmas area, the Coronation shale formation consists of a magnetic shale and a tilloid. The tilloid horizon (24 m) consists of fragments of angular to subangular quartz, quartzite, chert and red jasper with a highly argillaceous dark greenish gray to dark green groundmass. Inter-calated in the tilloid are quartzites (Button 1970). A seven metre thick shale with gradational upper and lower contacts overlies the tilloid and, according to Button (1970), may show "preconsolidation slump structures". The shale is often moderately magnetic but may in some sections be strongly magnetic.

In the Heidelberg area, well striated pebbles occur in a 6 m thick tillite. The boulders are composed dominantly of sandstone although slate and lava pebbles have been noted (Rogers 1922). The banded shale unit (19 m) overlying the tillite contains much magnetite and was correlated with the Coronation shales by Rogers (1922).

3.2.2.3 Witpoortjie Formation

This formation is about 584 m thick in the East Rand, 470 m in the Delmas area, 440 m in the South Rand and about 350 m thick in the Evander area. The Formation usually has a conglomerate at the base and a diamictite - the Blue Grit - at the top.

Directly above the shales containing the Coronation Shale Formation is a coarse basal grit or small pebble conglomerate (up to 5 cm thick) - the Coronation Reef - which is developed near Heidelberg. Pretorius (1964) has recognised an auriferous conglomerate on the South Rand which is locally developed at the Edenkop Mine as the Coronation Reef. At about the same stratigraphic level a sericitic and argillaceous quartzite occurs in the Delmas area compared with a shale on the Evander Goldfield.

The quartzites and shales which are developed between the Coronation quartzites and the next significant marker - the Government or Veldschoen Reef - have been described by Button (1970) and Rogers (1922) for the Delmas and Heidelberg area. (Table 3). The shales are all dark gray to black in colour and often grade into argillaceous quartzites which in turn may grade into a siliceous quartzite. The first quartzite below the Government Reef in the Delmas area is distinctive in that it is the only carbonate bearing reef in the Witpoortjie Formation (Button 1970). In the Evander area the Coronation Shale Formation is overlain by shale (54 m), 'puddingstone' or well rounded pebble conglomerate (4.5 m), quartzite (9 m), gritty shale (40 m), white quartzite (21 m) and finally the Blue Grit.

The Government Reef is the most persistent conglomerate in the West Rand Group succession near Heidelberg. It occurs at the base of a 50 m thick quartzite where it may locally be up to 1 m thick. The pebbles are often well packed and measure up to 2 cm in diameter. The "Government Stage" described by Pretorius (1964) is a 1 m thick conglomerate occurring at the base of a quartzite horizon (19 m) at Edenkop Mine on the South Rand. The Veldshoen Reef of the Delmas area occupies a similar stratigraphic position to the Government Reef on the East Rand. This reef occurs at the base of an 85 m siliceous quartzite and may in places be separated into two bands of gritty small pebbled conglomerates or grit. According to Button (1970) the pebbles are composed of vein quartz, chert and banded jasper with a matrix which is often mineralised. The term "Veldschoen Reef" had previously been used by Collender (1960) for the first quartzite below the Crown lava in the Klerksdorp area. Button notes (1970) that the "Slipper Horizon" in the Delmas area would coincide more correctly with the Veldschoen Reefs as developed in the Klerksdorp area.

Between the Government Reef and the next important marker horizon - the Blue Grit - there are about 135 meters of sediments in the Heidelberg area and possibly about 95 m on the South Rand (Rogers 1922; Pretorius 1964). In the Heidelberg area the sand/shale ratio for these sediments is less than 0.27. Near Delmas sericitic and argillaceous quartzites follow the Veldschoen Reef and are in turn overlain by a slightly magnetic shale unit measuring 71 m in thickness. According to Button (1970) the shale is broadly banded and is light greenish to grey in colour. In the Delmas area there is no horizon which can be correlated with the Blue Grit in the East Rand, South Rand and Evander basin. As there is only another 61 m of arenaceous sediments (Slipper Horizon) between the last named shale unit and the Crown lava it would be appropriate to include this shale with the Witpoortjie Formation and the Slipper Horizon with the dominantly arenaceous Florida Quartzite Formation of the Jeppes town Group.

The Blue Grit ranges in thickness from 0 to 590 m in the Evander basin, is 180 m near the Hex River Mine on the South Rand and is between 30 and 230 m in the Heidelberg area. The Blue Grit described by Rogers (1922) as a rock of "remarkable character" has a heterogeneous matrix composed of quartz, chlorite, sericite, hornblende, epidote, zoisite and calcite. Angular (1.5 to 75 mm) fragments and pebbles composed of quartz, fresh feldspar, hornblende, pyroxene, granite, syenite, porphyritic lava, quartzite, phyllite, slate and possibly tuff are randomly scattered throughout the unit. On the Evander Goldfield, occasional boulders up to 30 cm in size and with ill-defined outlines are present (Jansen et al 1972).

The termination of the Blue Grit on the Evander area is marked by a distinct unconformity with the overlying quartzite being incorporated into the Central Rand Group (Jansen et al 1972). The top of the Government Subgroup was placed by Rogers (1922) at the top of the quartzite horizon above the Blue Grit, primarily because the overlying beds (ie. those of the Jeppes-town Subgroup) are allegedly more argillaceous. Likewise, Pretorius (1964) included a ripple marked quartzite overlying the Blue Grit into the Government Subgroup.

However, subsurface mapping on the East Rand (Antrobus 1964) has revealed that the sand/shale ratio for the Jeppes-town Subgroup is 1.6 compared to the Government subgroups ratio of 1.4. According to Button (1968) there is no reason for dividing the Group into three subgroups and he suggests that "there are certain marker horizons which provide convenient points of reference in the stratigraphic column (eg. the Crown Lava)". The writer, in complying with SACS (1978) breakdown of the West Rand Group in the historic type area, ends the Witpoortjie formation with an argillaceous unit - that of the Blue Grit.

3.2.3 Jeppes-town Subgroup

The Jeppes-town Subgroup is poorly exposed in the Heidelberg-Delmas-Balfour area where it measures approximately 610 m near Heidelberg, 245 m near the Hex River Mine and is about 280 m near Delmas. There is a distinctive marker horizon in the middle of the Subgroup - the Crown lava - which is split into two lava flows south of the Sugarbush fault. The presence of Crown lava in all three areas makes it possible to divide the Jeppes-town Subgroup into its three formations as done on the Central Rand by SACS (1978).

3.2.3.1 Florida Quartzite

Near Heidelberg, a quartzite (10 m) overlies the Blue Grit and is in turn overlain by red weathered shales about 305 m thick containing about 33 m of sandstone. The shale is distinctive in that "thin bands of very ferruginous rock approaching the West Rand shale in character" occur throughout the Florida Quartzite Formation near Heidelberg (Rogers 1922).

On the South Rand a borehole (RT2 at the Heidelberg-Roodepoort Mine) penetrated 145 meters of sediments below an amygdaloidal lava underlying the basal conglomerate of the Central Rand Group (Pretorius 1964). The hole did not reach the Blue Grit but passed through 4.3 m of quartzite, 3.6 m of shale, 35.7 m of alternating thin quartzite and shale bands, 57.6 m of black shale and finally 43.8 m of quartzite before being stopped.

Near Delmas, a 61 m quartzite rests with a sharp, probably erosive, contact on the underlying shale (which the writer includes in the Witpoort-

jie Formation). At the base of this unit is a gritty quartzite, with disseminated crystalline and detrital pyrite and associated heavy minerals. This grit is locally known as the "Slipper Horizon". The quartzite is distinctive in that it is, according to Button (1970), 'black speckled, striped to varying degrees and banded'. The banding is due to the alteration of dark greenish grey argillaceous quartzite and a carbonate bearing greenish grey sub-siliceous quartzite.

3.2.3.2 Crown Lava

In the Heidelberg-Nigel area a succession of amygdaloidal lavas and coarse fragmental volcanic beds, the whole suite being not more than 30.5 m thick, lies on a feldspathic quartzite 3-5 m thick which in its upper parts contains splinters (varying in length from 0.2 mm to 10 cm) of an originally glassy volcanic rock. In places, these splinters and fragments are so abundant that the rock can be classified as an agglomerate (Rogers 1922; de Jager 1964; Cousins 1973). These rocks are, according to Rogers (1922), equivalent to the Crown Lava (or Jeppe Amygdaloid).

On the South Rand the amygdaloidal lava may locally (eg. Heidelberg-Roodepoort Mine) immediately underlie the Central Rand Group and reach a thickness of up to 76 m (Pretorius 1964). At the Hex River Mine the Jeppe Amygdaloid consists of two flows (Nel 1933), namely a dark lava with few amygdales and a lava devoid of amygdales but with a few feldspar phenocrysts. To the south east of the mine Leube (1956) found one flow only, 91.5 m thick, with feldspar phenocrysts but no amygdales.

Button (1970) describes the Crown Lava, which is about 65 m thick near Delmas, as a dark greenish grey lava, prominently amygdaloidal in its upper half. White calcite and zoned greenish black chlorite amygdales are the most common types. In the lower half the lava is sparsely amygdaloidal and often carries scattered feldspar phenocrysts with the last meter of lava being prominently amygdaloidal or occasionally pyroclastic.

3.2.3.3 Roodepoort Formation

The sediments between the Crown Lava and the Central Rand Group vary in thickness from 30 to 200 meters in the Heidelberg area, between 0 and 103 m in the South Rand and ^{measures} about 182 m near Delmas.

In the Heidelberg area the sediments above the lavas are chiefly shales, but thin beds of quartzite occur in them; a quartzite which lies about 90 m above the lavas to the south of the Heidelberg (Hourtpoort) is spotted due to the presence of many grains of microcline feldspar (Rogers 1922). De Jager (1964) found that this quartzite horizon proved to be a useful marker in certain mines (eg. Vlakfontein). A peculiar feature which Rogers records is the appearance of a great thickness (up to 76 m) of quartzite in

the upper part of the Roodepoort Formation in particular areas (eg. Groenfontein) which does not appear in other areas (eg. Houtpoort), although south of the Sugarbush fault the quartzite is again seen. The mineralogy of the upper Jeppestown subgroup shale according to de Jager (1964) is leucogene rich, except for the 3 to 5 meters immediately below the Main Conglomerate in which rutile is present.

In the South Rand area, the Roodepoort Formation was penetrated by a borehole in the Witkleifontein locality (Pretorius 1964). It intersected 14 m of shales, 7.6 m of quartzites, 44.8 m of shales (some bands of which are highly contorted or brecciated), 24 m of quartzites and 14 m of shale above an amygdaloidal lava flow into which the borehole penetrated for 3 m.

In the Delmas area, Button (1970) described the first 24 m of quartzite overlying the Crown Lava as a fine grained, dark gray, often striped quartzite which has a spotted appearance due to carbonate minerals. At one locality this quartzite was separated from the lava by a meter of grey, banded shale. Overlying the first major quartzite member is a 34.5 m shale which may be strongly magnetic in parts, a 94.5 m sericitic and argillaceous quartzite and finally a 29 m shale horizon. The shale below the Main Conglomerate has a weathered phase of lighter coloured material which overlies the darker green unweathered shale. According to Button (1970), this palaeosoil is attributed to "preMain Reef Horizon erosion". This erosion resulted in the decrease in thickness from 46 m in the western portion of the Bultfontein Basin to 12 m in the eastern and south eastern portions. Furthermore, a similar decrease in thickness of the same shale unit from 153 to 92 meters in the East Rand Basin was attributed to the same "pre-Main Reef Horizon erosion".

Button (1968) noted that the West Rand Group section near Delmas between the Main Reef Horizon and the Tilloid Horizon was not a deranged succession of conglomerate, quartzite and shale but can be shown to be made up of a well ordered series of sedimentary cycles. Furthermore, Button (1968) correlated sediments of the Delmas area to those of the Klerksdorp goldfields, Orange Free State goldfields and West Wits goldfields on the basis of repetitive sedimentary cycle patterns. Clearly, where borehole data are available or subsurface mapping is possible the cyclic sedimentation of the Jeppestown sediments serves as a useful stratigraphic marker (Figure 7).

3.3 Vredefort Area

Although deep drilling has disclosed the presence of West Rand Group rocks in the de Bron horst on the Orange Free State goldfield (Figure 2)

RAND GROUP SEDIMENTS

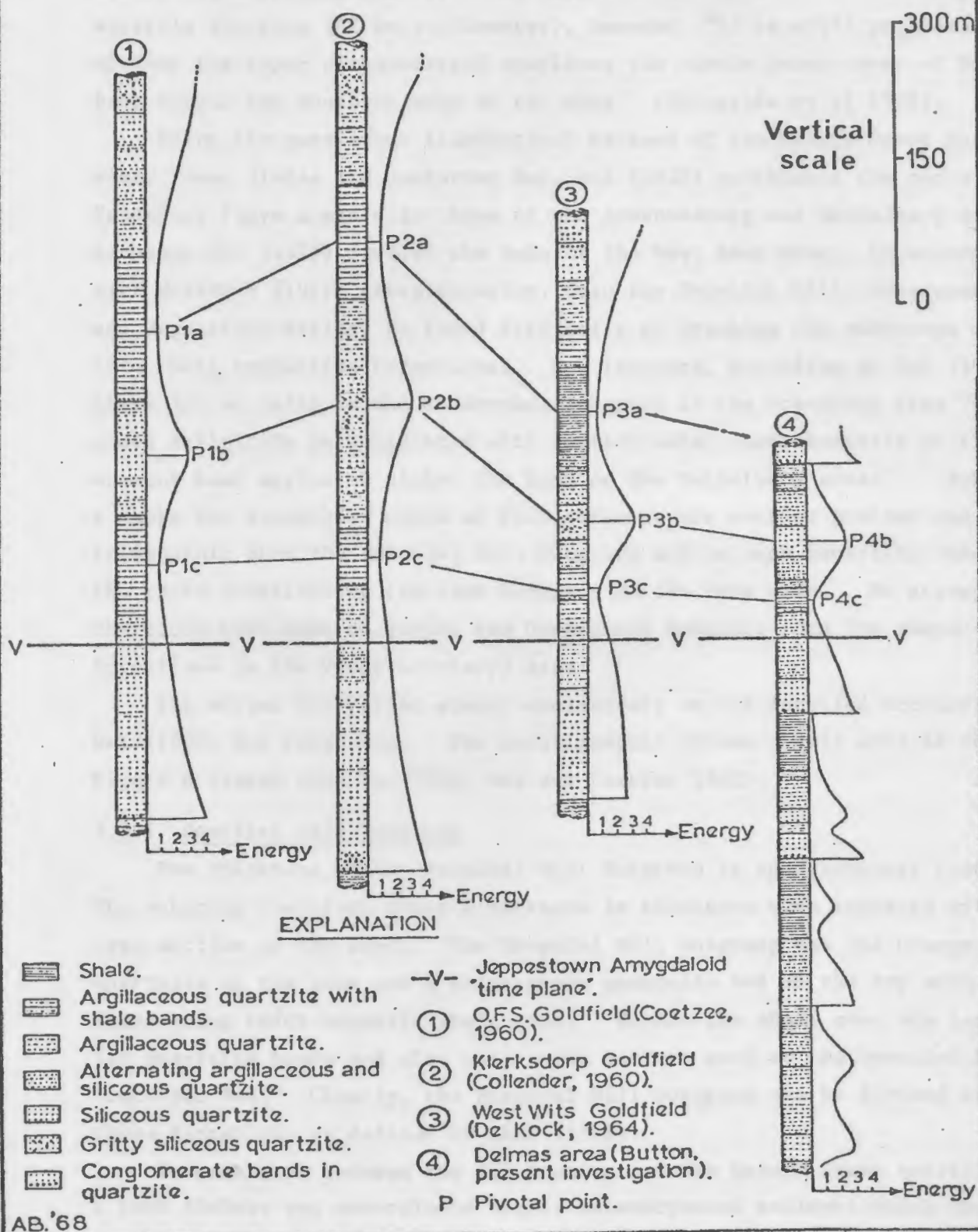


Figure 7: Cyclic sedimentation in same West Rand Group sediments (after Button 1968)

(Coetzee 1960), the most southerly outcrop of the Group is situated around the periphery of the Vredefort Dome, about 120 km south - south west of Johannesburg. The strata surrounding the northern half of the dome are overturned and intensely metamorphosed while those on the southern side are mildly metamorphosed and dip under Karoo cover. The West Rand Group rocks encircle the dome (42 km in diameter), however, "it is still problematic whether the Upper Witwatersrand completes the circle under cover of Karoo beds around the southern edge of the dome". (Whiteside et al 1976).

Using the persistent lithological markers of the Orange Grove Quartzite, Water Tower Slates and Contorted Bed, Nel (1927) correlated the rocks in the Vredefort Parys areas with those of the Johannesburg and Heidelberg areas. Although Nel (1927) divided the beds of the West Rand Group, in accordance with Mellor's (1917) classification, into the Hospital Hill, Government Reef and Jeppestown series, he found difficulty in breaking the subgroups down into their respective formations. For instance, according to Nel (1927), there are no units in the Government Subgroup in the Vredefort area "which could definitely be correlated with certain beds, characteristic of the Government Reef series of either the Rand or the Heidelberg areas". Taken as a whole the arenaceous units of this subgroup are coarser grained and more feldspathic than the Hospital Hill Subgroup and as such generally resemble the rocks constituting the same Subgroup on the type area. No attempt has therefore been made to divide the Government Subgroup into its respective formations in the Vredefort-Parys area.

The writer has relied almost exclusively on the detailed accounts by Nel (1927) for this area. The stratigraphic column of this area is shown on Figure 8 (taken from Nel 1933; Nel and Verster 1962).

3.3.1 Hospital Hill Subgroup

The thickness of the Hospital Hill Subgroup is approximately 1100 m. The subgroup therefore shows a decrease in thickness when compared with the type section of the Rand. The Hospital Hill subgroup has the Orange Grove quartzite at the base and a thick green quartzite bed at the top with an intervening thick magnetic shale zone. Within the shale zone are lenticular quartzite bands and also well known markers such as the Speckled Bed and Contorted Bed. Clearly, the Hospital Hill Subgroup can be divided into its three formations as defined by SACS (1978).

Intercalated between the Old Granite and the Orange Grove quartzites is a dark diabase and subordinate highly metamorphosed sediment which vary in thickness between 90 and 250 meters. The diabase was named an "amygdaloidal hornblende granulite" by Hall and Molengraaf (1925). Nel (1927) incorpor-

ated the admixture of volcanogenic and sedimentary material as a basal amygdaloid in the Hospital Hill Subgroup. However, these rocks are now correlated with the Dominion Group (Nel and Verster 1962).

3.3.1.1 The Orange Grove Quartzite

Directly overlying the Dominion Group sediments is an 82 to 143 m quartzite unit, 8 to 27 m shale unit and a 2 to 33 m top quartzite. The first quartzite unit may, as on the Central Rand, be split into three quartzite beds by intercalated shale horizons. The quartzites all "possess the same lithological character" and are white or light brown, fine to medium grained and glassy. The shales are soft and weather red with the exception of the top shale unit which weathers black.

Unlike the Orange Grove quartzite formation in the Heidelberg-Delmas-Balfour area the quartzites have no pebble beds or grits, either at the base or higher up. The great variation in thickness (minimum thickness of 54.8 m, maximum 165 m, average 114 m) of the formation in the Vredefort area differs from the formation on the Central Rand where the thickness remains fairly constant (200 m).

3.3.1.3 Parktown Shale

The Parktown Shale formation has an average thickness of about 670 m in the Vredefort area as compared to 700 m on the Central Rand.

Overlying the Orange Grove quartzite is a shale measuring about 185 m with a highly magnetic and frequently banded unit near its base. According to Nel these magnetic shales probably correspond to the Water Tower Shale described by Mellor (1911). No ripple marked quartzite marker has been identified. However, about 300 m above the base of the Hospital Hill Subgroup is a feldspathic quartzite which has been correlated with the Speckled Bed on the Central Rand. This marker consisting of quartz, feldspar (oligo-calc - albite) and microcline may, in places, reach a thickness of 30 m. A short distance (about 100 m) above the Speckled Bed is a dark strongly laminated shale, the Contorted Bed, which has all the distinctive features already described on the Central Rand and in the Heidelberg areas. A peculiar feature to the Contorted Bed in the Vredefort area is the presence of a narrow sheet of epidioritised dolerite. The shales between the Contorted Bed and the Brixton Formation embrace various argillaceous rocks. Zones of sandy shale which are banded due to the presence of light coloured quartzite laminae grade into brown or reddish weathering shales which in turn grade into green or black shales.

3.3.1.3 Brixton Formation

The Brixton Formation in the Vredefort area consists of two quartzite

units and three shale units. Its average thickness of 367 m is a marked decrease when compared to both the Heidelberg and Central Rand area.

The lower (41 m) and upper (107 m) quartzitic units are separated by a 183 m shale unit and overlying the upper quartzite is a 26 m shale unit.

The quartzites are light coloured, often green fine to medium grained and, where not recrystallised, sago structures are evident. The cross bedding and ripple marks within these units were used by Nel (1927), to prove the inversion of the beds on the north eastern area of the dome. The argillaceous unit between the quartzites consist of "sandy laminated shales" similar to those underlying the Brixton formation. The uppermost shale unit of the Brixton formation was incorporated into the Government Subgroup by Nel (1927) whereas the writer places it in the Brixton formation in order to conform with SACS (1978).

3.3.2 Government Subgroup

The Government Subgroup is about 1600 m thick and comprises a succession of about ten argillaceous units and ten arenaceous units. The shales are on the whole more siliceous in character than the ferruginous shales of the Hospital Hill Subgroup while the quartzites are generally more feldspathic.

The first quartzite (14 m) is reddish to yellowish and coarser grained when compared to the last Brixton quartzite and is overlain by a 53 m thick shale, 73 m quartzite and a 75 m shale.

The thickest quartzite (375 m) in the subgroup has several grit bands and occasional conglomerate lenses. The pebbles and coarser grains chiefly consist of quartz and are well rounded giving the rock a distinctive sago texture. The quartzites grade into shales which in turn are overlain by a peculiar dark grit. This grit is never more than about 5 m thick and consists of a dark bluish matrix with abundant small glassy quartz grains as well as a 'thin scattering of irregular fragments and rounded pebbles of quartz, quartzite, and shale' (Nel 1927).

The poor exposure of the succeeding 610 m of sediments, the numerous faults and the intrusion of dolerite sheets has resulted in no good markers being identified. The four arenaceous units and five argillaceous units have a sand/shale ratio of about 0.5.

The three remaining quartzites and two shales crop out relatively well and according to Nel, can be used as marker horizons. The lowest quartzite is a thin (9 m) light coloured quartzite with well developed cross bedding and occasional grit bands. The quartzite grade into shales, with a persistent thin dark grit (2 m) band being developed a few metres above the quartzite. The matrix of the rock is a dark slaty blue colour, in which glossy quartz and fragments (<0.7 mm) of quartz, quartzite and 'non-descript rock'

occur. Nel (1927) tentatively suggests that this unit may correspond to the blue grit of the Heidelberg-Delmas-Balfour area.

The dark grit is succeeded by a ferruginous shale (91 m) which in turn grades into argillaceous quartzite (216 m), which varies from a fine to a coarse grained rock. This quartzite is often thinly bedded, has a light-greyish colour and contains many bands of fine grained shaly sandstones which often display excellent cross bedding. The overlying shale (73 m) is laminated and ferruginous in character and is in turn overlain by a 45 metre hard, light coloured, fine to medium grained quartzite. This quartzite often has lenses of grit which locally develops into small, well rounded, pebble conglomerate and because it is an easily recognisable rock unit in the field, Nel (1927) used this quartzite to mark the top of the Government Subgroup.

3.3.3 Jeppestown Subgroup

The Jeppestown Subgroup is very variable in thickness because of the lens-like nature of some of its constituent beds. Nel and Verster (1962) give a maximum thickness of 1360 metres. Although Nel stated in 1927 that the Jeppestown amygdaloid was not developed in the Vredefort area, in later publications (Nel 1939; Nel and Verster 1962), he describes a zone of volcanic rocks (100 m thick) about three-quarters of the way up in the succession. This lava - the equivalent of the Crown Lava of the Central Rand - was in 1927 considered to be equivalent to the Bird amygdaloid lavas in the Central Rand Group. In the Vredefort area the Jeppestown subgroup has some lenticular auriferous conglomerates which are not developed on both the Central and East Rand areas.

Although the presence of the Crown Lava in the Vredefort area makes it convenient to divide the Jeppestown subgroup into its three formations, the individual units making up the formations show considerable discrepancies in number and thickness throughout the area. The tentative composite thickness of the formations quoted above are taken from Nel (1927) and Nel and Verster (1962).

3.3.3.1 Florida Quartzite

This formation begins with a 15 metre shale horizon which is followed by about a 6 metre sandstone. Above the second and thickest (250 m) shale unit a conglomerate is developed. Much time and money has been spent in testing this 'reef' - named the Veldschoen Reef - for its gold content. However, the workings were closed before the production stage was reached and, according to Whiteside *et al* (1976) only 'a small tonnage of payable ore was developed on Nooitgedacht 89, south of the Vaal River near Venterskroon'. Overlying this conglomerate are intercalated quartzites and shales measuring about 170 metres in thickness which in turn are followed by 115 metres of

dark red shales. The last unit of the Florida Quartzite formation is a 103 m fine to medium grained, dark coloured quartzite.

3.3.3.2 Crown Lava

Nel and Verster (1962) estimate the thickness of this amygdaloidal lava to be about 97 metres. The upper portion of the lava is brecciated. The amygdales consist of quartz and calcite with chlorite sometimes being present.

3.3.3.3 Roodepoort Formation

About 160 metres of argillaceous quartzites are developed between the lava and the topmost shale unit. Near the lavas they are black in colour, fine grained, and display well developed cross beds. These dominantly arenaceous sediments are succeeded by a 122 m thick shale unit through a gradual transition zone. In places numerous basic intrusions enhance the thickness of this formation.

3.4 Klerksdorp-Ventersdorp-Ottosdal Area

In the Klerksdorp-Ventersdorp region the Dominion Group strata, as in the Vredefort area separates the Witwatersrand sediments from the basement rocks. The region can be divided into three areas - the scattered outcrops between Klerksdorp and Ventersdorp (described by Nel 1934; Nel et al 1939) an oval shaped fold known as the Rietkuil Syncline, sixteen kilometres west of Klerksdorp (reviewed by Wilson et al 1964) and a thin veneer of West Rand group strata preserved south of Ottosdal (von Backström 1952).

Beetz (1936) and Collender (1960) presented detailed stratigraphic sections of borehole core which penetrated West Rand Group strata in the vicinity of Klerksdorp. The compilation of the composite stratigraphic sections in this area is complicated by the folding and faulting of the Witwatersrand strata which delayed the emergence of the Klerksdorp District as an important gold producing area by forty years. However, despite the structural complexity the presence of economic auriferous conglomerates within the Dominion Group and Government and Jeppestown subgroup has encouraged further exploratory drilling (Whiteside et al 1976).

Figure 8 compares the lithology and thickness of the West Rand Group in the Klerksdorp area with those on the Central, Odendaalsrus and Vredefort areas (Nel 1933; Coetzee 1960; Cousins 1960). The figure clearly illustrates the pronounced increase of arenaceous sediments in the Klerksdorp area.

3.4.1 Hospital Hill Subgroup

The thickness of the Hospital Hill Subgroup in the Klerksdorp-Ventersdorp area is about 2100 metres which is about 500 metres more than the thick-

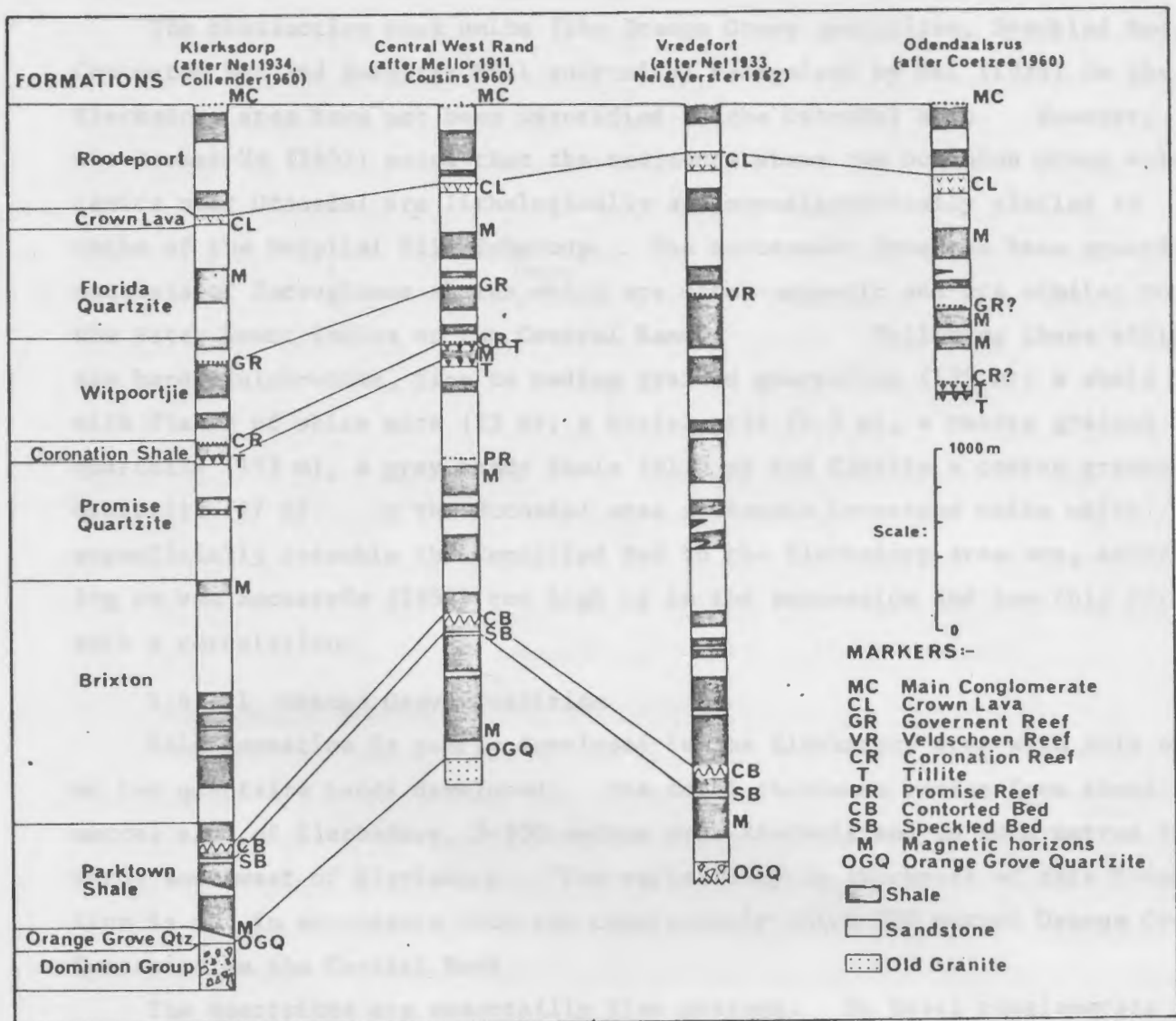


Figure 8: Comparison of lithology and thickness of West Rand Group stratigraphy in the Klerksdorp, Central-West Rand, Vredefort and Odendaalsrus areas.

ness on the Central Rand. The arenaceous members of this subgroup shows a progressive increase in thickness from the Central Rand towards the Klerksdorp area. West of Klerksdorp the sandstones thin until near Ottosdal instead of the normal 2100 metres of the Hospital Hill sediments the entire Witwatersrand succession only totals about 1370 metres (von Backström 1952).

The distinctive rock units (the Orange Grove quartzites, Speckled Bed, Contorted Bed and Hospital Hill quartzite) recognised by Nel (1934) in the Klerksdorp area have not been identified in the Ottosdal area. However, von Backström (1952) noted that the sediments above the Dominion Group volcanics near Ottosdal are lithologically and stratigraphically similar to rocks of the Hospital Hill Subgroup. The succession from the base upwards consists of ferruginous shales^(91.5 m) which are often magnetic and are similar to the Water Tower Shales on the Central Rand. Following these shales are hard bluish-white, fine to medium grained quartzites (155 m); a shale with flakes of white mica (23 m), a bluish grit (4.5 m), a coarse grained quartzite (152 m), a grey sandy shale (91.5 m) and finally a coarse grained quartzite (27 m). In the Ottosdal area siliceous ironstone units which superficially resemble the Contorted Bed in the Klerksdorp area are, according to von Backström (1952) too high up in the succession and too thin for such a correlation.

3.4.1.1 Orange Grove Quartzite

This formation is poorly developed in the Klerksdorp area with only one or two quartzite bands developed. The total thickness varies from about 160 metres east of Klerksdorp, 5-100 metres near Rietkuil and to zero metres towards southwest of Klerksdorp. The variability in thickness of this formation is not in accordance with the consistently thick 200 metres Orange Grove Quartzite on the Central Rand.

The quartzites are essentially fine grained. No basal conglomerate is developed. The top of the formation grades into black weathering shales and dark fine grained sandstone or quartzites belonging to the Parktown Shale formation. However, the yellowish colour, the hard compact nature of the rock and the absence of any feldspathic component in the quartzite makes the Orange Grove formation distinctive and may in places serve as a useful marker (Nel 1939).

3.4.1.2 Parktown Shale

The Parktown Shale formation is about 610 m thick in the Klerksdorp area (Nel 1934). Nel recognised the ferruginous Water Tower Shale Member and Contorted Bed in this area and tentatively correlated a feldspathic quartzite and a light weathering quartzite with the Speckled Bed and Ripple Marked

Quartzite respectively.

The Water Tower Shales consist of thick ferruginous shales with interbedded dark quartzites or siliceous ironstone bands. According to Nel 'occasional thin inconstant bands of ordinary light coloured quartzite' appear randomly within the argillaceous sequence. The Water Tower Shales are closely associated with the topmost Orange Grove Quartzite member and it is only in the Klerksdorp area that argillaceous units with the characteristics of the Water Tower Shales may, in places, underlie sandstones resembling the Orange Grove Quartzites. Overlying the Water Tower Shales are quartzites of varying thickness (0-60 m) which are the probable equivalents of the Ripple Marked Quartzite. Soft shales follow this arenaceous unit and about 430 metres above the Dominion Group, a 1-3 metre feldspathic quartzite which can 'safely be correlated with the similarly placed Speckled Bed in the Rand' serves as a useful marker (Nel 1934). Overlying this thin but consistent unit are argillaceous shales (183 m) which are in parts ferruginous and have minor thin bedded dark sandstone developed. Within these shales, approximately 52-61 metres above the Speckled Bed, the Contorted Bed with its alternations of jasper, chert and magnetite bearing laminae contorted into disharmonic folds is easily recognised and is a distinctive regional marker (Nel et al 1939). About 75 metres of alternating thinly bedded sandstone and shale bands make up the rest of the Parktown Shale Formation.

3.3.1.3 Brixton Formation

The Brixton Formation is about 1160 m thick in the Klerksdorp area as compared to 700 metres on the Central Rand and 1500 metres on the West Rand. Disregarding the argillaceous units of the formation the quartzites (particularly the topmost quartzite) generally shows a progressive increase in thickness from the Central Rand to the Klerksdorp-Ventersdorp area. The sand/shale ratio of this formation is 1.23 on the West and Central Rand as compared to 1.57 in the Klerksdorp area.

The succession from the base to the thickest shale of the Brixton Formation consists of coarse and gritty quartzites (107 m), 167 m siliceous shales, 30 m of sago textured quartzite and a 305 m shale unit which is ferruginous in parts. A 6 m sago quartzite divides the last named argillaceous unit. About 60 m above this quartzite is another coarse and gritty quartzite of about the same thickness. The rest of the Brixton succession is made up of thinly bedded argillaceous quartzite and shales (61 m), a coarse grit horizon with pebble conglomerates (442 m) and 105-120 m of black weathering shale.

The sago textures in the well rounded coarser quartzite, the small pebble conglomerates in the topmost arenaceous unit and the repetitive nature of the argillaceous beds between two fine grained quartzites and three coarse grained quartzites makes this formation in the Klerksdorp area 'an excellent

guide to the correlation of the strata and a valuable aid in deciphering the structure of the Witwatersrand beds' (Nel 1934).

3.3.2 The Government Subgroup

Nel (1934, Nel et al (1939), Collender (1960) and Wilson et al (1964) have remarked on the development of auriferous and uraniferous horizons within the Government and Jeppestown Subgroups in the Klerksdorp area. Cousins (1960) compared the Government and Jeppestown sections of the Central-West Rand with those of the Klerksdorp area and attempted a correlation bed for bed. According to Cousins 'certain shale beds of the Central Rand are represented only by argillaceous quartzite or by quartzite with shale bands in the Klerksdorp area'. Collender (1960) attempted a more logical classification by breaking up Nel's (1934) Lower and Upper sections of the Government Subgroup into five stages (Government Boulder, Government, Coronation, Promise and Bonanza), each stage representing a cycle of sedimentation.

In this review, the writer places the base of the Government Subgroup at the base of the first known conglomerate in the subgroup (after Collender 1960; SACS 1978) and not at the base of an interbedded shale (Nel 1934; Cousins 1960). The first persistent conglomerates within the West Rand Group in the Klerksdorp area are unlike the other outcrop areas in that they occur 460 metres below the Promise Reef. The Lower Tillite horizon below the Promise Reef in the Klerksdorp areas is dissimilar to the tillites in the Heidelberg-Delmas-Balfour area, the Evander basin and the West Rand, as it is closely associated with arenaceous sediments. However, the Upper Tillite in the Klerksdorp area 'can be closely correlated with the beds on the Rand through the presence of tillite associated with the shales' (Collender 1960). These argillaceous units demarcate the Coronation Shale Formation as defined by SACS (1978). An attempt shall therefore be made in this review to re-classify Collender's (1960) five stages of the Government Subgroup into the three formations (Promise, Quartzite, Coronation Shale, Witpoortjie) as proposed by SACS (1978) (Table 4).

Nel's (1934) average composite thickness of the individual units making up Collender's five stages is 1500 m, whereas Collender's estimate based on borehole data is 1400 metres.

3.3.2.1 Promise Quartzite Formation

This formation consists of a basal coarse grained arenaceous unit (365 m), a Lower Tillite (6 m), a shale unit (90 m) and finally a conglomerate and quartzite unit totalling about 185 metres.

The thick basal unit consisting of green, medium to coarse grained

quartzite has numerous scattered pyritic black grits and conglomerate in the upper section. The milky white quartz, white chert and light grey chert pebbles of the conglomerate have an average diameter of about 6 mm and rarely exceed 18 mm. A number of the conglomerates contain low gold and uranium values. The Old West Bonanza Mine exploited some of these conglomerates (Nel 1934) and between 1907 and 1912 produced 30611 ozs of gold with an average grade of 7.8 dwts per ton. According to Nel (1934) the basal coarse grained arenaceous unit is essentially composed of 'milky soft micaceous sandstones, probably shaly in parts, which include grit bands'. Conglomerates are rarely developed, although Nel (1934) described conglomerates that were 'made up of small pebbles less than an inch across and more or less of the same size, but now and again there are individuals as much as 4 inches in diameter'. The pebbles consist of glassy, milky and dark green quartz, banded chert, quartzite, red shale and a 'non-descript dense light greenish grey rock.'

The Lower and Upper Tillite units are, according to Collender (1960), between 183 to 228 metres apart. The Lower Tillite, with an average thickness of about 6 metres, becomes thinner in a south westerly direction and in places passes into a narrow dark gritty rock in which pebbles are rare (Nel 1934). The Lower Tillite Matrix consists predominantly of angular glassy quartz fragments. The pebbles and boulders - some of which are striated - are composed primarily of quartz and quartzite and secondary grit, chert (sometimes banded) and a cherty lava.

A shale which varies considerably in distribution, width and texture overlies the tillite (Collender 1960). Outside the Rietkuil Syncline the alternating shale and argillaceous quartzite total 245 m whereas in the Rietkuil area it varies from 61 to 107 m (Beetz 1936; Collender 1960) with the overlying Promise Reef either resting on light green fine grained quartzite or on fine grained shale (0.5 m) characterised by the presence of small (1.25 mm) white chert fragments. According to Collender (1960) the presence of the fragments within the shale is a helpful stratigraphic marker in distinguishing this shale from any other in the Government Subgroup.

Sixty-one metres of light coloured quartzite with numerous poorly mineralized bands of conglomerate overlie the alternating quartzite and shales. The lowermost band is taken to be the equivalent of the Promise Reef (Collender 1960). Boreholes less than 2 km apart show the bands of conglomerate thickening from 10 cm southeast of the Afrikander Mine to six beds of conglomerate each exceeding 1 m in thickness towards the south of the mine. The pebbles mostly consist of white quartz and are small (up to 1.5 cm). Pyrite is present in places, but mineralization is poor. According to

TABLE 4: Breakdown of Government subgroup in the Klerksdorp area

STAGE (after Collender 1960)	FORMATION (after SACS 1978)	UNITS	m
GOVERNMENT	WITPOORTJIE (665 m)	Quartzites	91
BOULDER (220 m)		Argillaceous Quartzites	52
REEF		Boulder Conglomerates	107
GOVERNMENT (260 m)		Magnetic-Shale	183
		Quartzite	62
		Conglomerate	15
CORONATION (185 m)		Shales	15
		Argillaceous Quartzites	61
		Conglomerate	107
PROMISE (275 m)	CORONATION SHALE (90 m)	Shale	61
	PROMISE QUARTZITE (640 m)	Upper Tillite	30
		Quartzites	122
		Conglomerate	62
BONANZA (455 m)		Shales with dark quartzites	90
		Lower Tillite	6
		Reef + Conglomerate	365

Collender (1960), granular carbon has been found within these conglomerates in some boreholes, but unlike the carbon-gold relationship in the Central Rand Group, these carry no gold. Between these conglomerates and the Upper Tillite is about 190 m of coarse, greenish coloured, often sago-textured quartzite, containing scattered fragments of chert and pebbles of blue quartz, alternating with dark quartzite shales.

3.4.2.2 Coronation Shale Formation

The average thickness of the Upper Tillite is about 30 metres. According to Collender 'it consists essentially of a consolidated mudstone, very dark in colour with numerous quarter inch chert and quartz fragments'. Nel (1934) noted that Upper Tillite boulders north of Klerksdorp are striated. Collender (1960) observed that where the tillite is thin a light very coarse yellow grey quartzite with light and dark chert occurs between the tillite and the overlying shale.

The sixty metres of shale within the Coronation Shale formation in the Klerksdorp area are weakly magnetic. It is composed of 'dense light green shales with occasional darker phases and thin light coloured lenses of quartzite' (Collender 1960). West of Klerksdorp (Elandslaagte) these shales are best developed and have a banded slaty appearance due to intercalated lenses of quartzite with specks of pyrite.

3.4.2.3 The Witpoortjie Formation

The Witpoortjie Formation consists of Collender's Coronation Stage, Government Shale Stage and Government Boulder Stage. Each stage begins with a conglomerate. The Witpoortjie Formation in the type area, on the other hand, has only two well developed conglomerates - the Coronation Reef and Government Reef. However, the quartzite developed between these two reefs is coarse grained on the Central Rand and as the sand/shale ratio for the formation on the Central Rand (1.19) is much lower than that for the Klerksdorp area (2.5) one would expect a more proximal conglomerate reef (ie. in the Klerksdorp area) to grade into a coarse grained quartzite in the type area.

According to Nel (1934) the base of this formation 'is economically one of the most important members of the Witwatersrand succession in the Klerksdorp area for in it are included the auriferous conglomerates which were exploited in the past by the old Buffelsdoorn, Pope and Elandshoogte mines and which are still being worked by the Afrikander and the recently re-started Rietkuil mines.' Collender describes these 1 m thick conglomerates distributed within 108 m of greenish coloured quartzite as 'well mineralized' with the pebbles consisting of mixed rock types. They are well rounded and well

with Collender's (1960) breakdown. The reasons why Collender's classifications are adhered to here include: (i) the shale grades into the underlying arenaceous sediments; (ii) the Florida Quartzite formation on the Central Rand consists of two arenaceous units separated by a magnetic argillaceous unit (SACS 1978); and (iii) according to Collender there is a distinct unconformity separating the two subgroups if Nel's 'Outer Basin Stage' is included in the Jeppestown Subgroup.

3.4.3.1 Florida Quartzite Formation

In the Klerksdorp area this formation consists of a zone of conglomerate (50-62 m), a dense 'marble' quartzite (6 m), argillaceous quartzite (30 m), magnetic shales (183 m) and finally a zone of auriferous reefs and quartzite (244 m).

Four conglomerate bands at the base of this formation have been mined at both the Babrosco and Afrikander mines (Wilson et al 1964). However, the various reefs consist of lenticular and discontinuous bands that, according to Collender (1960) were deposited 'as channel deposits on the old undulating Government Series land surface'. Definite correlation of the reefs is therefore difficult, as many terminate against the sides of the channels. At the Babrosco Mine three conglomerates - the Upper, Middle and Lower Reefs - have been mined, while at the Afrikander Lease Mine five conglomerates - the No. 1 to 5 reefs - were still being exploited up to 1960 (Collender 1960). The No. 5 Reef and the Upper Reef represent the same conglomerate as they are both overlain by a distinctive marker - the Marble Quartzite. Wilson et al (1964), presented a geological section of the Rietkuil area which depicts the 'generally accepted correlation' of reefs below the Marble Quartzite. The No. 5 and No. 4 Reefs correlate with the Upper Reef, the No. 3 with the Middle Reef and the No. 2 with the Lower Reef. Furthermore, below the No. 1 Reef on the Afrikander mine is a conglomerate that has been extensively mined and is locally known as the Contact Reef (Wilson et al 1964).

The conglomerates are loosely packed and are composed of quartz, banded red and grey chert and lava pebbles varying from 1.8 to about 3 cm in diameter. They are well rounded and each band shows inverse grading. According to Collender (1960) carbon is present in the upper and lower limits and in the latter it occurs as several crossbedded stringers which merge into individual lenses up to 5 cm in thickness. The quartzite between the reefs are very light in colour, coarse to gritty with numerous small fragments and black specks. Throughout they contain pyritic stringers and very fine grits (2 mm) producing persistent crossbedding (Collender 1960).

A 1.5 to 9 metre marker locally termed the 'Marble Quartzite' overlies the conglomerate zone. It is extremely dense and is clear white in colour.

Collender (1960) has named this distinctive horizon 'The White Bar'.

Above the White Bar, 30 metres of quartzite gradually become darker in colour and less speckled below the major shale horizon. In one borehole a pyritic grit was intersected near the top of this unit (Collender 1960).

The thick shale unit (183 m) with intercalated argillaceous quartzite represent the only thick development of shales of the Jeppestown Subgroup in the Klerksdorp area. The shale bands increase in number and thickness eastwards and decrease in frequency downwards with the lower half of the unit being definitely more quartzitic than shaly (Collender 1960). They are moderately magnetic (Paver 1939) with several of the narrow ferruginous bands being contorted. The shale bands are characterised by their mottling and colour banding.

The 90 metres of sediments which overlie the shale show a marked development of grit and conglomerate. Collender (1960) states that these bands of conglomerate, which Nel (1934) termed the 'Inner Basin Reefs', are only present in the Rietkuil Syncline where they have been mined in the Babrosco and Afrikander Mines for their gold and uranium content. On the Stilfontein Mine and the Townlands the quartzite carries seven poorly developed conglomerate bands which were locally called the 'Veldschoen Reefs'. The conglomerates are concentrated in the first 18 metres of quartzite and are lenticular. Collender (1960) states; "The lowest reef is known as the Contact Reef and lies directly on the shales. The pebbles are large, consisting of white quartz up to 2 inches across and poorly packed. The No. 1 reef is closely associated with the Contact Reef and occurs sporadically in the form of lenses. The position of the No. 2 reef varies from 10 to 35 feet above the contact reef and that of the No. 4 reef is 25 feet above the No. 2 reef. No. 3 reef is an intermediate marker band. The No. 2 and No. 4 reefs are the main gold carriers. They may be single reefs or they split up into a series of narrow conglomerates which merge again to form wider bands with a channel width of some 60 inches. The No. 4 reef is characterised by the presence of high uranium values".

3.4.3.2 Crown Lava

This persistent amygdaloidal lava is well developed throughout the Klerksdorp area. Its thickness varies from 40 to 65 metres. The lava is fine grained with a dark olive green colour. The amygdales are about 6 mm in diameter and are numerous within the upper 30 metres (Collender 1960).

3.4.3.3 Roodepoort Formation

More than 600 metres of dominantly arenaceous sediments are developed above the Crown Lava. Collender (1960) distinguishes two units - the Upper

Striped Quartzite and the Transition Zone - within this formation. Sharpe (1950), Collender (1960) and Cousins (1965) have all remarked on the absence of a true shale at the top of the Jeppetown Subgroup in the Klerksdorp area. Mellor (1911) used the top of this shale in the type area to delineate the West and Central Rand Groups. The writer places the division between the upper and lower portions of the Witwatersrand Supergroup in the Klerksdorp area at the base of the Main Reef (Ada May Reef) as suggested by Cousins (1965). Hence in this area the transitional beds about 60 m below the Main Reef Zone are included in the West Rand Group.

The Upper Striped Quartzites have an average thickness of about 550 metres and are so named due to the alternations of argillaceous zones with light beds. In the east of the area the quartzites are fine grained and the argillaceous zones are more shaly in texture (Collender 1960). Within the thick succession, Collender noted four zones, each zone having certain textural characteristics. Overlying the amygdaloidal lava is a zone of alternating siliceous and argillaceous striped quartzites (61 cm) showing no signs of contact metamorphism. About 245 m of quartzite follow the first zone and have a markedly striped appearance caused by 0.7 - 12 metre siliceous bands alternating with argillaceous quartzites. Peppery black speckling is common. Quartz and chert fragments are spread over a thickness of 30 metres in the middle of this zone. The third zone (120 mm) is very argillaceous with the development of numerous dark green shale bands up to 8 cm in thickness. The contact with the underlying striped quartzite is very sharp. The rest of the unit is made up of darkish grey quartzites with minute black specks.

The transitional zone consists of 60 metres of quartzite and grits. The base is marked by a number of thin argillaceous bands while towards the top beds are gritty with the development of a few lenticular grit to small pebble conglomerate bands. The overlying conglomerate termed the Carbon Leader in the Far West Rand and the Ada May Reef in the Klerksdorp area (named the Main Conglomerate by SACS 1978) lies on the transition zone quartzites with a marked unconformity.

3.5 Northernmost West Rand Group Outlier

On the western edge of the Johannesburg granite dome and separated from the Witwatersrand Supergroup of the Central and West Rand by the Muldersdrif Ultramafic Complex (Anhaeusser 1978) are Hospital Hill Subgroup sediments preserved within a synclinal structure (Hendriks 1961) (Figure 9).

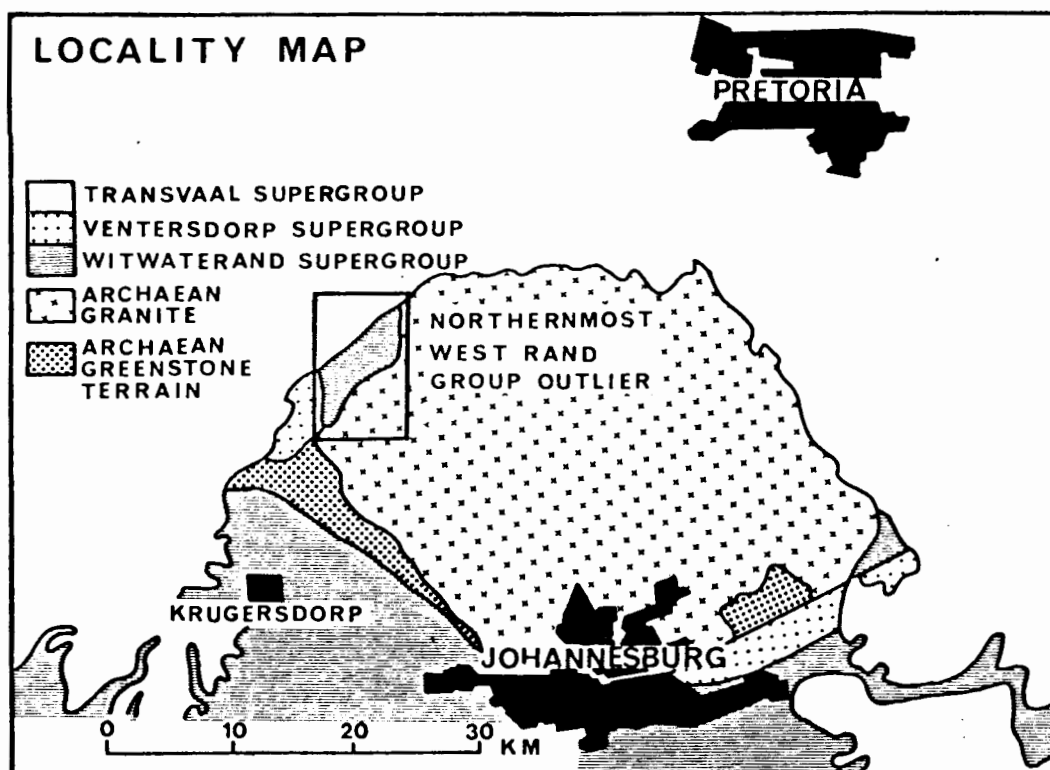


Figure 9: Map showing the location of the northernmost West Rand Group outlier.

The beds are locally sheared and brecciated and, according to Hendriks (1961), total about 620 metres compared to the 1600 metres of corresponding sediments preserved on the Central Rand.

3.5.1 Hospital Hill Subgroup

3.5.1.1 Orange Grove Quartzite

The Orange Grove Quartzite is approximately 100 metres thick. It is coarse grained at the base, becoming finer grained towards the top and is interbedded with a brownish to greyish, locally schistose slate (Jansen 1977). The lower quartzite unit contains several bands of conglomerate. The lower band, about 4.5 m from the base measures approximately 15 cm in thickness and is composed of pebbles of black and white vein quartz set in a sandy to gritty matrix. The second, and thickest conglomerate band (45 cm) is inversely graded with the top pebbles measuring about 5 cm in diameter.

The middle and upper quartzite units measure 14 m and 42 m in thickness respectively, and are yellow to white medium grained rocks (Jansen 1977).

3.5.1.2 Parktown Shale

The shale of the Parktown Shale Formation (approx. 260 m) is greenish in colour, weathering brown to reddish, and is often ferruginous. Several markers have been recognised and include the Water Tower Shale Member, Ripple Marked Quartzite, and the Speckled Bed and the Contorted Bed (Hendriks 1961).

The Water Tower Shale Member serves as a useful marker as it locally contains magnetite crystals and secondary chert. On weathering it displays a typical box structure (Jansen 1977). The other markers are not well exposed at most localities. The Rippled Marked Quartzite (2 m) is a yellowish white glassy rock composed of small round quartz grains surrounded by secondary quartz in a chloritic or feldspathic matrix. The Speckled Bed (1 m) is, as in all the other outcrop areas, a coarse grained feldspathic quartzite. The Contorted Bed has the same distinctive features as described in the Central Rand by Mellor (1911).

3.5.1.3 Brixton Formation

This formation is approximately 260 metres thick. The Parktown Shale Formation is followed by an arenaceous unit consisting of four bands of quartzite interbedded with shales. The total thickness of this unit is approximately 15 m and may serve as a useful marker due to its sago texture. The upper quartzite band (2 m) is coarse and locally contains gritty to conglomeratic layers.

The remaining quartzite units are typical of the Brixton Formation in their green colour and sago textures. The shale bands are mostly greenish in colour, but the upper shale is greyish blue, weathering brown. The shale

band under the upper quartzitic unit contains scattered pebbles of greenish quartzite.

3.6 Orange Free State Goldfield (Odendaalsrus Area)

Hospital Hill, Government and Jeppestown Subgroup sediments have been recognised in the Welkom-Odendaalsrus-Virginia region. For this area, the writer has almost wholly relied upon the review by Coetzee (1960). Jeppestown, and an incomplete Government Subgroup, composite columnar sections have been built up from borehole data. Unfortunately, a continuous succession of Hospital Hill sediments is not available at present due to the faulting and folding of the strata. Nevertheless, the correlation of the Jeppestown subgroup with an almost identical succession in the Klerksdorp area (Figure 8) has facilitated in the exploration of the overlying auriferous Main Conglomerate (Basal or Leader Reef). The shale of the West Rand Group and the Crown Lava were found to be valuable markers (Whiteside et al 1976).

3.6.1 Hospital Hill Subgroup

According to Coetzee (1960) various boreholes have passed through beds which, according to their lithological features and relative position in the structural interpretation of the area, probably belong to West Rand Group. But because a continuous succession cannot be established from borehole evidence as is the case for the Jeppestown and Government Subgroup their correlation must be regarded as being only tentative.

3.6.1.2 Parktown Shale Formation

About 10.6 km west-northwest of Odendaalsrus a borehole (WE 2) passed through the Ventersdorp Supergroup sediments and continued for about 390 metres in shale with an apparent dip of 60° . The lower 28.6 m consist of faintly banded to massive grey and black shales which grade into 2 m of finely banded grey and black dense silicified shale. Overlying these shales are 12.8 m of magnetic fine grained, massive, silicified arenaceous and strongly ferruginous red mudstone. Finally, 346 metres of black to grey shales which in places are magnetic and contorted, underly the lavas of the Ventersdorp Supergroup. Furthermore, a note appears on the borehole record stating that 'a band of finely laminated contorted shale suggests the possibility of these beds belonging to the Hospital Hill Series'. Clearly, the lithological appearance of the beds described above is that of the Parktown Shale Formation with the Contorted Bed being a distinctive marker.

3.6.1.3 Brixton Formation

Underlying Karoo cover and 7.7 km southwest of Welkom station a borehole (W1) penetrated 377 metres of quartzite and shale with an average dip of

The upper portion of the Government Subgroup consists of arenaceous sediments, carrying scattered grit bands, two intercalated shale bands and a conglomerate. The probable Government Reef is marked by a 7.5 cm thick layer containing chert and quartz pebbles resting directly on the underlying shale. The overlying quartzites are about 122 metres thick and are banded with white, glassy quartzites alternating with thick greenish grey argillaceous quartzites. These are followed by a 33 metre thick dark greenish to blackish shale which in turn is followed by alternating white, sandstones and argillaceous green quartzites. This quartzite between the two shale units is characterised by occasional small scattered quartz pebbles in the upper part and by coloured fragments in the lower part. Overlying these arenaceous sediments is an impersistent shale varying in thickness between 0.5 and 17 metres. The quartzite above the upper shale is whitish with a faint greenish-yellow tinge and carries scattered grit beds composed of quartz and chert pebbles.

3.6.3 Jeppetown Subgroup

The sediments comprising the Jeppetown Subgroup in the Odendaalsrus area are taken to include the rocks lying between the basal argillaceous quartzite (equivalent to Collender's (1960) 'Outer Basin Stage' in the Klerksdorp area) and the uppermost argillaceous unit (equivalent to Mellor's (1911) shale (T) on the Central Rand). The presence of the persistent Crown Lava in the Odendaalsrus area makes it convenient to divide the subgroup into its three formation.

3.6.3.1 Florida Quartzite Formation

The Florida Quartzite Formation is about 510 metres thick which is comparable with that measured in the Klerksdorp area.

From the base upwards, it consists of 76 metres of dark argillaceous quartzite, 82 metres of magnetic shale, 6 metres of argillaceous quartzite streaked with shale and finally a 186 metre quartzite.

3.6.3.2 Crown Lava

The Crown Lava is about 106 metres thick in the Odendaalsrus area, and according to Coetzee (1960) is an andesite.

In places, boreholes have penetrated a 1 m gritty tuff which rests on the Crown Lava and 'consists of angular grains of quartz, plagioclase, and altered rock, probably lava, set in a fine grained irresolvable matrix' (Coetzee 1960). The tuff is locally referred to as a "batwing" breccia.

The Crown Lava is dark greenish grey in colour, amygdaloidal in parts and, as in the South Rand area, built up of several flows. Intercalated fine grained tuffs carrying fragments of lava have been recorded and in one

borehole the upper 33 metres of the Crown Lava consists of fragments and bombs of black amygdaloidal lava intercalated in dense lava.

3.6.3.3 Roodepoort Formation

Overlying the Crown Lava are 33 metres of lightly banded grey quartzites, 107 metres of argillaceous quartzites with thin streaks of black shale, 122 metres of alternating bands of light grey to whitish, finely spotted quartzite and dark argillaceous quartzite and an upper argillaceous unit of 152 metres composed of numerous bands of dark arenaceous shale and pale quartzite.

4. MARKERS

It is unnecessary to enlarge upon the distinctive characteristics that 'markers' or key horizons within the West Rand Group possess. They have been dealt with above. This section summarizes the distribution of the markers and their geophysical (magnetic) properties.

Table 5 is an updated version of Nels (1933) compilation of the known, doubtful and absent markers in the outcrop areas. Included in the table is subsurface data from the Evander, Delmas and Orange Free State Goldfields areas (from Jansen et al 1972; Button 1968; Coetzee 1960).

Krahmann (1930) was the first to realize the possibility of the application of the magnetic geophysical methods for the tracing of the strongly magnetic and persistent shale units in the West Rand Subgroup. Following his experimental magnetic surveys on the West Rand various mining companies carried out a large scale geophysical programme (Weiss 1934). The success of the magnetic method in using strongly magnetic shale horizons (Water Tower Shale, Contorted Bed, Coronation Shale), even when covered by 3,000 metres of younger sediments, as markers for the determination of the approximate position of the zone of the Main Conglomerate is in itself, according to Weiss (1934), 'the greatest tribute to the enterprising mining companies and their distinguished magnetic experts'. Magnetometric traverses across the Witwatersrand sediments in the Klerksdorp and Vredefort areas has made it possible to correlate the relative magnetic anomalies arising from the shale units (Paver 1939). Table 6 is a comparison of the magnetic characteristics and the geological position of the anomalies observed in the West Rand Group of the Klerksdorp, Vredefort and West Rand areas (Krahmann 1934; Paver 1939).

The two major anomalies arising from the Water Tower Shale and Contorted

TABLE 5: Markers within the West Rand Group

AREA	HOSPITAL HILL SUBGROUP							GOVERNMENT SUBGROUP					JEPPESTOWN SUBGROUP	
	Orange Grove Quartzite	Water Tower Shale (magnetic)	Ripple Marked Quartzite	Speckled Bed	Contorted Bed	Black Hill Grit	Hospital Quartzite	Promise Reef	Tillite	Coronation Shale	Government Reef	Blue Grit	Cyclicity of Crown Lava	arenaceous/argill- aceous sediments
Central Rand	X	X	X	X	X	-	X	X	?	X	X	-	X	?
West Rand	X	X	X	X	X	-	X	X	X	X	X	-	X	X
Northernmost out- lier	X	X	X	X	X	-	X	-	-	-	-	-	-	-
Heidelberg area	X	X	?	-	X	X	X	X	X	X	X	X	X	?
South Rand area	?	-	-	-	X	X	X	?	?	?	X	X	X	?
Delmas area	X	X	?	?	?	?	?	?	X	X	X	X	X	X
Evander area	?	?	?	?	?	?	?	?	X	X	-	X	X	?
Vredefort area	X	X	-	X	X	-	X	?	?	X	-	?	X	?
Klerksdorp area	X	X	?	X	X	-	X	X	X	?	?	-	X	X
Ottosdal area	-	X	?	?	-	-	X	-	-	-	-	-	-	-
Orange Free State Goldfields	?	?	?	?	X	X	X	?	X	X	X	?	X	X

X = Exists or 'highly likely'

- = Absent

? = Doubtful

TABLE 6: Correlation of magnetic anomalies in West Rand Group

Shale Units	Approximate Distance above Base of Orange Grove Quartzite (m)	West Rand Anomalies	Klerksdorp area Anomalies	Vredefort area Anomalies
Water Tower Shale Member (B)	270	Major	Major	Major
Contorted Bed (F)	730	Major	Major	Major
Observatory Shale Member (F)	1255	Medium		
Lower Brixton Shale (G1)	1985		Medium	Medium
Middle Brixton Shale (G2)	2400	Medium		
Upper Brixton Shale		Medium	Medium	
Bottom Promise Quartzite Shale (J)				Medium
Top Promise Quartzite Shale (J)			Minor	Minor
Coronation Shale (L)	4155	Major	Minor	Major
Uppermost Witpoortjie Shale (O)	4790	Medium	Medium	Medium
Florida Quartzite Shale (Q)	5540	Medium	Medium	Medium

Symbols eg. (T) after Mellor (1917)

Major anomaly |6000 - 10000 γ |
medium anomaly |4000 - 6000 γ |
minor anomaly |2000 - 4000 γ |

Bed and the three anomalies caused by argillaceous shale units correlated with the Coronation Shale, last Witpoortjie shale and Florida Quartzite shale towards the top of the West Rand Group, are consistent features in all three areas. In the thick succession between these major anomalies, the magnetic anomalies are not so directly comparable. Paver (1939) noted that the total number of magnetic anomalies observed remained the same in the Klerksdorp, Vredefort and West Rand areas.

Clearly, the persistent lithological and geophysical markers of the Witwatersrand Supergroup have facilitated in the rapid identification and correlation of widely scattered outliers. Furthermore, the uniformity of the markers have enabled formations to be correlated unit for unit.

5. STRUCTURE

The structure of the Witwatersrand Supergroup is that of an elongated synclinorium stretching 320 km in a north easterly direction and 120 km in a north westerly direction. Widespread remnants of West Rand Group sediments not involved in the subsidence of the 'tectonic basin' are present near Ottosdal in the west and at Northcliff in the Central Rand (Brock and Pretorius 1964). Bordering, and in the centre of, the elongated basin are five distinctive outcropping hubs of granite. Drilling and geophysical investigations have proved that there are ten other granitic 'domes'.

Brock and Pretorius (1964) described the structure of the Witwatersrand Basin in terms of a grid pattern in which the superimposition of axial plane trace lines of major E-NE and NW folds give rise to culminations (Vredefort Hub, Johannesburg Dome, Devon Dome and De Bron Horst), and depressions (Potchefstroom Gap, Bothaville Gap, Blyvoor Segment Gap) arranged in a systematic manner. The formation of the folds may have been caused by differential subsidence due to the multistage rise of the Vredefort Hub and/or other domes which began in pre-Ventersdorp post-West Rand Group times. Brock and Pretorius (1964) suggested that as the domes were uplifted faults assisted basin deepening and were contemporaneous with sedimentation. These faults they named "Primary Basining Faults" and were intimately associated with the folding.

Button (1968) questioned this concept and suggested that the granitic domes were formed by post Transvaal tectonism acting on an originally more-or-less linear mass of granite trending in a northeast or east-northeast direction. Furthermore, the closure of the Witwatersrand basin defined by the exact outline of the rim is still unknown due to the paucity of diamond drill holes, especially along the south-western margin (Whiteside et al 1976).

Although numerous papers (eg. Mellor 1911, 1913; Krause 1912; Pelletier

1937; Ellis 1943; Roering 1968; Button 1968; Fripp and Gay 1972) and explanations of maps compiled by the Geological Survey (eg. Mellor 1917; Rogers 1922; Nel 1935; von Bockström 1962) have been published on the local structural features of the Witwatersrand Supergroup, the regional structural geology in relation to the other Supergroups and as an entity on its own has only recently been summarized by Pretorius (1974) and Whiteside et al (1976).

5.1 Folding

According to Pretorius (1974), the depositional axes of the Archaean and younger Proterozoic basins (Ventersdorp, Transvaal and Waterberg) all decrease in age up the regional palaeoslope from the Kaapvaal gravity low towards the Limpopo gravity high. Furthermore, the 'geometry of the gravity field over South Africa is a large scale portrayal of the areal and local tectonic fabric' (Pretorius 1978). For instance, the principal fabric of the Witwatersrand basin trends northeast, but has been deformed into an arcuate pattern by first order regional folding about northwesterly axes which follows the gravity trend. The superimposition of the folding on the fabric resulted in the formation of the large anticlines and synclines (average periodicity 40 - 50 km) which controlled the distribution of the granitic domes and major goldfields. In the South Rand area local smaller periodicities of 4-5 km, 1.5 - 2.5 km and 0.5 - 8 km, have been recorded (Pretorius 1964).

Detailed studies of folding within the Contorted Bed have been carried out by De Beer (1965), Truswell (1970) and Fripp and Gay (1972). The contortions are regarded by De Beer (1968) to be products 'of concentric folding of a competent layer with resultant bedding plane slip. The increasing curvature of a concentric fold causes an increasing lack of space in the core of the fold which often tends to develop local thrust faulting'. Truswell (1970) argued that the lack of pattern in the contortions and the fact that they do not affect strata above and below precluded a tectonic origin for the folds. Fripp and Gay (1972), on the other hand, support a tectonic origin for the contortions and state 'that in the Johannesburg area, at least, there exists good spatial and geometrical control on the attitude and shape of the folds. Only one contortion was found which the writers felt was undoubtedly of sedimentary origin but it is possible that initially, very gentle small-amplitude buckles were formed while the sediments were still soft'. The geometric control Fripp and Gay (1972) describe is that the 'fold axes are approximately parallel to each other, and most important, the axial surfaces are parallel and dip in the same direction as the bedding', hence refuting Truswell's (1970) slump theory. Folds within the shales of the West Rand Group are not well developed although locally good conjugate

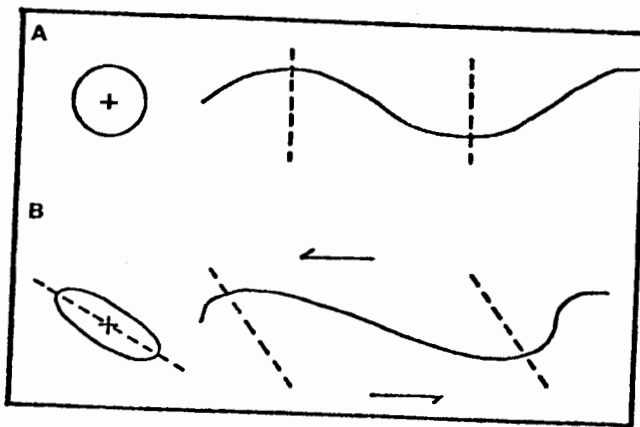


Figure 10: Fripp and Gay's (1972) model for the simultaneous formation of folds in the Contorted Bed and cleavage in the argillaceous rocks. Unit circle (A) demonstrates state of strain relative to strain ellipse (B). Under such deformation a gentle symmetrical flexure is flattened and deformed into an asymmetrical fold. Note that the major axis of the ellipse is not parallel to the axial plane of fold.

folds, kink bands, chevron folds and gentle flexure folds have been recorded (Fripp and Gay 1972).

Cleavage within the West Rand Group has been described by Roering (1968) in the Krugersdorp area and by Fripp and Gay (1972) in the Johannesburg area. Roering (1968) describes an east-west cleavage which has a fairly constant orientation over the area studied. The formation of the cleavage was thought to have formed after the folding and under a north-south compression. Fripp and Gay (1972) describe the cleavage developed in the argillaceous rocks in the Johannesburg area which has the same orientation as that described in the Krugersdorp area. They produced a model for the simultaneous formations of the folds in the Contorted Bed and cleavage in the argillaceous rocks. The model is reproduced on Figure 10.

The model is basically one of progressive deformation in which an initially symmetrical fold is distorted into an asymmetrical fold by simple shear.

On Figure 10 a unit circle is deformed into a strain ellipse whose axes rotate with the sense of shear. In this model the cleavage is thought to form perpendicular to the strain ellipse and hence it should normally be inclined at a shallower angle to the shear plane than the axial planes of the fold. Fripp and Gay's model (1972) therefore refutes Roering's (1968) concept in which cleavage is thought to have developed after folding on the basis that the average cleavage plane trace does not coincide with the fold axes. However, they all agree that the cleavage was formed under the action of a north-south directed compressive stress in both the West and Central Rand. Fripp and Gay (1972) conclude that 'this compression acting on the gently dipping rocks of the Hospital Hill Series could have caused the massive Hospital Hill Quartzites to ride over the underlying argillaceous rocks and the banded ironstones, thus causing these rocks to be deformed by a simple shear strain and leading to the formation of the cleavage in the relatively homogeneous argillaceous rocks and the asymmetric folds in the thinly bedded banded ironstones'.

5.2 Faulting

The distribution of faults in the Witwatersrand basin is depicted on Figure 11. Faulting can be classified into two groups - those which cut across the basin (radial or traverse faults) and those which are adjacent to the trend of maximum subsidence (strike faults).

Strike faulting has taken place in all four major outcrop areas and is more common in the older West Rand Group. The Rietfontein fault of the Central Rand, Witpoortjie and Roodepoort faults of the West Rand, the major

north-east trending faults (Buffelsdoorn, Kromdraai and East Buffelsfontein) in the Klerksdorp area and the de Bron fault in the Orange Free State are all more or less tangential to the basin and may be classified as strike faults (Whiteside et al 1976). The two most important radial faults are the Bank fault on the West Wits line and Sugarbush fault on the East Rand.

According to Whiteside et al (1976) the timing of the faults 'is essentially post-Ventersdorp and pre-Transvaal in age, but there is evidence suggesting that movements along the fault planes had probably been initiated prior to the extrusion of the lower Ventersdorp lava, and it is known that in some cases later movements took place on the same fault planes, even in post-Transvaal times'.

Brittle structures (extension joints, shear joints, and quartz-filled tension gashes and faults) are well developed in the Brixton and Orange Grove quartzites of the Central and West Rand. At a number of localities on the West Rand, transverse injective shale dykes have penetrated quartzite horizons. Roering (1968) interprets six of these shale dykes each varying in thickness between 12 cm and 3 m as representing a 'macro-boudinage type of phenomenon.'

Roering (1968) and Fripp and Gay (1972) studied the tension gash arrays in the Brixton quartzites on the West and Central Rand and concluded that they formed under the same conditions as the cleavage, ie. they were formed in response to a general north-south compressive force.

6. PETROLOGY

Fuller (1958) states that the 'gross features of Witwatersrand rocks are maintained over considerable distances, so that discussions of the petrology of relatively few specimens might lead to a better understanding of the System as a whole'. Macroscopic examination of rocks belonging to the West Rand group have been systematically described in each area in the section dealing with stratigraphy. In this section microscopic features (of the Crown Lava and Sandstones) and the mineralogy of the shales will be described.

6.1 Mineralogy Of The Shales

Fuller (1958), Danchin (1970) and Hofmeyer (1971) analysed shales of the West Rand Group both under the microscope and by X-ray diffraction techniques. The shales in the Parktown Shale Formation have never been as well scrutinized due to the lack of drill hole core and availability of fresh specimens. However, Fuller (1958) describes shales containing fine grained euhedral magnetite which are sufficiently magnetic to deflect a compass which may have been sampled within the Parktown Shale Formation. X-ray analysis of this

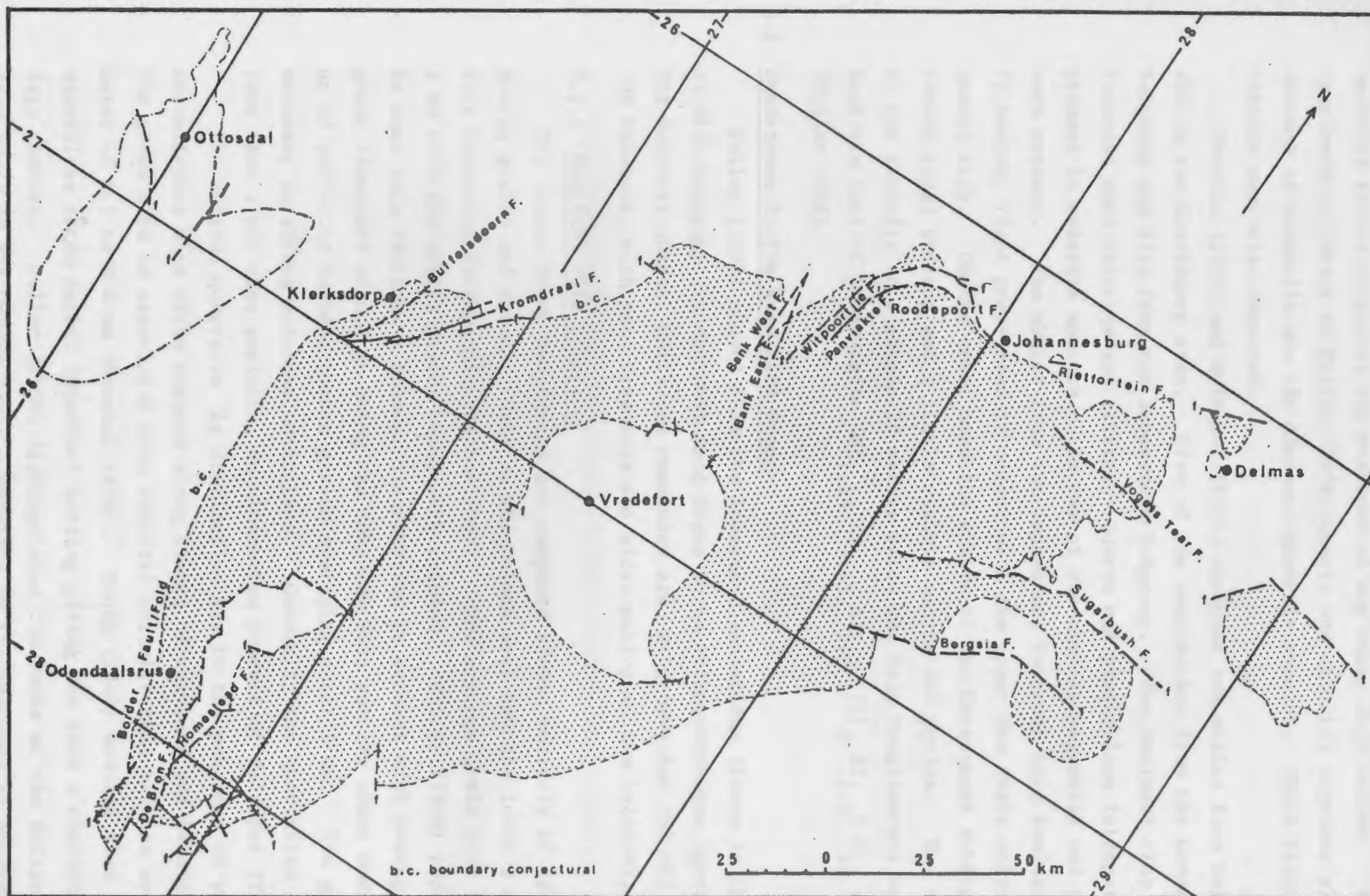


Figure 11: Map showing the periphery of the West Rand Group/Central Rand Group basins and the major faults (after Whiteside et al 1976).

material failed to reveal the presence of any other iron oxides. In all specimens collected by Fuller (1958) quartz and chlorite together with small amounts of muscovite are the dominant minerals present. Rare feldspar and calcite were also detected.

Danchin (1970) and Hofmeyer (1971) analysed ten shales from borehole JY8 in the Klerksdorp area. Five of the samples are from the Government Subgroup and five from the Jeppestown Subgroup. The dominant clay minerals recorded were chlorite and illite. Quartz and plagioclase feldspar were present in moderate amounts. In two of the samples magnetite and pyrite were present. The shales from the Jeppestown Subgroup were dominantly finely banded, light grey-green in colour with the upper two shale units being quartz rich. On the other hand the shales of the Government Subgroup often showed cross bedding and a little visible quartz and pyrite. The composition of the chlorite in a sample 20 metres below the Main Conglomerate on the East Rand was that of brunswigite ($\text{Mg}_{1.35} \text{Mg}_{3.65} \text{Al}_{1.0} (\text{Si}_3 \text{Al}_{1.0}) \text{O}_{10} (\text{OH})_8$) (Fuller 1958).

6.2 Sandstones In The West Rand Group

Fuller (1958) showed that the lowermost sandstones (those in the Hospital Hill Subgroup) in the West Rand Group to be orthoquartzites (greater than 95% detrital quartz) while the remainder are subgreywackes (50-60% quartz, 10% feldspar, with rock fragments and micas making up the balance).

6.2.1 Hospital Hill Subgroup

The Orange Grove Quartzites are composed almost entirely of detrital quartz grains and chert. Only in the Delmas area are the lower 3 metres of this formation feldspathic (Button 1968). The average grain size is about 1 mm with the quartz grains being well rounded. Fuller (1958) reports that in some thin sections a bimodal distribution is evident with average quartz grain diameters of 0.5 mm being the dominant mode and the minor mode is made up of perfectly rounded quartz grains averaging about 1 mm. The grains show moderate to strong undulose extinction. Generally the quartzites contain less than 1 per cent sericite, an alteration product of feldspar (Young 1907).

The Brixton quartzite is distinctive due to the presence of pale green chromiferous mica often present along planes of weakness and bedding surfaces. The green mica is associated with detrital chromite that have an average diameter of 0.1 to 0.4 mm (Frankel 1939). Young (1944) noticed that the Brixton quartzites often depict imperfect sorting giving the rock a characteristic sago texture. Fuller (1958) distinguishes the rocks of the Brixton Formation from those of the Orange Grove quartzites by the presence of recrystallised quartzite, relative freedom from inclusions, and by its normal extinction.

Styolites are a common feature in the Brixton quartzite (Young 1944).

6.2.2 Government and Jeppestown Subgroups

A variety of sandstone types occurs in the Government and Jeppestown subgroups and according to Fuller (1958) the range of composition of the principal components observed are as follows:-

	<u>Per cent</u>
Quartz	30 - 70
Feldspar	0 - 10
Rock Fragments	0 - 40
Matrix	0 - 20
Muscovite flakes	0 - 5
Biotite shreds	0 - 5

Fuller (1958) hence classifies the sandstones in the Government and Jeppestown subgroups as subgreywackes although he notes that Rogers (1922) described a sandstone with as much as 37 per cent feldspar. According to Fuller 'further work will be required before the full range of compositions represented in this thick succession of rocks is known'.

In this review only the general characteristics of the grains making up the subgreywackes will be discussed. The quartz grains are predominantly subangular and show weak to moderate extinction. Recrystallised quartzite is, according to Fuller (1958), absent in these two subgroups. The feldspar has a composition lying between Ab_{80} - Ab_{100} (oligoclase - albite) with traces of microcline being evident. Rock fragments occur as rounded to irregular grains and have approximately the same diameter of the associated quartz grains. In the Jeppestown Subgroup rock fragments occur which Fuller (1958) suggests 'are common in tuffaceous deposits and it is probable that they represent an admixture of volcanic material'. They occur throughout some 915 metres of section. The rock fragments may thus represent reworked Crown Lava. The matrix of the subgreywackes is composed almost entirely of sericite and calcite. Accessory minerals include leucoxene, crystalline pyrite and epidote. Fuller (1958) did a heavy mineral separation of Jeppestown subgreywacke and found that it was composed of biotite, chlorite and pyrite with small amounts of euhedral colourless crystals of apatite, zircon and tourmaline.

The Crown Lava has certain characteristics which are sufficiently diagnostic for it to be identified with certainty. According to Whiteside (1970) the Crown Lavas 'are generally dense andesites, pale grey to dark green in colour, which occasionally contain small, dark green, stubby phenocrysts, the amygdalae are filled with white quartz or dark green chlorite with a white rim, and often merges into each other giving rise to dumb-bell shapes.

Agglomerates and tuffs are sometimes present and these also have the same grey to dark green colour often with a brownish tinge'. Under the microscope the lava consists of felted or pilotaxitic groundmass of oligoclase-andesine ($An_{25} - An_{35}$) microliths. The groundmass consists of small corroded phenocrysts of plagioclase largely altered to sericite. The primary mafic minerals have altered to chlorite, sericite and a little calcite. In two thin sections (a lava and a tuff), Coetzee (1960) notes a variolitic texture formed by radiating fibres of plagioclase in the lava and rounding of detrital grains in a tuff and suggests that the Crown Lava was possibly poured out under water.

7. GEOCHEMISTRY

7.1 Shales

Marriott (1904) analysed five shale samples from the Parktown Shale Formation and noted that silica and iron constituted over 90 per cent of the mass, alumina another 6 per cent and the remaining 4 per cent were alkalies and other elements. Horwood (1910) cites an average of 10 analyses of Hospital Hill shales which are shown on Table 7. They are not included in the average West Rand Group shale due to their high iron content (ie. not representative). Hall (1938, p.151) lists three other analyses of ferruginous types taken within the Parktown Shale Formation. Ellis (1947, p.146) analysed a Jeppestown Subgroup shale (Table 7). Recently Danchin (1970) and Hofmeyer (1971) have analysed ten shale horizons within the Government and Jeppestown subgroups for major and trace elements respectively. These are listed on Table 7 (Major) and Table 8 (Trace and Alkali). Included in Table 8 are the boron contents of 10 West Rand Group shales done by Nel (1968).

The average MgO , total iron, P_2O_5 , Na_2O , Ni, Cr, and Co contents and the Ni/C and V/Cr ratios are far closer to the Fig Tree Subgroup than the average South African shale. According to Danchin (1970) and Hofmeyer (1971) this correlation indicates that the source rocks for the Witwatersrand Supergroup must have been similar in petrology to the source rocks of the Fig Tree sediments although they probably contained a smaller ultrabasic component as the Ni concentrations and therefore the Ni/Co ratios are significantly lower.

The Si/Al ratios for the two sets of shales (3.4 for the five Government Subgroup shales and 4.5 for the Jeppestown shales) are markedly different and suggest that the rate of deposition increased through West Rand Group time (Danchin 1970). However, further work on more closely spaced samples

TABLE 7: Major Element Analyses in the West Rand Group

HOSPITAL HILL SUBGROUP (after Horwood, 1910)		GOVERNMENT SUBGROUP (after Danchin, 1970)		JEPPESTOWN SUBGROUP (after Ellis 1947, Danchin 1970)		Average West Rand Shale (volatile free)	Average Fig Tree Group Shale (volatile free)	Average S.African Shale (volatile free)
Analyses	10	5	JP5 marker	5		10	22	323
C								
O ₂	54.48	58.04	46.43	65.9		62.73	63.41	66.21
O ₂	.51	0.68	0.39	0.49		0.61	0.63	0.90
2O ₃	12.11	15.42	9.79	13.22		14.44	14.31	18.79
O		8.56	20.00	3.89				
2O ₃		3.38	7.00	1.87				
Total Fe ₂ O ₃	25.38	12.90	29.09	5.71		12.11	10.56	6.18
O		0.01	0.14	.01				
O	0.95	4.64	3.81	3.82		4.61	5.47	1.86
O	3.4	0.96	1.64	1.66		1.44	1.02	0.78
2O	} 1.36	0.94	1.17	1.50				
O		2.21	0.41	2.03		2.04	2.47	3.26
2O ₅		0.09	0.09	0.07				
2		0.23	0.60	0.41				
		0.11	0.07	0.09				
		0.01	0.01	0.01				
L.O.I.	5	3.40	5.44	2.12				
TOTAL Average 100.19		99.55	99.31	99.63				
Range		(99.01 - 100.21)		(98.65 - 100.59)				

L.O.I. = Lost on Ignition

TABLE 7: Major Element Analyses in the West Rand Group

HOSPITAL HILL SUBGROUP (after Horwood, 1910)		GOVERNMENT SUBGROUP (after Danchin, 1970)		JEPPESTOWN SUBGROUP (after Ellis 1947, Danchin 1970)		Average West Rand Shale (volatile free)	Average Fig Tree Group Shale (volatile free)	Average S.African Shale (volatile free)
No of analyses		5		JP5 marker	5	10	22	323
SiO ₂	54.48	58.04		46.43	65.9	62.73	63.41	66.21
TiO ₂	.51	0.68		0.39	0.49	0.61	0.63	0.90
Al ₂ O ₃	12.11	15.42		9.79	13.22	14.44	14.31	18.79
FeO		8.56		20.00	3.89			
Fe ₂ O ₃		3.38		7.00	1.87			
Total Fe ₂ O ₃	25.38	12.90		29.09	5.71	12.11	10.56	6.18
MnO		0.01		0.14	.01			
MgO	0.95	4.64		3.81	3.82	4.61	5.47	1.86
CaO	0.4	0.96		1.64	1.66	1.44	1.02	0.78
Na ₂ O	} 1.36	0.94		1.17	1.50			
K ₂ O		2.21		0.41	2.03	2.04	2.47	3.26
P ₂ O ₅		0.09		0.09	0.07			
CO ₂		0.23		0.60	0.41			
S		0.11		0.07	0.09			
Cl		0.01		0.01	0.01			
L.O.I.	5	3.40		5.44	2.12			
TOTAL Average 100.19		99.55		99.31	99.63			
Range		(99.01 - 100.21)			(98.65 - 100.59)			

L.O.I. = Lost on Ignition

should provide useful information in this regard.

One of the shales (JP5) has a significantly smaller SiO_2 , Al_2O_3 , K_2O content and higher FeO , Fe_2O_3 and CO_2 values when compared to the other shale horizons (Table 7). The shale is dark, finely banded and fine grained with chlorite being the dominant clay mineral. It is the only shale horizon which does not contain any subordinate or trace amounts of plagioclase and illite. Unlike eight of the other shale horizons it contained magnetite. Clearly the geochemistry of this unit could be used as an argillaceous marker horizon in the Klerksdorp area.

Nel's (1968) study on the boron content of West Rand Group shales is of special importance as boron and other trace elements may be used to indicate their environment during deposition (Keith and Rogers, 1959; Johns 1963; Potter et al 1963; Shimp et al 1969). The basis of this concept is that certain trace elements such as boron, chlorine, lithium, sulphur and vanadium are concentrated more in sediments of marine origin than those of fresh water origin. The two Jeppestown and four Government Subgroup shales yields average boron contents of 11 p.p.m. (range 5-21 p.p.m.) and the average boron/potassium ratio is 8.2 (range 4.4 - 13). Although Nel (1968) concludes that the shales 'are comprised of the weathering products of igneous rocks deposited in a fresh water environment' he does emphasise the probability that little or no boron absorption occurred due to the small amounts of illite (which has a high absorptive capacity of boron (Harder 1961)).

7.2 Sandstones

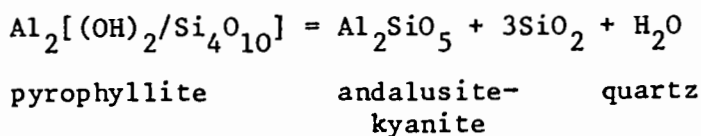
Only one analysis of a sandstone from the West Rand Group has been done. The analysis below is that of a specimen from the Jeppestown Subgroup from the Klerksdorp District (Fuller 1958):-

SiO_2	83.05
Al_2O_3	8.87
Fe_2O_3	.82
FeO	1.11
MgO	1.04
CaO	.06
Na_2O	.66
K_2O	3.19
H_2O	1.41
TiO_2	.32
P_2O_5	.02
S	.48
C	.03
	<hr/>
	100.08 Less O = S 99.9

T A B L E 9

SUBGROUP	MEMBERS AND BEDS	METAMORPHIC RESULTS
JEPPESTOWN SUBGROUP	Jeppestown Amygdaloid Quartzites Slates	Hornblende Granulite Recrystallisation Biotite Hornfels
GOVERNMENT REEF SUBGROUP	Quartzites Thin slates and ferrug- enous rocks Ferruginous Band Slates	Recrystallisation Biotite Hornfels Garnet Amphibole hornfels Garnet Amphibole hornfels Andalusite Cordierite hornfels
HOSPITAL HILL SUBGROUP	Upper Hospital Hill quartzite	Recrystallisation
	Hospital Hill slates	Cordierite hornfels and Andalusite Cordierite hornfels
	Lower Hospital Hill quartzite	Recrystallisation
	Hospital Hill slates	Cordierite hornfels and Andalusite Cordierite hornfels
	Water Tower slates	Garnet hornfels and garnet amphibole hornfels
	Orange Grove quartzite	Recrystallisation
DOMINION GROUP	Basal Amygdaloid	Hornblende granulite

The complete absence of kyanite, andalusite, cordierite and staurolite (except for the Vredefort area) and the presence of chlorite, illite, sericite, plagioclase feldspar, quartz, chloritoid, muscovite, pyrophyllite and pumpellyite within the Witwatersrand Supergroup indicates that the metamorphic minerals were formed in the very low grade or low grade regions of metamorphism as defined by Winkler (1974). Furthermore, as the breakdown reaction of pyrophyllite:-



has not occurred (except in the Vredefort area) it is unlikely that temperatures reached 400°C at 1.0 Kb (Kerrick 1968).

9. BASIN ANALYSIS

An impressive volume of information has been synthesised for the Witwatersrand basin (Brock and Pretorius 1964a,b; Pretorius 1965, 1974; Vos 1975). In this review three major aspects of basin analysis will be described. These are the arrangement and type of sedimentary and volcanic fill, the tectonic setting and the depositional environment of the West Rand Group.

9.1 Arrangement And Type Of Fill

The thickness of the West Rand Group sediments decreases from the Klerksdorp area towards the Central Rand, Heidelberg and ^{South Rand} area (Nel 1933). The sand/shale ratio of the different subgroups in their respective areas, together with the composite stratigraphical thickness and volcanic/sediment ratio of the West Rand Group and areally related Central Rand, Dominion and Klipriviersberg Group (Pretorius 1974) are depicted on Table 10. The high sand/shale ratio in the Klerksdorp area is taken to indicate a proximal facies while the Central Rand area appears to be more of a distal facies (Pretorius 1965). Also the West Rand Group in the Vredefort and South Rand areas might have been deposited on the opposite side of the Basin to that laid down in the Welkom, Klerksdorp, West Rand, Central Rand, Delmas and Heidelberg areas. The thickness and sand/shale ratio in the West Rand Group sediments together with the following features of the main conglomerate of the overlying Central Rand succession - a decrease in average pebble size from north-northwest to south-southwest (Pirow 1920) and the pattern of payshoots fanning to the south east indicating a south easterly direction of flow (Reinecke 1927; du Toit 1954; Hargraves 1962) - lead one to conclude that the source for the sediments of some of the West Rand Group sediments is the same as that of the Main Conglomerate in the Central Rand Group (ie. northerly to northwesterly source).

In 1964 Brock and Pretorius (1964a,b) published a comprehensive account of the tectonic framework, basin geometry, stratigraphy and sedimentation in the Witwatersrand Supergroup and presented an overall conceptual model. They visualised the Witwatersrand Basin as a structurally closed continental basin with the West Rand Group deposits occurring over a larger area than those of the Central Rand Group, the basin being broader during the early stages of filling. Using mines, boreholes and outcrops as their control points they published isopach maps for the Hospital Hill, Government and Jeppes- town subgroups. The isopachs depict the West Rand Group as lying in a gradually sinking ovoid shaped basin whose long axis is directed to the northeast and decreases from 440 km during Hospital Hill times to about 370 km in Jeppes- town times. Furthermore, the maps indicate that the south eastern shore- line of the depression was practically static throughout West Rand Group times, although elsewhere the waters gradually regressed. Pretorius (1974) modified the composite isopachs (Figure 12) of the West Rand Group taking into consideration the manner in which the strata had been deformed. The geometry of the basin was defined by basin edge phenomena such as overlaps, unconformities, disconformities and the mine lease areas of economic gold

TABLE 10: Composite stratigraphic thickness of West Rand Group and areally and structurally related Groups

Groups	Total (m)	Sand/Shale Ratio			Volcanic/Sediment Ratio
		Hospital Hill	Government	Jeppestown	
West Rand Group Areas					
Central Rand	3 600*	0.54	1,48	0.77	
West Rand		0.55	2,50		
Heidelberg	2 800	0.56	1.48	0.54	
South Rand	1 700		1.70	0.68	
Vredefort	4 000	0.70	1.85	0.65	
Klerksdorp	4 750	0.80	2.60	1.27	
Klipriveersberg	3 050		0.70		8.80
Central Rand Group	3 160		12.6		0.1
West Rand Group	4 970		1.0		0.1
Dominion Group	2 720		6.0		37,9
Witwatersrand Supergroup	13 900		1.9		0.8

*Government and Jeppestown thickness after Cousins (1960), Hospital Hill thickness after Mellor 1911.

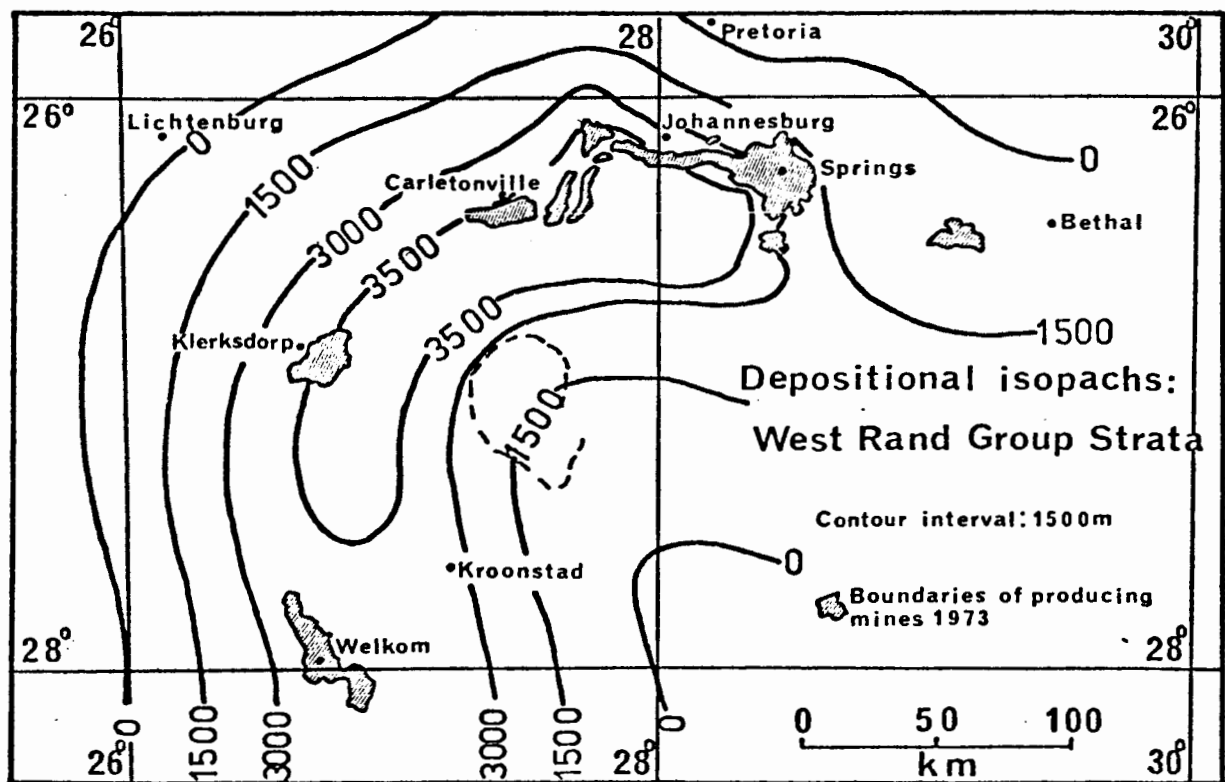


Figure 12: The extrapolated isopachs (metres) of the West Rand Group (after Pretorius 1974).

deposits located along the basin margins.

Vos (1975) devised a model of the evolution of the Witwatersrand basin from available data and from analogies with present depositional environments in which sediments of similar character are being deposited. He attempted to answer the question of why there is a marked concentration of gold in the Central Rand Group while the West Rand Group is devoid of any significant economic deposits (except in the Rietkuil Syncline). Figure 13 is a schematic illustration of the proposed manner of evolution for the Witwatersrand Basin according to Vos (1975).

The inward migration of the basin margins is seen to have occurred contemporaneously with marginal uplift and basin subsidence. The proximal coarse grained sediments along the margin edge are thus uplifted and reworked into Central Rand Group sediments which prograde out over the remnant distal West Rand Group portion of the sequence.

9.2 Tectonic Setting

The tectonic setting of the West Rand Group and Witwatersrand basin is one for which certain questions remain to be answered. The knowledge of the basin that has been gained so far, include its size and extent, the proportions of sediments that have filled it, the approximate position of the source lands that supplied its sediments, the nature of the source land, the subsequent deformation and metamorphism. The questions that remain to be answered are (i) what type of crust underlies the basin? (ii) what relation, if any, does the basin have to sutures of Archaean age? (iii) if it was situated in an intracratonic basin how does it relate to a continent-wide, regional palaeogeography? and finally (iv) if the sediments were subjected to marine processes what can one ascertain, if anything, about its open ocean margin? Some of these questions may be very difficult to answer due to the cover of large amounts of post Archaean sediments. Others may be answered by further studies of West and Central Rand Group sediments which might according to Potter and Pettijohn (1977) require a 'systematic inventory of facts' which include:-

1. the facies distribution and thickness within the basin at various stages of its filling.
2. the palaeocurrent pattern of each facies.
3. the relation of facies and palaeocurrents to both contemporaneous and later deformation and
4. the petrology of its fill (which may include both fluid inclusion studies and geochemistry).

The Witwatersrand Supergroup in places unconformably overlies older rocks which are granitic and rocks which contain great volumes of high - Mg basalts or basaltic komatiites (Anhaeusser 1978). The granites display a

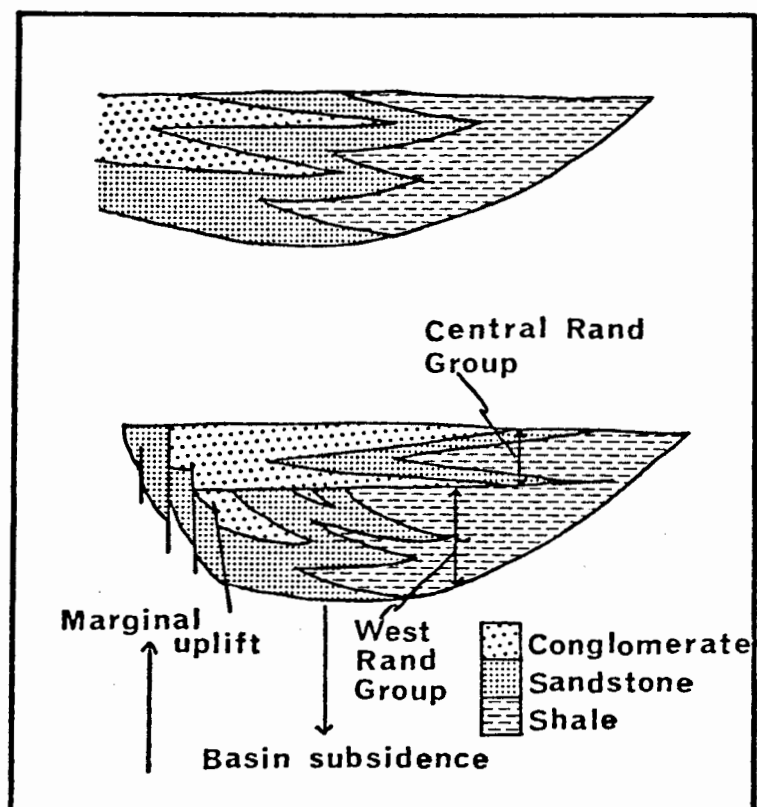


Figure 13: Schematic illustration of Vos's (1975) proposed manner of evolution for the Witwatersrand basin.

marked weathered profile (Button and Tyler, in press) and Vos (1975) interprets the quartzites of the Hospital Hill Subgroup as being deposited upon a broad semi-stable "platform" which 'had undergone a long period of geochemical separation leaving only the resistant quartz fraction which went to form the mineralogically mature othoquartzite'.

In the Klerksdorp area the Witwatersrand Supergroup is underlain by the Dominion Group and overlain by the Ventersdorp Supergroup. The Dominion Group and Ventersdorp Supergroup are almost wholly volcanic (Table 9) and according to Brock and Pretorius (1964a) "their relationships suggests that the three systems collectively constitute a major geological cycle". The ratio of volcanics to sediments is, according to Pretorius (1974), a pointer to the general order of infilling of the Archaean and Proterozoic basins on the Kaapvaal craton in South Africa. He noted that the Witwatersrand succession is situated between moderate periods of crustal instability in which 'most of the material entering the basin was drawn from the simatic lithosphere, with only limited quantities of sediments being mixed with the volcanics'. These conclusions conform with Henthorn's (1972) work on palaeomagnetism within the Witwatersrand Triad in which the direction obtained from the Jeppetown amygdaloid (D-253, I=22) circle of confidence (which is large), includes the palaeopoles of both the Great Dyke of Rhodesia (McElhinny and Gough 1963) and the Gaberones granite (Evans 1967). The Gaberones granite has a date of 2480 ± 50 m.y. (McElhinny 1967) and the Great Dyke 2500 m.y. (Wilson et al 1978). According to Henthorn (1973) these dates are of comparable age to the estimated time span of the Witwatersrand system and 'may indicate a moderately static pole during the deposition of the Witwatersrand system'.

9.3 Depositional Environment

Attempts to reconstruct West Rand Group sedimentary environments have been made by numerous geologists (eg. Hatch 1906; Mellor 1915, 1916; Rogers 1926; Reinecke 1927; Sharpe 1949; du Toit 1954; Wiebols 1955; Antrobus 1956; Brock and Pretorius 1964; Vos 1976) and many diverse settings have been invoked and are presented in a chronological review of speculations and observations on the depositional environment of the Witwatersrand sediments by Pretorius (1975). Geologists have, until recently considered the Witwatersrand basin to be closed (Brock 1950; de Villiers 1959) and since 1964 no marine environment has been suggested for the deposition of the Witwatersrand sediments. The reason for this could be due to the conclusion of Brock and Pretorius (1964a) that 'the frequency of reference to "encroaching oceans" in connection with the Witwatersrand System, even in recent years, discloses that the continental environment of the closed basin has not been

fully appreciated. Oceans are quite incompatible with the great thicknesses of shallow water sediments confined to a synclinal depression in the heart of a sub-continent'. However, work done by Sharpe (1949), Hargraves (1962) and Eriksson (in press) all suggest that marine processes played a part in the formation of the thick alternating shale and sandstone units of the West Rand Group. Until further work is done on the palaeo-current and facies distribution of the West Rand Group, the following depositional environments for the West Rand Group must be regarded only as tentative general candidates.

9.3.1 Alluvial And Lacustrine

Reinecke (1927), Pretorius (1966) and Vos (1975) presented depositional patterns for the West and Central Rand Group sediments which fit a braided alluvial plain and lacustrine model. Reinecke (1927) invoked earth movements for the increase in grain size from the West Rand to the Central Rand Group and for the presence of unconformities between the two groups. The widespread distribution of the conglomerate bands at different horizons and lying unconformably on shale horizons within the Government Subgroup Reinecke (1927) attributed to the sudden drainage of lakes dammed by glaciers or landslides and followed by periodic flooding and slumping. Vos's (1975) model (Figure 13) is one in which he interprets the West Rand Group deposits to be a thick accumulation of mainly lower braided alluvial plain and lacustrine sediments. The lacustrine setting being the locus for the fine grained sediments, silts and clays and the alluvial plain setting is that of sandstones and conglomerates. The thick alternating sandstone and shale horizons are explained by a shifting depositional system (sourceward and basinward) controlled by tectonism in the basin and source area.

In 1966 Pretorius synthesised the detailed sedimentological work done in the previous five years and introduced two new concepts - the identification of local depositional conditions as deduced from fan facies, and the employment of energy levels as controlling factors in the nature of the sedimentary responses to the varying depositional processes. He regarded the sediments of the West Rand Group as being deposited in a distal lacustrine environment.

9.3.2 Deltaic and Marine

Pretorius (1975) states that 'Carrick (1896) drew the attention of the various authors, that Fred Struben, the original pioneer of the Witwatersrand area, at the very beginning of his mining of the conglomerates in the Lower Division of the Witwatersrand Sequence considered the banket to be an ocean-beach deposit. At the same time Garinier (1896) put forward the first suggestion that the beaches had formed along a closed sea that was surrounded by high mountains, some of which formed a vast amphitheatre on the northern

side. Streams converged in all directions towards the basin'. Hatch (1906) considered the source area to lie to the west, the sea to the east and that the shales and sands of the West Rand Group were laid down on a subsiding ocean floor. Mellor (1915, 1916) considered the spectacular change from shale to sandstones to be produced on an extensive delta. The delta model, according to Mellor (1915), could explain the continual increase in coarseness from the West Rand to the Central Rand Group.

Alternate rising and sinking of a marine area was invoked as a possible mechanism for the development of the predominantly arenaceous Government Subgroups between two predominantly argillaceous Hospital Hill and Jeppes-town subgroups (Sharpe 1949). The smaller scaled alternations of quartzite - shale, Sharpe termed a cyclothem and were thought to have been caused by earth movements of a more local character which modified the conditions of deposition. As well as shoaling of the basin, elevation and erosion of the source area has been held responsible for the coarsening of the sediments arriving in the basin. Although no published reports of palaeocurrent measurements have been recorded within the West Rand Group, Hargraves (1962) noted that the orientation of the current bedding on the East Rand within the overlying Main Conglomerates was bimodal and that the crests of the transverse ripples lie in a northwest-southeast direction. Hargraves therefore postulated tidal movement from southeast to northwest.

R E F E R E N C E S

- Allsopp, H.L., 1964. Rubidium-Strontium ages from the western Transvaal. *Nature*, 204 (4956) : 361-363.
- Allsopp, H.L., Roberts, H.R., and Schreiner, G.D.L., and Hunter, D.R., 1962. Rb-Sr age measurements of various Swaziland granites. *J. Geophys. Res.*, 67(13).
- Anhaeusser, C.R., 1978. The geology and geochemistry of the Muldersdrif ultramafic complex. Inform. Circ. econ. Geol. Res. Unit, Univ. Witwatersrand, Johannesburg, 117 : 14 pp.
- Antrobus, E.S.A., 1956. The origin of the auriferous reefs of the Witwatersrand System. *Trans. geol. Soc. S. Afr.*, 59 : 1-22.
- Antrobus, E.S.A., 1964. Notes on the geological column of the East Rand. In : Haughton, S.H. (Editor), *The Geology of Some Ore Deposits in Southern Africa*, Geol. Soc. S. Afr., Johannesburg, Vol 1: 113-123.
- Bain, G.W., 1955. Discussion of paper "The occurrence and origin of gold and radioactive minerals in the Witwatersrand System, the Dominion Reef, the Ventersdorp Contact Reef and the Black Reef" by Liebenberg, W.R., *Trans. geol. Soc. S. Afr.*, 58 : 236.
- Bain, G.W., 1960. Patterns to ores in layered rocks : *Econ. Geol.*, 55(4) : 695-731.
- Becker, G.F., 1896. The Witwatersrand blanket with notes on other gold-bearing pudding-stones. *Annu. Rep. U. S. Geol. Surv.*, 18(5) : 153-184.
- Beetz, P.F.W., 1936. Contributions to the geology of the Klerksdorp district from the results of the drilling activities by the Western Reefs Exploration and Development Company. *Trans. geol. Soc. S. Afr.*, 39 : 223-261.
- Borchers, R. , 1961. Exploration of the Witwatersrand System and its Extensions. *Proc. geol. Soc. S. Afr.*, 64 : 67.
- Borchers, R., 1964. Exploration of the Witwatersrand System and its Extensions. In : S.H. Haughton (Editor), *The Geology of Some Ore Deposits in Southern Africa*. Geol. Soc. of S. Afr., Johannesburg, Vol. 1 : 1-23.
- Bosazza, V.L., 1939. Discussion on paper 'The sampling of mine dusts' by H.S. Patterson. *J. Chem. met Min. Soc. S. Afr.*, 40 : 227.
- Brock, B.B., 1950. The Vredefort ring. *Trans. geol. Soc. S. Afr.*, 53 : 131.
- Brock, B.B. and Pretorius, D.A., 1964a. An introduction to the stratigraphy and structure of the Rand Goldfield. In: S.H. Haughton (Editor), *The Geology of Some Ore Deposits in Southern Africa*. Geol. Soc. of S. Afr., Johannesburg, Vol. 1 : 25-61.
- Brock, B.B. and Pretorius, D.A., 1964b. Rand basin sedimentation and tectonics. In: S.H. Haughton (Editor), *The Geology of Some Ore Deposits in Southern Africa*. Geol. Soc. of S. Afr., Johannesburg, Vol. 1 : 449-499.
- Button, A., 1968. Subsurface stratigraphic analysis of the Witwatersrand and Transvaal sequences in the Irene-Delmas-Devon area, Transvaal. Unpub. M.Sc. thesis, Univ. Witwatersrand, Johannesburg, 120 pp.

REFERENCES

- Allsopp, H.L., 1964. Rubidium-Strontium ages from the western Transvaal. *Nature*, 204 (4956) : 361-363.
- Allsopp, H.L., Roberts, H.R., and Schreiner, G.D.L., and Hunter, D.R., 1962. Rb-Sr age measurements of various Swaziland granites. *J. Geophys. Res.*, 67(13).
- Anhaeusser, C.R., 1978. The geology and geochemistry of the Muldersdrif ultramafic complex. Inform. Circ. econ. Geol. Res. Unit, Univ. Witwatersrand, Johannesburg, 117 : 14 pp.
- Antrobus, E.S.A., 1956. The origin of the auriferous reefs of the Witwatersrand System. *Trans. geol. Soc. S. Afr.*, 59 : 1-22.
- Antrobus, E.S.A., 1964. Notes on the geological column of the East Rand. In : Haughton, S.H. (Editor), *The Geology of Some Ore Deposits in Southern Africa*, Geol. Soc. S. Afr., Johannesburg, Vol 1: 113-123.
- Bain, G.W., 1955. Discussion of paper "The occurrence and origin of gold and radioactive minerals in the Witwatersrand System, the Dominion Reef, the Ventersdorp Contact Reef and the Black Reef" by Liebenberg, W.R., *Trans. geol. Soc. S. Afr.*, 58 : 236.
- Bain, G.W., 1960. Patterns to ores in layered rocks : *Econ. Geol.*, 55(4) : 695-731.
- Becker, G.F., 1896. The Witwatersrand banket with notes on other gold-bearing pudding-stones. *Annu. Rep. U. S. Geol. Surv.*, 18(5) : 153-184.
- Beetz, P.F.W., 1936. Contributions to the geology of the Klerksdorp district from the results of the drilling activities by the Western Reefs Exploration and Development Company. *Trans. geol. Soc. S. Afr.*, 39 : 223-261.
- Borchers, R. , 1961. Exploration of the Witwatersrand System and its Extensions. *Proc. geol. Soc. S. Afr.*, 64 : 67.
- Borchers, R., 1964. Exploration of the Witwatersrand System and its Extensions. In : S.H. Haughton (Editor), *The Geology of Some Ore Deposits in Southern Africa*. Geol. Soc. of S. Afr., Johannesburg, Vol. 1 : 1-23.
- Bosazza, V.L., 1939. Discussion on paper 'The sampling of mine dusts' by H.S. Patterson. *J. Chem. met Min. Soc. S. Afr.*, 40 : 227.
- Brock, B.B., 1950. The Vredefort ring. *Trans. geol. Soc. S. Afr.*, 53 : 131.
- Brock, B.B. and Pretorius, D.A., 1964a. An introduction to the stratigraphy and structure of the Rand Goldfield. In: S.H. Haughton (Editor), *The Geology of Some Ore Deposits in Southern Africa*. Geol. Soc. of S. Afr., Johannesburg, Vol. 1 : 25-61.
- Brock, B.B. and Pretorius, D.A., 1964b. Rand basin sedimentation and tectonics. In: S.H. Haughton (Editor), *The Geology of Some Ore Deposits in Southern Africa*. Geol. Soc. of S. Afr., Johannesburg, Vol. 1 : 449-499.
- Button, A., 1968. Subsurface stratigraphic analysis of the Witwatersrand and Transvaal sequences in the Irene-Delmas-Devon area, Transvaal. Unpub. M.Sc. thesis, Univ. Witwatersrand, Johannesburg, 120 pp.

- Button, A., 1970. The stratigraphy of the Witwatersrand System in the Delmas area, Transvaal. Inform. Circ. econ. Geol. Res. Unit, Univ. Witwatersrand, Johannesburg, 58 : 20 pp.
- Button, A., 1973. A regional study of the stratigraphy and development of the Transvaal basin in the eastern and northeastern Transvaal. Unpub. Ph.D. thesis, Univ. Witwatersrand, Johannesburg, 352 pp.
- Button, A. 1978. Correlation of the Godwan Formation based on stratigraphic trends in the Witwatersrand basin. Trans. geol. Soc. S.Afr., 81 : 109-114.
- Button A. and Tyler, N., (in press) Precambrian paleoweathering and erosion surfaces in Southern Africa - Review of their character and economic significance. Inform. Circ. econ. Geol. Res. Unit, Univ. Witwatersrand, Johannesburg, 135.
- Carrick, T.J., 1896. On faulting along the Main reef line. Trans. geol. Soc. S. Afr., 2 : 39-41
- Cloud, P., 1976. Major features of crustal evolution. A.L. du Toit Memorial Lecture No. 14, Geol. Soc. of S. Afr., Johannesburg. Annex. to Vol. LXXIX, 33 pp.
- Coetzee, C.B., 1960. The geology of the Orange Free State goldfield. Mem. geol. Surv. S. Afr. 49 : 198 pp.
- Collender, D.F., 1960. The Witwatersrand System in the Klerksdorp area as revealed by diamond drilling. Trans. geol. Soc. S. Afr., 63 : 189-226.
- Corstorphine, G.S., 1904. The geological relation of the Old Granite to the Witwatersrand Series. Trans. geol. Soc. S. Afr., 7 : 9-12.
- Cousins, C.A., 1960. Discussion on paper 'The Witwatersrand System in the Klerksdorp area as revealed by diamond drilling' by F.D. Collender. Trans. geol. Soc. S.Afr., 63 : 227-229.
- Cousins, C.A., 1965. Disconformities in the Main Reef Zone of the Witwatersrand System, and their bearing on reef correlation, with particular reference to the east, central and west Witwatersrand. Trans. geol. Soc. S. Afr., 68 : 121-142.
- Cousins, C.A., 1973. Discussion on paper 'Suggestions for the revision of the existing Witwatersrand stratigraphic classification and nomenclature' by G.F. Wagener. Trans. geol. Soc. S. Afr., 76(2) 181-182.
- Danchin, R.V., 1970. Aspects of the geochemistry of some selected South African fine grained sediments. Unpub. Ph.D. thesis, Univ. Cape Town, Cape Town, 215 pp.
- Davies, R.D., Allsopp, H.L., Erlank, A.J. and Manton, W.I., 1969. Sr-isotopic studies on various layered mafic intrusions in southern Africa. In : Symposium on the Bushveld Igneous Complex and Other Layered Intrusions. Spec. Publ. geol. Soc. S. Afr., 1 : 576-593.
- De Beer, J.H., 1966. A detailed geological and soil map of the Johannesburg city area. Unpub. Ph.D. thesis, Univ. Witwatersrand, Johannesburg.

- De Jager, F.S.J., 1964. The Witwatersrand System in the Springs-Nigel-Heidelberg sector of the East Rand Basin. In: S.H. Haughton (Editor) *The Geology of Some Ore Deposits in Southern Africa*, Geol. Soc. of S.Afr., Johannesburg. Vol. 1 : 161-190.
- De Villiers, J.E., 1941. Optical properties and crystallography of zoned pumpellyite from the Witwatersrand. *Amer. Min.*, 26 : 237-246.
- De Villiers, J., 1959. Mineral Resources of the Union of S. Afr., Geol. Surv. S. Afr., Pretoria.
- Draper, D., 1896. The Primary Systems of South Africa with special reference to the conglomerate beds of the Witwatersrand. *Trans. geol. Soc. S. Afr.*, 1 : 12-26.
- Draper, D., 1897a. On the connection between the conglomerate beds of the Witwatersrand and those situated in the districts of Potchefstroom and Klerksdorp. *Trans. geol. Soc. S. Afr.*, 2 : 5-14.
- Draper, D., 1897b. The extension of the Main Reef westwards on the farm Witpoortjie. *Trans. geol. Soc. S. Afr.*, 2 : 5-14.
- Du Toit, A.L., 1954. *The Geology of South Africa*. 3rd Edition, Oliver and Boyd, Edinburgh, 611 pp.
- Ellis, J., 1940. A tear-fault in the Far East Rand. *Trans. geol. Soc. S. Afr.*, 43 : 127-142.
- Ellis, J., 1947. The Marievale granophyre, a metamorphic rock. *Trans. geol. Soc. S. Afr.*, 50 : 121-160.
- Eriksson, K.A; Turner, B.R. and Vos, R.G. (in press). Evidence of tidal processes from the lower part of the Witwatersrand Supergroup, South Africa.
- Evans, M.E., 1967. A Paleomagnetic study of the Gaberones granite of Botswana. *Geophys.J.* , 12 : 491-498.
- Fox, E.F., 1939. The geophysical and geological investigation of the Far East Rand. *Trans. geol. Soc. S. Afr.*, 51 : 213-247.
- Frankel, J.J. , 1939. The green colour of the Hospital Hill quartzites. *Trans. geol. Soc. S. Afr.*, 42 : 15-17.
- Frankel, J.J., 1944. On silicates and dusts from the Witwatersrand Gold Mines. *J.S. Afr. chem. Soc.*, 44 : 169-179.
- Frey, M., 1970. The step from diagenesis to metamorphism in pelitic rocks during Alpine orogenesis. *Sedimentol.* 15 : 261-279.
- Fripp, R.E.P. and Gay, N.C., 1972. Some structural aspects of the Hospital Hill series on the north-central margin of the Witwatersrand Basin. *Trans. geol. Soc. S. Afr.*, 75(3) : 187-196.
- Frost, A., McIntyre, R.C., Papenfus, E.B. and Weiss O., 1946. The discovery and prospecting of a potential goldfield near Odendaalsrus in the Orange Free State Union of South Africa. *Trans. geol. Soc. S. Afr.*, 49 : 1-33.

- Fuller, A.O., 1958. A contribution to the petrology of the Witwatersrand System. *Trans. geol. Soc. S. Afr.*, 61 : 19-50.
- Garnier, J., 1896. Gold and diamonds in the Transvaal and the Cape. *Trans. geol. Soc. S. Afr.*, 2 : 91-103, 109-120.
- Graton, L.C., 1930. Hydrothermal origin of the Rand gold deposits, Part 1. *Econ. Geol.*, 25 (Suppl.) : 185 pp.
- Gregory, J.W., 1908. The origin of the gold in the Rand Banket. *Trans. Instn. Min. Metall, Lond.*, 17 : 2-41.
- Gruner, J.W., 1944. The hydrothermal alteration of feldspars in acid solutions between 300° and 400°C. *Econ. Geol.*, 39 : 578-589.
- Hall, A.L., 1911. The geology of Sekukuniland. Explanation of sheet 8. *Geol. Surv. S. Afr.*, Pretoria, 40 pp.
- Hall, A.L., 1925. On the metamorphism of the Lower Witwatersrand System in the Vredefort Mountain Land. *Trans. geol. Soc. S. Afr.* 9 : 10-15.
- Hall, A.L., 1938. Analyses of rocks, minerals, ores, coals, soils, and waters from Southern Africa. *Mem. Geol. Surv. S. Afr.*, Pretoria, 32 : 876 pp.
- Hall, A.L. and Molengraaff, G.A.F., 1925. The Vredefort mountain land in the southern Transvaal and the northern Orange Free State. *Amst. Verh. Kon. Akad. Wet. Tweede Sectie, Deel 24(3)* : 183 pp.
- Harder, H., 1961. Beitrag zur geochemie des Bors 111. Bor in metamorphen gesteinen und im geochem-ischen Kreislauf. *Nachr. Adkad. Wiss. Göttingen. Math-Phys. Kl. No. 1* : 1.
- Hargraves, R.B., 1962. Crossbedding and ripple marking in the Main Bird Series of the Witwatersrand System in the East Rand area. *Trans. geol. Soc. of S. Afr.*, 65 : 263-279.
- Hatch, F.H., 1898. A geological survey of the Witwatersrand. *Quart. J. geol. Soc. Lond.*, 54 : 73-100.
- Hatch, F.H. 1904. The extension of the Witwatersrand eastward under the Dolomite and Eccca Series of the Southern Transvaal. *Trans. geol. Soc. S. Afr.*, 7 : 57-69.
- Hatch, F.H. 1906. The geological history of the South African formations. *Proc. geol. Soc. S. Afr.*, 9 : 21-34.
- Hatch, F.H., 1913. Inpoverishment with depth on the Rand. (Letter to Editor). *Min. Mag., Lond.*, 9 : 450-451.
- Hendriks, L.P., 1961. Die voor-Transvaalse gesteentes op Zwartkop 82 en omstreke, noord van Krugersdorp, Transvaal. Unpub. M.Sc. thesis, Univ. Pretoria, Pretoria, 76 pp.
- Henthorn, D.I., 1972. Paleomagnetism of the Witwatersrand Triad, Republic of South Africa and related topics. Unpub. Ph.D. thesis, Univ. Leeds, Leeds.

- Hofmeyr, P.K., 1971. The abundances and distribution of some trace elements in some selected South African shales. Unpub. Ph.D. thesis, Univ. Cape Town, Cape Town, 218 pp.
- Horwood, C.B., 1910. Notes and analyses of typical Transvaal rocks. Trans. geol. Soc. S. Afr., 13 : 29-55.
- Humphrey, W.A. and Krige, L.J., 1931. The Geology of the country south of Piet Retief. Explanation of Sheet No. 68 (Piet Retief). Geol. Surv. S. Afr., Pretoria, 67 pp.
- Jansen, H., 1974. Explanatory notes. Sheet 2426 (Thabazimbi), Geol. Surv. S. Afr., Pretoria.
- Jansen, H., Schalk, K.E., Leube, A., Snyman, A.A., Steyn, A.P.A., de Jager, F.S.J. and Beer, H.M., 1972. Geology of the country around Standerton. Explanation of sheets 2628D and 2629C. Geol. Surv. S. Afr., Pretoria, 27 pp.
- Jansen, H., 1977. The geology of the country around Pretoria. Explanation of sheets 2527DA, DB, DC, DD and 2528CA, CB, CC, CD. Geol. Surv. S. Afr., Pretoria, S. Afr., 141 pp.
- Johns, W.D., 1963. Die verteilung von Chlor in rezenten marinen und nicht marinen Sedimenten. Fortschr. Geol. Rheinland Westfalen, 10 : 215-230.
- Keith, M.L. and Rogers, E.T., 1959. Geochemical indicators of marine and fresh-water sediments. In: P.H. Abelson (Editor), Researches in Geochemistry. Wiley, New York, 38-61.
- Kerrick, D.M., 1968. Experiments on the upper stability limit of pyrophyllite at 1.8 kb and 3.9 kb water pressure. Am. J. Sci., 266 : 204-214.
- Krahmann, R., 1930. Magnetic investigations as an aid to economic geology. Trans. geol. Soc. S. Afr., 33 : 65-87.
- Krahmann, R., 1936. The geophysical magnetometric investigations on west Witwatersrand areas between Randfontien and Potchefstroom, Transvaal. Trans. geol. Soc. S. Afr., 39 : 1-44.
- Krause, H.L., 1912. A contribution to the structural geology of the East Rand. Trans. geol. Soc. S. Afr., 15 : 93-99.
- Kynaston, H., 1911. The geology of a portion of the Rustenburg district lying north of the Pilandsberg. Ann. Rep. Geol. Surv. S. Afr., Pretoria, 63-73.
- Leube, A., 1956. The geology of the Greylingstad-Vaal River area. Unpub. Report, Geol. Surv. S. Afr., Pretoria.
- Liebenberg, W. R., 1955. The occurrence and origin of gold and radioactive minerals in the Witwatersrand System, the Dominion Reef, the Ventersdorp Contact Reef and the Black Reef. Trans. geol. Soc. S. Afr., 58 : 101-223.
- Marriott, H.F., 1904. Notes on the chemical composition of the Hospital Hill shales. Trans. geol. Soc. S. Afr., 7 : 27-29.
- Martini, J.E.J., 1975-76. Preliminary report on the deep borehole drilled on Tweefontein 441JP, Rustenbrug District, Western Transvaal. Ann. Geol. Surv. S. Afr., Pretoria, 11 : 73-76.

- McElhinny, M.W., 1967. The paleomagnetism of the southern continents; a survey and analysis. In: Symposium on Continental Drift (UNESCO/IUGS), Montevideo, Uruguay, 24 pp. Also in: 1972, Trans. Am. Geophys. Union, 52 : 176-197.
- McElhinny, M.W., and Gough, D.I., 1963. The paleomagnetism of the Great Dyke of Southern Rhodesia. Geophys. 7 : 287-303.
- Mellor, E.T., 1911. The normal section of the Lower Witwatersrand System. Trans. geol. Soc. of S. Afr., 14 : 93-131.
- Mellor, E.T., 1913. Structural features of the Western Witwatersrand. Trans. geol. Soc. S. Afr., 16 : 1-32.
- Mellor, E.T., 1916. The conglomerates of the Witwatersrand. Trans. Instn. Min. Metall. 25 : 226-348. Also in J.S. Afr. Chem. Soc., 16 : 144-180.
- Mellor, E.T., 1917. The geology of the Witwatersrand : Explanation of Sheet 52 (Johannesburg) . Geol. Surv. S. Afr., Pretoria, No 3 : 46 pp.
- Molengraaff, G.A.F., 1904. Notes on the geology of a portion of Klerksdorp district with special reference to the development of the Lower Witwatersrand beds and the Vaal River System. Trans. geol. Soc. S. Afr., 7 : 16-25.
- Molengraaff, G.A.F., 1905. Note on the geology of a portion of the Klerksdorp district with special reference to the development of the Lower Witwatersrand beds. Trans. geol. Soc. S. Afr., 8 : 16-25.
- Nel. L.T., 1927. The geology of the Country around Vredefort. Spec. Publ. geol. Surv. S. Afr., Pretoria. No 6.
- Nel. L.T., 1933. The Witwatersrand System outside the Rand. Proc. geol. Soc. S. Afr., 36 : 23-48.
- Nel. L.T., 1934. The Witwatersrand rocks in the Klerksdorp and Ventersdorp districts. Trans. geol. Soc. S. Afr., 37 : 103-143.
- Nel. L.T., 1935. The geology of the Klerksdorp-Ventersdorp area. Explanation of geological map No 37, Soec. Publ. geol. Surv. S. Afr., Pretoria, No 9.
- Nel. L.T., Truter, F.C., Willemsse, J. and Mellor, E.T., 1939. The geology of the country around Potchefstroom and Klerksdorp. Explanation of Sheet No 61 (Potchefstroom). Geol. Surv. S. Afr., Pretoria, 156 pp.
- Nel. L.T. and Verster, W.C., 1962. Die geologie van die gebied tussen Bothaville en Vredefort. Explanations of Sheets 2726B and 2727A. Geol. Surv. S. Afr., Pretoria.
- Nel. W.A., 1968. The estimation and distribution of boron in fine grained South African Sediments. Unpub. M.Sc. thesis, Univ. Cape Town, Cape Town, 69 pp.
- Nicolaysen, L.O., Burgher, A.J. and Liebenberg, W.R., 1962. Evidence for the extreme age of certain minerals from the Dominion Reef conglomerates and the underlying granite in the Western Transvaal. Geochim. cosmochim. Acta, 26 : 15-23.

- Paver, G.L., 1939. Magnetic anomalies in the Witwatersrand System. In: Nel, L.T., Compiler, The geology of the Country around Potchefstroom and Klerksdorp: Explanation of Sheet No 61 (Potchefstroom). Geol. Surv. S. Afr., Pretoria, 156 pp.
- Pegg, C.W., 1950. A contribution to the geology of the West Rand area. Trans. geol. Soc. S. Afr., 53 : 209-227.
- Pelletier, R.A., 1937. Contributions to the geology of the Far West Rand. Trans. geol. Soc. S. Afr., 40: 127-162.
- Pirow, H., 1920. Distribution of pebbles in the Rand basin and other features of the rock. Trans. geol. Soc. S. Afr., 23 : 64-97.
- Potter, P.E. and Pettijohn, F.J., 1977. Paleocurrents and Basin Analysis. 2nd Edition. Springer - Verlag, New York-Berlin, 425 pp.
- Potter, P.E., Shimp, N.F. and Witters, J., 1963. Trace elements in marine and fresh-water argillaceous sediments. Geochim. Cosmochim. Acta, 27 : 669-694.
- Pretorius, D.A., 1964. The geology of the Central Rand Goldfield. In: S.H. Haughton (Editor), The Geology of Some Ore Deposits in Southern Africa. Geol. Soc. of S. Afr., Johannesburg. Vol 1: 219-282. Also in: Inform. Circ. econ. Geol. Res. Unit., Univ. Witwatersrand, Johannesburg, 13 : 69 pp.
- Pretorius, D.A. 1964. The geology of the South Rand Goldfield. In: S.H. Haughton (Editor), The Geology of Some Ore Deposits in Southern Africa, Geol. Soc. of S. Afr., Johannesburg, Vol 1 : 219-282.
- Pretorius, D.A., 1965. Revision of the Lower Witwatersrand Stratigraphy. Unpub. report to Ad Hoc Committee for stratigraphy, 5 pp.
- Pretorius, D.A., 1966. Recorrelation of alleged Witwatersrand correlatives. Ann. Rep. Econ. Geol. Res. Unit. Univ. Witwatersrand, Johannesburg, 8 : 17 pp.
- Pretorius, D.A., 1966. Conceptual geological models in the exploration for gold mineralisation in the Witwatersrand Basin. Inform. Circ. Econ. Geol. Res. Unit. Univ. Witwatersrand, Johannesburg, 33 : 39 pp. Also in: S. Afr. Inst. Min. Metall., March, 1966 : 225-275.
- Pretorius, D.A., 1974. The nature of the Witwatersrand gold - uranium deposits. Inform. Circ. Econ. Geol. Res. Unit, Univ. Witwatersrand, Johannesburg, 86 : 50 pp.
- Pretorius, D.A., 1975. The depositional environment of the Witwatersrand goldfields, a chronological review of speculations and observations. Minerals Sci. Engng. 7(1): 18-47.
- Pretorius, D.A., 1978. The broader aspects of the gravity field over Southern Africa. Inform. Econ. Res. Unit, Univ. Witwatersrand, Johannesburg, 113: 10 pp.

- Ramdohr, P., 1958. On the occurrence of uranium in ancient conglomerate (discussion). *Econ. Geol.* 53 : 620.
- Ramsay, J.G., 1967. Folding and fracturing of rocks. McGraw Hill Book Co. Inc., New York, 568 pp.
- Reimer, T.O., 1975. The age of the Witwatersrand System and other gold - uranium placers: Implications on the origin of the mineralisation. *N. Jb. Miner. Mh.*, 79-98.
- Reinecke, L., 1927. The location of payable ore bodies in the gold bearing reefs of the Witwatersrand. *Trans. geol. Soc. S. Afr.*, 30 : 89-120.
- Reinecke, L. and Krahmann, R. 1935. Magnetometric prospecting on the Witwatersrand. *Amer. Inst. Min. Met. Engng.*, Fe. 1935.
- Roberts, E.R. and Kransdorff, D., 1938. The Upper Witwatersrand System at Randfontein Estates. *Trans. geol. Soc. S. Afr.*, 41 : 225-248.
- Roering, C., 1968. The tectonics of the West Rand syncline: a field study of brittle failure in the Witwatersrand Basin. *Inform. Circ. Econ. Geol. Res. Unit., Univ. Witwatersrand, Johannesburg*, 48 : 28 pp.
- Rogers, A.W., 1921. The geology in the neighbourhood of Heidelberg. *Trans. geol. Soc. S. Afr.*, 24 : 17-52.
- Rogers, A.W. 1922. The Geology of the Country around Heidelberg. *Expl. of Geol. Map., Spec. Publ. Geol. Surv. S. Afr.*, Pretoria, No 4.
- Rundle, C.C. and Snelling, N.J., 1977. The geochronology of uraniferous minerals in the Witwatersrand Triad., an interpretation of new and existing U-Pb age data on rocks and minerals from the Dominion Reef, Witwatersrand and Ventersdorp Supergroups. *Phil. Trans. R. Soc. Lond. A.*, 286 : 567-583. Also in: J.E.T. Horne and Sir Kingsley Dunham (Editors), *Mineralogy: Towards the Twenty-First Century*. The Royal Society, London (1977), 404 pp.
- Sacs, 1978. Lithostratigraphic subdivisions of the Witwatersrand Supergroup. South African Committee for Stratigraphy, *Geol. Surv. S. Afr.*, Pretoria.
- Sawyer, A.R., 1904. The South Rand Goldfield, Transvaal. *Trans. Inst. Min. Eng. Newcastle (England)*, Vol 27.
- Sawyer, A.R., 1907. New Rand Goldfield, Orange River Colony. *Trans. Inst. Min. Eng. Newcastle (England)*, Vol 33.
- Sawyer, A.R., 1911. Some structural features of the Witwatersrand System on the central Rand, with a note on the Rietfontein Series (discussion). *Proc. geol. Soc. S. Afr.*, 14 : 35.
- Schutte, I.C., Seeger, K.G. and Wilke, D.P., 1960. Die geologie van 'n gedeelte van die gebied 2426 (Skaal 1: 250 000) langs die Krokodilrivier, ten weste van Thabazimbi. *Unpub. Rept. geol. Surv. S. Afr.*, Pretoria, 7-25.
- Shimp, N.F., Witters, J., Potter, P.E. and Schleidher, J.A., 1969. Distinguishing marine and fresh-water muds. *J. Geol.*, 77 : 566-580.

- Sharpe, J.W.N., 1949. The economic auriferous banket of the Upper Witwatersrand beds and their relationship to sedimentation features. Trans. geol. Soc. S. Afr., 52: 265-300.
- Toens, P.O. and Griffiths G.H., 1964. The geology of the West Rand. In: S.H. Haughton (Editor), The Geology of Some Ore Deposits in Southern Africa. Geol. Soc. of S. Afr. Johannesburg, Vol 1: 283-321.
- Truswell, J.F. , 1967. A critical review of stratigraphic Terminology as applied to South Africa. Trans. geol. Soc. S. Afr., 70: 81-116.
- Truswell, J.F., 1977. The geological evolution of South Africa. Purnell, Cape Town-Johannesburg-London, 218 pp.
- Truter, F.C., 1949. A review of volcanism in the geological history of South Africa. Proc. geol. Soc. S. Afr. , 52 : 29-89.
- Tyler, N., 1978. The stratigraphy of the early-Proterozoic Buffalo Springs Group in the Thabazimbi Area, west-central Transvaal. Inform. Circ. econ. geol. Res. Unit, Univ. Witwatersrand, Johannesburg, 120: 16 pp.
- Van Eeden, O.R., de Wet, N.P. and Strauss, C.Z., 1963. The geology of the area round Schweizer-Renecke. Explanation of Sheets 2724B and 2725A. Geol. Surv. S. Afr., Pretoria, 76 pp.
- Van Niekerk, C.B. and Burger, A.J., 1964. The age of the Ventersdorp System. Ann. geol. Surv. S. Afr., Pretoria, 3: 75-86.
- Van Niekerk, C.B., 1968. The suitability of extrusive rocks for U-Pb radiometric dating. Unpub. Ph.D. thesis, Univ. Cape Town, Cape Town.
- Van Niekerk, C.B., 1969a. The uranium-lead isotopic dating of South African acid lavas, Bull. Volcan 32(3): 481-498.
- Van Niekerk, D.B. and Burger, 1969b. Lead isotopic data relating to the age of the Dominion Reef lava. Trans. geol. Soc. S. Afr., 72: 37-45.
- Van Niekerk, C.B. and Burger, A.J., 1978. A new age for the Ventersdorp acidic lavas. Trans. geol. Soc. S. Afrd., 81(2) : 155-164.
- Van Rooyen, D.P., 1947. Sekere pre-Transvaal rotse noord-oos van Potgietersrus. Trans. geol. Soc. S. Afr., 50: 63-70.
- Verwoerd, W.J., 1964. Stratigraphic classification: A critical review. Trans. geol. S. Afr., 67: 263-282.
- Von Backström, J.W., 1952. The Dominion Reef and Witwatersrand Systems between Wolmaransstad and Ottosdal, Transvaal. Trans. geol. Soc. S. Afr., 55: 53-71.
- Von Backström, J.W., 1962. Die geologie van die gebied om Ottosdal, Transvaal. Explanation of Sheets 2625D and 2626C. Geol Surv. S. Afr., Pretoria.
- Vos, R.G., 1975. An alluvial plain and lacustrine model for the Precambrian Witwatersrand deposits of South Africa. J. Sed. Petrol 45(2): 480-493.
- Wagener, G.F., 1972. Suggestions for the revision of the existing Witwatersrand Stratigraphic classification and nomenclature. Trans. geol. Soc. S. Afr., 75(2): 77-84.

- Weiss, O., 1934. The applications and limitations of geophysical prospecting methods in the Witwatersrand area. *J.S. Afr. chem. Soc.*, 34, 10:
- Weiss, O., 1936. Typical magnetic anomalies of Lower Witwatersrand shales and younger dykes in the Witwatersrand. *J.S. Afr.chem, Soc.*, 34: 227-234.
- Weiss, O., 1950. Gravimeter results in prospecting for Witwatersrand quartzites in the Transvaal and Orange Free State. (abs) *Geophysics*, 15: 311.
- Winter, H. de la R., 1978. Subdivisions of the Witwatersrand triad : the Dominion Group, the Witwatersrand Supergroup and the Ventersdorp Group. Unpubl. provisional stratigraphic subdivisions. S. Afr. committee for stratigraphy, Geol. Surv., Pretoria.
- Whiteside, H.C., 1970. Volcanic rocks of the Witwatersrand triad. In: T.N. Clifford and I.G. Gass (Editors), "African Magmatism and Tectonics". Oliver and Boyd, Edinburgh, 461 pp.
- Whiteside, H.C.M., Glasspool, K.R., Hiemstra, S.A., Pretorius, D.A. and Antrobus, E.S., 1976. Gold in the Witwatersrand Triad. In: C.B. Coetzee (Editor). Mineral Resources of the Republic of South Africa., Geol. Surv. S. Afr., Pretoria, 462 pp.
- Wiebols, J.H., 1955. Note on chloritoid in the Witwatersrand System. *Trans. geol. Soc. S. Afr.*, 64: 85-98.
- Wilson, J.F., Bickle, M.J., Hawkesworth, C.J., Martin, A., Nisbet, E.G. and Orphen, J., 1978. Granite-greenstone terrains of the Rhodesian Archaean craton. *Nature*, 278(5640): 23-27.
- Wilson, N.L., Toens, P.D. and van der Schyff, D.B., 1964. The geology of the Rietkuil Syncline. In: S.H. Haughton (Editor), *The Geology of Some Ore Deposits in Southern Africa*. geol. Soc. of S. Afr., Johannesburg Vol 1: 393-398.
- Winkler, H.G.F., 1974. *Petrogenesis of Metamorphic Rocks*. 3rd Edition. Springer-Verlag, New York-Berlin, 326 pp.
- Winkler, H.G.F., 1967. *Petrogenesis of Metamorphic Rocks*. 3rd Edition. Springer-Verlag, New York-Berlin, 220 pp.
- Young, R.B., 1907. The alteration of the feldspars in the feldspathic quartzite underlying the Hospital Hill slate. *Trans. geol. Soc. S. Afr.*, 10: 62-64.
- Young, R.B., 1917. *The Banket of the South African Goldfields*. Gurney and Jackson, London.
- Young, R.B., 1944. Stylolitic solution in Witwatersrand quartzites. *Trans. geol. Soc. S. Afr.*, 47: 137-142.

APPENDIX TWO

Computer programme for the correction of crossbedding data (an expanded and updated version of van Eden's (1969) programme).

- Aim :
- (a) to establish a programme which computes the original current direction from crossbedding within dipping strata
 - (b) to process the orientation data at each locality into statistically meaningful parameters
 - (c) to format the output in a simple concise manner.

- Method :
- (a) The problem of correcting primary structure for tilt of the bedding can be solved by using a stereographic net or employing trigonometric formulas. The latter method can be adapted to a computer programme, which makes the whole exercise of correction automatic and effortless. In the field the following parameters are collected and constitute the input data (the alphabetic symbols in brackets represent the input data in the functions shown on computer printout -1).

Input Data : Azimuth bedding (A) - azimuthal direction of dip of the bedding in degrees.

Dip Bedding (B) - angle of dip of the bedding in degrees.

Azimuth X-bedding (C) - azimuthal direction of the foreset of the cross-bedded unit.

Dip X-bedding (D) - angle of dip of the cross-bedded unit.

Procedure : Next a two step rotational procedure involving the rotation of the normal to the bedding plane about the vertical axis into the YZ plane and a rotation of the normal to the bedding plane about the X axis into a vertical position is accomplished. The rotational formulae of van Eden (1969) were modified for fortran language and used on the UCT 1000 Univac Computer. Also inserted in the programme are a few 'ELSE IF' clauses introducing negligible small constants to avoid zero and infinite values.

Output Data: Corrected azimuth X-bedding (E) - 'primary' azimuthal direction of dip of the tilt corrected foreset
Corrected dip X-bedding (F) - original angle of repose of foreset.

- (b) Once (E) and (F) are known the programme computes several calculations for the number of observations in each locality. These calculations include :

$$V = \sum_{i=1}^n n_i \cos X_i$$

$$W = \sum_{i=1}^n n_i \sin X_i$$

$$VM = \arctan W/V$$

$$R = (V^2 + W^2)^{1/2}$$

$$L = (R/n) \cdot 100$$

$$MDip = F/n$$

Where : X is the the mid-point azimuth of the i th class interval or for ungrouped data is the azimuthal angle measured.

VM is the azimuth of the resultant vector

n_i the number of observations in each class

n the total number of observations

R the magnitude or length of the resultant vector

L the magnitude of the resultant vector in terms of per cent ; and

$MDip$ the arithmetic mean corrected dip.

The magnitude of the vector (L) is a measure of the concentration of azimuths, the greater L the greater the concentration. The ratio R/n was called the consistency ratio by Reiche (1938) and embodies the statistical "standard deviation" within circular normal distributions. If the consistency ratio were perfect, the consistency ratio would equal unity, whereas, were there no grouping the resultant vector would be zero, as would the consistency ratio by definition.

- (c) The format of the programme was designed so that it prints out the name of the study area (e.g. West Rand Group paleocurrent analysis-Heidelberg area), the station at which crossbed data were measured (e.g. Government Reef Unit, T14), the input and output data (A,B,C,D,E and F), and the relevant statistics for that station (vector mean azimuth, vectoral magnitude, consistency ratio and arithmetic mean corrected dip). Because of programme specification the input cards were sequenced as follows :

@ E O F

card (1)	STATION LOCALITY
card (2+n)	DATA CARDS

The number of measurements (A,B,C,D) recorded at any one station locality must not exceed 6788 (a most generous restriction !). The format of the card is punched as below :

n A B C D

A THRU A }

J T H U K

[illegible]

Following the last data card, a card with the numbers 6789 punched in its first 4 columns instructs the programme to start processing the next Group of data obtained at a different locality. The format at each station locality is exactly the same as above i.e. starting with a station locality card, followed by data cards and ending with a 6789 card. The last card of the last locality which terminates the input data must not be a 6789 card but rather a card with 9999 punched in its first 4 columns.

Results : Examples of the printouts obtained for both unimodal and bimodal distributions are shown on "computer printout -2".

COMPUTER PRINTOUT 1

IRUN PCSTF,A0216-R101/HHGF,GEOCHEM,S20,20

FTN,CS
FTN BR1

*01/22/80-11:19

```

1.      REAL L
2.      DIMENSION TITLE(20)
3.      SUME=0.
4.      SUMSIN=0.
5.      SUMF=0.
6.      SUMCOS=0.
7.      SUMESQ=0.
8.      PI=3.141592654
9.      NN=0
10.
11.      190 SUMESQ=0.0
12.
13.      SUME=0.0
14.      MEANAZ=0
15.      MDIP=0
16.      SUMF=0.0
17.      SUMCOS=0.0
18.      SUMSIN=0.0
19.      WRITE(5,105)
20.
21.
22.      105 FORMAT(1H1,16X,'WEST RAND GROUP PALAEOCURRENT DIRECTION ANALYSIS-H
23.      *EIDELBERG AREA',///)
24.
25.
26.      READ(8,203)TITLE
27.      WRITE(5,106)TITLE
28.
29.      203 FORMAT(20A4)
30.
31.      106 FORMAT(//,8X,20A4,/)
32.
33.      WRITE(5,100)
34.
35.
36.      100 FORMAT( 9X,'LOCALITY',4X,'AZIMUTH',6X,'DIP',9X,'AZIMUT',6X,
37.      *'DIP',8X,'CORRECTED',2X,'CORRECTED')
38.
39.
40.      WRITE(5,101)
41.
42.
43.      101 FORMAT(10X,'NUMBER',5X,'BEDDING',4X,'BEDDING',6X,'CBEDDING',4X,
44.      *'CBEDDING',6X,'AZIMUTH',6X,'DIP',/)
45.
46.
47.      200 READ(8,201,END=202)N,A,B,C,D
48.
49.      IF(N.EQ.6789)GO TO 202
50.
51.      IF(N.EQ.9999)GO TO 999
52.
53.      N1=N
54.
55.      201 FORMAT(I4,4F3.0)
56.
57.
58.

```

```

59.
60.      NN=NN+1
61.      A=A/57.3
62.      B=B/57.3
63.      C=C/57.3
64.      D=D/57.3
65.      PI6=270./57.3
66.      PI4=90./57.3
67.
68.      X=SIN(D)*SIN(A-C)
69.
70.      IF (D.EQ.PI4) D=D+0.0001
71.
72.      IF (D.EQ.PI6) D=D+0.0001
73.
74.      S=TAN(D)*COS(A-C)
75.
76.      IF (S.EQ.0.) S=0.00000001
77.
78.      W=ATAN(1/S)+B
79.
80.      G=ABS(A-C)
81.
82.      IF ((G.LT.PI6).AND.(G.GT.PI4)) THEN
83.
84.          Y=-SQRT(1-X*X)*COS(W)
85.
86.      ELSE
87.
88.          Y=SQRT(1-X*X)*COS(W)
89.
90.      END IF
91.
92.      GO TO 901
93.
94. 901 Z=SQRT(1-X*X)*SIN(W)
95.
96.      IF (X.EQ.0) X=0.00000001
97.
98.      E=ATAN2(Y,X)+A-PI4
99.
100.     IF (E.LT.0) E=E+(360/57.3)
101.
102.     IF (Z.EQ.0) Z=0.00000001
103.
104.     ZZ=SQRT(1-Z*Z)/Z
105.
106.     F=ABS(ATAN(ZZ))
107.
108.     ALFA=E
109.
110.     SUMCOS=SUMCOS+COS(ALFA)
111.
112.     SUMSIN=SUMSIN+SIN(ALFA)
113.
114.     A=A*57.3
115.     B=B*57.3
116.     C=C*57.3
117.     D=D*57.3
118.     E=E*57.3
119.     F=F*57.3
120.

```

1
1
1
1
1
1
1
1

```

121.
122.
123.      WRITE(5,102)N,A,B,C,D,E,F
124.
125. 102 FORMAT(10X,I4,7X,F7.3,4X,F7.3,7X,F7.3,4X,F7.3,7X,F7.3,4X,F7.3,/)
126.
127.      SUME=SUME+E
128.
129.      SUMF=SUMF+F
130.
131.      SUMESQ=SUMESQ+E**2
132.
133.      GO TO 200
134.
135. 202 CONTINUE
136.
137.      N=N1
138.
139.      V=SUMCOS
140.
141.      W=SUMSIN
142.
143.      VM=ATAN2(W,V)
144.
145.      IF (VM.LE.0) VM=(2*PI)+VM
146.
147.      VMN=VM*57.3
148.
149.      VSQ=V*V
150.
151.      WSQ=W*W
152.
153.      R=SQRT(VSQ+WSQ)
154.
155.      L=(R/N)*100
156.
157.      MDIP=SUMF/N
158.
159.      WRITE(5,104)VMN,R,L,MDIP
160.
161. 104 FORMAT('0',11X,'VECTOR MEAN AZIMUTH='F5.0,///,
162.
163.      *12X,'VECTORAL MAGNITUDE='F5.2,///,
164.
165.      *12X,'CONSISTENCY RATIO='F6.2,///,
166.
167.      *12X,'ARITHMETIC MEAN CORRECTED DIP='I3)
168.
169.      GO TO 190
170.
171. 999 STOP
172.      END
173.
174.
175.

```

ND FTN 273 IBANK 293 DBANK

ENTERING USER PROGRAM

COMPUTER PRINTOUT 2

WEST RAND GROUP PALAEOCURRENT DIRECTION ANALYSIS-HEIDELBERG REA

TR17 JEPPESTOWN-1STQTZ

LOCALITY NUMBER	AZIMUTH BEDDING	DIP BEDDING	AZIMUTH CBEDDING	DIP CBEDDING	CORRECTED AZIMUTH	CORRECTED DIP
1	260.000	29.000	232.000	40.000	192.505	19.064
2	260.000	29.000	235.000	41.000	199.077	18.495
3	260.000	29.000	234.000	32.000	171.340	13.435
4	260.000	29.000	235.000	42.000	201.035	19.269
5	260.000	29.000	229.000	35.000	176.352	17.291
6	260.000	29.000	248.000	43.000	228.228	15.619
7	260.000	29.000	225.000	30.000	157.871	17.057
8	260.000	29.000	235.000	40.000	196.958	17.743
9	260.000	29.000	240.000	44.000	213.086	18.982
10	260.000	29.000	218.000	44.000	182.47	28.426
11	260.000	29.000	212.000	42.000	173.606	29.883
12	260.000	29.000	226.000	32.000	164.814	17.309
13	260.000	29.000	218.000	35.000	166.375	22.616
14	260.000	29.000	218.000	43.000	181.004	27.702
15	260.000	29.000	231.000	46.000	201.478	24.135

VECTOR MEAN AZIMUTH= 187.

VECTORAL MAGNITUDE=14.19

CONSISTENCY RATIO= 94.61

ARITHMETIC MEAN CORRECTED DIP= 20

WEST RAND GROUP PALAEOCURRENT DIRECTION ANALYSIS-HEIDELBERG AREA

TR7-SR3 - BINOMIAL -MODE A

LOCALITY NUMBER	AZIMUTH BEDDING	DIP	AZIMUTH CBEDDING	DIP CBEDDING	CORRECTED AZIMUTH	CORRECTED DIP
1	256.000	26.000	248.000	37.000	231.71	11.746
2	256.000	26.000	250.000	45.000	243.082	19.297
3	256.000	26.000	233.000	42.000	207.074	20.290
4	256.000	26.000	265.000	36.000	264.823	10.997
5	256.000	26.000	245.000	40.000	228.072	15.178
6	256.000	26.000	233.000	46.000	211.963	23.847
7	256.000	26.000	235.000	50.000	216.75	26.970
8	256.000	26.000	235.000	46.000	215.246	23.256
9	256.000	26.000	206.000	35.000	162.393	26.119
10	256.000	26.000	232.000	43.000	206.796	21.493
11	256.000	26.000	235.000	27.000	162.606	9.379
12	256.000	26.000	253.000	46.000	249.709	20.072
13	256.000	26.000	227.000	44.000	200.421	24.093
14	256.000	26.000	238.000	52.000	224.906	28.129
15	256.000	26.000	230.000	34.000	185.815	15.102
16	256.000	26.000	230.000	41.000	200.706	20.475
17	256.000	26.000	220.000	36.000	177.895	20.674
18	256.000	26.000	225.000	45.000	198.815	25.677
19	256.000	26.000	250.000	48.000	244.179	22.271
20	256.000	26.000	220.000	43.000	189.625	25.945
21	256.000	26.000	225.000	35.000	161.664	17.866
22	256.000	26.000	230.000	46.000	243.482	20.287
23	256.000	26.000	230.000	30.000	148.796	25.716
24	256.000	26.000	245.000	39.000	226.772	14.233
25	256.000	26.000	245.000	39.000	226.772	14.233
26	256.000	26.000	255.000	35.000	252.344	9.014
27	256.000	26.000	238.000	49.000	193.997	31.747
28	256.000	26.000	235.000	45.000	214.19	22.342

VECTOR MEAN AZIMUTH= 212.

VECTORAL MAGNITUDE=24.35

CONSISTENCY RATIO= 86.95

ARITHMETIC MEAN CORRECTED DIP= 20

WEST RAND GROUP PALAEOCURRENT DIRECTION ANALYSIS-HEIDELBERG AREA

TR7-GR3 (CONTD.) - MODE B

LOCALITY NUMBER	AZIMUTH BEDDING	DIP BEDDING	AZIMUTH CORRECTED	DIP CORRECTED	CORRECTED AZIMUTH	CORRECTED DIP
1	256.000	26.000	305.000	28.000	3.268	21.780
2	256.000	26.000	325.000	17.000	35.968	25.114
3	256.000	26.000	312.000	17.000	34.313	21.378
4	256.000	26.000	322.000	15.000	40.272	23.890
5	256.000	26.000	300.000	26.000	5.945	18.902
6	256.000	26.000	317.000	34.000	359.744	30.232
7	256.000	26.000	303.000	30.000	357.298	21.895
8	256.000	26.000	345.000	41.000	12.029	46.892
9	256.000	26.000	330.000	25.000	21.751	30.041
10	256.000	26.000	258.000	16.000	72.825	10.024
11	256.000	26.000	302.000	33.000	350.015	23.124
12	256.000	26.000	77.000	15.000	76.393	40.998
13	256.000	26.000	5.000	25.000	38.511	41.044
14	256.000	26.000	315.000	25.000	15.092	24.493
15	256.000	26.000	175.000	10.000	98.83	26.226
16	256.000	26.000	295.000	35.000	339.444	21.305
17	256.000	26.000	305.000	30.000	358.652	22.752
18	256.000	26.000	280.000	40.000	309.719	18.926

VECTOR MEAN AZIMUTH= 20.

VECTORAL MAGNITUDE=14.84

CONSISTENCY RATIO= 82.43

ARITHMETIC MEAN CORRECTED DIP= 26

APPENDIX THREE

ROCK TYPE CODE

- | | |
|-------------------------|-----------------------|
| 1. = West Rand Group | A = shale |
| 2. = Central Rand Group | B = Greywacke |
| 3. = Fig Tree Group | C = Tillite |
| 4. = Mozaan Group | D = Ferruginous shale |
| | E = Sandstone |
| | F = Granitic paleosol |

WEST RAND GROUP SEDIMENTS-HEIDELBERGAREA, EASTERN TRANSVAAL

	PCS-1	PCS-2	PCS-4	PCS-8	PCS-11	PCS-13	PCS-16	PCS-18	PCS-25	PCS-26
* * * MAJOR ELEMENTS * * *										
S102	58.60	60.68	53.49	53.81	57.11	48.36	55.62	51.78	73.04	89.48
T102	1.09	1.02	.65	.54	.50	.35	.65	.59	.34	.11
AL203	23.84	22.41	13.84	12.74	11.07	8.67	14.39	13.47	9.66	5.32
FE203	3.76	5.55	20.40	20.98	19.43	9.52	16.14	21.26	6.67	1.36
FeO	-	-	-	-	-	-	-	-	-	-
MNO	.02	.04	.17	.17	.17	.15	.09	.09	.05	.02
MGO	1.58	2.28	5.79	5.65	5.22	14.11	6.40	6.54	4.32	.97
CAO	.03	.02	.15	.28	.35	6.94	.17	.25	.40	.14
NA2O	.19	.16	.01	.01	.01	.01	.02	.01	1.37	.05
K2O	6.78	5.91	.45	.43	.22	.01	1.64	.59	.64	1.55
P2O5	.01	.02	.09	.07	.09	.01	.09	.11	.01	.01
H2O+	3.93	3.70	3.43	4.58	4.24	10.74	4.65	4.99	2.59	1.09
H2O-	.17	.12	.13	.14	.13	.16	.17	.10	.15	.11
CO2	-	-	-	-	-	-	-	-	-	-
TOTAL	99.90	101.91	98.60	99.40	98.54	99.03	100.03	99.78	99.24	100.21
* * * TRACE ELEMENTS * * *										
CS	-	-	-	-	-	-	-	-	-	-
RB	221.	190.	16.9	20.3	9.81	ND	71.6	26.2	23.5	49.4
BA	-	-	-	-	-	-	-	-	-	-
SR	16.4	13.2	3.72	7.14	.69	221.	25.0	6.55	87.8	7.70
TH	-	-	-	-	-	-	-	-	-	-
U	12.7	1.60	ND	1.00	ND	ND	ND	ND	ND	ND
ZR	190.	170.	154.	132.	126.	32.9	136.	127.	101.	48.4
HF	-	-	-	-	-	-	-	-	-	-
NB	12.0	10.5	8.68	7.39	7.87	ND	7.02	7.63	4.26	ND
CR	1412.	1370.	780.	642.	599.	1971.	670.	683.	462.	78.6
V	276.	227.	142.	127.	123.	140.	148.	144.	62.8	23.0
SC	-	-	-	-	-	-	-	-	-	-
NI	280.	332.	333.	286.	242.	428.	308.	299.	151.	33.5
CO	72.6	48.3	40.3	34.2	30.7	73.6	37.3	39.8	28.8	6.10
GA	27.6	25.8	17.4	16.9	14.7	8.50	16.5	17.0	10.1	5.45
PB	-	-	-	-	-	-	-	-	-	-
ZN	-	-	-	-	-	-	-	-	-	-
CU	-	-	-	-	-	-	-	-	-	-
Y	-	-	-	-	-	-	-	-	-	-
LA	-	-	-	-	-	-	-	-	-	-
CE	-	-	-	-	-	-	-	-	-	-
PR	-	-	-	-	-	-	-	-	-	-
ND	-	-	-	-	-	-	-	-	-	-
SM	-	-	-	-	-	-	-	-	-	-
EU	-	-	-	-	-	-	-	-	-	-
GD	-	-	-	-	-	-	-	-	-	-
TB	-	-	-	-	-	-	-	-	-	-
DY	-	-	-	-	-	-	-	-	-	-
HO	-	-	-	-	-	-	-	-	-	-
ER	-	-	-	-	-	-	-	-	-	-
TM	-	-	-	-	-	-	-	-	-	-
YB	-	-	-	-	-	-	-	-	-	-
87/86	-	-	-	-	-	-	-	-	-	-
I-SR	-	-	-	-	-	-	-	-	-	-

WEST RAND GROUP SEDIMENTS-HEIDELBERGAREA, EASTERN TRANSVAAL

	PCS-1	PCS-2	PCS-4	PCS-8	PCS-11	PCS-13	PCS-16	PCS-18	PCS-25	PCS-26
* * * ELEMENT RATIOS * * *										
ZR/NB	15.8	16.2	17.7	17.8	16.0	-	19.4	16.7	23.7	-
ZR/Y	-	-	-	-	-	-	-	-	-	-
ZR/HF	-	-	-	-	-	-	-	-	-	-
K/RB	254.	258.	221.	176.	186.	-	190.	187.	227.	261.
K/BA	-	-	-	-	-	-	-	-	-	-
K/SR	3.432+003	3.708+003	1.004+003	500.	2.647+003	.375	545.	748.	60.5	1.671+003
K/ZR	296.	289.	24.3	27.1	14.5	2.52	103.	38.5	52.7	266.
K/NB	4.683+003	4.695+003	430.	483.	232.	-	1.939+003	642.	1.247+003	-
K/Y	-	-	-	-	-	-	-	-	-	-
BA/RB	-	-	-	-	-	-	-	-	-	-
BA/SR	-	-	-	-	-	-	-	-	-	-
BA/ZR	-	-	-	-	-	-	-	-	-	-
RB/SR	13.5	14.4	4.54	2.84	14.2	-	2.87	4.00	.267	6.41
NI/CO	3.86	6.87	8.26	8.38	7.86	5.81	8.24	7.44	5.24	4.99
CR/NI	5.03	4.13	2.34	2.24	2.48	4.61	2.18	2.37	3.07	2.58
TI/P	150.	70.1	9.92	10.6	7.63	48.1	9.92	7.37	46.7	15.1
GA/AL	2.188-004	2.180-004	2.376-004	2.507-004	2.518-004	1.852-004	2.436-004	2.378-004	1.935-004	1.936-004
TH/U	-	-	-	-	-	-	-	-	-	-
LA/YB	-	-	-	-	-	-	-	-	-	-
EU/EU*	-	-	-	-	-	-	-	-	-	-
CA/AL	1.698-003	1.204-003	1.462-002	2.965-002	4.266-002	1.08	1.594-002	2.504-002	5.587-002	3.551-002
MG #	115.	116.	125.	126.	126.	104.	117.	122.	110.	109.
* * * C.I.P.W. NORMS * * *										
OZ	29.16	33.73	43.01	43.28	47.93	14.72	39.59	39.49	55.35	81.54
CO	16.16	15.75	13.28	11.92	10.39	-	12.49	12.62	6.01	3.33
OR	40.36	34.92	2.66	2.54	1.30	.06	9.69	3.49	3.78	9.16
PL	1.69	1.35	.24	1.02	1.23	23.67	.42	.61	13.51	1.05
PL-AB	1.61	1.35	.08	.08	.08	.08	.17	.08	11.59	.42
PL-AN	.08	-	.16	.93	1.15	23.58	.26	.52	1.92	.63
LC	-	-	-	-	-	-	-	-	-	-
NE	-	-	-	-	-	-	-	-	-	-
KP	-	-	-	-	-	-	-	-	-	-
NO	-	-	-	-	-	-	-	-	-	-
DI	-	-	-	-	-	7.90	-	-	-	-
DI-NO	-	-	-	-	-	4.24	-	-	-	-
DI-EN	-	-	-	-	-	3.66	-	-	-	-
DI-FS	-	-	-	-	-	-	-	-	-	-
HY	3.94	5.68	14.42	14.07	13.00	31.48	15.94	16.29	10.76	2.42
HY-EN	3.94	5.68	14.42	14.07	13.00	31.48	15.94	16.29	10.76	2.42
HY-FS	-	-	-	-	-	-	-	-	-	-
OL	-	-	-	-	-	-	-	-	-	-
OL-FO	-	-	-	-	-	-	-	-	-	-
OL-FA	-	-	-	-	-	-	-	-	-	-
CS	-	-	-	-	-	-	-	-	-	-
MT	-	-	-	-	-	-	-	-	-	-
IL	.04	.09	.36	.36	.36	.32	.19	.19	.11	.74
AP	.02	.04	.21	.17	.21	.02	.21	.26	.02	.02
CC	-	-	-	-	-	-	-	-	-	-
AN/PL	4.94	-	64.86	91.67	93.14	99.64	60.14	86.04	14.20	59.79
FO/OL	-	-	-	-	-	-	-	-	-	-
D.I.	70.83	70.01	45.76	45.91	49.32	14.86	49.44	43.06	70.73	91.12

WEST RAND GROUP SEDIMENTS-HEIDELBERGAREA,EASTERN TRANSVAAL

	PCS-31	PCS-32	PCS-36	TILL-A	TILL-B	P&R	APGS	P.GR.	01/09	04/13
* * * ELEMENT RATIOS * * *										
ZR/NB	16.1	17.9	20.5	23.7	14.9	26.8	18.6	12.6	23.4	14.1
ZR/Y	-	-	-	-	-	-	-	-	-	-
ZR/HF	-	-	-	-	-	-	-	-	-	-
K/RB	216.	208.	216.	194.	192.	213.	200.	190.	145.	138.
K/BA	-	-	-	-	-	-	-	-	-	-
K/SR	2.094+003	1.025+003	2.675+003	1.949+003	1.155+003	184.	714.	1.655+003	1.567+003	2.385+003
K/ZR	127.	129.	164.	122.	115.	103.	91.2	308.	70.1	193.
K/NB	2.053+003	2.313+003	3.366+003	2.897+003	1.715+003	2.753+003	1.699+003	3.394+003	1.640+003	2.722+003
K/Y	-	-	-	-	-	-	-	-	-	-
BA/RB	-	-	-	-	-	-	-	-	-	-
BA/SR	-	-	-	-	-	-	-	-	-	-
BA/ZR	-	-	-	-	-	-	-	-	-	-
RB/SR	9.68	4.92	12.4	10.0	6.03	.865	3.57	8.72	10.8	17.3
NI/CO	7.81	6.74	7.63	6.96	5.59	6.21	6.94	26.3	8.25	6.52
CR/NI	2.20	2.43	2.27	2.48	3.54	3.35	2.29	.276	2.45	2.70
TI/P	15.1	9.77	8.93	14.4	57.7	14.7	9.46	20.6	1.60	10.4
GA/AL	2.291-004	2.350-004	2.441-004	2.290-004	2.207-004	2.249-004	2.526-004	2.172-004	2.293-004	2.418-004
TH/U	-	-	-	-	-	-	-	-	-	-
LA/YB	-	-	-	-	-	-	-	-	-	-
EU/EU*	-	-	-	-	-	-	-	-	-	-
CA/AL	9.862-003	4.383-002	6.067-002	4.993-003	1.246-003	.582	.126	7.302-004	3.119-003	1.007-003
HG #	113.	116.	114.	133.	130.	105.	117.	107.	125.	133.
* * * C.I.P.A. NORMS * * *										
QZ	37.99	40.17	36.93	59.13	60.55	26.64	33.15	48.44	50.48	46.44
CO	12.76	11.61	10.83	8.62	8.85	.15	10.30	12.69	10.80	10.08
OR	11.94	11.52	16.61	11.88	10.46	11.40	9.16	34.57	11.70	17.85
PL	.41	2.34	2.92	.08	.34	29.63	6.18	1.27	.17	.25
PL-AB	.25	.59	.25	.08	.34	3.13	.17	1.27	.17	.25
PL-AN	.15	1.74	2.67	-	-	26.50	6.01	-	-	-
LC	-	-	-	-	-	-	-	-	-	-
NE	-	-	-	-	-	-	-	-	-	-
KP	-	-	-	-	-	-	-	-	-	-
NO	-	-	-	-	-	-	-	-	-	-
DI	-	-	-	-	-	-	-	-	-	-
DI-NO	-	-	-	-	-	-	-	-	-	-
DI-EN	-	-	-	-	-	-	-	-	-	-
DI-FS	-	-	-	-	-	-	-	-	-	-
HY	16.99	14.22	14.30	6.03	6.48	16.26	16.09	.65	6.02	7.10
HY-EN	16.99	14.22	14.30	6.03	6.48	16.26	16.09	.65	6.02	7.10
HY-FS	-	-	-	-	-	-	-	-	-	-
OL	-	-	-	-	-	-	-	-	-	-
OL-FO	-	-	-	-	-	-	-	-	-	-
OL-FA	-	-	-	-	-	-	-	-	-	-
CS	-	-	-	-	-	-	-	-	-	-
MT	-	-	-	-	-	-	-	-	-	-
IL	.15	.15	.19	.09	.09	.24	.24	.02	.36	.47
AP	.14	.21	.24	.07	.02	.14	.21	.02	.35	.02
CC	-	-	-	-	-	-	-	-	-	-
AN/PL	37.71	74.64	91.32	-	-	89.43	97.26	-	-	-
FO/OL	-	-	-	-	-	-	-	-	-	-
D.I.	50.18	52.28	53.79	71.09	71.35	41.18	42.48	64.26	62.35	64.54

WEST RAND GROUP SEDIMENTS-HEIDELBERG AREA, EASTERN TRANSVAAL

	05/01	09/10	13/11	15/14	16/01	17/01	E-J.S.
* * * MAJOR ELEMENTS * * *							
S102	50.69	65.14	75.88	52.85	59.20	62.99	61.26
T102	.44	.81	.24	.40	.44	.65	-
AL203	11.60	13.17	6.49	11.20	11.53	16.92	17.30
FE203	27.69	8.33	6.64	22.70	19.90	6.11	1.36
FeO	-	-	-	-	-	-	7.98
MNO	.26	.05	.11	.03	.03	.04	-
MGO	2.58	5.36	6.75	2.66	2.83	4.72	1.67
CAO	.01	.01	.41	.35	.03	.01	.84
NA2O	.02	.05	.01	.02	.05	.10	4.79
K2O	2.19	2.01	.02	1.03	1.90	3.30	3.03
P2O5	.05	.09	.01	.01	.02	.01	-
H2O+	3.90	4.06	3.63	5.92	3.96	4.68	2.20
H2O-	.56	.18	.11	2.09	.37	.28	-
CO2	-	-	-	-	-	-	.16
TOTAL	99.99	99.26	100.30	99.26	100.26	99.81	100.59
* * * TRACE ELEMENTS * * *							
CS	-	-	-	-	-	-	-
RB	137.	78.7	50.	62.6	112.	118.	-
BA	-	-	-	-	-	-	-
SR	9.75	22.7	10.3	20.7	11.4	16.7	-
TH	-	-	-	-	-	-	-
U	ND	1.48	.56	ND	ND	ND	-
ZR	115.	240.	368.	57.9	104.	249.	-
HF	-	-	-	-	-	-	-
NB	7.19	6.94	5.00	3.14	7.33	12.0	-
CR	460.	1769.	868.	312.	364.	675.	-
V	108.	140.	93.1	78.5	95.5	149.	-
SC	-	-	-	-	-	-	-
NI	1.94	343.	807.	158.	247.	580.	-
CO	27.5	25.2	44.1	26.5	29.3	34.6	-
GA	16.2	15.0	6.75	15.7	14.7	19.7	-
PB	-	-	-	-	-	-	-
ZN	-	-	-	-	-	-	-
CU	-	-	-	-	-	-	-
Y	-	-	-	-	-	-	-
LA	-	-	-	-	-	-	-
CE	-	-	-	-	-	-	-
PR	-	-	-	-	-	-	-
ND	-	-	-	-	-	-	-
SM	-	-	-	-	-	-	-
EU	-	-	-	-	-	-	-
GD	-	-	-	-	-	-	-
TB	-	-	-	-	-	-	-
DY	-	-	-	-	-	-	-
HO	-	-	-	-	-	-	-
ER	-	-	-	-	-	-	-
TH	-	-	-	-	-	-	-
YB	-	-	-	-	-	-	-
87/86	-	-	-	-	-	-	-
I-SR	-	-	-	-	-	-	-

WEST RAND GROUP SEDIMENTS-HEIDELBERGAREA,EASTERN TRANSVAAL

	05/01	09/10	13/11	15/14	16/01	17/01	E-J.S.
* * * ELEMENT RATIOS * * *							
ZR/NB	15.9	34.6	73.5	18.5	14.3	20.6	-
ZR/Y	-	-	-	-	-	-	-
ZR/HF	-	-	-	-	-	-	-
K/RB	132.	212.	332.	137.	141.	233.	-
K/BA	-	-	-	-	-	-	-
K/SR	1.865+003	735.	16.1	414.	1.390+003	1.640+003	-
K/ZR	159.	69.5	.452	148.	151.	110.	-
K/NB	2.529+003	2.404+003	33.2	2.723+003	2.152+003	2.275+003	-
K/Y	-	-	-	-	-	-	-
BA/RB	-	-	-	-	-	-	-
BA/SR	-	-	-	-	-	-	-
BA/ZR	-	-	-	-	-	-	-
RB/SR	14.1	3.47	4.840-002	3.03	9.86	7.04	-
NI/CO	7.052-002	13.6	18.3	5.97	8.43	16.8	-
CR/NI	237.	5.16	1.07	1.97	1.48	1.16	-
TI/P	12.1	12.4	33.0	54.9	30.2	89.3	-
GA/AL	2.647-004	2.159-004	1.965-004	2.649-004	2.409-004	2.206-004	-
TH/U	-	-	-	-	-	-	-
LA/YB	-	-	-	-	-	-	-
EU/EU*	-	-	-	-	-	-	-
CA/AL	1.163-003	1.025-003	8.524-002	4.217-002	3.511-003	7.975-004	6.552-002
MG	252.	110.	106.	192.	165.	108.	27.8
* * * C.I.P.W. NORMS * * *							
QZ	38.35	49.17	64.83	44.11	47.41	42.74	11.79
CO	9.20	10.91	5.73	9.44	9.38	13.18	4.98
OR	12.94	11.88	.12	6.09	11.23	19.50	17.91
PL	.17	.42	2.05	1.84	.44	.85	43.69
PL-AB	.17	.42	.08	.17	.42	.85	40.53
PL-AN	-	-	1.97	1.67	.02	-	3.16
LC	-	-	-	-	-	-	-
NE	-	-	-	-	-	-	-
KP	-	-	-	-	-	-	-
MO	-	-	-	-	-	-	-
DI	-	-	-	-	-	-	-
DI-WO	-	-	-	-	-	-	-
DI-EN	-	-	-	-	-	-	-
DI-FS	-	-	-	-	-	-	-
HY	6.43	13.35	16.81	6.62	7.05	11.76	17.69
HY-EN	6.43	13.35	16.81	6.62	7.05	11.76	4.16
HY-FS	-	-	-	-	-	-	13.53
OL	-	-	-	-	-	-	-
OL-FO	-	-	-	-	-	-	-
OL-FA	-	-	-	-	-	-	-
CS	-	-	-	-	-	-	-
MT	-	-	-	-	-	-	1.97
IL	.56	.11	.24	.06	.06	.09	-
AP	.02	.02	.02	.02	.05	.02	-
CC	-	-	-	-	-	-	.36
AN/PL	-	-	95.88	90.80	4.12	-	7.22
FO/OL	-	-	-	-	-	-	-
D.I.	51.46	61.47	65.04	50.36	59.06	63.09	70.23

* * * SAMPLE DIRECTORY * * *

SAMPLE #	DATABASE #	ROCK TYPE	LOCALITY	REFERENCE
PCS-1	0	1A	SHALE IN CONTACT WITH MAIN REEF, HEIDELBERG, TVL.	1
PCS-2	0	1A	0.1M BELOW MAIN REEF, HEIDELBERG AREA, EAST TVL.	1
PCS-4	0	1A	7.1M BELOW MAIN REEF, HEIDELBERG AREA, EAST TVL.	1
PCS-8	0	1A	21.4M BELOW MAIN REEF, HEIDELBERG AREA, EAST TVL.	1
PCS-11	0	1A	24.7M BELOW MAIN REEF, HEIDELBERG AREA, EAST TVL.	1
PCS-13	0	1A	30M BELOW MAIN REEF, HEIDELBERG AREA, EAST TVL.	1
PCS-16	0	1A	39M BELOW MAIN REEF, HEIDELBERG AREA, EAST TVL.	1
PCS-18	0	1A	55M BELOW MAIN REEF, HEIDELBERG AREA, EAST TVL.	1
PCS-25	0	1B	430M BELOW MAIN REEF, HEIDELBERG AREA, EAST TVL.	1
PCS-26	0	1E	324M BELOW MAIN REEF, HEIDELBERG AREA, EAST TVL.	1
PCS-31	0	1A	380M BELOW MAIN REEF, HEIDELBERG AREA, EAST TVL.	1
PCS-32	0	1A	180M BELOW MAIN REEF, HEIDELBERG AREA, EAST TVL.	1
PCS-36	0	1A	104M BELOW MAIN REEF, HEIDELBERG AREA, EAST TVL.	1
TILL-A	0	1C	1300M BELOW MAIN REEF, HEIDELBERG AREA, EAST TVL.	1
TILL-B	0	1C	1300M BELOW MAIN REEF, HEIDELBERG AREA, EAST TVL.	1
P#R	0	1A	84M BELOW MAIN REEF, HEIDELBERG AREA, EAST TVL.	1
#PGS	0	1A	480M BELOW MAIN REEF, HEIDELBERG AREA, EAST TVL.	1
P.GR.	0	1F	PALEOSOL OF GRANITE, >260M, EAST TVL, BELOW OGQ.	1
1/09	0	1A	3050M BELOW MAIN REEF, HEIDELBERG AREA, EAST TVL.	1
4/13	0	1A	2200M BELOW MAIN REEF, HEIDELBERG AREA, EAST TVL.	1
5/01	0	1A	1950M BELOW MAIN REEF, HEIDELBERG AREA, EAST TVL.	1
9/10	0	1A	790M BELOW MAIN REEF, HEIDELBERG AREA, EAST TVL.	1
13/11	0	1B	750M BELOW MAIN REEF, HEIDELBERG AREA, EAST TVL.	1
15/14	0	1A	830M BELOW MAIN REEF, HEIDELBERG AREA, EAST TVL.	1
17/01	0	1A	585M BELOW MAIN REEF, HEIDELBERG AREA, EAST TVL.	1
16/01	0	1A	770M BELOW MAIN REEF, HEIDELBERG AREA, EAST TVL.	1
E-J.S.	0	1A	MARIEVALE MINE, 'FAR EAST RAND'	1

27 SAMPLES IN THIS DIRECTORY

REFERENCES

REFERENCE LIST FOR SAMPLE DIRECTORIES

- 1 CAMDEN-SMITH, P.M., 1979. UNPUB. DATA. ANALYSED AT GEOCHEMISTRY DEPT.,
UNIV. CAPE TOWN, CAPE TOWN.
- 10 ELLIS, J., 1947. THE MARIEVALE GRANOPHYRE, A METAMORPHIC ROCK. TRANS.
GEOL. SOC. S. AFR., 50: 121-160.

WEST RAND GROUP SHALES-KLERKSDORP AREA, WESTERN TVL.

	JP1	JP2	JP3	JP4	JP5	JP6	JP7	JP8	JP9	JP10
* * * MAJOR ELEMENTS * * *										
S102	63.42	65.67	67.97	71.20	46.43	57.23	59.85	60.73	56.53	55.87
T102	.60	.65	.38	.44	.39	.73	.64	.62	.45	.96
AL203	12.88	12.93	14.80	11.63	9.79	20.18	16.03	14.42	11.43	15.06
FE203	1.76	1.99	2.53	1.71	7.00	2.30	1.19	.61	10.32	2.60
FeO	4.02	4.17	2.15	3.02	20.00	3.88	6.61	10.04	10.78	11.50
MNO	.01	.01	.01	.01	.14	.01	.01	.01	.01	.01
MGO	5.36	5.72	2.79	3.54	3.81	4.56	5.07	5.25	3.61	4.73
CAO	2.84	1.51	1.41	1.70	1.64	.62	1.16	1.11	.99	.92
NA2O	1.64	1.60	.21	2.56	1.17	1.17	1.13	.50	1.20	.72
K2O	1.52	1.43	3.90	1.28	.41	3.71	2.13	1.53	1.89	1.83
P2O5	.08	.07	.08	.05	.09	.10	.10	.10	.05	.11
H2O+	2.62	3.22	2.79	1.89	5.44	3.97	3.45	3.83	1.84	3.91
H2O-	-	-	-	-	-	-	-	-	-	-
CO2	1.45	.25	.10	.50	.60	.10	.50	.35	.10	.10
TOTAL	98.20	99.19	99.12	99.53	96.91	98.56	97.83	99.10	98.90	98.52

* * * TRACE ELEMENTS * * *

CS	-	-	-	-	-	-	-	-	-	-
RB	-	-	-	-	-	-	-	-	-	-
BA	-	-	-	-	-	-	-	-	-	-
SR	-	-	-	-	-	-	-	-	-	-
TH	10.0	3.00	22.0	7.00	17.0	4.00	ND	7.00	2.00	12.0
U	-	-	-	-	-	-	-	-	-	-
ZR	136.	130.	506.	99.0	137.	158.	130.	127.	111.	168.
HF	-	-	-	-	-	-	-	-	-	-
NB	3.00	1.30	17.0	1.00	1.00	4.00	1.00	5.00	12.0	6.00
CR	876.	1290.	56.0	780.	530.	900.	935.	1125.	478.	710.
V	143.	123.	19.0	89.0	67.0	187.	135.	120.	67.0	123.
SC	16.0	16.0	6.60	12.0	16.0	21.0	18.0	15.0	14.0	17.0
NI	298.	352.	20.0	205.	215.	252.	258.	316.	186.	232.
CO	45.0	43.0	6.40	30.0	21.0	40.0	36.0	32.0	20.0	32.0
GA	14.0	14.0	21.0	11.0	11.0	21.0	19.0	16.0	13.0	17.0
PB	-	-	-	-	-	-	-	-	-	-
ZN	88.0	88.0	104.	61.0	63.0	97.0	98.0	77.0	55.0	90.0
CU	61.0	64.0	10.0	44.0	32.0	60.0	46.0	42.0	41.0	85.0
Y	16.0	18.0	69.0	10.0	6.00	28.0	16.0	15.0	15.0	24.0
LA	-	-	-	-	-	-	-	-	-	-
CE	-	-	-	-	-	-	-	-	-	-
PR	-	-	-	-	-	-	-	-	-	-
ND	-	-	-	-	-	-	-	-	-	-
SM	-	-	-	-	-	-	-	-	-	-
EU	-	-	-	-	-	-	-	-	-	-
GD	-	-	-	-	-	-	-	-	-	-
TB	-	-	-	-	-	-	-	-	-	-
DY	-	-	-	-	-	-	-	-	-	-
HO	-	-	-	-	-	-	-	-	-	-
ER	-	-	-	-	-	-	-	-	-	-
TM	-	-	-	-	-	-	-	-	-	-
YB	-	-	-	-	-	-	-	-	-	-
87/86	-	-	-	-	-	-	-	-	-	-
I-SR	-	-	-	-	-	-	-	-	-	-

WEST RAND GROUP SHALES-KLERKSDORP AREA, WESTERN T.V.L.

	JP1	JP2	JP3	JP4	JP5	JP6	JP7	JP8	JP9	JP10
	* * * ELEMENT RATIOS * * *									
ZR/NB	45.3	130.	29.8	99.0	137.	39.5	130.	21.4	9.25	31.3
ZR/Y	8.50	7.22	7.33	9.90	22.8	5.64	8.13	6.69	7.40	7.83
ZR/HF	-	-	-	-	-	-	-	-	-	-
K/RB	-	-	-	-	-	-	-	-	-	-
K/BA	-	-	-	-	-	-	-	-	-	-
K/SR	-	-	-	-	-	-	-	-	-	-
K/NB	92.8	91.3	64.0	107.	24.8	195.	134.	119.	141.	80.6
K/Y	4.206+003	1.187+004	1.904+003	1.063+004	3.404+003	7.700+003	1.743+004	2.540+003	1.307+003	2.532+003
BA/RB	789.	660.	469.	1.063+003	567.	1.100+003	1.093+003	794.	1.046+003	633.
BA/SR	-	-	-	-	-	-	-	-	-	-
BA/ZR	-	-	-	-	-	-	-	-	-	-
RB/SR	-	-	-	-	-	-	-	-	-	-
NI/CO	-	-	-	-	-	-	-	-	-	-
CR/NI	6.62	8.19	3.13	6.83	10.2	6.30	7.17	9.67	9.30	7.25
T/P	2.94	3.66	2.80	12.1	2.47	3.57	3.62	3.56	2.57	3.06
GA/AL	10.3	12.8	6.52	12.1	5.95	10.0	8.79	8.52	12.4	12.0
TH/U	2.054-004	2.051-004	2.681-004	1.787-004	2.123-004	1.966-004	2.244-004	2.097-004	2.149-004	2.133-004
LA/YB	-	-	-	-	-	-	-	-	-	-
EU/EU*	-	-	-	-	-	-	-	-	-	-
CA/AL	298	158	129	197	226	4.146-002	9.782-002	104	117	6.243-002
MG #	72.0	72.7	73.8	69.8	26.6	70.0	58.6	49.6	41.2	43.5
* * * C.I.P.W. NORMS * * *										
OZ	35.92	37.75	44.57	42.44	15.84	26.82	32.25	35.29	30.31	26.39
CO	6.92	6.72	9.09	4.22	6.05	13.58	11.16	10.97	5.96	10.72
OR	8.99	8.45	23.05	7.56	2.42	21.92	12.41	9.04	11.17	10.81
PL-AB	18.28	18.99	7.62	26.61	13.66	11.69	11.50	4.87	14.11	9.31
PL-AN	13.88	13.54	1.78	21.66	9.90	9.90	9.56	4.23	10.15	6.09
LC	4.40	5.45	5.84	4.95	3.76	1.79	1.94	2.64	3.95	3.21
NE	-	-	-	-	-	-	-	-	-	-
KP	-	-	-	-	-	-	-	-	-	-
#O	-	-	-	-	-	-	-	-	-	-
DI-WO	-	-	-	-	-	-	-	-	-	-
DI-EN	-	-	-	-	-	-	-	-	-	-
DI-FS	-	-	-	-	-	-	-	-	-	-
HY	18.30	19.20	8.20	12.24	40.05	15.39	22.74	30.00	19.78	29.02
HY-EN	13.35	14.25	6.95	8.82	9.49	11.36	12.63	13.08	8.99	11.78
HY-FS	4.96	4.96	1.25	3.42	30.56	4.04	10.12	16.93	10.79	17.24
OL	-	-	-	-	-	-	-	-	-	-
OL-FO	-	-	-	-	-	-	-	-	-	-
OL-FA	-	-	-	-	-	-	-	-	-	-
CS	-	-	-	-	-	-	-	-	-	-
MT	2.55	2.89	3.67	2.48	10.15	3.33	1.73	1.62	14.33	4.06
IL	1.14	1.23	.72	.84	.74	1.39	1.22	1.18	.85	1.82
AP	.19	.17	.19	.12	.21	.24	.24	.24	.12	.26
CC	3.30	.57	.23	1.14	1.36	.23	1.14	.80	.23	.26
AN/PL	24.08	28.71	76.67	18.59	27.50	15.31	16.87	38.43	28.02	34.53
FO/OL	-	-	-	-	-	-	-	-	-	-
D.I.	58.78	59.74	69.40	71.66	29.16	58.64	54.22	48.56	51.64	45.30

.DIR

* * * SAMPLE DIRECTORY * * *

SAMPLE #	DATABASE #	ROCK TYPE	LOCALITY	REFERENCE
JP1	0	1A	AN.AM.CORP.BOREHOLEJY8-NEAR KLERKSDORP, DATUM	2
JP2	0	1A	61M BELOW JP1 JY8BOREHOLE	2
JP3	0	1A	442METRES BELOW JP1-JY8BOREHOLE	2
JP4	0	1A	472METRES BELOW JP1-JY8BOREHOLE	2
JP5	0	1A	854METRES BELOW JP1-JY8BOREHOLE	2
JP6	0	1A	1043METRES BELOW JP1-JY8BOREHOLE	2
JP7	0	1A	1128METRES BELOW JP1-JY8BOREHOLE	2
JP8	0	1A	1211METRES BELOW JP1-JY8BOREHOLE	2
JP9	0	1A	1593METRES BELOW JP1-JY8BOREHOLE	2
JP10	0	1A	1616METRES BELOW JP1-JY8BOREHOLE	2

10 SAMPLES IN THIS DIRECTORY

REFERENCES

REFERENCE LIST FOR SAMPLE DIRECTORIES

- 2A DANCHIN, R.V., 1970. ASPECTS OF THE GEOCHEMISTRY OF SOME SELECTED SOUTH AFRICAN FINE GRAINED SEDIMENTS. UNPUB. PH.D. THESIS, UNIV. CAPE TOWN, CAPE TOWN, 215PP.
- 2B HOFMEYR, P.K., 1971. THE ABUNDANCES AND DISTRIBUTION OF SOME TRACE ELEMENTS IN SOME SELECTED SOUTH AFRICAN SHALES. UNPUB. PH.D. THESIS, UNIV. CAPE TOWN, CAPE TOWN, 218PP.

WEST RAND GROUP SEDIMENTS-MARIEVALE, EASTERN TRANSVAAL.

	UG/01	UG/02	UG/03	UG/04	UG/05	UG/06	UG/07	UG/08	UG/09	UG/10
	* * * MAJOR ELEMENTS * * *									
S102	68.18	71.41	66.30	62.94	75.74	77.47	67.00	94.49	73.25	67.73
T102	.77	.56	.66	.62	.46	.30	1.53	.07	.55	.87
AL203	17.25	12.99	12.98	13.41	10.28	8.64	12.19	3.78	11.39	10.03
FE203	4.55	7.12	11.15	12.51	3.92	3.11	8.18	.69	5.79	8.84
FeO	-	-	-	-	-	-	-	-	-	-
MNO	.04	.05	.09	.11	.08	.10	.07	.01	.04	.07
MGO	1.98	2.63	4.05	5.06	3.58	3.19	3.95	.37	3.80	6.33
CAO	.05	.04	.08	.09	.93	2.10	.03	.02	.07	.60
NA2O	.20	.10	.07	.05	.09	.07	.11	.06	.05	.01
K2O	4.13	2.39	1.56	1.26	1.89	1.61	2.26	1.00	2.34	1.01
P2O5	.06	.03	.06	.06	.05	.03	.04	.01	.05	.10
H2O+	3.26	3.46	3.90	4.37	3.75	4.33	4.79	.80	3.30	4.99
H2O-	.11	.29	.10	.11	.08	.04	.05	.04	.05	.07
CO2	-	-	-	-	-	-	-	-	-	-
TOTAL	100.58	101.07	101.00	100.59	100.85	100.99	100.19	101.34	100.68	100.65
	* * * TRACE ELEMENTS * * *									
CS	-	-	-	-	-	-	-	-	-	-
RB	131.	76.0	51.0	40.0	65.0	54.0	79.0	31.0	83.0	39.0
BA	-	-	-	-	-	-	-	-	-	-
SR	30.0	16.0	11.0	10.0	26.0	37.0	18.0	7.00	9.00	15.0
TH	-	-	-	-	-	-	-	-	-	-
U	-	-	-	-	-	-	-	-	-	-
ZR	122.	115.	132.	140.	212.	105.	1117.	44.0	183.	353.
HF	-	-	-	-	-	-	-	-	-	-
NB	8.00	7.00	9.00	8.00	6.00	3.00	22.0	-	7.00	10.0
CR	1059.	660.	776.	559.	456.	475.	3762.	67.0	1084.	2202.
V	168.	125.	142.	78.0	56.0	48.0	130.	11.0	105.	134.
SC	-	-	-	-	-	-	-	-	-	-
NI	236.	384.	409.	415.	186.	140.	449.	26.0	359.	570.
CO	29.0	54.0	56.0	31.0	30.0	23.0	89.0	6.00	37.0	58.0
GA	-	-	-	-	-	-	-	-	-	-
PB	-	-	-	-	-	-	-	-	-	-
ZN	77.0	100.	139.	144.	77.0	63.0	183.	33.0	101.	134.
CU	46.0	85.0	77.0	64.0	56.0	34.0	180.	9.00	30.0	133.
Y	20.0	17.0	22.0	21.0	15.0	12.0	37.0	5.00	17.0	26.0
LA	-	-	-	-	-	-	-	-	-	-
CE	-	-	-	-	-	-	-	-	-	-
PR	-	-	-	-	-	-	-	-	-	-
ND	-	-	-	-	-	-	-	-	-	-
SM	-	-	-	-	-	-	-	-	-	-
EU	-	-	-	-	-	-	-	-	-	-
GD	-	-	-	-	-	-	-	-	-	-
YB	-	-	-	-	-	-	-	-	-	-
DY	-	-	-	-	-	-	-	-	-	-
HO	-	-	-	-	-	-	-	-	-	-
ER	-	-	-	-	-	-	-	-	-	-
TM	-	-	-	-	-	-	-	-	-	-
YB	-	-	-	-	-	-	-	-	-	-
87/86	-	-	-	-	-	-	-	-	-	-
1-SR	-	-	-	-	-	-	-	-	-	-

WEST RAND GROUP SEDIMENTS-MARIEVALE, EASTERN TRANSVAAL.

	UG/01	UG/02	UG/03	UG/04	UG/05	UG/06	UG/07	UG/08	UG/09	UG/10
* * * ELEMENT RATIOS * * *										
ZR/NB	15.2	16.4	16.5	17.5	35.3	35.0	50.8	-	26.1	35.3
ZR/Y	6.10	6.76	6.00	6.67	14.1	8.75	30.2	8.80	10.8	13.6
ZR/HF	-	-	-	-	-	-	-	-	-	-
K/RB	262.	261.	254.	261.	241.	248.	237.	268.	234.	215.
K/BA	-	-	-	-	-	-	-	-	-	-
K/SR	1.143+003	1.243+003	1.177+003	1.046+003	633.	361.	1.042+003	1.186+003	2.158+003	559.
K/ZR	281.	173.	98.1	74.7	74.0	127.	16.8	139.	106.	23.8
K/NB	4.286+003	2.834+003	1.619+003	1.307+003	2.615+003	4.455+003	853.	-	2.775+003	838.
K/Y	1.714+003	1.167+003	589.	498.	1.046+003	1.114+003	507.	1.660+003	1.143+003	322.
BA/RB	-	-	-	-	-	-	-	-	-	-
BA/SR	-	-	-	-	-	-	-	-	-	-
BA/ZR	-	-	-	-	-	-	-	-	-	-
RB/SR	4.37	4.75	4.64	4.00	2.50	1.46	4.39	4.43	9.22	2.60
NI/CO	8.14	7.11	7.30	13.4	6.20	6.09	5.04	4.33	9.70	9.83
CR/NI	4.49	1.72	1.90	1.35	2.45	3.39	8.38	2.58	3.02	3.86
TI/P	17.6	25.6	15.1	14.2	12.6	13.7	52.5	9.62	15.1	12.0
GA/AL	-	-	-	-	-	-	-	-	-	-
TH/U	-	-	-	-	-	-	-	-	-	-
LA/YB	-	-	-	-	-	-	-	-	-	-
EU/EU*	-	-	-	-	-	-	-	-	-	-
CA/AL	3.911-003	4.155-003	8.316-003	9.056-003	.122	.328	3.323-003	7.139-003	8.292-003	8.072-002
MG #	115.	118.	118.	116.	107.	106.	113.	112.	109.	109.
* * * C.I.P.#. NORMS * * *										
QZ	48.26	57.76	53.88	50.26	60.80	61.73	51.82	89.75	58.33	53.37
CO	12.45	10.24	11.17	11.94	6.52	3.04	9.55	2.59	6.77	8.07
OR	24.41	14.12	9.22	7.45	11.17	9.51	13.35	5.91	13.83	5.97
PL	1.69	.85	.60	.48	5.05	10.81	.93	.54	.44	2.41
PL-AB	1.69	.85	.59	.42	.76	.59	.93	.51	.42	.06
PL-AN	-	.00	.00	.05	4.29	10.22	-	.03	.02	2.32
LC	-	-	-	-	-	-	-	-	-	-
NE	-	-	-	-	-	-	-	-	-	-
KP	-	-	-	-	-	-	-	-	-	-
#0	-	-	-	-	-	-	-	-	-	-
DI	-	-	-	-	-	-	-	-	-	-
DI-#0	-	-	-	-	-	-	-	-	-	-
DI-EN	-	-	-	-	-	-	-	-	-	-
DI-FS	-	-	-	-	-	-	-	-	-	-
HY	4.93	6.55	10.09	12.60	8.92	7.94	9.84	.92	9.46	15.76
HY-EN	4.93	6.55	10.09	12.60	8.92	7.94	9.84	.92	9.46	15.76
HY-FS	-	-	-	-	-	-	-	-	-	-
OL	-	-	-	-	-	-	-	-	-	-
OL-F0	-	-	-	-	-	-	-	-	-	-
OL-FA	-	-	-	-	-	-	-	-	-	-
CS	-	-	-	-	-	-	-	-	-	-
MT	-	-	-	-	-	-	-	-	-	-
IL	.09	.11	.19	.24	.17	.21	.15	.02	.09	.15
AP	.09	.07	.14	.14	.12	.07	.05	.02	.12	.24
CC	-	-	-	-	-	-	-	-	-	-
AN/PL	-	.29	.82	11.41	84.92	94.52	-	6.26	4.64	95.49
F0/OL	-	-	-	-	-	-	-	-	-	-
D.I.	74.36	72.73	63.69	58.13	72.73	71.84	66.11	96.16	72.58	59.42

WEST RAND GROUP SEDIMENTS-MARIEVALE, EASTERN TRANSVAAL.

	UC/01	UC/02	UA/01	UA/02	UA/03	UA/04
* * * MAJOR ELEMENTS * * *						
S102	62.77	60.18	54.87	57.72	63.46	66.50
T102	.70	.72	.66	.60	.66	.51
AL203	14.75	15.37	15.09	13.04	14.70	9.97
FE203	11.50	11.89	21.11	19.08	10.37	5.38
FeO	-	-	-	-	-	-
MNO	.09	.10	.09	.11	.08	.11
MGO	4.50	5.98	3.22	4.42	5.22	5.09
CAO	.11	.06	.29	.04	.15	4.88
NA2O	.09	.08	.04	.02	.08	.06
K2O	1.78	1.73	.74	.29	2.00	1.24
P2O5	.09	.04	.21	.05	.05	.04
H2O+	4.28	4.93	4.39	4.82	4.37	7.36
H2O-	.19	.25	.07	.30	.13	.20
CO2	-	-	-	-	-	-
TOTAL	100.85	101.33	100.78	100.49	101.27	101.34

* * * TRACE ELEMENTS * * *						
CS	-	-	-	-	-	-
RB	58.0	57.0	23.0	11.0	70.0	44.0
BA	-	-	-	-	-	-
SR	15.0	13.0	9.00	5.00	16.0	48.0
TH	-	-	-	-	-	-
U	-	-	-	-	-	-
ZR	133.	90.0	143.	128.	151.	152.
HF	-	-	-	-	-	-
NB	9.00	9.00	10.0	9.00	8.00	6.00
CR	998.	933.	824.	769.	804.	853.
V	159.	173.	173.	129.	137.	88.0
SC	-	-	-	-	-	-
NI	363.	391.	304.	313.	294.	279.
CO	46.0	47.0	54.0	47.0	43.0	39.0
GA	-	-	-	-	-	-
PB	-	-	-	-	-	-
ZN	122.	142.	122.	117.	87.0	87.0
CU	49.0	35.0	47.0	38.0	57.0	66.0
Y	18.0	18.0	29.0	18.0	19.0	18.0
LA	-	-	-	-	-	-
CE	-	-	-	-	-	-
PR	-	-	-	-	-	-
ND	-	-	-	-	-	-
SM	-	-	-	-	-	-
EU	-	-	-	-	-	-
GD	-	-	-	-	-	-
TB	-	-	-	-	-	-
DY	-	-	-	-	-	-
HO	-	-	-	-	-	-
ER	-	-	-	-	-	-
TM	-	-	-	-	-	-
YB	-	-	-	-	-	-
87/86	-	-	-	-	-	-
1-SR	-	-	-	-	-	-

WEST RAND GROUP SEDIMENTS-MARIEVALE, EASTERN TRANSVAAL.

	UC/D1	UC/D2	UA/D1	UA/D2	UA/D3	UA/D4
* * * ELEMENT RATIOS * * *						
ZR/NB	14.8	10.0	14.3	14.2	18.9	25.3
ZR/Y	7.39	5.00	4.93	7.11	7.95	8.44
ZR/HF	-	-	-	-	-	-
K/RB	255.	252.	267.	219.	237.	234.
K/BA	-	-	-	-	-	-
K/SR	985.	1.105+003	683.	481.	1.038+003	214.
K/ZR	111.	160.	43.0	18.8	110.	67.7
K/NB	1.642+003	1.596+003	614.	267.	2.075+003	1.716+003
K/Y	821.	798.	212.	134.	874.	572.
BA/RB	-	-	-	-	-	-
BA/SR	-	-	-	-	-	-
BA/ZR	-	-	-	-	-	-
RB/SR	3.87	4.38	2.56	2.20	4.38	.917
NI/CO	7.89	8.32	5.63	6.66	6.84	7.15
CR/NI	2.75	2.39	2.71	2.46	2.73	3.06
TI/P	10.7	24.7	4.32	16.5	18.1	17.5
GA/AL	-	-	-	-	-	-
TH/U	-	-	-	-	-	-
LA/YB	-	-	-	-	-	-
EU/EU*	-	-	-	-	-	-
CA/AL	1.006-002	5.267-003	2.593-002	4.139-003	1.377-002	.660
MG H	117.	113.	158.	132.	113.	106.

* * * C.I.P.W. NORMS * * *						
QZ	48.73	44.17	46.98	49.91	47.38	43.62
CO	12.68	13.35	14.20	12.69	12.25	-
OR	10.52	10.22	4.37	1.71	11.82	7.33
PL	.76	.71	.41	.17	1.09	23.78
PL-AB	.76	.68	.34	.17	.68	.51
PL-AN	-	.04	.07	-	.42	23.27
LC	-	-	-	-	-	-
NE	-	-	-	-	-	-
KP	-	-	-	-	-	-
WO	-	-	-	-	-	-
DI	-	-	-	-	-	-
DI-WO	-	-	-	-	-	-
DI-EN	-	-	-	-	-	-
DI-FS	-	-	-	-	-	-
HY	11.21	14.89	8.02	11.01	13.00	12.68
HY-EN	11.21	14.89	8.02	11.01	13.00	12.68
HY-FS	-	-	-	-	-	-
OL	-	-	-	-	-	-
OL-FO	-	-	-	-	-	-
OL-FA	-	-	-	-	-	-
CS	-	-	-	-	-	-
MT	-	-	-	-	-	-
IL	.19	.21	.19	.24	.17	.24
AP	.20	.09	.50	.07	.12	.09
CC	-	-	-	-	-	-
AN/PL	-	5.09	16.46	-	38.15	97.87
FO/OL	-	-	-	-	-	-
D-I.	60.01	55.07	51.69	51.79	59.88	51.46

.DIR

* * * SAMPLE DIRECTORY * * *

SAMPLE #	DATABASE #	ROCK TYPE	LOCALITY	REFERENCE
UG/01	0	A	0.05M BELOW BASE OF M.R.Q.	11
UG/02	0	A	0.34M BELOW BASE OF M.R.Q.	11
UG/03	0	A	3.39M BELOW BASE OF M.R.Q.	11
UG/04	0	A	7.69M BELOW BASE OF M.R.Q.	11
UG/05	0	A	14.2M BELOW BASE OF M.R.Q.	11
UG/06	0	A	14.9M BELOW BASE OF M.R.Q.	11
UG/07	0	A	26.6M BELOW BASE OF M.R.Q.	11
UG/08	0	A	26.9M BELOW BASE OF M.R.Q.	11
UG/09	0	A	27.6M BELOW BASE OF M.R.Q.	11
UG/10	0	A	28.5M BELOW BASE OF M.R.Q.	11
UC/01	0	A	0.85M BELOW BASE OF M.R.Q.	11
UC/02	0	A	4.98M BELOW BASE OF M.R.Q.	11
UA/01	0	A	0.00M BELOW BASE OF M.R.Q.	11
UA/02	0	A	2.00M BELOW BASE OF M.R.Q.	11
UA/03	0	A	8.10M BELOW BASE OF M.R.Q.	11
UA/04	0	A	15.3M BELOW BASE OF M.R.Q.	11

16 SAMPLES IN THIS DIRECTORY

REFERENCES

REFERENCE LIST FOR SAMPLE DIRECTORIES

11

SPRAGUE, A. R. G., 1979, UNPUB. DATA. ANALYSED AT GEOCHEM. DEPT.,
UNIV. CAPE TOWN.

CENTRAL RAND GROUP

	UR1140	439-2	439-3	615-7	615-8	615-9	730-4	730-5	730-6	V56-56
* * * MAJOR ELEMENTS * * *										
SI02	59.89	50.87	54.18	57.00	54.24	55.13	50.87	51.09	54.09	53.98
TI02	.55	.63	.60	.81	.92	.85	.72	.75	.95	.71
AL203	13.57	17.81	18.52	19.86	22.57	21.37	19.22	18.94	22.99	19.00
FE203	9.77	12.85	9.86	7.54	6.41	7.13	11.37	10.67	6.39	6.81
FeO	-	-	-	-	-	-	-	-	-	-
MnO	.16	.14	.12	.04	.03	.03	.06	.08	.03	.08
MgO	7.05	7.64	6.58	5.45	4.62	4.97	7.43	7.75	4.83	9.08
CaO	.84	.10	.09	.14	.21	.13	.11	.12	.09	.56
Na2O	.09	.09	.17	.49	.63	.53	.17	.14	.33	.50
K2O	.88	1.30	2.08	2.51	3.46	3.01	1.87	1.70	4.11	2.83
P2O5	.06	.09	.10	.09	.14	.09	.08	.08	.07	.07
H2O+	5.84	7.64	6.65	5.99	5.86	6.10	7.48	7.33	5.89	6.58
H2O-	.17	.30	.34	.14	.20	.24	.36	.22	.23	.12
CO2	.72	.29	.22	.24	.29	.26	.26	.24	.20	.24
TOTAL	99.69	99.75	99.51	100.30	99.68	99.84	100.00	99.31	100.20	100.56

* * * TRACE ELEMENTS * * *

CS	-	-	-	-	-	-	-	-	-	-
RB	32.5	49.8	77.6	98.7	98.0	116.	67.5	63.6	145.	112.
BA	278.	258.	408.	399.	505.	473.	298.	299.	579.	552.
SR	17.4	20.8	33.4	75.8	95.0	83.8	28.2	26.2	44.6	36.8
TH	5.91	3.05	5.17	6.29	4.94	7.11	4.50	4.93	8.14	6.84
U	-	-	-	-	-	-	-	-	-	-
ZR	134.	107.	94.6	153.	139.	143.	114.	121.	145.	129.
HF	-	-	-	-	-	-	-	-	-	-
NB	4.50	5.30	7.20	92.0	9.80	7.00	6.70	9.20	11.0	8.40
CR	1117.	1161.	1164.	1215.	1170.	1161.	1178.	1124.	1324.	970.
V	121.	189.	179.	191.	228.	201.	192.	193.	223.	168.
SC	23.0	28.0	28.0	30.0	36.0	32.0	28.0	29.0	35.0	27.0
NI	507.	570.	572.	558.	610.	561.	629.	563.	570.	466.
CO	66.9	49.2	56.1	73.4	83.8	75.2	74.2	46.8	75.1	66.2
GA	-	-	-	-	-	-	-	-	-	-
PB	-	-	-	-	-	-	-	-	-	-
ZN	140.	120.	96.0	84.0	84.0	77.0	124.	121.	111.	116.
CU	32.0	48.8	42.9	57.1	124.	45.0	53.2	45.7	84.2	40
Y	12.1	20.9	21.3	24.5	30.0	25.2	22.1	22.5	30.0	11.7
LA	-	-	-	-	-	-	-	-	-	-
CE	-	-	-	-	-	-	-	-	-	-
PR	-	-	-	-	-	-	-	-	-	-
ND	-	-	-	-	-	-	-	-	-	-
SM	-	-	-	-	-	-	-	-	-	-
EU	-	-	-	-	-	-	-	-	-	-
GD	-	-	-	-	-	-	-	-	-	-
TB	-	-	-	-	-	-	-	-	-	-
DY	-	-	-	-	-	-	-	-	-	-
HO	-	-	-	-	-	-	-	-	-	-
ER	-	-	-	-	-	-	-	-	-	-
TM	-	-	-	-	-	-	-	-	-	-
YB	-	-	-	-	-	-	-	-	-	-
87/86	-	-	-	-	-	-	-	-	-	-
I-SR	-	-	-	-	-	-	-	-	-	-

CENTRAL RAND GROUP

	UR1140	439-2	439-3	615-7	615-8	615-9	730-4	730-5	730-6	V56-58
* * * ELEMENT RATIOS * * *										
ZR/NB	29.9	20.1	13.1	1.66	14.2	20.4	17.0	13.1	13.2	15.4
ZR/Y	11.1	5.10	4.44	6.24	4.64	5.66	5.16	5.37	4.83	11.0
ZR/HF	-	-	-	-	-	-	-	-	-	-
K/RB	225.	217.	223.	211.	293.	216.	230.	222.	235.	209.
K/BA	26.3	41.8	42.3	52.2	56.9	52.8	52.1	47.2	58.9	42.6
K/SR	420.	519.	517.	275.	302.	298.	550.	539.	765.	636.
K/ZR	54.4	101.	183.	136.	206.	175.	136.	117.	235.	182.
K/NB	1.623+003	2.036+003	2.398+003	226.	2.931+003	3.570+003	2.317+003	1.534+003	3.102+003	2.797+003
K/Y	604.	516.	811.	850.	957.	992.	702.	627.	1.137+003	2.006+003
BA/RB	8.55	5.18	5.26	4.04	5.15	4.09	4.41	4.70	3.98	4.92
BA/SR	16.0	12.4	12.2	5.26	5.32	5.64	10.6	11.4	13.0	15.0
BA/ZR	2.07	2.42	4.31	2.61	3.63	3.31	2.61	2.48	4.00	4.27
RB/SR	1.87	2.39	2.32	1.30	1.03	1.38	2.39	2.43	3.26	3.05
NI/CO	7.58	11.6	10.2	7.60	7.28	7.46	8.48	12.0	7.59	7.04
CR/NI	2.20	2.04	2.03	2.18	1.92	2.07	1.87	2.00	2.32	2.08
TI/P	12.6	9.62	8.24	12.4	9.03	13.0	12.4	12.9	18.6	13.9
GA/AL	-	-	-	-	-	-	-	-	-	-
TH/U	-	-	-	-	-	-	-	-	-	-
LA/YB	-	-	-	-	-	-	-	-	-	-
EU/EU*	-	-	-	-	-	-	-	-	-	-
CA/AL	8.291-002	7.576-003	6.557-003	9.512-003	1.250-002	8.208-003	7.722-003	8.549-003	5.282-003	3.977-002
MG *	108.	110.	109.	108.	108.	109.	109.	109.	108.	104.
* * * C.I.P.N. NORMS * * *										
QZ	45.49	33.98	35.42	36.42	30.45	33.12	31.65	32.22	29.24	26.36
CO	12.57	16.25	15.99	16.34	17.89	17.24	16.92	16.87	18.00	14.82
OR	5.20	7.68	12.29	14.83	20.45	17.79	11.05	10.05	24.29	16.72
PL	.76	.76	1.44	4.15	5.33	4.48	1.44	1.18	2.79	5.03
PL-AB	.76	.76	1.44	4.15	5.33	4.48	1.44	1.18	2.79	4.23
PL-AN	-	-	-	-	-	-	-	-	-	.80
LC	-	-	-	-	-	-	-	-	-	-
NE	-	-	-	-	-	-	-	-	-	-
KP	-	-	-	-	-	-	-	-	-	-
WO	-	-	-	-	-	-	-	-	-	-
DI	-	-	-	-	-	-	-	-	-	-
DI-WO	-	-	-	-	-	-	-	-	-	-
DI-EN	-	-	-	-	-	-	-	-	-	-
DI-FS	-	-	-	-	-	-	-	-	-	-
HY	17.56	19.03	16.39	13.57	11.51	12.38	18.50	19.30	12.03	22.61
HY-EN	17.56	19.03	16.39	13.57	11.51	12.38	18.50	19.30	12.03	22.61
HY-FS	-	-	-	-	-	-	-	-	-	-
OL	-	-	-	-	-	-	-	-	-	-
OL-FO	-	-	-	-	-	-	-	-	-	-
OL-FA	-	-	-	-	-	-	-	-	-	-
CS	-	-	-	-	-	-	-	-	-	-
MT	-	-	-	-	-	-	-	-	-	-
IL	.34	.30	.26	.09	.06	.06	.13	.17	.06	.17
AP	.14	.18	.16	.21	.33	.21	.19	.19	.16	.17
CC	1.36	-	-	.04	.05	.02	.01	.03	-	.55
AN/PL	-	-	-	-	-	-	-	-	-	15.96
FO/OL	-	-	-	-	-	-	-	-	-	-
D.I.	51.45	42.43	49.15	55.40	56.23	55.39	44.14	43.45	56.32	47.31

CENTRAL RAND GROUP

	GV2-28	UC-760	AOF-1	KAMT-1	KAMT-2	KAMT-7	KAMT-8	E-MQ
* * * MAJOR ELEMENTS * * *								
S102	52.59	49.47	50.31	53.90	53.10	52.40	53.70	90.49
T102	.59	.79	.52	.01	.01	.01	.01	-
AL203	15.84	19.03	18.52	20.10	21.60	20.70	23.10	4.95
FE203	14.18	12.19	8.15	11.70	12.50	8.70	8.50	.17
FeO	-	-	-	-	-	-	-	.17
MnO	.23	.12	.10	.01	.01	.01	.01	-
MgO	7.27	8.08	11.76	7.70	6.50	8.80	6.50	.38
CaO	.12	.15	.70	.50	.50	.50	.50	.89
Na2O	.03	.25	.33	.09	.12	.16	.25	1.13
K2O	.67	1.12	2.15	1.77	1.66	1.24	1.57	1.25
P2O5	.09	.07	.11	.01	.01	.01	.01	-
H2O+	7.31	7.62	6.72	5.00	5.20	6.10	5.60	.58
H2O-	.21	.25	.14	-	-	-	-	-
CO2	.28	.25	.01	.01	.01	.01	.01	.32
TOTAL	99.41	99.39	99.52	100.80	101.22	98.64	99.76	100.33

* * * TRACE ELEMENTS * * *

CS	-	-	-	-	-	-	-	-
RB	24.9	48.0	-	-	-	-	-	-
BA	205.	317.	-	-	-	-	-	-
SR	91.0	65.9	-	-	-	-	-	-
TH	3.05	8.04	-	-	-	-	-	-
U	-	-	-	-	-	-	-	-
ZR	105.	108.	-	-	-	-	-	-
HF	-	-	-	-	-	-	-	-
NB	7.20	7.20	-	-	-	-	-	-
CR	1219.	1154.	-	-	-	-	-	-
V	170.	196.	-	-	-	-	-	-
SC	25.0	30.0	-	-	-	-	-	-
NI	654.	681.	-	-	-	-	-	-
CO	62.3	62.7	-	-	-	-	-	-
GA	-	-	-	-	-	-	-	-
PB	-	-	-	-	-	-	-	-
ZN	172.	177.	-	-	-	-	-	-
CU	38.7	9.70	-	-	-	-	-	-
Y	20.3	22.5	-	-	-	-	-	-
LA	-	-	-	-	-	-	-	-
CE	-	-	-	-	-	-	-	-
PR	-	-	-	-	-	-	-	-
ND	-	-	-	-	-	-	-	-
SM	-	-	-	-	-	-	-	-
EU	-	-	-	-	-	-	-	-
GD	-	-	-	-	-	-	-	-
TB	-	-	-	-	-	-	-	-
DY	-	-	-	-	-	-	-	-
HO	-	-	-	-	-	-	-	-
ER	-	-	-	-	-	-	-	-
TM	-	-	-	-	-	-	-	-
YB	-	-	-	-	-	-	-	-
87/86	-	-	-	-	-	-	-	-
I-SR	-	-	-	-	-	-	-	-

CENTRAL RAND GROUP

	GV2-28	UC-76D	ADF-1	KAMT-1	KAMT-2	KAMT-7	KAMT-9	E-MQ
* * * ELEMENT RATIOS * * *								
ZR/NB	14.5	15.0	-	-	-	-	-	-
ZR/Y	5.16	4.79	-	-	-	-	-	-
ZR/HF	-	-	-	-	-	-	-	-
K/RB	223.	194.	-	-	-	-	-	-
K/BA	27.1	29.3	-	-	-	-	-	-
K/SR	61.1	141.	-	-	-	-	-	-
K/ZR	53.1	86.3	-	-	-	-	-	-
K/NB	773.	1.291+003	-	-	-	-	-	-
K/Y	274.	413.	-	-	-	-	-	-
BA/RB	8.23	6.60	-	-	-	-	-	-
BA/SR	2.25	4.81	-	-	-	-	-	-
BA/ZR	1.96	2.94	-	-	-	-	-	-
RB/SR	.274	.728	-	-	-	-	-	-
NI/CO	10.5	10.9	-	-	-	-	-	-
CR/NI	1.86	1.69	-	-	-	-	-	-
TI/P	9.01	15.5	6.49	1.37	1.37	1.37	1.37	-
GA/AL	-	-	-	-	-	-	-	-
TH/U	-	-	-	-	-	-	-	-
LA/YB	-	-	-	-	-	-	-	-
EU/EU*	-	-	-	-	-	-	-	-
CA/AL	1.022-002	1.064-002	5.100-002	3.356-002	3.123-002	3.259-002	2.921-002	.243
MG #	112.	109.	104.	109.	112.	106.	108.	82.5

* * * C.I.P.W. NORMS * * *								
QZ	39.02	31.69	21.47	34.11	35.35	32.59	35.53	77.46
CO	15.07	17.41	14.66	17.17	18.74	18.23	20.13	.86
OR	3.96	6.62	12.70	10.46	9.81	7.33	9.28	7.39
PL	.25	2.12	5.48	3.11	3.37	3.71	4.47	11.95
PL-AB	.25	2.12	2.79	.76	1.02	1.35	2.12	9.56
PL-AN	-	-	2.69	2.35	2.35	2.35	2.35	2.39
LC	-	-	-	-	-	-	-	-
NE	-	-	-	-	-	-	-	-
KP	-	-	-	-	-	-	-	-
NO	-	-	-	-	-	-	-	-
DI	-	-	-	-	-	-	-	-
DI-NO	-	-	-	-	-	-	-	-
DI-EN	-	-	-	-	-	-	-	-
DI-FS	-	-	-	-	-	-	-	-
HY	18.11	20.12	29.29	19.18	16.19	21.92	16.19	1.12
HY-EN	18.11	20.12	29.29	19.18	16.19	21.92	16.19	.95
HY-FS	-	-	-	-	-	-	-	.17
OL	-	-	-	-	-	-	-	-
OL-FO	-	-	-	-	-	-	-	-
OL-FA	-	-	-	-	-	-	-	-
CS	-	-	-	-	-	-	-	-
MT	-	-	-	.00	.00	.00	.00	.25
IL	.49	.26	.21	.02	.02	.02	.02	-
AP	.21	.17	.26	.02	.02	.02	.02	-
CC	.00	.10	.02	.02	.02	.02	.02	.73
AN/PL	-	-	49.07	75.54	69.85	63.47	52.65	20.01
FO/OL	-	-	-	-	-	-	-	-
D.I.	43.23	40.42	36.97	45.33	46.17	41.27	46.93	94.40

.DIR

*** SAMPLE DIRECTORY ***

SAMPLE #	DATABASE #	ROCK TYPE	LOCALITY	REFERENCE
UR1140	0	2A	MARIEVALE CONS. MINES LTD., NIGEL DISTRICT	3
439-2	0	2A	BH.439, LESLIE GOLD MINE, EVANDER AREA	3
439-3	0	2A	BH.439, LESLIE GOLD MINE, EVANDER AREA	3
615-7	0	2A	BH.615, FARM TWISTORAAI, EVANDER AREA.	3
615-8	0	2A	BH.615, FARM TWISTDRAAI, EVANDER AREA.	3
615-9	0	2A	BH.615, FARM TWISTDRAAI, EVANDER AREA.	3
730-4	0	2A	BH.730, KINROSS, EVANDER AREA.	3
730-5	0	2A	BH.730, KINROSS, EVANDER AREA.	3
730-6	0	2A	BH.730, KINROSS, EVANDER AREA.	3
V56-58	0	2A	BH.V56, VAN DYK PROP. MINES LTD., EAST RAND.	3
GV2-28	0	2A	GROOTVLEI GOLD MINING CO., EAST RAND.	3
UC-760	0	2A	MARIEVALE CONS. MINES LTD., NIGEL DISTRICT.	3
ADF-1	0	2A	FARM WITHOK, SPRINGS DISTRICT, EAST RAND.	4
KAMT-1	0	2A	LESLIE GOLD MINE-BH.258, EVANDER GOLDFIELD.	5
KAMT-2	0	2A	LESLIE GOLD MINE-BH.208, EVANDER GOLDFIELD.	5
KAMT-7	0	2A	LESLIE GOLD MINE, EAST DRIVE, EVANDER GOLDFIELD.	5
KAMT-8	0	2A	LESLIE GOLD MINE, EAST DRIVE, EVANDER GOLDFIELD.	5
E-MQ	0	2E	MARIEVALE MINE, FAR EAST RAND	10

18 SAMPLES IN THIS DIRECTORY

REFERENCES

REFERENCE LIST FOR SAMPLE DIRECTORIES

- 3 FULLER, A.D., 1978 AND 1979. UNPUB. DATA. ANALYSED AT GEOCHEMISTRY DEPT.,
UNIV. CAPE TOWN, CAPE TOWN.
- 4 FULLER, A.D., 1958. A CONTRIBUTION TO THE PETROLOGY OF THE WITWATERS-
RAND SYSTEM. TRANS. GEOL. SOC. S. AFR., 61: 235-256.
- 5 TWEEDIE, K.A.M., 1968. THE STRATIGRAPHY AND SEDIMENTARY STRUCTURES OF
KIMBERLY SHALES IN THE EVANDER GOLDFIELD, EASTERN TRANSVAAL, SOUTH
AFRICA. TRANS. GEOL. SOC. S. AFR., 71: 235-256.
- 10 ELLIS, J., 1947. THE MARIEVALE GRANOPHYRE, A METAMORPHIC ROCK. TRANS.
GEOL. SOC. S. AFR., 50: 121-160.

FIG TREE GROUP-SHEBA FORMATION

	C-3	C-5	V-1	V-2	K-1	C-4	C-6	C-7	C-8	C-9
* * * MAJOR ELEMENTS * * *										
SI02	56.00	63.70	54.11	63.32	63.88	65.10	66.00	63.80	72.00	70.60
TI02	.46	.72	1.00	.59	.59	.50	.45	.56	.60	.54
AL203	10.30	12.30	17.54	10.79	10.97	9.48	11.50	10.50	9.34	10.30
FE203	14.40	11.00	8.88	6.96	6.67	7.88	6.26	7.74	6.82	8.55
FeO	-	-	-	-	-	-	-	-	-	-
MNO	.16	.04	.06	-	-	.14	.10	.07	.07	.07
MGO	-	.13	-	5.67	5.50	3.35	-	-	.80	-
CAO	2.17	.81	.22	1.95	1.70	3.18	2.05	1.51	1.22	1.67
NA2O	.28	1.70	2.14	2.09	1.27	1.78	2.80	1.30	1.54	1.71
K2O	.72	-	2.72	1.44	1.63	1.35	.90	1.81	-	.97
P2O5	-	-	-	-	-	-	-	-	-	-
H2O+	-	-	-	-	-	-	-	-	-	-
H2O-	-	-	-	-	-	-	-	-	-	-
CO2	-	-	-	-	-	-	-	-	-	-
TOTAL	84.49	90.40	86.67	92.81	92.21	92.76	90.06	87.29	92.39	94.41
* * * TRACE ELEMENTS * * *										
CS	-	-	-	-	-	-	-	-	-	-
RB	28.0	83.0	-	-	-	53.0	46.0	73.0	73.0	36.0
BA	516.	316.	-	-	-	408.	156.	296.	331.	243.
SR	85.0	16.0	-	-	-	142.	129.	81.0	41.0	80.0
TH	-	-	-	-	-	-	-	-	-	-
U	-	-	-	-	-	-	-	-	-	-
ZR	34.0	112.	-	-	-	113.	140.	150.	166.	123.
HF	-	-	-	-	-	-	-	-	-	-
NB	-	-	-	-	-	-	-	-	-	-
CR	-	-	-	-	-	-	-	-	-	-
V	-	-	-	-	-	-	-	-	-	-
SC	28.0	21.0	-	-	-	13.0	10.0	14.0	13.0	13.0
NI	958.	400.	-	-	-	264.	232.	362.	280.	291.
CO	-	-	-	-	-	-	-	-	-	-
GA	-	-	-	-	-	-	-	-	-	-
PB	-	-	-	-	-	-	-	-	-	-
ZN	-	-	-	-	-	-	-	-	-	-
CU	-	-	-	-	-	-	-	-	-	-
Y	-	-	-	-	-	-	-	-	-	-
LA	-	-	-	-	-	-	-	-	-	-
CE	-	-	-	-	-	-	-	-	-	-
PR	-	-	-	-	-	-	-	-	-	-
ND	-	-	-	-	-	-	-	-	-	-
SM	-	-	-	-	-	-	-	-	-	-
EU	-	-	-	-	-	-	-	-	-	-
GD	-	-	-	-	-	-	-	-	-	-
TB	-	-	-	-	-	-	-	-	-	-
DY	-	-	-	-	-	-	-	-	-	-
HO	-	-	-	-	-	-	-	-	-	-
ER	-	-	-	-	-	-	-	-	-	-
TM	-	-	-	-	-	-	-	-	-	-
YB	-	-	-	-	-	-	-	-	-	-
87/86	-	-	-	-	-	-	-	-	-	-
I-SR	-	-	-	-	-	-	-	-	-	-

FIG TREE GROUP-SHEBA FORMATION

	C-3	C-5	V-1	V-2	K-1	C-4	C-6	C-7	C-8	C-9
* * * ELEMENT RATIOS * * *										
ZR/NB	-	-	-	-	-	-	-	-	-	-
ZR/Y	-	-	-	-	-	-	-	-	-	-
ZR/HF	-	-	-	-	-	-	-	-	-	-
K/RB	213.	-	-	-	-	211.	162.	215.	-	224.
K/BA	11.6	-	-	-	-	27.5	47.9	52.5	-	33.1
K/SR	70.3	-	-	-	-	78.9	57.9	136.	-	101.
K/ZR	176.	-	-	-	-	99.2	53.4	100.	-	65.5
K/NB	-	-	-	-	-	-	-	-	-	-
K/Y	-	-	-	-	-	-	-	-	-	-
BA/RB	18.4	3.81	-	-	-	7.70	3.39	4.09	4.53	6.75
BA/SR	19.7	19.7	-	-	-	2.87	1.21	3.53	8.07	3.04
BA/ZR	15.2	2.82	-	-	-	3.61	1.11	1.91	1.99	1.98
RB/SR	.329	5.19	-	-	-	.373	.357	.864	1.78	.450
NI/CO	-	-	-	-	-	-	-	-	-	-
CR/NI	-	-	-	-	-	-	-	-	-	-
TI/P	-	-	-	-	-	-	-	-	-	-
GA/AL	-	-	-	-	-	-	-	-	-	-
TH/U	-	-	-	-	-	-	-	-	-	-
LA/YB	-	-	-	-	-	-	-	-	-	-
EU/EU*	-	-	-	-	-	-	-	-	-	-
CA/AL	.284	8.886-002	1.692-002	.244	.209	.453	.241	.194	.176	.219
HG #	-	-	-	107.	107.	115.	-	-	192.	-

* * * C.I.P.A. NORMS * * *										
QZ	46.97	51.88	30.78	33.02	38.41	38.18	41.88	46.08	59.24	53.36
CO	5.11	8.03	10.68	2.25	4.03	-	2.19	3.66	4.59	3.40
OR	4.25	-	16.07	8.51	9.63	7.98	5.32	10.70	-	5.73
PL	13.13	18.40	19.20	27.36	19.18	28.95	33.86	18.49	19.08	22.75
PL-AB	2.37	14.38	18.11	17.68	10.75	15.06	23.69	11.00	13.03	14.47
PL-AN	10.77	4.02	1.09	9.67	8.43	13.89	10.17	7.49	6.05	8.28
LC	-	-	-	-	-	-	-	-	-	-
NE	-	-	-	-	-	-	-	-	-	-
KP	-	-	-	-	-	-	-	-	-	-
NO	-	-	-	-	-	-	-	-	-	-
DI	-	-	-	-	-	.54	-	-	-	-
DI-NO	-	-	-	-	-	.29	-	-	-	-
DI-EN	-	-	-	-	-	.25	-	-	-	-
DI-FS	-	-	-	-	-	-	-	-	-	-
HY	-	.32	-	14.12	13.70	8.09	-	-	1.99	-
HY-EN	-	.32	-	14.12	13.70	8.09	-	-	1.99	-
HY-FS	-	-	-	-	-	-	-	-	-	-
OL	-	-	-	-	-	-	-	-	-	-
OL-FO	-	-	-	-	-	-	-	-	-	-
OL-FA	-	-	-	-	-	-	-	-	-	-
CS	-	-	-	-	-	-	-	-	-	-
MT	-	-	-	-	-	-	-	-	-	-
IL	.34	.09	.13	-	-	.30	.21	.15	.15	.15
AP	-	-	-	-	-	-	-	-	-	-
CC	-	-	-	-	-	-	-	-	-	-
AN/PL	81.96	21.84	5.68	35.36	43.97	47.98	30.03	40.51	31.72	36.41
FO/OL	-	-	-	-	-	-	-	-	-	-
D.I.	53.59	66.27	64.96	59.22	58.79	61.22	70.89	67.77	72.27	73.56

FIG TREE GROUP-SHEBA FORMATION

	C-10	C-11	C-12	C-13	C-14	C-15	C-16	C-17B	C-18	C-25
* * * MAJOR ELEMENTS * * *										
S102	66.20	66.20	70.60	68.00	67.00	66.80	65.20	67.00	66.00	57.20
T102	.69	.51	.47	.46	.49	.49	.51	43.00	.53	.42
AL203	12.50	10.30	9.97	10.10	10.00	9.61	10.70	10.30	10.30	9.48
FE203	8.23	7.02	6.40	7.05	9.14	6.07	7.21	5.42	6.87	4.95
FeO	-	-	-	-	-	-	-	-	-	-
MnO	.06	13.00	.08	.12	.09	.13	.09	.11	.10	.08
MgO	-	-	3.50	-	-	-	-	-	-	-
CaO	1.34	2.29	1.51	2.47	1.47	3.00	2.21	2.43	2.39	1.60
Na2O	2.13	2.06	1.84	1.50	1.34	1.76	1.55	1.64	1.70	2.90
K2O	1.13	1.26	1.26	1.55	1.32	1.35	1.98	2.14	1.45	1.18
P205	-	-	-	-	-	-	-	-	-	-
H2O+	-	-	-	-	-	-	-	-	-	-
H2O-	-	-	-	-	-	-	-	-	-	-
CO2	-	-	-	-	-	-	-	-	-	-
TOTAL	92.08	102.64	95.63	91.25	90.85	89.21	89.45	132.04	89.34	77.81
* * * TRACE ELEMENTS * * *										
CS	-	-	-	-	-	-	-	-	-	-
RB	49.0	43.0	52.0	49.0	45.0	47.0	67.0	83.0	.43	61.0
BA	274.	285.	207.	315.	224.	231.	526.	502.	2.84	519.
SR	59.0	126.	78.0	109.	50.0	101.	97.0	115.	1.04	164.
TH	-	-	-	-	-	-	-	-	-	-
U	-	-	-	-	-	-	-	-	-	-
ZR	206.	120.	124.	127.	104.	123.	109.	115.	.31	157.
HF	-	-	-	-	-	-	-	-	-	-
NB	-	-	-	-	-	-	-	-	-	-
CR	-	-	-	-	-	-	-	-	-	-
V	-	-	-	-	-	-	-	-	-	-
SC	15.0	13.0	12.0	12.0	13.0	12.0	13.0	11.0	14.0	11.0
NI	342.	283.	287.	266.	306.	280.	317.	257.	319.	256.
CO	-	-	-	-	-	-	-	-	-	-
GA	-	-	-	-	-	-	-	-	-	-
PB	-	-	-	-	-	-	-	-	-	-
ZN	-	-	-	-	-	-	-	-	-	-
CU	-	-	-	-	-	-	-	-	-	-
Y	-	-	-	-	-	-	-	-	-	-
LA	-	-	-	-	-	-	-	-	-	-
CE	-	-	-	-	-	-	-	-	-	-
PR	-	-	-	-	-	-	-	-	-	-
ND	-	-	-	-	-	-	-	-	-	-
SM	-	-	-	-	-	-	-	-	-	-
EU	-	-	-	-	-	-	-	-	-	-
GD	-	-	-	-	-	-	-	-	-	-
TB	-	-	-	-	-	-	-	-	-	-
DY	-	-	-	-	-	-	-	-	-	-
HO	-	-	-	-	-	-	-	-	-	-
ER	-	-	-	-	-	-	-	-	-	-
TM	-	-	-	-	-	-	-	-	-	-
YB	-	-	-	-	-	-	-	-	-	-
87/86	-	-	-	-	-	-	-	-	-	-
I-SR	-	-	-	-	-	-	-	-	-	-

FIG TREE GROUP-SHEBA FORMATION

	C-10	C-11	C-12	C-13	C-14	C-15	C-16	C-17B	C-18	C-23
* * * ELEMENT RATIOS * * *										
ZR/NB	-	-	-	-	-	-	-	-	-	-
ZR/Y	-	-	-	-	-	-	-	-	-	-
ZR/HF	-	-	-	-	-	-	-	-	-	-
K/RB	191.	243.	201.	263.	244.	238.	245.	214.	2.799+004	161.
K/BA	34.2	36.7	50.5	40.8	48.9	48.5	31.2	35.4	4.238+003	18.9
K/SR	159.	83.0	134.	118.	219.	111.	169.	154.	1.157+004	59.7
K/ZR	45.5	87.2	84.4	101.	105.	91.1	151.	154.	3.883+004	62.4
K/NB	-	-	-	-	-	-	-	-	-	-
K/Y	-	-	-	-	-	-	-	-	-	-
BA/RB	5.59	6.63	3.98	6.43	4.98	4.91	7.85	6.05	6.60	8.51
BA/SR	4.64	2.26	2.65	2.89	4.48	2.29	5.42	4.37	2.73	3.16
BA/ZR	1.33	2.37	1.67	2.48	2.15	1.88	4.83	4.37	9.16	3.31
RB/SR	.831	.341	.667	.450	.900	.465	.691	.722	.413	.372
NI/CO	-	-	-	-	-	-	-	-	-	-
CR/NI	-	-	-	-	-	-	-	-	-	-
TI/P	-	-	-	-	-	-	-	-	-	-
GA/AL	-	-	-	-	-	-	-	-	-	-
TH/U	-	-	-	-	-	-	-	-	-	-
LA/YB	-	-	-	-	-	-	-	-	-	-
EU/EU*	-	-	-	-	-	-	-	-	-	-
CA/AL	.145	.300	.204	.330	.198	.421	.279	.318	.313	.226
HG #	-	-	111.	-	-	-	-	-	-	-
* * * C.I.P.N. NORMS * * *										
QZ	46.41	36.50	46.62	48.05	51.00	45.09	43.87	44.06	45.44	32.39
CO	5.34	1.38	2.83	1.46	3.69	-	1.99	.87	1.59	.52
OR	6.68	7.45	7.45	9.16	7.80	7.98	11.70	12.65	8.57	6.97
PL	24.67	28.79	23.06	24.95	18.63	29.23	24.08	25.93	26.24	32.48
PL-AB	18.02	17.43	15.57	12.69	11.34	14.89	13.12	13.88	14.36	24.54
PL-AN	6.65	11.36	7.49	12.25	7.29	14.33	10.96	12.06	11.86	7.94
LC	-	-	-	-	-	-	-	-	-	-
NE	-	-	-	-	-	-	-	-	-	-
KP	-	-	-	-	-	-	-	-	-	-
NO	-	-	-	-	-	-	-	-	-	-
DI	-	-	-	-	-	-	-	-	-	-
DI-NO	-	-	-	-	-	-	-	-	-	-
DI-EN	-	-	-	-	-	-	-	-	-	-
DI-FS	-	-	-	-	-	-	-	-	-	-
HY	-	17.54	8.72	-	-	-	-	-	-	-
HY-EN	-	-	8.72	-	-	-	-	-	-	-
HY-FS	-	17.54	-	-	-	-	-	-	-	-
OL	-	-	-	-	-	-	-	-	-	-
OL-FO	-	-	-	-	-	-	-	-	-	-
OL-FA	-	-	-	-	-	-	-	-	-	-
CS	-	-	-	-	-	-	-	-	-	-
MT	-	10.18	-	-	-	-	-	-	-	-
IL	.13	.97	.17	.26	.19	.28	.19	.24	.21	.17
AP	-	-	-	-	-	-	-	-	-	-
CC	-	-	-	-	-	-	-	-	-	-
AN/PL	26.95	39.46	32.48	49.12	39.14	49.05	45.53	46.49	45.18	24.44
FO/OL	-	-	-	-	-	-	-	-	-	-
D-I.	71.12	61.38	69.64	69.90	70.14	67.96	68.69	70.59	68.39	53.90

.DIR

* * * SAMPLE DIRECTORY * * *

SAMPLE #	DATABASE #	ROCK TYPE	LOCALITY	REFERENCE
C-3	0	3A	SHEBA FARM, ULUNDI SYNCLINE, BARBETON MTN. LAND.	6
C-5	00	3A	SHEBA FARM, ULUNDI SYNCLINE, BARBETON MTN. LAND.	6
V-1	00	3A	SHEBA FORMATION, ULUNDI SYNCLINE.	
V-2	00	3B	SHEBA FORMATION, ULUNDI SYNCLINE.	
K-1	0	3B	SHEBA FORMATION, ULUNDI SYNCLINE.	8
C-4	00	3B	SHEBA FARM, ULUNDI SYNCLINE, BARBETON MTN. LAND.	6
C-6	00	3B	SHEBA FARM, ULUNDI SYNCLINE, BARBETON MTN. LAND.	6
C-7	00	3B	SHEBA FARM, ULUNDI SYNCLINE, BARBETON MTN. LAND.	6
C-8	00	3B	SHEBA FARM, ULUNDI SYNCLINE, BARBETON MTN. LAND.	6
C-9	00	3B	SHEBA FARM, ULUNDI SYNCLINE, BARBETON MTN. LAND.	6
C-10	00	3B	SHEBA FARM, ULUNDI SYNCLINE, BARBETON MTN. LAND.	6
C-11	00	3B	SHEBA FARM, ULUNDI SYNCLINE, BARBETON MTN. LAND.	6
C-12	00	3B	SHEBA FARM, ULUNDI SYNCLINE, BARBETON MTN. LAND.	6
C-13	00	3B	SHEBA FARM, ULUNDI SYNCLINE, BARBETON MTN. LAND.	6
C-14	00	3B	SHEBA FARM, ULUNDI SYNCLINE, BARBETON MTN. LAND.	6
C-15	00	3B	SHEBA FARM, ULUNDI SYNCLINE, BARBETON MTN. LAND.	6
C-16	00	3B	SHEBA FARM, ULUNDI SYNCLINE, BARBETON MTN. LAND.	6
C-17B	00	3B	SHEBA FARM, ULUNDI SYNCLINE, BARBETON MTN. LAND.	6
C-18	00	3B	SHEBA FARM, ULUNDI SYNCLINE, BARBETON MTN. LAND.	6
C-25	0	3B	SHEBA FARM, ULUNDI SYNCLINE, BARBETON MTN. LAND.	6

20 SAMPLES IN THIS DIRECTORY

REFERENCES

REFERENCE LIST FOR SAMPLE DIRECTORIES

- 6 CONDIE, K.E.; MACKE, J.E. AND REIMER, T.O., 1970. PETROLOGY AND GEOCHEMISTRY OF EARLY PRECAMBRIAN GRAYWACKES FROM THE FIG TREE GROUP, SOUTH AFRICA. GEOL. SOC. AM. BULL. 81: 2759-2776.
- 7 VISSER, D.L.J., (COMPILER) 1956. THE GEOLOGY OF THE BARBETON AREA. S.AFR. GEOL. SURVEY SPEC. PUB. 15: 251 PP.
- 8 KOEN, G.W., 1947. DIE GEOLOGIE VAN DIE SHEBAGEBIED IN DIE BARBETONSE DISTRIK. UNPUB. M.SC. THESIS, PRETORIA UNIV., PRETORIA.

FIG TREE GROUP-BELVUE ROAD FORMATION

	C-1	C-2	C-24	C-26	C-27	C-28	C-29
* * * MAJOR ELEMENTS * * *							
SI02	65.80	65.20	59.30	51.90	51.20	60.80	64.43
TI02	.50	.53	.67	.69	.66	.38	.43
AL203	12.40	12.60	14.50	14.30	15.00	10.06	10.73
FE203	5.65	5.38	7.63	8.73	8.89	4.72	4.89
FeO	-	-	-	-	-	-	-
MNO	.07	.06	.09	.13	.10	.12	.08
MGO	2.07	-	-	-	-	-	-
CAO	2.44	2.24	2.98	4.49	3.10	4.99	2.36
NA2O	1.62	2.10	3.45	3.04	3.32	2.48	3.01
K2O	-	2.32	2.03	3.20	3.07	2.00	1.36
P2O5	-	-	-	-	-	-	-
H2O+	-	-	-	-	-	-	-
H2O-	-	-	-	-	-	-	-
CO2	-	-	-	-	-	-	-
TOTAL	90.55	90.43	90.65	86.48	85.34	85.55	87.23
* * * TRACE ELEMENTS * * *							
CS	-	-	-	-	-	-	-
RB	65.0	106.	95.0	124.	109.	81.0	53.0
BA	571.	476.	610.	1090.	701.	489.	455.
SR	283.	215.	363.	507.	568.	318.	222.
TH	-	-	-	-	-	-	-
U	-	-	-	-	-	-	-
ZR	146.	165.	206.	228.	245.	153.	150.
HF	-	-	-	-	-	-	-
NB	-	-	-	-	-	-	-
CR	-	-	-	-	-	-	-
V	-	-	-	-	-	-	-
SC	-	-	-	-	-	-	-
NI	272.	142.	53.0	114.	101.	234.	202.
CO	-	-	-	-	-	-	-
GA	-	-	-	-	-	-	-
PB	-	-	-	-	-	-	-
ZN	-	-	-	-	-	-	-
CU	-	-	-	-	-	-	-
Y	-	-	-	-	-	-	-
LA	-	-	-	-	-	-	-
CE	-	-	-	-	-	-	-
PR	-	-	-	-	-	-	-
ND	-	-	-	-	-	-	-
SH	-	-	-	-	-	-	-
EU	-	-	-	-	-	-	-
GD	-	-	-	-	-	-	-
TB	-	-	-	-	-	-	-
DY	-	-	-	-	-	-	-
HO	-	-	-	-	-	-	-
ER	-	-	-	-	-	-	-
TH	-	-	-	-	-	-	-
YB	-	-	-	-	-	-	-
B7/B6	-	-	-	-	-	-	-
I-SR	-	-	-	-	-	-	-

FIG TREE GROUP-3ELVUE ROAD FORMATION

	C-1	C-2	C-24	C-26	C-27	C-28	C-29
* * * ELEMENT RATIOS * * *							
ZR/NB	-	-	-	-	-	-	-
ZR/Y	-	-	-	-	-	-	-
ZR/HF	-	-	-	-	-	-	-
K/RB	-	182.	177.	214.	234.	205.	213.
K/BA	-	40.5	27.6	24.4	36.4	34.0	24.8
K/SR	-	89.6	46.4	52.4	44.9	52.2	50.9
K/ZR	-	117.	81.8	117.	104.	109.	75.3
K/NB	-	-	-	-	-	-	-
K/Y	-	-	-	-	-	-	-
BA/RB	8.78	4.49	6.42	8.79	6.43	6.04	8.58
BA/SR	2.02	2.21	1.68	2.15	1.23	1.54	2.05
BA/ZR	3.91	2.88	2.96	4.78	2.86	3.20	3.03
RB/SR	.230	.493	.262	.245	.192	.255	.239
NI/CO	-	-	-	-	-	-	-
CR/NI	-	-	-	-	-	-	-
TI/P	-	-	-	-	-	-	-
GA/AL	-	-	-	-	-	-	-
TH/U	-	-	-	-	-	-	-
LA/YB	-	-	-	-	-	-	-
EU/EU*	-	-	-	-	-	-	-
CA/AL	.266	.240	.277	.424	.279	.669	.298
MG #	118.	-	-	-	-	-	-
* * * C.I.P.N. NORMS * * *							
OZ	48.06	39.31	25.08	13.72	13.50	31.13	36.64
CO	5.30	2.56	1.21	-	.58	-	-
OR	-	13.71	12.00	18.91	18.14	11.82	8.04
PL	25.81	28.88	43.98	41.65	43.47	31.40	37.14
PL-AB	13.71	17.77	29.19	25.72	28.09	20.99	25.47
PL-AN	12.10	11.11	14.78	15.92	15.38	10.41	11.67
LC	-	-	-	-	-	-	-
NE	-	-	-	-	-	-	-
KP	-	-	-	-	-	-	-
NO	-	-	-	1.86	-	5.63	-
DI	-	-	-	-	-	-	-
DI-NO	-	-	-	-	-	-	-
DI-EN	-	-	-	-	-	-	-
DI-FS	-	-	-	-	-	-	-
HY	5.16	-	-	-	-	-	-
HY-EN	5.16	-	-	-	-	-	-
HY-FS	-	-	-	-	-	-	-
OL	-	-	-	-	-	-	-
OL-FO	-	-	-	-	-	-	-
OL-FA	-	-	-	-	-	-	-
CS	-	-	-	-	-	-	-
MT	-	-	-	-	-	-	-
IL	.15	.13	.19	.28	.21	.26	.17
AP	-	-	-	-	-	-	-
CC	-	-	-	-	-	-	-
AN/PL	46.89	38.48	33.62	38.23	35.38	33.16	31.42
FO/OL	-	-	-	-	-	-	-
D.I.	61.77	70.79	66.27	58.36	59.73	63.93	70.15

.DIR

* * * SAMPLE DIRECTORY * * *

SAMPLE #	DATABASE #	ROCK TYPE	LOCALITY	REFERENCE
C-1	D	3B	BELVUE RD.FORMATION,ULUNDI SYNCLINE,BAR.MTN.LAND	6
C-2	O	3B	BELVUE RD.FORMATION,ULUNDI SYNCLINE,BAR.MTN.LAND	6
C-24	O	3B	BELVUE RD.FORMATION,ULUNDI SYNCLINE,BAR.MTN.LAND	6
C-26	O	3B	BELVUE RD.FORMATION,ULUNDI SYNCLINE,BAR.MTN.LAND	6
C-27	O	3B	BELVUE RD.FORMATION,ULUNDI SYNCLINE,BAR.MTN.LAND	6
C-28	O	3B	BELVUE RD.FORMATION,ULUNDI SYNCLINE,BAR.MTN.LAND	6
C-29	D	3B	BELVUE RD.FORMATION,ULUNDI SYNCLINE,BAR.MTN.LAND	6

7 SAMPLES IN THIS DIRECTORY

REFERENCES

REFERENCE LIST FOR SAMPLE DIRECTORIES

6

CONDIE, K.E.; MACKE, J.E. AND REIMER, T.D., 1970. PETROLOGY AND GEOCHEMISTRY OF EARLY PRECAMBRIAN GRAYWACKES FROM THE FIG TREE GROUP, SOUTH AFRICA. GEOL. SOC. AM. BULL. 81: 2759-2776.

FIG TREE GROUP-FORMATION UNIDENTIFIED

	FG-15	SF-2	SF-3	SF-4B	SH-7	FG-1	FG-2	FG-8	FG-9	FG-10
* * * MAJOR ELEMENTS * * *										
S102	68.60	63.71	65.94	67.03	65.68	56.91	42.66	69.45	48.85	58.15
T102	.45	.56	.43	.49	.43	.67	.46	.39	.42	.81
AL203	10.26	11.26	9.29	12.01	9.67	10.84	7.28	5.10	7.44	13.41
FE203	2.30	13.07	6.02	3.54	6.60	3.39	29.64	14.94	31.30	12.78
FeO	4.17	-	-	4.30	-	17.95	9.45	2.73	4.89	1.72
MNO	.19	.03	.04	.03	.16	.05	.16	.68	.23	.12
MGO	4.07	5.23	4.38	4.14	4.23	3.18	2.28	2.35	1.60	3.11
CAO	1.53	.16	2.58	.10	2.80	.01	.01	.21	.03	-
NA2O	1.55	.93	.86	.40	1.70	.01	-	-	-	-
K2O	1.64	.75	1.56	2.23	1.50	.82	.43	.34	1.57	1.94
P2O5	.37	.09	.08	.09	.08	.02	.13	.05	.05	.08
H2O+	2.23	4.26	6.23	4.61	6.19	3.50	6.11	3.02	3.01	6.72
H2O-	-	-	-	-	-	-	-	-	-	-
CO2	2.55	-	-	.10	-	.10	.10	.30	.10	.10
TOTAL	99.61	100.05	97.40	99.07	99.04	97.45	98.68	99.56	99.49	98.94
* * * TRACE ELEMENTS * * *										
CS	-	-	-	-	-	-	-	-	-	-
RB	-	-	-	-	-	-	-	-	-	-
BA	-	-	-	-	-	-	-	-	-	-
SR	-	-	-	-	-	-	-	-	-	-
TH	3.00	5.00	9.00	6.00	9.00	1.00	3.00	6.00	1.00	8.00
U	-	-	-	-	-	-	-	-	-	-
ZR	89.0	105.	112.	91.0	111.	51.0	40.0	37.0	60.0	78.0
HF	-	-	-	-	-	-	-	-	-	-
NB	1.30	4.00	19.0	3.00	4.00	1.00	4.00	1.00	2.00	3.00
CR	706.	824.	820.	768.	694.	977.	573.	811.	346.	1590.
V	86.0	74.0	70.0	89.0	68.0	122.	83.0	73.0	57.0	192.
SC	15.0	15.0	12.0	15.0	21.0	20.0	18.0	16.0	15.0	28.0
NI	277.	443.	444.	570.	666.	414.	341.	338.	207.	1200.
CO	36.0	36.0	22.0	32.0	34.0	24.0	22.0	44.0	22.0	74.0
GA	10.0	12.0	12.0	13.0	13.0	11.0	8.00	5.00	9.00	15.0
PB	-	-	-	-	-	-	-	-	-	-
ZN	69.0	89.0	90.0	89.0	70.0	70.0	65.0	52.0	82.0	190.
CU	58.0	45.0	44.0	40.0	33.0	33.0	41.0	76.0	19.0	94.0
Y	12.0	15.0	46.0	18.0	17.0	20.0	26.0	11.0	80.0	28.0
LA	-	-	-	-	-	-	-	-	-	-
CE	-	-	-	-	-	-	-	-	-	-
PR	-	-	-	-	-	-	-	-	-	-
ND	-	-	-	-	-	-	-	-	-	-
SM	-	-	-	-	-	-	-	-	-	-
EU	-	-	-	-	-	-	-	-	-	-
GD	-	-	-	-	-	-	-	-	-	-
TB	-	-	-	-	-	-	-	-	-	-
DY	-	-	-	-	-	-	-	-	-	-
HO	-	-	-	-	-	-	-	-	-	-
ER	-	-	-	-	-	-	-	-	-	-
TM	-	-	-	-	-	-	-	-	-	-
YB	-	-	-	-	-	-	-	-	-	-
87/86	-	-	-	-	-	-	-	-	-	-
I-SR	-	-	-	-	-	-	-	-	-	-

FIG TREE GROUP-FORMATION UNIDENTIFIED

	FG-15	SF-2	SF-3	SF-4B	SH-7	FG-1	FG-2	FG-8	FG-9	FG-10
* * * ELEMENT RATIOS * * *										
ZR/NB	89.0	26.2	5.89	30.3	27.7	51.0	10.0	37.0	30.0	26.0
ZR/Y	7.42	7.00	2.43	5.06	6.53	2.55	1.54	3.36	.750	2.79
ZR/HF	-	-	-	-	-	-	-	-	-	-
K/RB	-	-	-	-	-	-	-	-	-	-
K/BA	-	-	-	-	-	-	-	-	-	-
K/SR	-	-	-	-	-	-	-	-	-	-
K/ZR	153.	59.3	115.	203.	112.	133.	89.2	76.3	217.	206.
K/NB	1.361+004	1.557+003	677.	6.171+003	3.113+003	6.807+003	892.	2.823+003	6.517+003	5.366+003
K/Y	1.135+003	415.	280.	1.028+003	732.	340.	137.	257.	163.	575.
BA/RB	-	-	-	-	-	-	-	-	-	-
BA/SR	-	-	-	-	-	-	-	-	-	-
BA/ZR	-	-	-	-	-	-	-	-	-	-
RB/SR	-	-	-	-	-	-	-	-	-	-
NI/CO	7.69	12.3	20.2	17.8	19.6	17.2	15.5	7.68	9.41	16.2
CR/NI	2.55	1.86	1.85	1.35	1.04	2.36	1.68	2.40	1.67	1.32
TI/P	8.83	8.55	7.38	7.48	7.38	46.0	6.32	10.7	11.5	13.9
GA/AL	1.842-004	2.014-004	2.441-004	2.045-004	1.954-004	1.917-004	2.076-004	1.852-004	2.286-004	2.114-004
TH/U	-	-	-	-	-	-	-	-	-	-
LA/YB	-	-	-	-	-	-	-	-	-	-
EU/EU*	-	-	-	-	-	-	-	-	-	-
CA/AL	.201	1.917-002	.375	1.123-002	.391	1.245-003	1.853-003	5.556-002	5.441-003	-
MG N	65.8	116.	108.	66.4	110.	24.7	41.7	81.1	69.0	95.3
* * * C.I.P.N. NORMS * * *										
QZ	44.80	47.55	43.17	48.08	37.97	35.70	37.62	64.65	40.46	46.09
CO	5.94	8.84	1.70	8.94	.35	9.94	6.81	4.73	5.74	11.31
OR	9.69	4.43	9.16	13.18	8.86	4.85	2.54	2.01	9.28	11.46
PL	13.12	8.08	19.55	3.38	27.75	.08	-	-	-	-
PL-AB	13.12	7.87	7.28	3.38	14.38	.08	-	-	-	-
PL-AN	-	.21	12.28	-	13.37	-	-	-	-	-
LC	-	-	-	-	-	-	-	-	-	-
NE	-	-	-	-	-	-	-	-	-	-
KP	-	-	-	-	-	-	-	-	-	-
NO	-	-	-	-	-	-	-	-	-	-
DI	-	-	-	-	-	-	-	-	-	-
DI-NO	-	-	-	-	-	-	-	-	-	-
DI-EN	-	-	-	-	-	-	-	-	-	-
DI-FS	-	-	-	-	-	-	-	-	-	-
HY	15.50	13.03	10.91	14.53	10.53	37.07	5.69	5.85	3.98	7.75
HY-EN	10.14	13.03	10.91	10.31	10.53	7.92	5.68	5.85	3.98	7.75
HY-FS	5.37	-	-	4.22	-	29.15	-	-	-	-
OL	-	-	-	-	-	-	-	-	-	-
OL-FO	-	-	-	-	-	-	-	-	-	-
OL-FA	-	-	-	-	-	-	-	-	-	-
CS	-	-	-	-	-	-	-	-	-	-
MT	3.33	-	-	5.13	-	4.92	29.64	9.89	15.29	3.59
IL	.85	.06	.09	.93	.34	1.27	.87	.74	.80	1.54
AP	.17	.21	.19	.18	.19	.02	.02	.12	.05	-
CC	2.57	-	-	-	-	-	-	.26	-	-
AN/PL	-	2.55	62.78	-	48.17	-	-	-	-	-
FO/OL	-	-	-	-	-	-	-	-	-	-
D-I.	67.60	59.85	59.61	64.64	61.22	40.63	40.16	66.66	49.73	57.55

FIG TREE GROUP-FORMATION UNIDENTIFIED

	FG-11	FG-12	FG-13	FG-14	FG-16	FG-17	SF-4A	SF-5	SF-6	SH-2
* * * MAJOR ELEMENTS * * *										
SIO2	56.83	54.20	51.74	56.99	56.01	57.24	52.67	59.21	52.48	59.18
TIO2	.42	.72	.73	.78	.64	.57	.71	.72	.54	.51
AL2O3	7.07	16.66	16.79	17.52	13.14	14.24	18.17	16.42	14.15	11.01
FE2O3	24.23	6.69	6.66	2.97	3.66	10.11	10.05	1.63	17.49	7.92
FeO	3.59	5.39	5.96	4.74	7.69	2.87	-	5.67	-	-
MNO	.03	.08	.12	.09	.06	.12	.04	.03	.04	.21
MGO	2.22	5.33	6.09	5.30	6.05	4.00	5.57	5.31	6.90	5.43
CAO	.01	.15	.13	.10	.16	.06	.11	.20	.12	3.50
NA2O	-	.97	.85	.73	.87	.01	9.30	1.05	1.06	1.40
K2O	.34	3.38	3.13	3.97	1.44	3.90	3.93	3.35	.98	1.73
P2O5	.04	.11	.11	.09	.09	.08	.10	.10	.09	.09
H2O+	4.86	5.92	5.85	5.42	5.20	5.52	6.60	4.66	5.94	5.36
H2O-	-	-	-	-	-	-	-	-	-	-
CO2	.10	.10	.10	.10	.10	.10	.10	.10	-	2.25
TOTAL	99.74	99.70	98.26	98.80	95.11	98.82	107.35	98.45	99.69	98.59
* * * TRACE ELEMENTS * * *										
CS	-	-	-	-	-	-	-	-	-	-
RB	-	-	-	-	-	-	-	-	-	-
BA	-	-	-	-	-	-	-	-	-	-
SR	-	-	-	-	-	-	-	-	-	-
TH	1.00	9.00	5.00	3.00	10.0	7.00	7.00	11.0	10.0	5.00
U	-	-	-	-	-	-	-	-	-	-
ZR	59.0	88.0	90.0	130.	102.	83.0	99.0	120.	77.0	114.
HF	-	-	-	-	-	-	-	-	-	-
NB	6.00	2.00	5.00	10.0	7.00	4.00	8.00	5.00	8.00	8.00
CR	524.	1147.	1059.	1245.	946.	879.	1070.	1090.	945.	775.
V	50.0	179.	169.	220.	117.	127.	194.	148.	105.	85.0
SC	15.0	26.0	26.0	26.0	21.0	21.0	28.0	23.0	20.0	16.0
NI	339.	658.	737.	451.	475.	430.	600.	526.	496.	420.
CO	29.0	61.0	87.0	38.0	32.0	36.0	39.0	25.0	32.0	32.0
GA	8.00	18.0	19.0	19.0	15.0	19.0	20.0	18.0	16.0	12.0
PB	-	-	-	-	-	-	-	-	-	-
ZN	53.0	156.	164.	102.	132.	173.	116.	103.	122.	136.
CU	36.0	62.0	74.0	60.0	71.0	56.0	54.0	46.0	48.0	44.0
Y	75.0	29.0	27.0	32.0	24.0	29.0	35.0	25.0	25.0	26.0
LA	-	-	-	-	-	-	-	-	-	-
CE	-	-	-	-	-	-	-	-	-	-
PR	-	-	-	-	-	-	-	-	-	-
ND	-	-	-	-	-	-	-	-	-	-
SM	-	-	-	-	-	-	-	-	-	-
EU	-	-	-	-	-	-	-	-	-	-
GD	-	-	-	-	-	-	-	-	-	-
TB	-	-	-	-	-	-	-	-	-	-
DY	-	-	-	-	-	-	-	-	-	-
HO	-	-	-	-	-	-	-	-	-	-
ER	-	-	-	-	-	-	-	-	-	-
TM	-	-	-	-	-	-	-	-	-	-
YB	-	-	-	-	-	-	-	-	-	-
87/86	-	-	-	-	-	-	-	-	-	-
I-SR	-	-	-	-	-	-	-	-	-	-

FIG TREE GROUP-FORMATION UNIDENTIFIED

	FG-11	FG-12	FG-13	FG-14	FG-16	FG-17	SF-4A	SF-5	SF-6	SH-2
* * * ELEMENT RATIOS * * *										
ZR/NB	9.33	44.0	18.0	13.0	14.6	20.7	12.4	24.0	9.62	14.2
ZR/Y	.787	3.03	3.33	4.06	4.25	2.86	2.83	4.80	3.08	4.38
ZR/HF	-	-	-	-	-	-	-	-	-	-
K/RB	-	-	-	-	-	-	-	-	-	-
K/BA	-	-	-	-	-	-	-	-	-	-
K/SR	-	-	-	-	-	-	-	-	-	-
K/ZR	47.8	319.	289.	254.	117.	390.	330.	232.	106.	126.
K/NB	473.	1.403+004	5.197+003	3.296+003	1.708+003	8.094+003	4.078+003	5.562+003	1.017+003	1.795+003
K/Y	37.6	968.	962.	1.030+003	498.	1.116+003	932.	1.112+003	325.	552.
BA/RB	-	-	-	-	-	-	-	-	-	-
BA/SR	-	-	-	-	-	-	-	-	-	-
BA/ZR	-	-	-	-	-	-	-	-	-	-
RB/SR	-	-	-	-	-	-	-	-	-	-
NI/CO	11.7	10.8	8.47	11.9	14.8	11.9	15.4	21.0	15.5	13.1
CR/NI	1.55	1.74	1.44	2.76	1.99	2.04	1.78	2.07	1.91	1.85
TI/P	14.4	8.99	9.12	11.9	9.77	9.79	9.75	9.89	8.24	7.78
GA/AL	2.138-004	2.042-004	2.138-004	2.049-004	2.157-004	2.521-004	2.080-004	2.071-004	2.137-004	2.059-004
TH/U	-	-	-	-	-	-	-	-	-	-
LA/YB	-	-	-	-	-	-	-	-	-	-
EU/EU*	1.908-003	1.215-002	1.045-002	7.701-003	1.643-002	5.685-003	8.169-003	1.643-002	1.144-002	.429
CA/AL	82.9	68.4	68.7	69.0	63.5	81.6	111.	63.8	117.	109.
MG W	-	-	-	-	-	-	-	-	-	-
* * * C.I.P.#. NORMS * * *										
QZ	52.22	26.16	23.71	27.32	31.80	36.29	-	26.76	32.28	35.22
CO	6.70	11.41	12.00	12.02	10.15	10.00	-	11.07	11.34	5.90
OR	2.01	19.97	18.50	23.46	8.51	23.05	23.22	19.80	5.79	10.22
PL	-	8.21	7.19	6.18	7.36	.08	30.15	8.88	8.98	14.40
PL-AB	-	8.21	7.19	6.18	7.36	.08	30.15	8.88	8.97	11.85
PL-AN	-	-	-	-	-	-	-	-	.01	2.55
LC	-	-	-	-	-	-	-	-	-	-
NE	-	-	-	-	-	-	22.44	-	-	-
KP	-	-	-	-	-	-	-	-	-	-
NO	-	-	-	-	-	-	-	-	-	-
DI	-	-	-	-	-	-	-	-	-	-
DI-NO	-	-	-	-	-	-	-	-	-	-
DI-EN	-	-	-	-	-	-	-	-	-	-
DI-FS	-	-	-	-	-	-	-	-	-	-
HY	5.53	16.60	19.63	18.33	25.22	9.96	-	21.16	17.18	13.52
HY-EN	5.53	13.27	15.17	13.20	15.07	9.96	-	13.22	17.18	13.52
HY-FS	-	3.33	4.46	5.13	10.15	-	-	7.93	-	-
OL	-	-	-	-	-	-	9.72	-	-	-
OL-FO	-	-	-	-	-	-	9.72	-	-	-
OL-FA	-	-	-	-	-	-	-	-	-	-
CS	-	-	-	-	-	-	-	-	-	-
MT	10.45	9.70	9.66	4.31	5.31	7.99	-	2.36	-	-
IL	.80	1.37	1.39	1.48	1.22	1.08	.09	1.37	.09	.45
AP	.02	.26	.23	.18	.21	.11	.20	.24	.21	.21
CC	-	.01	-	-	.07	-	-	.12	-	5.12
AN/PL	-	-	-	-	-	-	-	-	.08	17.72
FO/OL	-	-	-	-	-	-	-	-	-	-
D.I.	54.23	54.34	49.40	56.95	47.67	59.43	75.82	57.44	47.04	57.29

FIG TREE GROUP-FORMATION UNIDENTIFIED

SH-3 FG.COM

* * * MAJOR ELEMENTS * * *

S102	57.10	58.87
T102	.63	.51
AL203	13.69	12.09
FE203	10.64	2.80
FE0	-	8.15
MNO	.12	.08
MGO	6.46	5.73
CAO	1.57	1.17
NA2O	1.54	1.20
K2O	1.53	1.22
P2O5	.10	.08
H2O+	6.22	3.59
H2O-	-	-
CO2	-	2.25
TOTAL	99.60	97.74

* * * TRACE ELEMENTS * * *

CS	-	-
RB	-	-
BA	-	-
SR	-	-
TH	5.00	14.0
U	-	-
ZR	85.0	96.0
HF	-	-
NB	1.00	8.00
CR	903.	763.
V	136.	94.0
SC	23.0	17.0
NI	463.	526.
CO	46.0	33.0
GA	16.0	13.0
PB	-	-
ZN	114.	90.0
CU	18.0	46.0
Y	19.0	19.0
LA	-	-
CE	-	-
PR	-	-
ND	-	-
SM	-	-
EU	-	-
GD	-	-
TB	-	-
DY	-	-
HO	-	-
ER	-	-
TM	-	-
YB	-	-
87/86	-	-
I-SR	-	-

FIG TREE GROUP-FORMATION UNIDENTIFIED

SH-3

FG.COM

* * * ELEMENT RATIOS * * *

ZR/NB	85.0	12.0
ZR/Y	4.47	5.05
ZR/HF	-	-
K/RB	-	-
K/BA	-	-
K/SR	-	-
K/ZR	149.	105.
K/NB	1.270+004	1.266+003
K/Y	668.	533.
BA/RB	-	-
BA/SR	-	-
BA/ZR	-	-
RB/SR	-	-
NI/CO	10.1	15.9
CR/NI	1.95	1.45
TI/P	8.65	8.76
GA/AL	2.208-004	2.032-004
TH/U	-	-
LA/YB	-	-
EU/EU*	-	-
CA/AL	.155	.131
MG #	110.	57.2

* * * C.I.P.N. NORMS * * *

QZ	29.58	33.23
CO	6.89	8.80
OR	9.34	7.21
PL	20.17	10.15
PL-AB	13.03	10.15
PL-AN	7.14	-
LC	-	-
NE	-	-
KP	-	-
NO	-	-
DI	-	-
DI-NO	-	-
DI-EN	-	-
DI-FS	-	-
HY	16.09	26.23
HY-EN	16.09	14.27
HY-FS	-	11.96
OL	-	-
OL-FO	-	-
OL-FA	-	-
CS	-	-
MT	-	4.06
IL	.26	.97
AP	.24	.19
CC	-	1.90
AN/PL	35.38	-
FO/OL	-	-
D.I.	51.65	50.60

.DIR

*** SAMPLE DIRECTORY ***

SAMPLE #	DATABASE #	ROCK TYPE	LOCALITY	REFERENCE
FG-15	0	3B	BETWEEN SHEBA AND FAIRVIEW GOLD MINES, ULUNDI S.	2A
SF-2	0	3B	WEST OF SHEBA MINE, NORTH LIMB-ULUNDI SYNCLINE.	2:
SF-3	0	3B	WEST OF SHEBA MINE, NORTH LIMB-ULUNDI SYNCLINE.	2B
SF-4B	0	3B	WEST OF SHEBA MINE, NORTH LIMB-ULUNDI SYNCLINE.	2:
SH-7	0	3B	BH.2K40, SHEBA MINE.	2A
FG-1	0	3B	FARM JOSEF'S DAL. RD. FROM HAVELOCK TO BARBETON.	2A
FG-2	0	3D	FARM JOSEF'S DAL. RD. FROM HAVELOCK TO BARBETON.	2A
FG-8	0	3D	31 DEGREES 01 AND 3/4 MIN. EAST, 26 DEGREES 13 MIN. STH.	2A
FG-9	0	3D	WEST OF PIGGS PEAK	2A
FG-10	0	3D	NGWENHA IRON DEPOSIT	2B
FG-11	0	3D	NGWENHA IRON DEPOSIT	2B
FG-12	0	3A	BETWEEN SHEBA AND FAIRVIEW GOLD MINES, ULUNDI S.	2A
FG-13	0	3A	BETWEEN SHEBA AND FAIRVIEW GOLD MINES, ULUNDI S.	2A
FG-14	0	3A	BETWEEN SHEBA AND FAIRVIEW GOLD MINES, ULUNDI S.	2A
FG-16	0	3A	FARM LOUIEVILLE 467, LOUW'S CREEK.	2B
FG-17	0	3A	FARM LOUIEVILLE 467, LOUW'S CREEK.	2B
SF-4A	0	3A	WEST OF SHEBA MINE, NORTH LIMB-ULUNDI SYNCLINE.	2:
SF-5	0	3A	WEST OF SHEBA MINE, NORTH LIMB-ULUNDI SYNCLINE.	2:
SF-6	0	3A	WEST OF SHEBA MINE, NORTH LIMB-ULUNDI SYNCLINE.	2:
SH-2	0	3A	BH.2K40, SHEBA MINE.	2A
SH-3	0	3A	BH.2K40, SHEBA MINE.	2A
FG.COM	0	3A	WEST OF SHEBA MINE, NORTH LIMB-ULUNDI SYNCLINE.	2A

22 SAMPLES IN THIS DIRECTORY

REFERENCES

REFERENCE LIST FOR SAMPLE DIRECTORIES

- 2A DANCHIN, R.V., 1970. ASPECTS OF THE GEOCHEMISTRY OF SOME SELECTED SOUTH AFRICAN FINE GRAINED SEDIMENTS. UNPUB. PH.D. THESIS, UNIV. CAPE TOWN, CAPE TOWN, 215PP.
- 2B HOFMEYR, P.K., 1971. THE ABUNDANCES AND DISTRIBUTION OF SOME TRACE ELEMENTS IN SOME SELECTED SOUTH AFRICAN SHALES. UNPUB. PH.D. THESIS, UNIV. CAPE TOWN, CAPE TOWN, 218PP.

MOZAAN GROUP

	MZ-1	MZ-2	MZ-3	MZ-4	MZ-5	MZ-6	MZ-7
* * * MAJOR ELEMENTS * * *							
S102	40.30	51.10	58.32	50.73	74.04	50.68	42.45
T102	.12	2.03	.65	.43	.51	.49	.44
AL203	2.29	.78	16.13	11.72	13.41	13.32	11.95
FE203	42.63	44.43	13.50	28.16	3.50	24.45	31.11
FEO	10.63	1.51	.29	1.94	.29	1.51	.86
MNO	.14	.02	.09	.02	-	.04	2.31
MGO	1.52	.12	.58	.17	.37	.12	.38
CAO	.78	.01	-	.02	.02	-	-
NA2O	.10	.10	.10	.10	.10	.10	.10
K2O	.14	-	2.31	.03	2.33	.01	1.03
P2O5	.04	.04	.05	.03	.17	.05	.08
H2O+	1.01	2.00	6.84	6.51	4.12	8.49	7.82
H2O-	-	-	-	-	-	-	.10
CO2	.40	.10	.10	.15	.10	.10	-
TOTAL	99.90	102.24	98.96	100.01	98.96	99.36	98.60

* * * TRACE ELEMENTS * * *

CS	-	-	-	-	-	-	-
RB	-	-	-	-	-	-	-
BA	-	-	-	-	-	-	-
SR	-	-	-	-	-	-	-
TH	-	-	-	-	-	-	-
U	-	-	-	-	-	-	-
ZR	-	-	-	-	-	-	-
HF	-	-	-	-	-	-	-
NB	-	-	-	-	-	-	-
CR	-	-	-	-	-	-	-
V	-	-	-	-	-	-	-
SC	-	-	-	-	-	-	-
NI	-	-	-	-	-	-	-
CO	-	-	-	-	-	-	-
GA	-	-	-	-	-	-	-
PB	-	-	-	-	-	-	-
ZN	-	-	-	-	-	-	-
CU	-	-	-	-	-	-	-
Y	-	-	-	-	-	-	-
LA	-	-	-	-	-	-	-
CE	-	-	-	-	-	-	-
PR	-	-	-	-	-	-	-
ND	-	-	-	-	-	-	-
SM	-	-	-	-	-	-	-
EU	-	-	-	-	-	-	-
GD	-	-	-	-	-	-	-
TB	-	-	-	-	-	-	-
DY	-	-	-	-	-	-	-
HO	-	-	-	-	-	-	-
ER	-	-	-	-	-	-	-
TH	-	-	-	-	-	-	-
YB	-	-	-	-	-	-	-
87/86	-	-	-	-	-	-	-
I-SR	-	-	-	-	-	-	-

-DIR

* * * SAMPLE DIRECTORY * * *

SAMPLE #	DATABASE #	ROCK TYPE	LOCALITY	REFERENCE
MZ-1	0	4D	MOOIHOEK-KABUTA AREA	2A
MZ-2	0	4D	MOOIHOEK-KABUTA AREA	2A
MZ-3	0	4A	MOOIHOEK-KABUTA AREA	2A
MZ-4	0	4D	MOOIHOEK-KABUTA AREA	2A
MZ-5	0	4A	MOOIHOEK-KABUTA AREA	2A
MZ-6	0	4D	MOZAAN OUTLIER WEST OF MHLOSHENI	2A
MZ-7	0	4D	MOZAAN OUTLIER WEST OF MHLOSHENI	2A

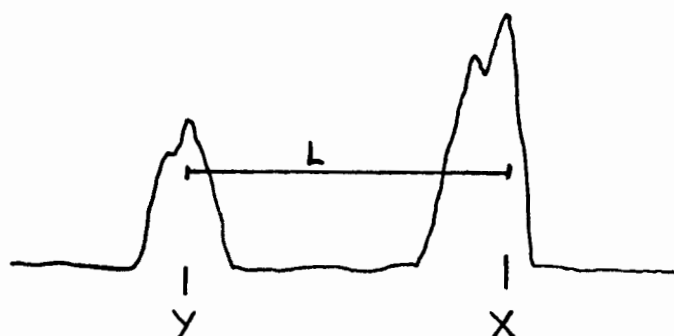
7 SAMPLES IN THIS DIRECTORY

APPENDIX FOUR

Settings and calculations for
 b_0 determination by XRD

INSTRUMENT SETTINGS: 50 KV
 25 mA
 Time constant: 2
 Preset seconds or counts: 4×10^3
 Range (θ /S): variable, mostly $2 \times 10^4 - 4 \times 10^4$
 Scanning speed: $\frac{1}{2}^\circ 2\theta/\text{min}$ (1)
 Chart drive: 2 cm/min. (2)
 From (1) and (2) $1^\circ 2\theta = 40 \text{ mm}$ (3)
 Slit: 1°

METHOD: Scan between $59.50^\circ 2\theta$ and $62.50^\circ 2\theta$ to cover quartz (060) and white mica (060) peak, using quartz (060) as an internal standard, which according to ASTM cards appears at 'X' = $59.98^\circ 2\theta$ for $\text{Cu } K\alpha$ radiation. The distance between quartz and white mica peak is measured at $\frac{3}{4}$ height in mm. Let this distance be 'L' and the white mica peak be at 'Y' $^\circ 2\theta$. We want to find Y, hence $d(060)$ and hence b_0 .



Now $n\lambda = 2d \sin \theta$, where $n = 1$ (1st order spacing) in this case.

$$\therefore d = \frac{\lambda}{2 \sin \theta}$$

for $\text{Cu } K\alpha$ radiation $\lambda = 1.54056$

therefore if measure L we can find Y $^\circ 2\theta$.

$$\text{From (3) } Y = 59.98^\circ 2\theta + \frac{L}{40}$$

$$\text{but want } \theta, \text{ not } 2\theta, \quad \theta = \frac{59.98 + \frac{L}{40}}{2}$$

$$\text{but } b_0 = 6 \times d(060) = \frac{3 \lambda}{\sin \theta} = \frac{4.62168}{\sin \left(\frac{59.98 + \frac{L}{40}}{2} \right)}$$

APPENDIX FIVE

T A B L E 1

Estimated precision and detection limit of major oxides
 (Geochemistry Department, University of Cape Town)

Precision (Pr) is expressed as % of average concentration.
 Detection Limit (DL) expressed as weight % oxide.

OXIDE	AVERAGE	PR.	DL
Fe_2O_3	5.0	0.3	0.04
MnO	0.2	2.5	0.006
T_1O_2	0.5	0.4	0.004
CaO	5.0	0.3	0.01
K_2O	2.5	0.8	0.002
S_1O_2	55.0	0.5	0.05
Al_2O_3	15.0	0.5	0.03
MgO	4.0	1.0	0.05
Na_2O	3.0	1.3	0.08

TABLE 2

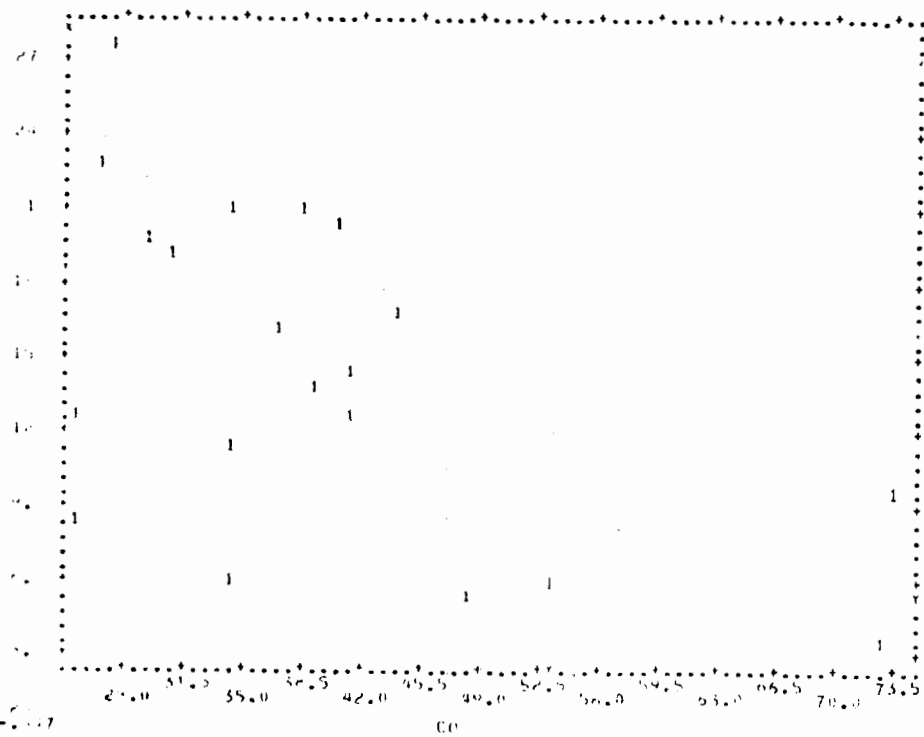
Counting errors and detection limits for trace elements analysed by XRF.
All data in ppm.

SD (100) = 2 error (95 percent confidence) at 100 ppm
SD (10) = 2 error at 10 ppm
DL = Detection limit at 99 percent confidence
G = Granitic matrix
B = Basaltic matrix

Element		SD (100)	SD (10)	DL
Ba	G	2.0	2.0	3
	B	6.2	4.0	7
Rb	G	0.6	0.4	0.8
	B	0.6	0.5	1.0
Zr	G	1.0	0.9	2.0
	B	1.4	1.2	2.6
Nb	G	1.2	1.1	2.3
	B	1.6	1.4	2.9
Th	G	0.8	0.5	1.9
	B	1.0	0.7	2.1
Pb	G	0.8	0.5	1.9
	B	1.0	0.7	2.1
Y	G	1.0	0.9	1.9
	B	1.2	1.1	2.2
Zn	G	0.8	0.5	1.0
	B	1.0	0.7	1.0
Sr	G	0.6	0.4	0.7
	B	0.6	0.5	0.9
Cu	G	1.0	0.8	1.7
	B	1.2	1.0	2.0
Co	G	3.4	3.2	7
	B	4.4	4.2	9
Ni	G	1.2	1.0	2.1
	B	1.6	1.2	2.6
Cr	G	1.6	1.2	2.5
	B	2.0	1.5	3.1
V	G	3.0	2.8	5.6
	B	3.0	2.8	5.6

The decimal fractions in the trace element data are not significant but have been included in order to allow accurate rounding off.

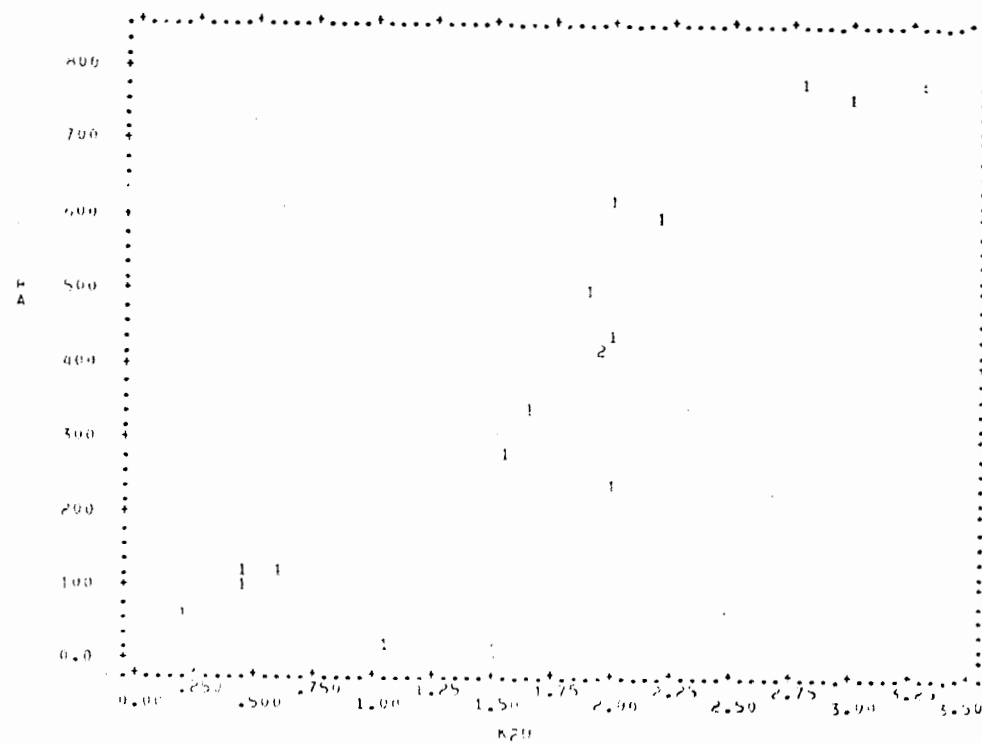
APPENDIX SIX

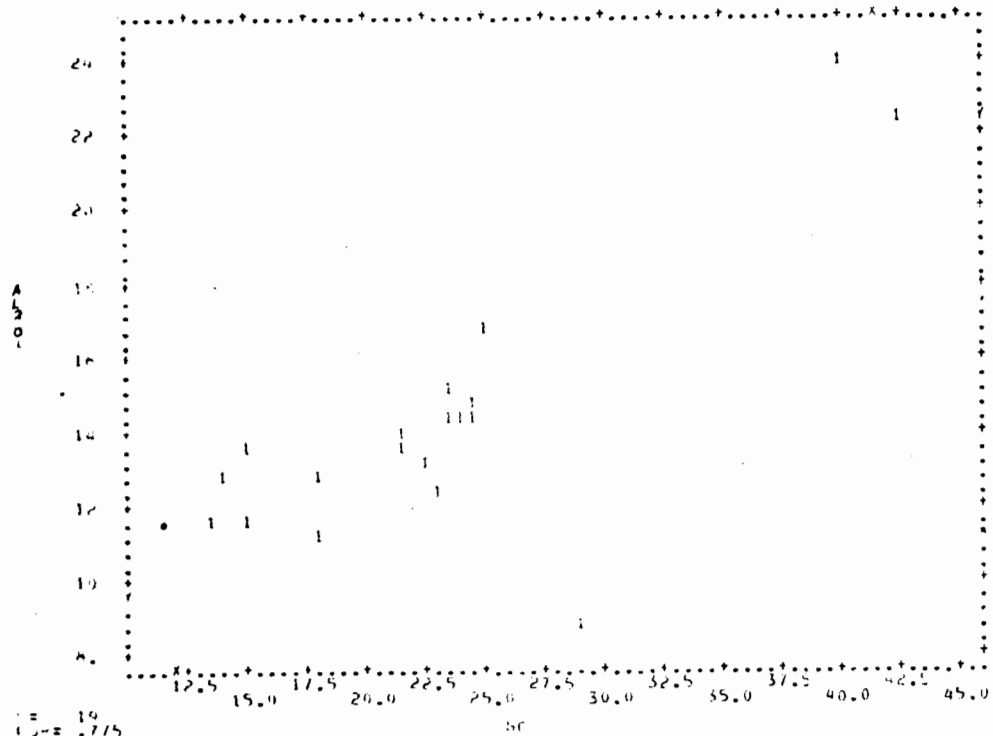


1-1.17

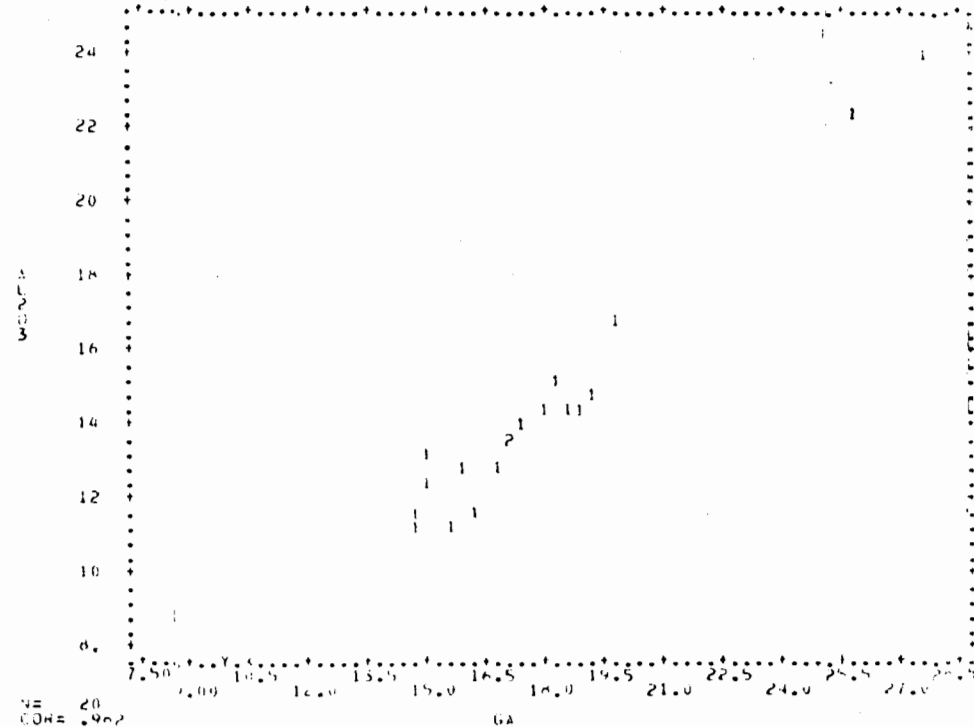
CO

STATISTICS REGRESSION LINE PFS.85.
 13.583 13.583 13.583 13.583 13.583 13.583
 13.583 13.583 13.583 13.583 13.583 13.583

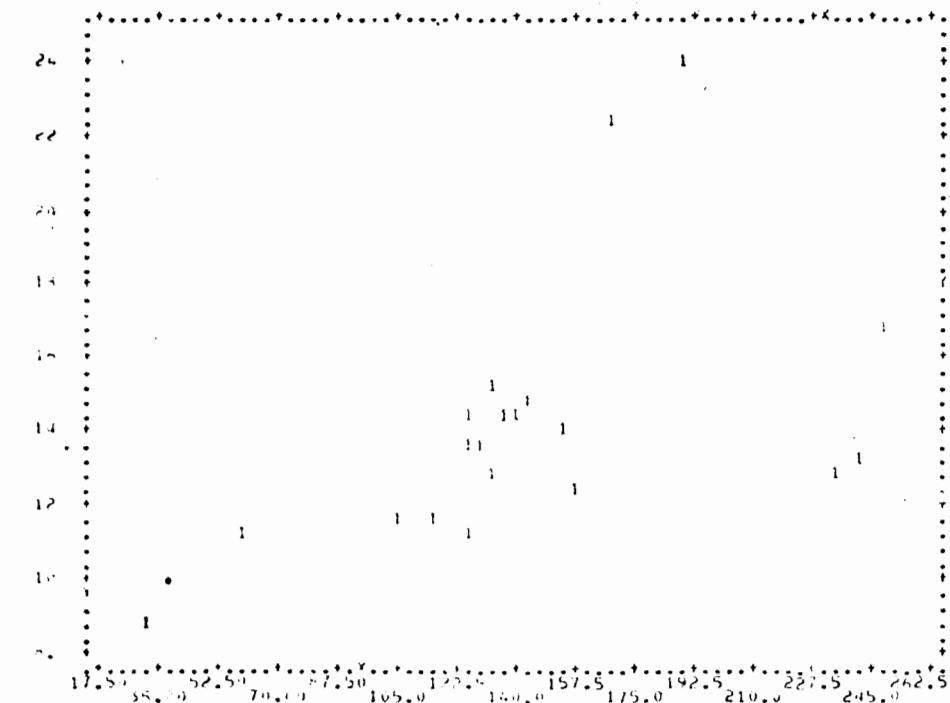




MEAN STDEV REGRESSION LINE RES.SS
X 25.000 7.7169 Y 1.6657 * X - 6.9144 25.142
Y 14.275 3.5842 Y = 1.6657 * X - 6.9144 5.4511

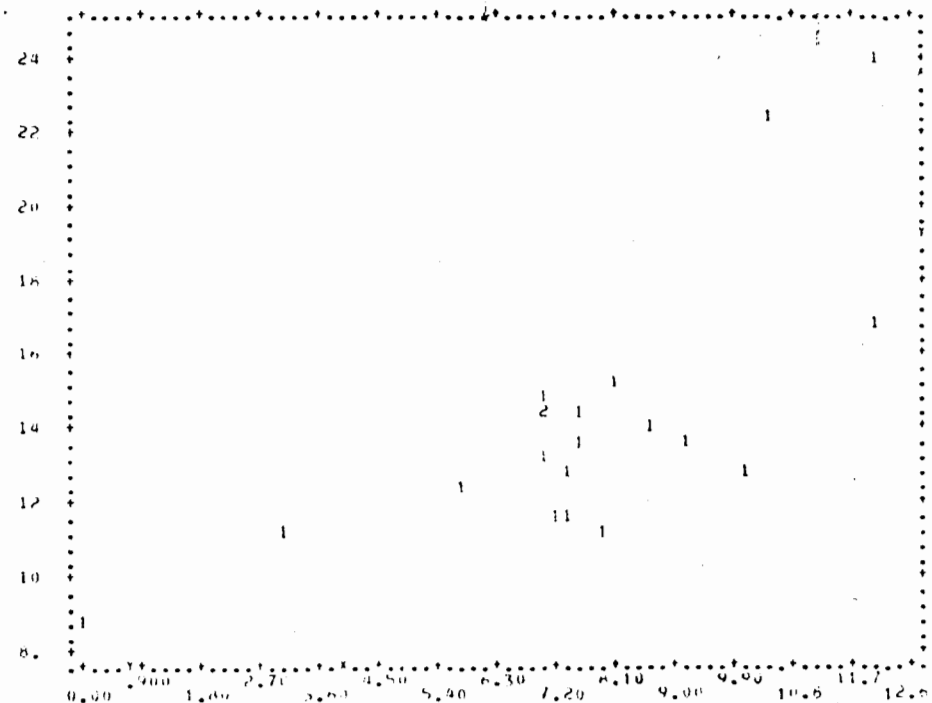


MEAN STDEV REGRESSION LINE RES.SS
X 17.515 5.9841 Y 0.9609 * X - 2.5502 1.2576
Y 14.121 3.5605 Y = 0.9609 * X - 2.5502 1.0044

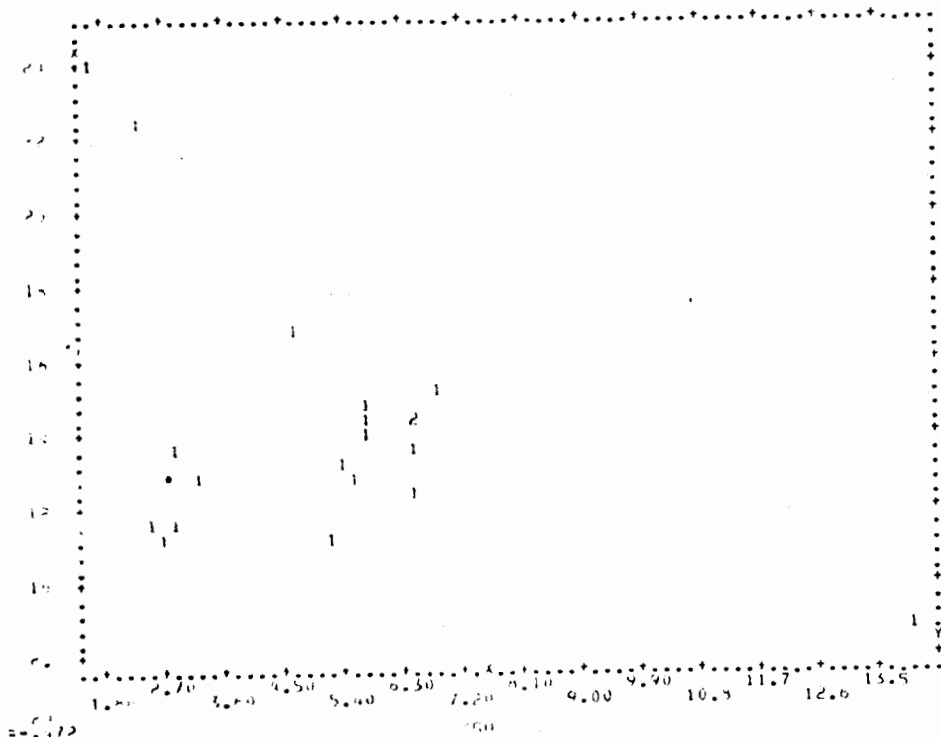


N= 20
 MEAN 55.850 ST. DEV. 3.5585
 REGRESSION LINE
 $X = 7.8674 + Y + 30.872$
 $Y = .05541 * X + 9.2851$
 RES. MS. 3.9167

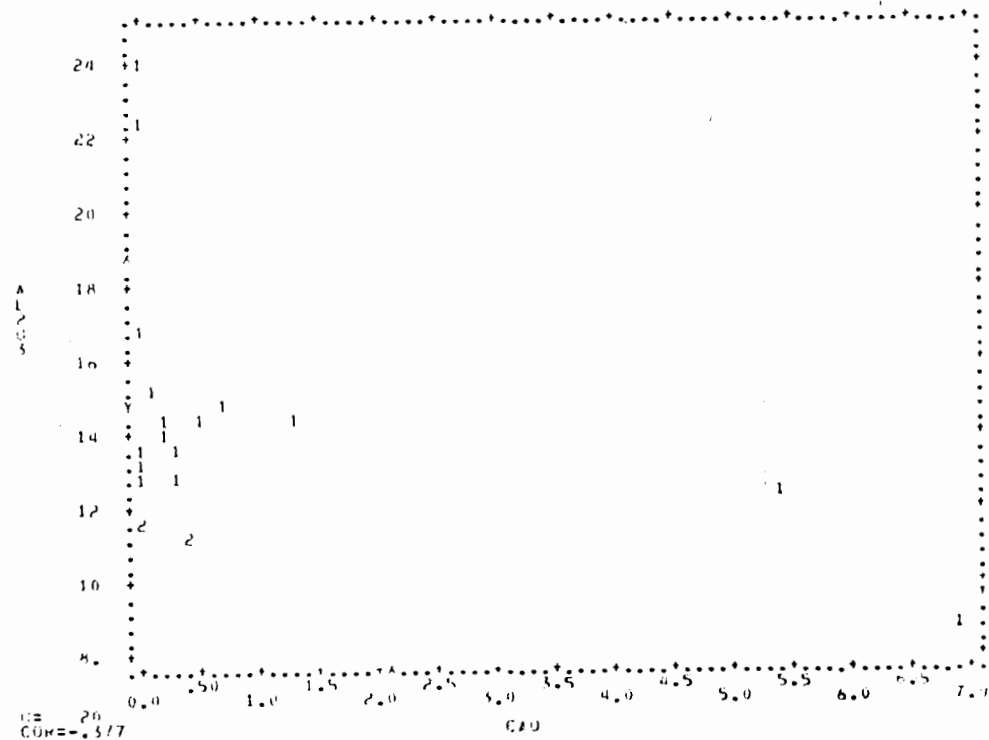
A
 1
 2
 11
 1



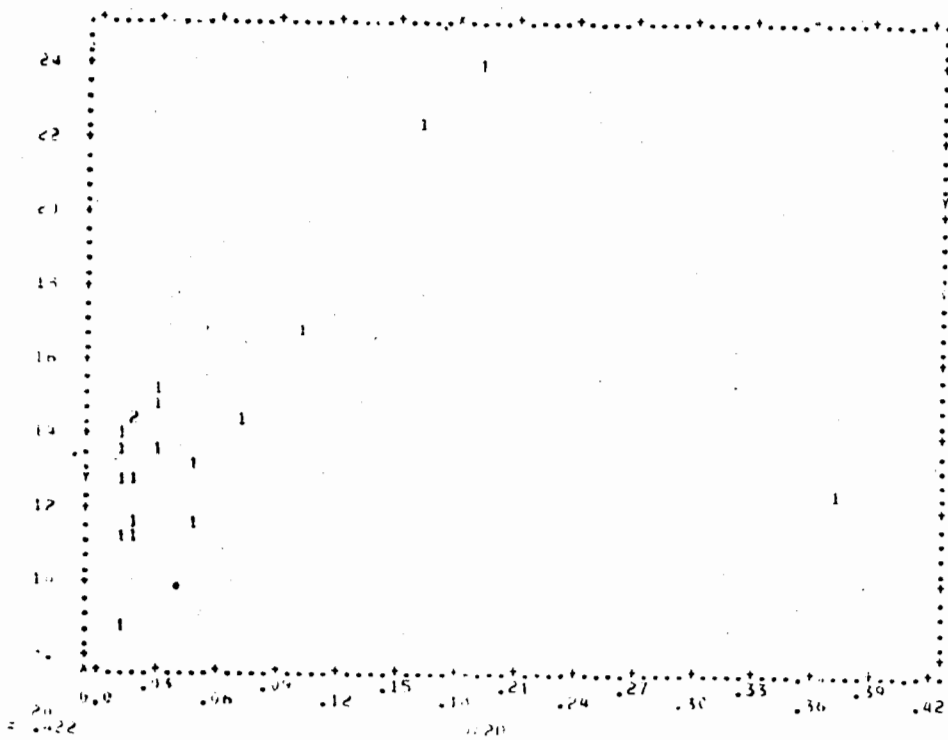
N= 20
 MEAN 7.0220 ST. DEV. 2.7136
 REGRESSION LINE
 $X = .55587 * Y + .19920$
 $Y = .95550 * X + 0.5541$
 RES. MS. 3.0677



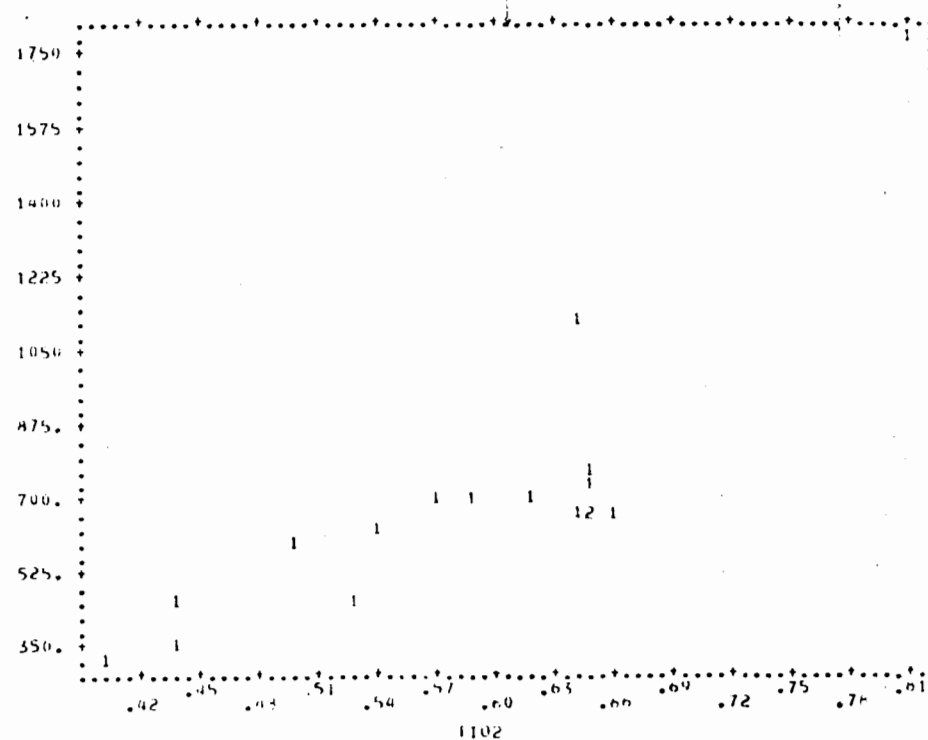
$R^2 = .772$
 $R = .879$
 $SE = 1.15$
 $Y = 3.5605$
 $X = -1.5984$
 $Y = -1.6184$
 $Y = 17.510$
 $Y = 10.805$

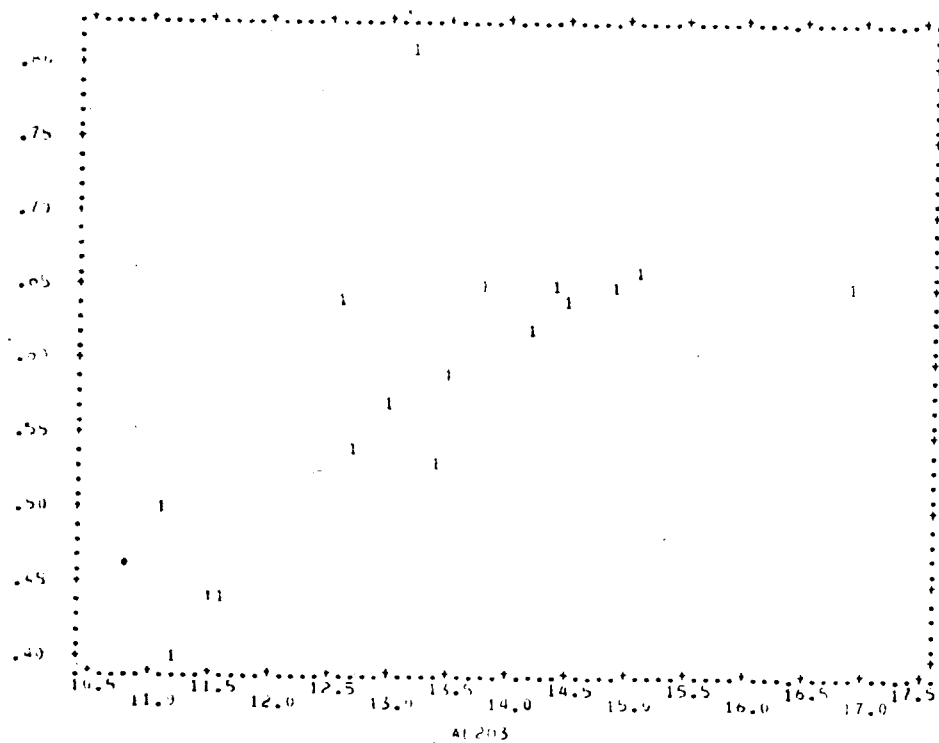


$R^2 = .26$
 $R = .517$
 $SE = 1.15$
 $Y = 3.5605$
 $X = -1.5984$
 $Y = -1.6184$
 $Y = 17.510$
 $Y = 10.805$

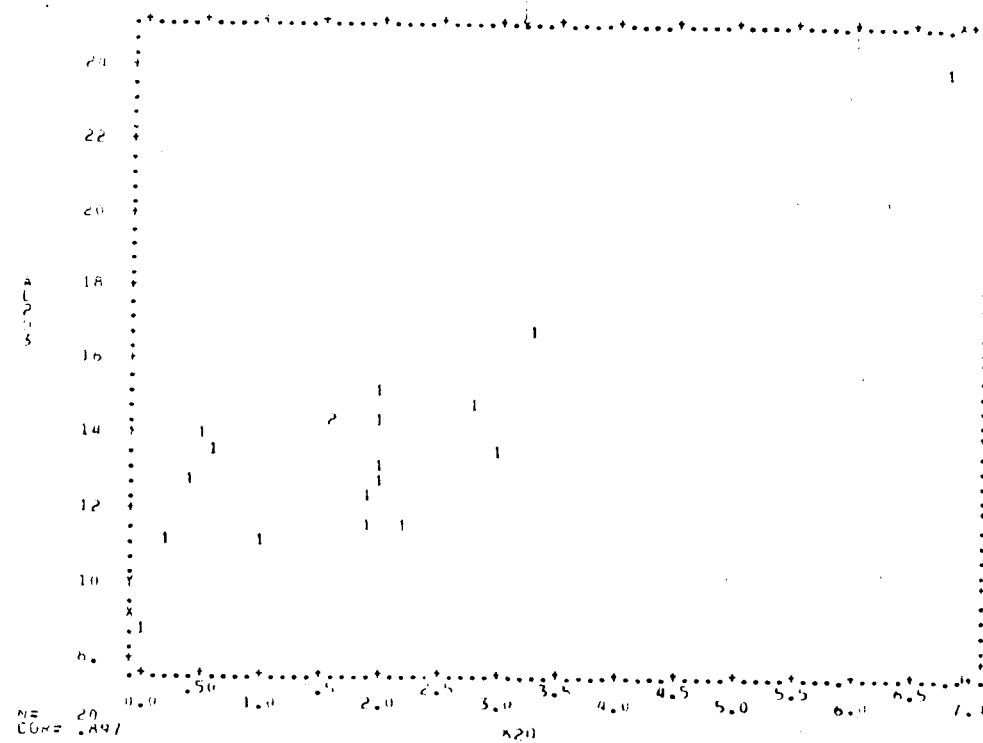


	ST. DEVI.	REGRESSION LINE	S.S. RES.
0.0150	0.0027	$x = 0.1906 + r = 0.0029$	0.0076
19.121	3.5605	$y = 17.917x + 15.074$	11.000





AL 203



N= 20
 CORR= .897
 MEAN 2.0860 ST. DEV. 1.7275
 X 2.0860 Y 14.121
 REGRESSION LINE
 X= .45510 Y= 6.1598
 Y= 1.6978 X+ 10.264
 RES. S.S. 2.6174